INFLUENCE OF SUBSOIL STRENGTH ON PERFORMANCE OF GEOSYNTHETIC-REINFORCED FOUNDATIONS

A Thesis

Submitted in Partial Fulfillment of the Requirements

for the Degree of

DOCTOR OF PHILOSOPHY

by

ARGHADEEP BISWAS

Department of Civil Engineering
Indian Institute of Technology Guwahati
Guwahati

February 2016

…Dedicated to all "Suddha-Sattwa" s who have furthered me to blossom in the garden of life…

STATEMENT

I do hereby declare that the matter embodied in this thesis is the result of investigations carried out by me in the Department of Civil Engineering, Indian Institute of Technology Guwahati, Guwahati, Assam, India.

In keeping with the general practice of reporting scientific observations, due acknowledgements have been made wherever the work described is based on findings of other investigators.

Guwahati — Arghadeep Biswas

Date:

CERTIFICATE

This is to certify that the thesis entitled "**Influence of Subsoil Strength on Performance of Geosynthetic-Reinforced Foundations**" submitted by **Arghadeep Biswas** (Roll No. 10610418), to the Indian Institute of Technology Guwahati, for the award of degree of Doctor of Philosophy in Civil Engineering is a record of bonafide research work carried out by him under my supervision and guidance. The thesis work, in my opinion, has reached the requisite standard fulfilling the requirement for the degree of Doctor of Philosophy.

The results contained in this thesis have not been submitted in part or full to any other University or Institute for award of any degree or diploma.

Dr. A. Murali Krishna
Associate Professor
Department of Civil Engineering
Indian Institute of Technology Guwahati
Guwahati-781039, India

ACKNOWLEDGEMENTS

It is an opportunity and gives me immense pleasure to convey my wholehearted gratitude to all the generous people I have been associated at IIT Guwahati.

The work reported in this thesis was carried out under the esteemed supervision and guidance of **Dr. A. Murali Krishna.** However, my special thanks to **Dr. Sujit Kr. Dash** who has introduced me in the field and supervise at initial stage of my research. I remain deeply grateful to them not only for their guidance and constant encouragement throughout the course, but also for their invaluable advice and encouragement that enriched my doctoral study.

I would like to thank my Doctoral Committee members, Dr. Sredeep S., Dr. N. Sahoo and Dr. B. Pradhan, for sparing their valuable time in reviewing my work. I extend my sincere thanks to the other faculty members of the Geotechnical Engineering Division of IIT Guwahati for their cooperation whenever required. I would like to thank Head of the Department, Dr. S. Dutta, and the former Heads of the Department, Dr. S.K. Deb and Dr. A.K. Sharma, for the facilities provided for conducting the research.

I express my heartfelt gratitude and thanks to the former scientific officer of Civil Engineering Department Dr. Kumar Pallav for extending all possible support. I gratefully acknowledge the unstinted help provided by Mr. Hari Ram Upadhyaya, Md. Bazal Hoque and Mr. Upen Gohain during different phases of my research work. Furthermore, I would like to thank the office staff of Civil Engineering Department, for their support in administrative works.

A very special gratitude is due to former M.Tech. students, Md. Asfaque, Bino, Ramesh and Bikash, for their cooperation in the laboratory works. I take this opportunity to thank Raju and Tapan for their invaluable help in conducting the experiments.

My time at IITG, 'the home away from home', was made enjoyable due to many friends who became a part of my life. I want to thank them all: Akash, Abhijit, Pranjal, Pawan, Sabyasachi, Awadhesh, Shiv, Bali, Suchit, Deepjyoti, Srikanth, Sudheer, Bhanu, Janarul, Jagori, Yagom, Jumrik, Arindam, Nabin, and many others; I was touched by their friendly affection, timely help, and moral support. My special thanks to Prof. Madhusudan Chakraborty, Dr. Mukul Bora and Dr. Arup Bhattacharjee for their valuable suggestions, effective co-operation and encouraging interactions which help me to improve my skills.

Lastly, but most importantly, I want to acknowledge the greatest supports, love and encouragements received from my parents (Baba and Ma), wife (Sumana) and our loving son, Suddhasattwa, without which it would never be possible.

Arghadeep Biswas

ABSTRACT

The ever increasing infrastructure development requires adequate competent ground which is becoming scarce. Therefore, developing techniques for improving the weak subsoil (low bearing capacity and/or excessive settlements) into a competent acceptable condition is a major task in geotechnical engineering practice. In this perspective, the concept of reinforcing the soil is being practiced since long. For the last few decades, the soil-reinforcement technique has been vividly applied in different fields of civil engineering, such as foundations, slopes, retaining walls, embankments, and pavements.

The benefits of using reinforcement for foundation applications in different forms (planar and/or three-dimensional) have been demonstrated by several researchers. Several influencing factors investigated in most of the studies were, reinforcement material, form, geometry; its placement depth and filled materials etc., to determine their optimum values, but mostly concerning about the softer clay or loose sand. In practice, natural ground (subgrade) may exist at different strength levels and situations may arise where reasonably strong soils also fail to meet the design requirements which need to be improved. In such situations, performance of reinforced foundations with different subgrade strengths should be considered which hasn't been addressed yet. Besides, it has been observed from the literature that different reinforcement systems, such as planar geogrid, three-dimensional geocells, and their combination haven't investigated systematically, especially with the varying clay subgrades. In view of the above, the present study aimed for developing an understanding of the performance of the geosynthetic-reinforced foundation systems with different reinforcement forms and having clay subgrades of varying strengths.

The objective of the present study was achieved through physical model tests, which were planned in five different series of tests in such a way that effect of each foundation configuration can be evaluated. Model tests were carried out on a circular footing of 150 mm diameter (D) resting on 1 m × 1 m × 1 m foundation bed having clay subgrades of different undrained shear strengths (c_u), ranging from 7 to 60 kPa. Different series of laboratory model tests were performed on homogeneous and layered foundation systems. The layered systems were comprised of unreinforced and reinforced sand of varying layer thicknesses (H = 0.63 to 2.19D) overlying the clay subgrades. The reinforcements used in these tests were planar geogrid, geocells, and geocell-geogrid combined. The foundation beds were prepared in the laboratory in a test tank and foundation performances were monitored under a rigid circular footing.

The tests on different foundation systems are presented in different chapters of this thesis, sequentially as unreinforced, geogrid reinforced, geocell reinforced, and geocell-geogrid reinforced foundation systems. The results are presented in terms of bearing pressure-settlement and surface deformation profiles. Besides, different bearing pressure ratios are introduced to compare the foundation behavior and reinforcement contributions. It was noticed that reinforcement of any form can improve the performance of clay subgrades, depending on footing settlement, layer thickness, and subgrade strength. In general, the improvement factors were decreased with increase in subgrade strengths (c_u). A maximum of about 12-fold improvement in bearing pressure was obtained for very soft clay subgrade of 7 kPa with geocell-geogrid configuration; while, the maximum bearing pressure of about 720 kPa was noted for the similar reinforcement configuration with c_u = 60 kPa. Optimum height of geocell-mattress for softer subgrades ($c_u \leq$ 15 kPa) was 1.57D. In the case of stiffer subgrades (c_u > 15 kPa) the optimum height was 1.05D. Beyond these optimum

heights buckling of geocell-walls and sand squeezing influenced the performance negatively. The geocells contribution, in improved bearing pressures, was higher for stiffer subgrades, while geogrid contribution was higher for softer subgrades.

Regression models were developed, based on the selected test data, to evaluate the bearing pressure at a given settlement level for a foundation system with any clay subgrade and reinforcement configuration. A detailed illustration of the applicability of the regression equations, highlighting the importance of subgrade strength in optimizing reinforced foundation design, was presented.

TABLE OF CONTENTS

LIST OF FIGURES

LIST OF TABLES

NOTATIONS AND ABBREVIATIONS

α	Level of significance
β_i	Regression coefficients
γ_b	Bulk unit weight of the clay
γ_d	Dry unit weight of the sand
δ	Surface deformation
δ_s	Interfacial friction angle of sand-geogrid
σ_3	Minor principal stress
σ_n	Normal stress
φ	Frictional angle of sand
ψ	Dilation angle of sand
b	Width of the geocell mattress
C_c	Coefficient of curvature of the sand
c_u	Undrained shear strength of clay
C_u	Coefficient of uniformity of the sand
d	Pocket size of the geocell mattress
D	Diameter of the footing
df	Degrees of freedom
D_r	Relative density of sand
e_i	Errors: difference between the dependent and the predicted value
E_s	Standard error
G	Specific gravity of sand and clay
h	Height of the geocell mattress
H	Thickness of unreinforced and reinforced sand layer
I_{fbg}	Bearing pressure improvement factor: q_{sgcg} / q_{sgc}
I_{fg}	Bearing pressure improvement factor: q_{sg} / q_s
I_{fgc}	Bearing pressure improvement factor: q_{sgcg} / q_s
I_{fs}	Bearing pressure improvement factor: q_s / q_c
I_{fsg}	Bearing pressure improvement factor: q_{sg} / q_c
I_{fsgc}	Bearing pressure improvement factor: q_{sgc} / q_c
I_{fsgcg}	Bearing pressure improvement factor: q_{sgcg} / q_c
k	Number of variables

n	Number of observations
q_c	Bearing pressure of homogeneous clay bed
q_{os}	Bearing pressure of homogeneous sand bed
q_s	Bearing pressure of unreinforced layered foundations
q_{sg}	Bearing pressure of geogrid reinforced foundations
q_{sgc}	Bearing pressure of geocell reinforced foundations
q_{sgcg}	Bearing pressure of geocell-geogrid reinforced foundations
R^2	Correlation in regression analysis
s	Footing settlement
u	Placement depth of the geocell mattress below the footing
$\hat{y}_i$	Predicted values
$\bar{y}$	Mean of dependent variables
y_i	Observed values
SSR	Sum of squares due to regression
SST	Total sum of squares
MSR	Mean square due to regression
MSE	Mean square due to errors

Chapter 1. INTRODUCTION

1.1 INTRODUCTION

The ever increasing demand of competent land for infrastructure development has been a challenge for geotechnical engineers to develop optimized methodology of transforming comparatively week subsoil into an acceptable condition. In most of the cases, the inadequacy arises in terms of unsatisfactory bearing capacity of the soil. In view of this, different ground improvement techniques are invented which increases strength and stiffness of soil, reduces compressibility and vulnerability to liquefaction, prevent adverse physical or chemical changes upon environmental effects and minimize the natural unpredictability of borrow materials and foundation soils. Amongst the various ground improvement techniques, such as replacement with good-filling soil, preloading with vertical drains, different types of compactions, grouting, deep soil mixing, and chemical treatments etc, the soil-reinforcement in different forms is being widely appreciated for its versatility and technical, economical, and environmental feasibility.

1.2 SOIL REINFORCEMENT

The concept of reinforcing the earth is being practiced since centuries in various forms like straw, reed, bamboo, logs, timber planks etc. (Dewar, 1962; Jones, 1996; Saran, 2005). However, the credit of introducing the systematic concept of soil-reinforcement has been with Vidal (1969). Over the time, soil-reinforcement has been modified according to new inventions and needs, in terms of material and shape. The metallic strip-reinforcements in the beginning were replaced by polymeric sheet-type-

reinforcement and afterwards, the versatile geosynthetics in different forms superseded all. In the process of modification, eventually, the three dimensional geocells were devised by Webster and Watkins (1977). Geocells are the honeycombing confining system, generally made of geosynthetics such as geogrids and geotextiles.

Most of the applications of soil-reinforcement in improving the bearing capacity are investigated through foundation systems of different configurations. Studies indicating metallic-strip form of reinforcements were the most primitive type, started with the pioneer work of Binquet and Lee (1975). For the last few decades, apart from the foundation applications, the soil-reinforcements in planar form are used in several fields of civil engineering applications, such as construction of pavements, retaining walls, embankments etc. The benefits of planar reinforcements considering several aspects, such as material-strength, geometry, placement depths, and number of layers etc., for its optimized use, has been demonstrated by several investigators (Akinmusuru and Akinbolade, 1981; Fragaszy and Lawton, 1984; Love et al., 1987; Shin et al., 1993; Michael and Collin, 1997; Alawaji, 2001; Alamshahi and Hataf, 2009; Choudhary et al., 2010; Latha et al., 2013).

Similar as the planar reinforcements, geocells were also used in foundations, roadways, railways, embankments, slopes etc. to improve the load-bearing capacity of soils. Several field applications (Johnson, 1982; Cowland and Wong, 1993; Raymond, 2001; Emersleben and Meyer, 2008) and laboratory studies (Rea and Mitchell, 1978; Shimizu and Inui, 1990; Lau et al., 2001; Sitharam et al., 2007; Zhang et al., 2010; Mehrjardi et al. 2013; Tafreshi et al., 2013) have been reported highlighting the benefits of three dimensional geocell types of reinforcements.

1.3 IMPORTANCE OF SUBGRADES

A typical reinforced-foundation, with planar reinforcement, is shown in Fig. 1.1. The diameter (or width) of the footing is '*D*'; while, the depth of the reinforced zone is '*H*'. Two types of soils can be noticed, indicating the filled-soil (Type-1) and the in-situ soil (Type-2). In most of the cases, the soil-combinations can be found as sand-sand, sand-clay, and clay-clay. However, as per the general practice, granular materials such as sand or gravel are used as filling-soil.

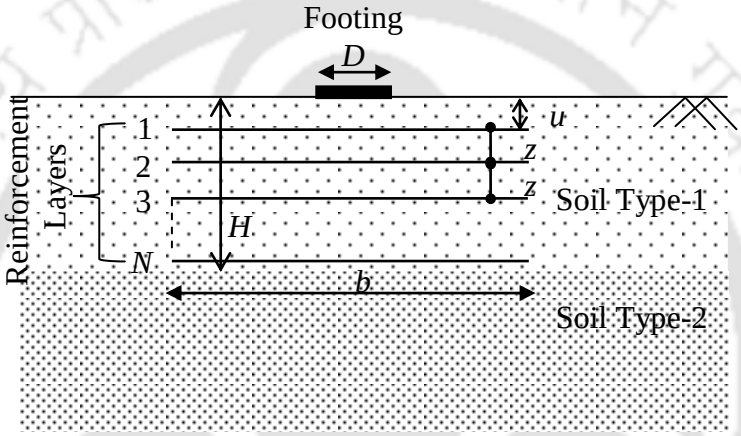

Fig. 1.1 Typical reinforced (planar) foundation (modified after Khing et al., 1993)

In the context of foundations, comparative performance of different forms of reinforcement (i.e. planar, three-dimensional, and combination of planar and three-dimensional) have been studied many occasions by varying different parameters such as reinforcement-geometry, placement depth, and filled materials etc. It is noticed that most of the studies were focused on improving the bearing capacity of soft subgrades only. However, as can be seen in Fig. 1.1, the behavior of foundations is largely dependent on the underlying subgrade. Besides, in practice, situations may arise where reasonably strong soil also fails to meet the design requirements or marginally competent ground needs to be improved. In such situations, quantification of performance of geosynthetics-reinforced systems is yet to be fully exploited, especially when clay is considered as subgrade.

1.4 BROAD OBJECTIVE OF THE STUDY

Present study envisages to develop an understanding of the performance of foundation systems having different reinforcement-configurations overlying clay subgrades of varying strength through physical model tests.

1.5 ORGANIZATION OF THE THESIS

The thesis is organized in 9 chapters.

In **Chapter 2,** selected studies on reinforced-foundation systems of different form of reinforcement, such as planar, three-dimensional geocells, and in combination of the two, are reviewed. The chapter concludes with the critical appraisal drawn on literature reviewed and detailed scope of the present study.

Chapter 3 deals with the details of materials used, its characterization, and methodology adopted in the study. Details of test program, test set-up, preparation of foundation beds and experimental procedure are also explained in this chapter.

Chapter 4 presents the results obtained from the tests performed on homogeneous (clay and sand) and unreinforced layered foundations. The homogeneous foundations were consisted of saturated clay having different undrained shear strengths and a sand bed at dense condition. The unreinforced layered foundations were comprised of different thickness of sand layers overlain the clay subgrades of different strengths. The results from this chapter are used to evaluate the reinforcement effects in further chapters.

Chapter 5 covers the foundation responses investigated with a single layer of geogrid placed at sand-clay interface. The foundation configurations were kept similar as followed in unreinforced-layered case. The influence of layer thickness and the

subgrade strength on the beneficial effect of the planar geogrid were the investigated parameters for this test series.

Chapter 6 discusses the responses of geocell-reinforced foundations having varying clay subgrades underneath. The heights of geocell-mattress were so selected that in combination with the sand cushion thickness, the total depth of the reinforced-sand layer from footing bottom will be the same as used in unreinforced and geogrid-reinforced foundations. The chapter provides a comparative performance of geocell-reinforced foundation with respect to previous systems.

In **Chapter 7**, effect of an additional planar geogrid placed at the bottom of the geocell-sand mattress is presented keeping the foundation configurations as similar as the geocell-alone case. A comparative performance of the geocell-geogrid with the geocell-foundations is also presented.

A discussion on the comparative foundation performance is presented in **Chapter 8** to highlight the design implications of the study**.** Besides, a regression analysis, to correlate the variables, is also performed. An illustrative design example is presented to describe the use of the regression equations generated.

Chapter 9 summarizes and concludes the present study with the conclusions drawn from the present research work. A brief note on the future scope of work has also been presented.

Chapter 2. LITERATURE REVIEW

2.1 INTRODUCTION

Behaviors of foundation system in different configurations, such as unreinforced and reinforced, were being investigated through either field or simulated laboratory model studies. As the objective of the present study is to investigate the effect of subgrade soil on the performance of different foundation configurations, studies pertaining to different model studies on shallow foundations were reviewed.

In this chapter, a brief discussion on unreinforced foundations in homogeneous and layered configuration followed by the review on reinforced foundations, such as planar and geocell reinforced foundations studies, are presented. Critical appraisal of the literature reviewed and a detailed objective of the present study have concluded the chapter.

2.2 UNREINFORCED FOUNDATIONS

The unreinforced foundations can be considered as homogeneous and layered configurations. Studies on unreinforced foundation systems (homogeneous and layered) are discussed in the following sections.

2.2.1 Foundations on Homogeneous Soil

Foundation behavior on homogeneous soil was, probably, initiated by Pauker (1889). In the study, the foundation behavior was investigated on homogeneous sand and analyzed based on the earth pressure theory proposed by Rankine (1857). The Pauker's model was modified by Bell (1915) by considering both the cohesion and friction of homogeneous soil. Subsequently, Prandtl (1921) has developed an

analytical solution, based on experimental results, to define the ultimate bearing capacity of soil. Terzaghi (1943) has extended Prandtl's model with a semi empirical equation based on principle of superposition. In this model, the non-linear behavior of the foundation responses, cohesion and friction, weight of the soil, and the embedment depth of foundations were considered. Different 'bearing capacity factors', such as N_c, N_q and N_γ, were proposed as a function of the friction angle of soil. In Fig. 2.1, different modes of plastic flow of foundation soil (after failure) under varying footing conditions are presented, as described by Terzaghi. Later, the theory was further revised to take care of effects of footing shape and different modes of failures. Afterwards, considering different aspects of foundation configurations, such as effect of soil-saturation (Skempton, 1951), loading eccentricity and inclination (Meyerhof, 1951, 1953, 1957, 1963, 1965; Teng, 1969; Hansen, 1970; Hanna and Meyerhof, 1981; Highter and Anders, 1985), compressibility of soil (Vesic, 1973, 1975) were studied by different researchers. However, most of the modifications have considered bearing capacity theory and factors proposed by Terzaghi.

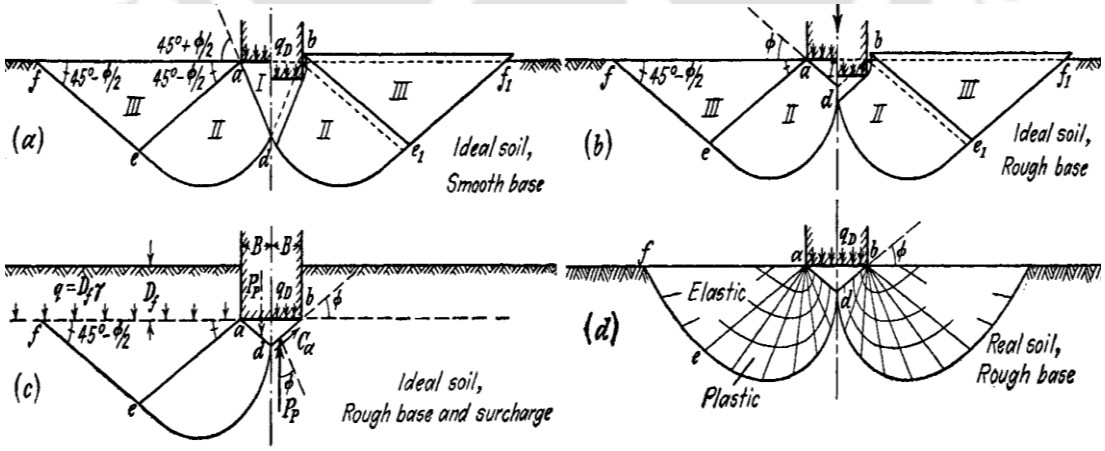

Fig. 2.1 Boundaries of zone of plastic flow after failure under different foundation conditions (after Terzaghi, 1943)

2.2.2 Foundations on Layered Soil

In practice, due to Earth's natural stratigraphic nature, foundations are mostly encountering the layered soils underneath. Behavior of the foundations on layered soil was initiated by Button (1953) with saturated clay. Brown and Meyerhof (1969) had conducted several model tests on saturated clay of varying strength in layered configuration under rigid strip and circular surface footing. Later, Meyerhof (1974) has developed the theory of layered soil based on laboratory model studies. Two types of layered configurations were considered: dense sand over soft clay and loose sand over stiff clay. Fig. 2.2 presents the failure mechanisms suggested by Meyerhof (1974). Later, it was modified by Meyerhof and Hanna (1978) considering inclined loading, as presented in Fig. 2.3.

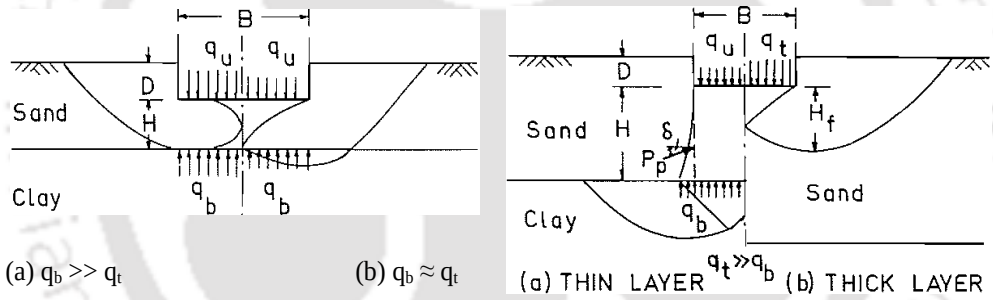

Fig. 2.2 Failure mechanisms defined by Meyerhof (1974)

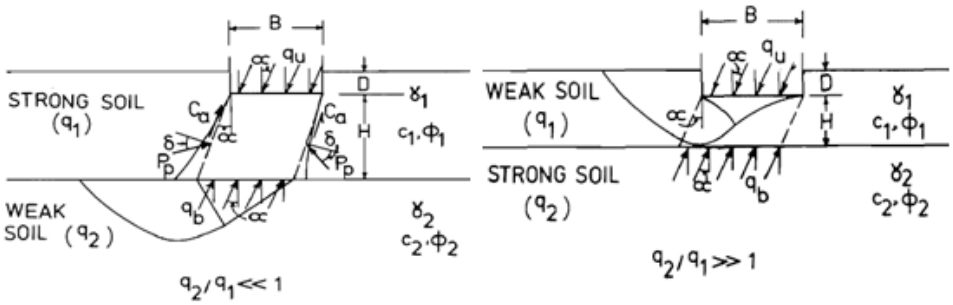

Fig. 2.3 Failure mechanisms for inclined load (after Meyerhof and Hanna, 1978)

Afterwards, several studies have enriched the topic with different parametric variations (Vesic, 1975; Tournier and Milovic, 1977; Pfeifle and Das, 1979; Hanna and Meyerhof, 1980; Hanna, 1981, 1982; Siraj-Eldine and Bottero, 1987; Cooke,

1988; Tani and Craig, 1995; Burd and Frydman, 1997; Cerato and Lutenegger, 2006). In most of the studies, sand and/or clay was used in varying parametric combinations in different configurations.

2.3 REINFORCED FOUNDATIONS

Traditionally, deep foundations are adopted to avoid the shallow soft soil and to transfer the structural loads to a comparatively stronger stratum. However, it is not economical always; not even the other ground improvement methods, such as excavation of soft soil and filling with good material, use of stone column, different compaction methods or chemical treatments to overcome the inadequacy of the strength (Robertson and Gilchrist, 1987; Paul, 1988; Hendricker et al., 1998; Palmeira et al., 2008). In several such situations 'soil reinforcement' is found to be the most viable alternative due to several advantages. Reinforced soil structures perform much better with greater control compared to conventional soil structures and ground improvement methods.

Various forms of soil reinforcement are available and used in different occasions. The metallic strip soil-reinforcement is the most primitive type (Binquest and Lee, 1975 a, b; Fragaszy and Lawton, 1984; Samtani and Sonpal, 1989; Huang and Tatsuoka, 1990) among the different soil-reinforcements. However, the metallic reinforcements are corrosive, not economic, and having limited beneficial effects in planar form. Hence, depending on performances, environmental feasibility, cost effectiveness etc, the soil-reinforcements are modified in terms of material and configurations. The metallic strip reinforcements were replaced by sheet-type reinforcement which was superseded by three dimensional geocells. Besides, the invention of polymeric geosynthetics, such as geotextiles and geogrids, has added a completely new dimension in this technology. The polymeric geosynthetics are cost

effective, environment-friendly, easy to use having high performance improvements (Guido et al., 1986; Mandal and Sah, 1992; Michael and Collin, 1997; Sitharam and Sireesh, 2004; Latha and Somwanshi, 2009; Rajyalakshmi et al., 2012; Kazi et al., 2015). Geocells, the three-dimensional soil-reinforcement, usually made of geotextiles or geogrids, are comparatively new inclusion in this technology. Several studies are reported (Rea and Mitchell, 1978; Jonson, 1982; Buthurst and Jarrett, 1998; Bush et al, 1990; Cowland and Wong, 1993; Krishnaswamy et al., 2000; Dash et al., 2001, 2003, 2007, 2012; Zhou and Wen, 2008; Pokharel et al., 2010; Tafreshi et al., 2013) stating its superiority since its invention by Webster and Watkins (1977).

In general, to evaluate improvements in load bearing capacity of the reinforced-soil, geotechnical structures like foundations and embankments are considered in most of the cases. However, as per the scope of the present study, selected studies on reinforced foundation systems comprised of planar and geocell-reinforcements are discussed in the following sections.

2.3.1 Studies with Planar Reinforcement

Binquet and Lee (1975a, b) pioneered the studies on the behavior of the reinforced foundation systems with planar reinforcement. In their study, the sandy-soil was reinforced with aluminum strips under a strip footing of width (B) 0.3 inch in a test tank of length 60 inches. Three different foundation configurations were considered such as homogeneous sand, soft soil under the sand layer, and a deep finite pocket of very soft material under the sand bed. The mechanisms of foundation failures were attributed as ‘general shear’, ‘tie-pullout’, and ‘tie-break’, shown in Fig. 2.4.

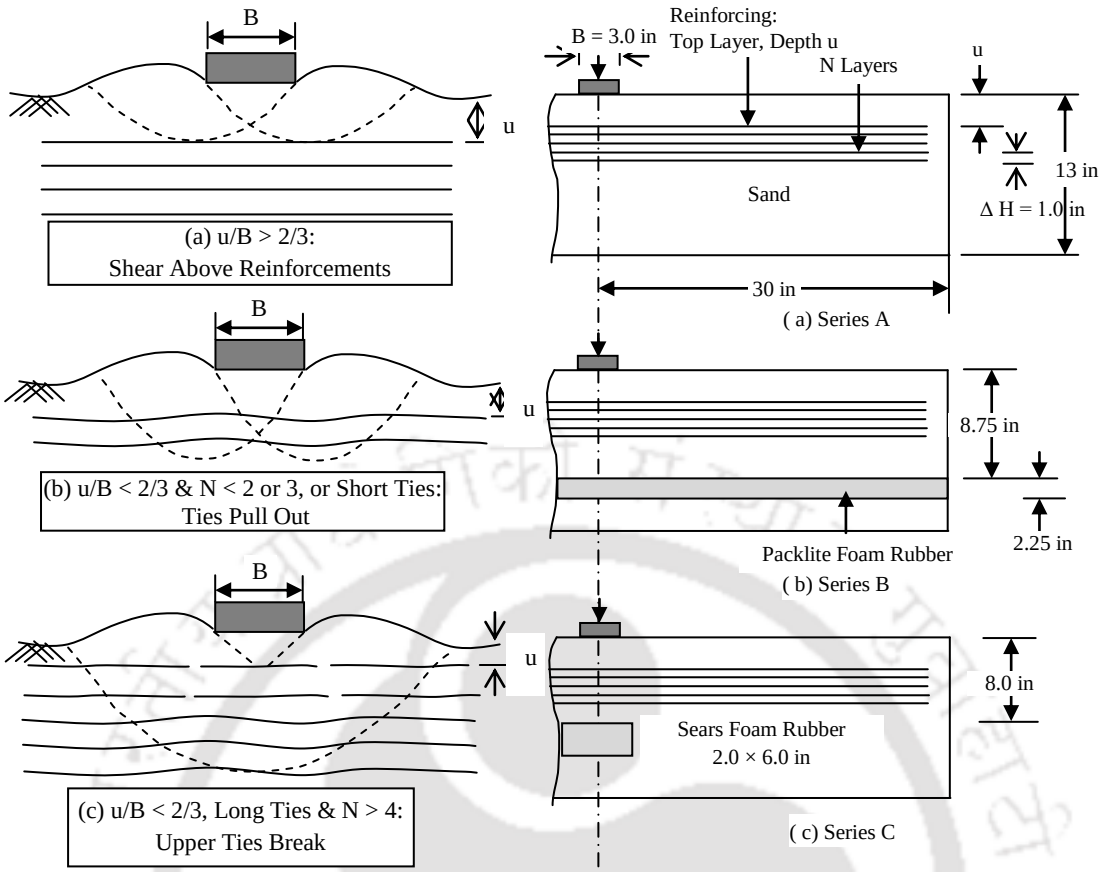

Fig. 2.4 Arrangement of model tests and modes of failure (reproduced after Binquet and Lee, 1975 a, b)

Selected studies on reinforced foundations using planar reinforcements are summarized in Table 2.1. A typical geometric configuration, shown in Fig. 2.5, was considered in most of the studies. In the figure, the '*q*' is signifying the loading intensity on the footing of width '*B*'. The other parameters shown in the figure are: '*u*' – the placement depth of the first layer reinforcement from footing bottom, '*h*' – the vertical spacing between the reinforcements, '*b*' – the reinforcement width, '*N*'- the number of reinforcement layers, and '*d*' – is the total depth of reinforced soil. As per the general practice, there might be two types of soil, the filling-soil in between and above the reinforcement layers, and the native soil below the reinforced-soil layer.

Table 2.1: Summary of selected studies with planar reinforcement

Study	Footing Type	Reinforcement Type	Optimum Parameters Found				
			u/B	b/B	Δh/B	N	BCR
Binquet and Lee (1975)	Strip	Aluminum strip	0.33	20	0.33	6	2-4
Akinmusuru and Akinbolade (1981)	Square	Rope fiber	0.5	10	0.5	3	2.9
Fragaszy and Lawton (1984)	Rectangular	Aluminum strip	0.33	6	0.33	3	1.7
Guido et al. (1986)	Square	Geogrid/geotextile	0.25	3	0.25	3	2.8
Love et al. (1987)	Strip	Geotextile/Geogrid	-	-	-	-	-
Kim and Cho (1988)	Strip	Geotextile	0.5-1.0	-	-	-	
Samatani and Sonpal (1989)	Strip	Metal strip	-	-	-	-	-
Huang and Tatsuoka (1990)	Strip	Metal Strip	0.5	6	0.5	3	6.34
Mandal and Sah (1992)	Square	Geogrid	0.175	-	0.2	1	1.56
Shin et al. (1993)	Strip	Geogrid	0.4	10	0.4	5	1.4
Khing et al. (1993)	Square	Geogrid	0.25-0.4	11	0.4	6	4
Omar et al. (1993)	Rectangular/strip	Geogrid	0.33	8	0.33	6-7	3-4.5
Khing et al. (1994)	Strip	Geogrid	0.67	6	0.67	1	1.3
Das and Khing (1994)	Strip	Geogrid	0.67	6	0.67	1	1.3-1.4
Alawaji (2001)	Circular	Geogrid	0.1	4	0.1	1	3.2
Das and Omar (1994)	Strip	Geogrid	0.33	8	0.33	-	3-5.5
Michael and Collin (1997)	Square	Geogrid/geocell	0.25	-	0.5	3	2.6
Sitharam and Sireesh (2004)	Circular	Geogrid	0.3	6	0.4	6	3.24
Basudhar et al. (2007)	Circular	Geotextile	0.25	3.5	1	3	5.5
Sawwaf (2007)	Strip	Geogrid	0.6	5	0.5	4	2
Latha and Somwanshi (2009)	Square	Geogrid	0.1	5 – 6	0.5	4	2- 2.5

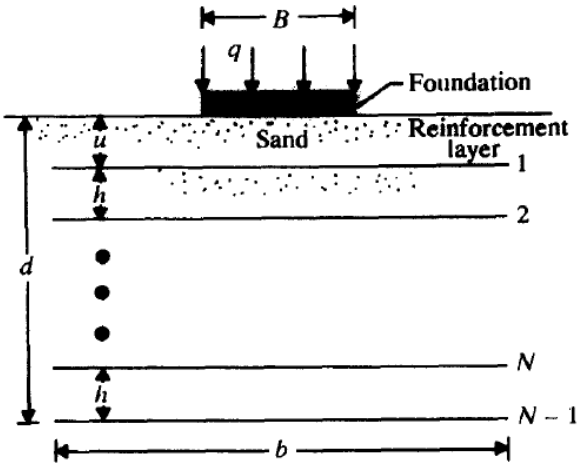

Fig. 2.5 Typical geogrid-reinforced foundation (after Khing et al., 1993)

Fragaszy and Lawton (1984) studied the effect of soil density (D_r = 51, 61, 70, 80, and 90%), reinforcement geometry, and the number of reinforcement layers on the load-settlement behavior of a rectangular footing. Household aluminum strips were used as the reinforcement in the study. In the experiments, reinforcements were observed to be broken at higher density of soil ($D_r \geq 70\%$), as reported by Binquet and Lee (1975). It was also reported that improvement in bearing capacity was independent of soil-density beyond a settlement level of 10% of '*B*'.

Guido et al. (1986) compared the performances of geogrid and geotextile reinforcement in medium dense sand (D_r = 55%). The reinforcing mechanism for geogrid was attributed to the soil-geogrid interlocking; while, the same for the geotextile was assigned to frictional force only. The optimum values of the various parameters were reported as $u = 0.25B$, $N = 3$, $b = 2\text{-}3B$ (ref. Fig. 2.5).

Love et al. (1987) investigated the performance of geogrid reinforcement placed at the sand-clay layer-interface. In the study, the undrained shear strengths (c_u) of the clay subgrades were considered as 6, 9, and 14 kPa. Substantial reduction in stress transferred onto the clay subgrade was found with inclusion of the reinforcements. It was observed that the reduction was depended on clay strength and

layer thickness. The additional benefit in bearing capacity attributed to 'membrane action' which is a function of strain mobilization at the level of reinforcement placed and interfacial properties of the reinforcement.

Mandal and Sah (1992) performed model tests on square footing rested over geogrid reinforced clay subgrade (c_u = 27 kPa). Photograph of the test set up is shown in Fig. 2.6. Effect of the placement depth of geogrid on foundation behaviors was investigated in the study. The improvement in bearing capacity was reported in terms of bearing capacity ratio (BCR), defined as the ratio of bearing capacities of reinforced and unreinforced foundations. Maximum BCR was found as 1.56 (with u/B = 0.25) and about 45% reduction in settlement was reported in the study.

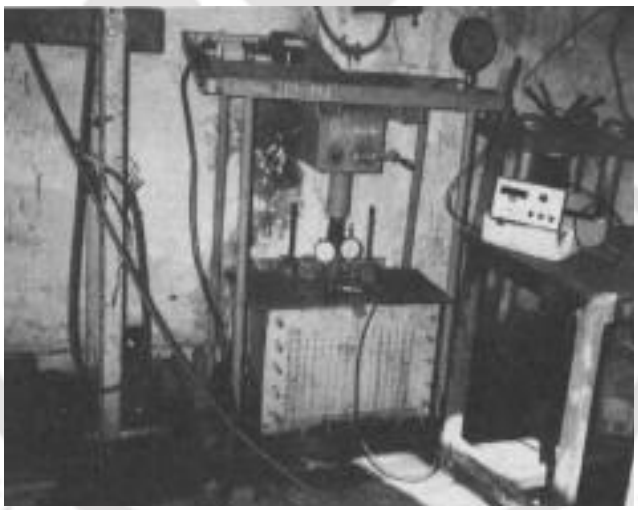

Fig. 2.6 Photograph of foundation set up (after Mandal and Sah, 1992)

Shin et al. (1993) conducted laboratory model tests on a strip footing supported by geogrid-reinforced clay. Two different clay strengths were considered in the study, such as c_u = 3.14 and 6.02 kPa. The reinforcement-mechanism, as defined in the study, is presented in Fig. 2.7. In the figure, zone-1 was considered as 'increased stiffness zone'; while, development of the passive and frictional resistances were considered to be happened at zone-2. The maximum improvement, in terms of BCR, was found as 1.4, for b/B = 10 and u = 0.4B. However, for b/B > 6, marginal

improvement was observed. The other optimum parameters were reported as N = 5 and d = 1.8B.

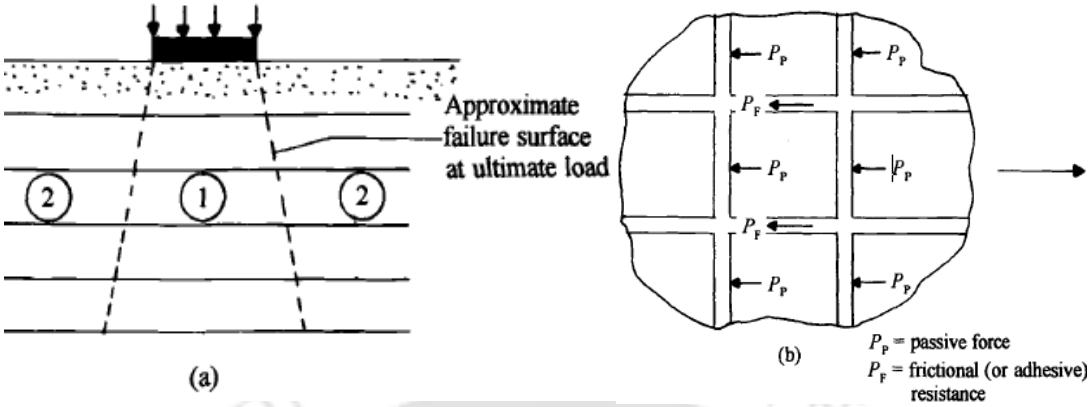

Fig. 2.7 Reinforcing mechanism as defined by Shin et al. (1993)

Khing et al. (1993) investigated the behavior of a strip footing on geogrid reinforced-sand bed. The schematic of the foundation configuration was presented in Fig. 2.5. The optimal values of the parameters were found as: u = 0.25-0.4B, N = 6, h = 0.375B and b = 10.75B. Maximum about 4-fold improvements in bearing capacity was achieved in the study.

Michael and Collin (1997) performed large scale model tests on geogrid-reinforced foundations. A test tank of 5.4 m × 6.9 m × 6 m, with varying footing sizes as 0.30, 0.46, 0.61, and 0.91 m^2, was considered for the study. The parametric study considered the effect of reinforcement area, vertical spacing, and number of reinforcement layers. Maximum about 2.6-fold improvement in bearing capacity was found for 3-layers of geogrid reinforcements.

Sitharam and Sireesh (2004) studied the performance of an embedded circular footing on geogrid-reinforced sand. Effect of embedment depths of footing, surface deformations, strain in geogrid, and pressure distribution under the footing were investigated, keeping the relative density of sand constant at 70%. A high localized strain in geogrid was observed just below the footing which was almost negligible at

about 2*D* from footing center. Higher load distribution and squeezing out of the sand from footing bottom were noticed for the reinforcements placed at relatively lower depths. Improvement in bearing capacity in the range of 3.0 was reported in the study.

Basudhar et al. (2007) investigated the behavior of geotextile-reinforced foundations on sand (D_r = 45%) under circular footing. Analytical and numerical analysis were performed to compare the experimental responses. The study highlighted the effect of footing size, reinforcement layer, reinforcement pattern, and relative density of soil on load-settlement behavior. Results showed maximum of 5.5-fold improvement in bearing capacity with 3-layers of reinforcements.

Latha and Somwanshi (2009) presented a model test, accompanied by a numerical simulation in FLAC^{3D}, on square footing resting on reinforced-sand. Variations in bearing capacity with the change in layout and configuration of reinforcements, type, tensile strength and amount of reinforcements were the investigated parameters. The improvement in bearing capacity was in the range of 2-2.5 times that of the unreinforced bed. The schematic test configuration is presented in Fig. 2.8.

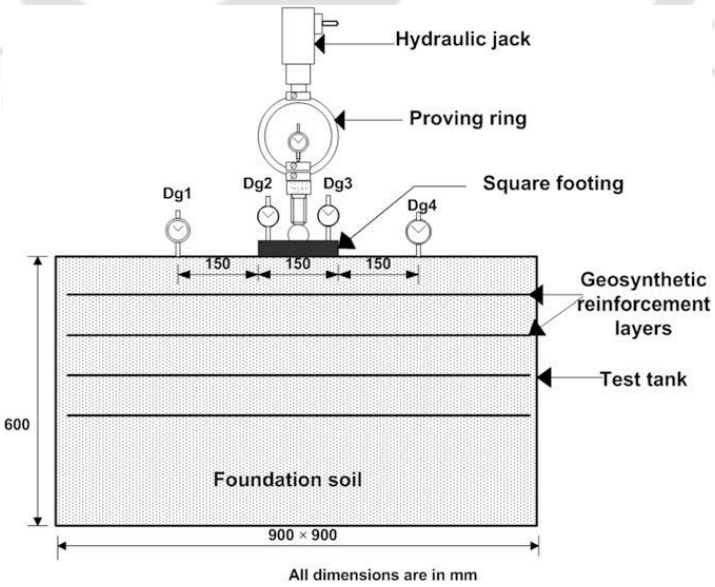

Fig. 2.8 Schematic test configurations adopted by Latha and Somwanshi (2009)

Regression analysis was considered in various studies to evaluate the interrelationship between the dependent and independent variables considered. Ranjan et al. (1996), Bera et al. (2005), Latha et al. (2013) adopted the non-linear regression models for defining the foundation behavior in terms of bearing pressures with respect to different influencing parameters, such as layer thickness, footing settlements, reinforcement geometry etc. The predicted behaviors showed reasonably good agreements with that of the experimental values. A typical regression model as proposed by Bera et al. (2005) is presented in Eq. 2.1.

$$q_{rs} = a_{10}.q_s^{a11}.(s/B)^{a12}.N^{a13}.f^{a14}.(L_s/B)^{a15}.a_{16}^{(u/B)}.a_{17}^{(Sv/B)} \quad (2.1)$$

Where, 'q_s' and 'q_{rs}' is the unreinforced and reinforced bearing pressures, respectively, at any settlement level (s/B). The B, L_s, N, f, u, S_v are the footing width, reinforcement lengths, number of reinforcement layers, friction ratio, depth of first layer reinforcement, and vertical spacing between the reinforcements, respectively. The a_{10}, a_{11}, a_{12}, a_{13}, … a_{ij}, etc. are the regression coefficients. Where 'i' is the 'number of observations' and 'j' represents the 'number of independent variables or predictors'. The a_{10} (where $i = 1$ and $j = 0$) represents the regression coefficients for the first observation having the independent (or predictor) variable as '1' producing the intercept term for the equation.

2.3.2 Studies with Geocell Reinforcement

Geocell is a three dimensional soil-reinforcement introduced by Webster and Watkins (1977). However, the concept of soil-confinement is considered to be initiated in the form the traditional triaxial compression tests which estimate the variation in strength parameters by altering the confinements. Henkel and Gilbert (1952) studied the effect of membrane stiffness and different modes of deformations

in triaxial tests. It was found that, correction considering the hoop tension is not required unless the membrane is not firmly attached to the specimen. Duncan and Seed (1967) considered both the axial and volumetric stain in estimating the axial and lateral stress. Rochelle et al. (1988) reported an empirical relation between the confining stress and axial strain considering the hoop stresses.

Bathurst and Karpurapu (1993) performed a large-scale single-cell triaxial compression tests with geocell-reinforced specimens. In the tests, the sample diameter was 200 mm having an aspect ratio (height to diameter) as unity. Rajagopal et al. (1999) performed a series of triaxial tests on geocell-confined granular soils of 100 mm diameter with aspect ratio 2:1, in single and multiple cell configurations as presented in Fig. 2.9. Similar trends of failures, by bursting of the seams, were found by Bathurst and Karpurapu (1993). Besides, it was found that the increase in the strength and stiffness of the soil is a function of cell diameter, strength, and stiffness of geocell material. Rajagopal et al. (1999) found that geocell system in the field can be simulated by the three interconnected cells in the triaxial test.

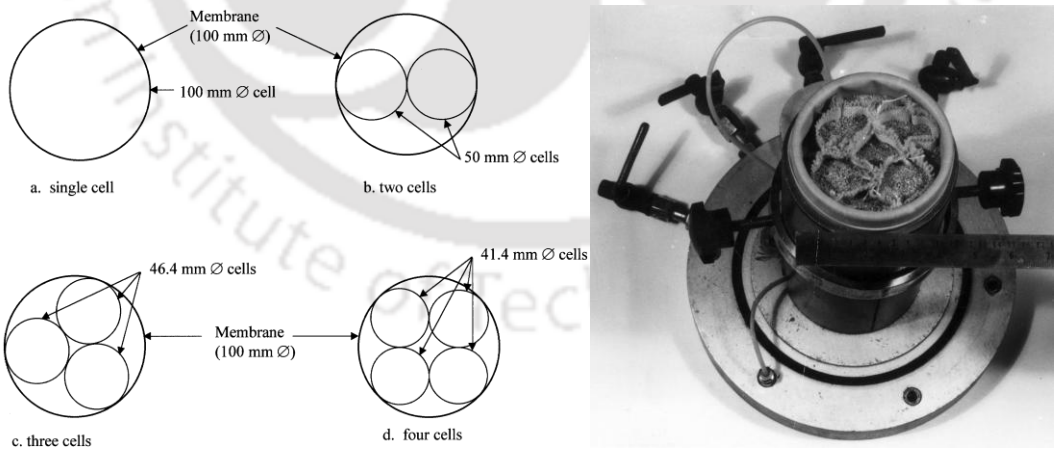

Fig. 2.9 Test configurations considered by Rajagopal et al. (1999)

Latha and Murthy (2007) compared the performance of different forms of reinforcements, such as horizontal, geocell, and randomly distributed fibers, made from geotextile, geogrid, and polyester, through triaxial tests. The schematic of the

test specimens are shown in Fig. 2.10. Wu and Hong (2009) studied the stress-strain response, effect of encapsulation, mobilized apparent-cohesion and variation in friction angle through triaxial compression tests**.**

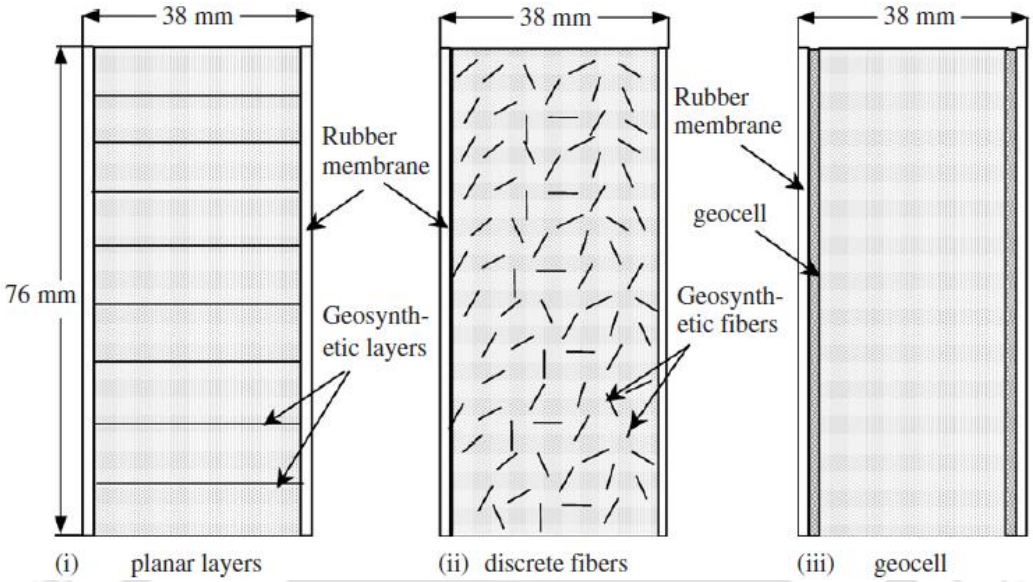

Fig. 2.10 Different forms of reinforcements used by Latha and Murthy (2007)

The results obtained from the triaxial tests indicated the development of additional apparent cohesion in the in-filled soil depending on tensile strength of the confinement materials. Besides, the soil-behavior was dependent on type, quantity and size of the reinforcements used. Thus, though, the triaxial compression test is an indicator of behavior of an individual confining system, but, it is always useful in estimating the effect of parametric alteration of a geocell-system. However, the model tests are inevitable for simulating the actual field conditions to estimate the overall behavior of the geocell-reinforced foundations.

A typical geocell-reinforced foundation system is shown in Fig. 2.11. Different parameters indicated are: height (*h*) and width (*b*) of the geocell-mattress; diameter of geocell-pockets (*d*); and the placement depth of reinforcement below the footing bottom (*u*). Two types of soils, such as sand-sand, sand-clay and clay-clay, generally noticed in most of the cases. However, as per general practice, the geocell-

pockets are filled with granular materials such as sand or gravel. Table 2.2 summarizes selected model studies on geocell-reinforced systems.

Table 2.2: Summary of selected studies with geocell reinforcement

Researches	**Footing Type**	**Reinforcement/ Geocell material**	**Optimum Parameters Found**				
			u/B	***b/B***	***d/B***	***h/B***	***BCR***
Mandal and Gupta (1994)	Rectangular	Geogrid	-	2	0.55	1.5	8
Mhaiskar and Mandal (1996)	Rectangular	Geogrid	0	3.4	0.625	2.8	3
Bathurst and Jarrett (1988)	Strip	Geoweb/Geogrid	-	-	-	-	-
Krishnaswamy et al. (2000)	Strip	Geogrid	-	-	-	0.5	-
Dash et al. (2001a,b; 2003a, b; 2004; 2007; 2008; 2010; 2012)	Strip	Geogrid, non-oriented polymer	0.1	12	1.2	3.14	8
	Strip	Geogrid, non-oriented polymer	0.1	8	1.2	2	9
	Circular	Geogrid	0.1	4	0.7	0.8	4
	Circular	Geogrid	0.33	6	0.8	1.68	7
	Strip	Geogrid	0.1	8	1.2	2.75	8
	Strip	Geogrid	0.1	10	1.2	1.6	-
	Strip	Geogrid	0.1	12	1.2	3.14	8
	Circular	Geogrid	0.1	8	1.2	1.6	6
	Strip	Geogrid	0.1	8	1.6	1.2	4.5
Sitharam et al. (2005)	Circular	Geogrid	0	5.5	0.8	2.4	6
Yoon et al. (2008)	Square	Waste tire thread	0.2	4.17	0.54	0.39	3
Zhou and Wen (2008)	Circular	Geogrid	-	1	0.13	0.1	3
Emersleben and Mayer (2008)	Circular	Geogrid	0	-	0.77	0.67	1.5
Sireesh et al. (2009)	Circular	$FLAC^{3D}$	0.4	5	0.8	1.8	4
Minaxi Rai (2010)	Circular	Geogrid	0.1	6.67	0.4	0.8	14
Zhang et al. (2010)	Circular	Geogrid	0.85	5.5	-	0.13	8
Pokharel et al. (2010)	Circular	Geogrid	0.13	1.37	1.37	0.67	2.5
Tafreshi and Dawson (2010)	Strip	Geogrid/geotextile	0.1	4.2	0.67	1.33	3
Tanyu et al. (2013)	Circular	Textured HDPE	-	-	-	-	-

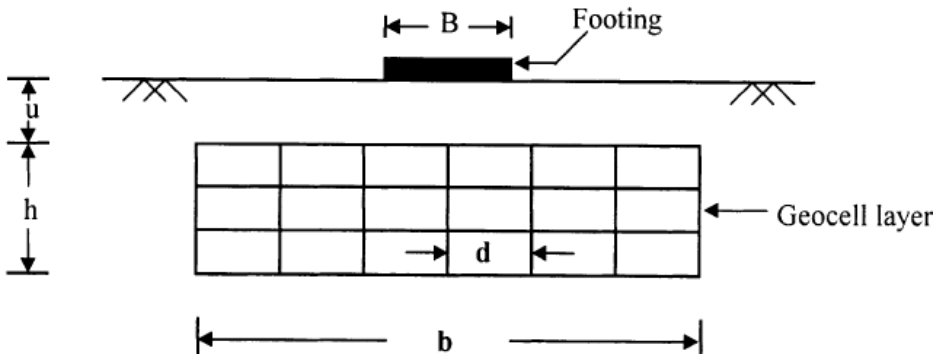

Fig. 2.11 Typical geocell-reinforced foundation systems (after Dash et al., 2001a)

Webster and Watkins (1977) used an array of soil-filled plastic tubes over the soft subgrade for an access road. Webster and Alford (1978) performed full scale traffic load tests on soft subgrade reinforced with sand-filled-aluminum-cell. Significant improvement in load carrying capacity was noted which reduced the thickness of unreinforced crushed stone layer by 1.6 times. Webster (1979) reported better performance of a square and hexagonal geocells in comparison to that in rectangular shape. Johnson (1982) considered geocell-reinforcement in a bridge construction. The geocell-mattress was placed over a soft estuarine silt layer and overlain by an approach embankment. Reduced lateral strain and about 50% reductions in predicted settlement were reported in the study. Robertson and Gilchrist (1987) reported the suitability of geocell-reinforcement in constructing a 4 m high embankment over soft clay. The geocell was reported as better alternative compared to excavation-filling, in terms of cost effectiveness and performance. A similar performance of geocell reinforcement in an embankment construction was reported by Paul (1988). The application of geocell was found to be the most convenient and effective method as compared to staged construction with provision of accelerated drainage and excavation-filling.

Bush et al. (1990) presented the details of field-construction method of geocell-reinforced embankment over soft ground. The geocell-mattress was fabricated with polymeric geogrids with the help of bodkin joints. The procedure of 'no cell was filled to full height before its neighbor was at least half filled' was adopted to avoid the possible distortion of the cells. An overfilling of about 150 mm was provided to encounter the compaction settlement due to normal constructional traffic (Fig. 2.12).

Fig. 2.12 Filling of geocell-mattress (after Bush et al. 1990)

A fully instrumented field investigation and construction process of a geocell-reinforced road embankment over soft clay was reported by Cowland and Wong (1993). An average improvement in shear strengths in the range of 2-3 as compared to that of the initial native soil was reported after a year of completion.

Mandal and Gupta (1994) studied the performance of geocell-reinforced model foundation on sand over soft marine clay (c_u = 20 kPa, D_r = 60%). Different foundation configurations were considered. However, h = 1.5B was found as optimum thickness with a maximum bearing capacity improvement in the order of 8.0.

Mhaiskar and Mandal (1996) investigated the effect of geocell (geotextile made) geometry and relative density of the infill soil on the overall performance of foundations on the soft marine clay having c_u = 10 kPa. The schematic of the test

configuration is shown in Fig. 2.13. Significant improvement in load carrying capacity and reduction in settlement was reported with geocell-reinforcements. A finite element analysis performed in ANSYS, to compare the foundation behavior, depicted a reasonably good agreement to the model test results.

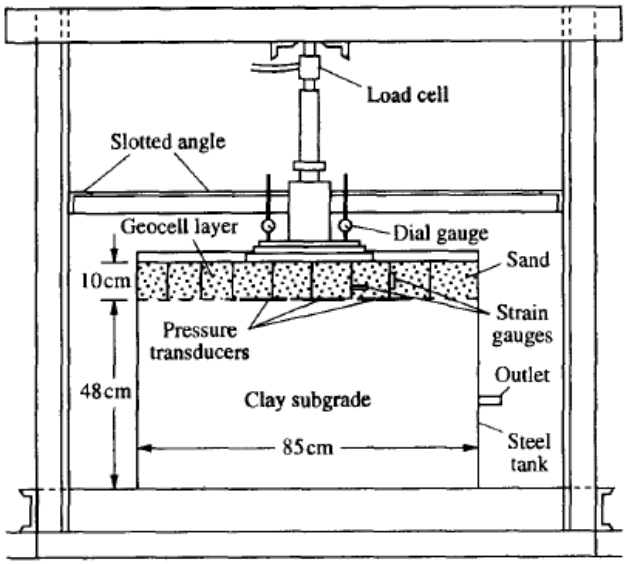

Fig. 2.13 Experimental set up prepared by Mhaiskar and Mandal (1996)

Koerner (1997) reported a case study on geocell-reinforced pavement filled with compacted sand over soft subgrade. A layer of emulsified asphalt was sprayed at the top of geocell-sand mattress. The pavement was tested under tandem-axle truck for 10,000 passes. The reinforced system resulted in slight rutting as compared to deep ruts occurred only after 10 passes over the unreinforced subgrade.

Krishnaswamy et al. (2000) conducted a series of model tests on geocell supported embankments constructed over soft clay having c_u = 20 kPa. The schematic of the test set up is presented in Fig. 2.14. Different uniaxial and biaxial geogrids were used for fabricating the geocells. The study revealed that the load carrying capacity was depended on the pocket size, height, and pattern of geocell formation, type of in-filled soil and the geogrid-stiffness.

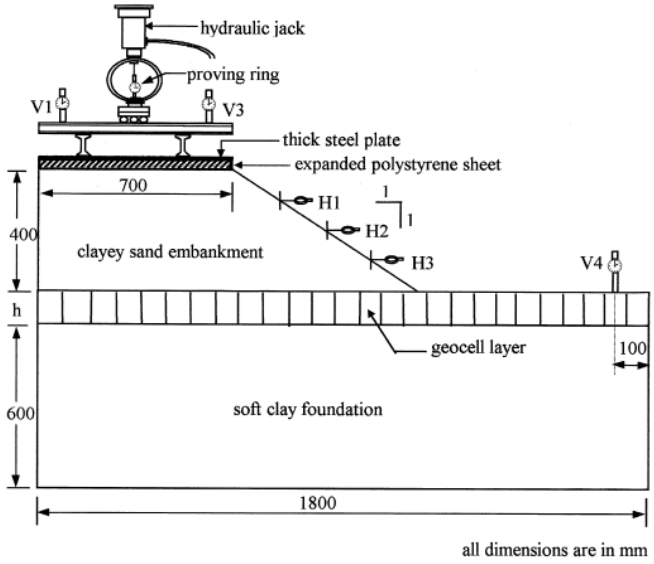

Fig. 2.14 Model test set up adopted by Krishnaswamy et al. (2000)

Dash et al. (2001a) conducted a detailed parametric study on geocell-reinforced foundations**.** Optimum values of various parameters, in terms of *B*, were reported as u = 0.1B, h = 3.14B, b = 12B, and d = 1.2B with a maximum 8-fold improvement in bearing capacity. In the testing program, no clear failure plane was observed till a settlement level of 50% of the footing-width. The study reported better performance of 'Chevron pattern' of geocell-formation, shown in Fig. 2.15, as compared to 'Diamond pattern'. About 30% further improvements in bearing capacity were reported with an additional planar geogrid at the bottom of the geocell-mattress (Dash et al., 2001b).

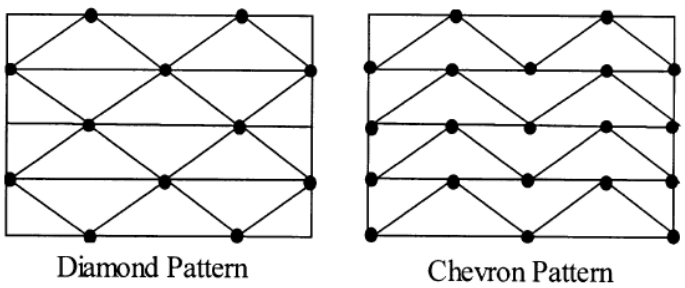

Fig. 2.15 Geocell formation patterns (after Dash et al., 2001a)

Dash et al. (2003a) investigated the effects of geocell-geometry and a base geogrid on the foundation behavior having a soft clay subgrade of 3.13 kPa (c_u). The

obtained results indicated maximum about 7-fold improvements in bearing capacity. The parametric optimums reported were: h = 1.68D, b = 5D and d = 0.8D. A comparative performance of different reinforcements, such as geocell, planar geogrid and randomly distributed mesh elements in uniform sand (with a constant D_r as 70%), under strip loading was investigated by Dash et al. (2004). The improvement in bearing capacity of the foundations having randomly distributed mesh elements was about twice that of the unreinforced bed; whereas, it was about 4-fold for the planar geogrid and 8-fold with geocell which was further enhanced by about 20% with a base geogrid. A detailed load-dispersion mechanism, shown in Fig. 2.16, was suggested by Dash et al. (2007) based on an instrumented study on strip footing supported by geocell-reinforced sand bed. Dash et al. (2008) studied the effect of height, width, and pocket size and embedment depth of the geocell layer on the subgrade modulus of geocell-reinforced sand foundations. The optimum values of u, b, h, and d were found to be 0.1, 12, 3.14, and 1.2 times B (footing width), respectively, to achieve the maximum improvement about 8.2-fold. It was further reported that the in-filled soil density (Dash, 2010) and aperture size with grid-orientation of geogrids for making the geocells (Dash, 2012) are also influences the foundation performance.

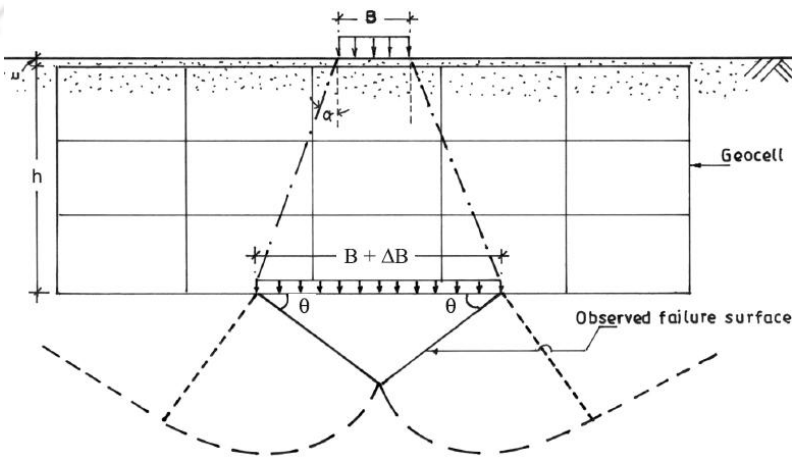

Fig. 2.16 Load-dispersion mechanism proposed by Dash et al. (2007)

Sitharam et al. (2005) investigated the performance of geocell-reinforced clay (c_u = 5.6 kPa) foundation system under circular footing. In this case, placing the footing directly over the geocell-mattress (i.e. u = 0) produced the optimum performance. Besides, an additional 20% improvement in bearing capacity was achieved with a base geogrid.

Emersleben and Mayer (2008) performed model tests on circular footing and compared the results with in-situ test on the geocell-reinforced subgrade (Fig. 2.17). A special type of soil, *Glyben*, was used to simulate the soft subgrade having c_u = 15 kPa. In model tests, about 1.5-fold improvement in bearing capacity and about 30% reduction in vertical stresses was noticed. The in-situ tests, such as 'vehicle crossing and vertical stress measurements' and 'falling weight deflectometer', showed reasonably good agreements with the model test results.

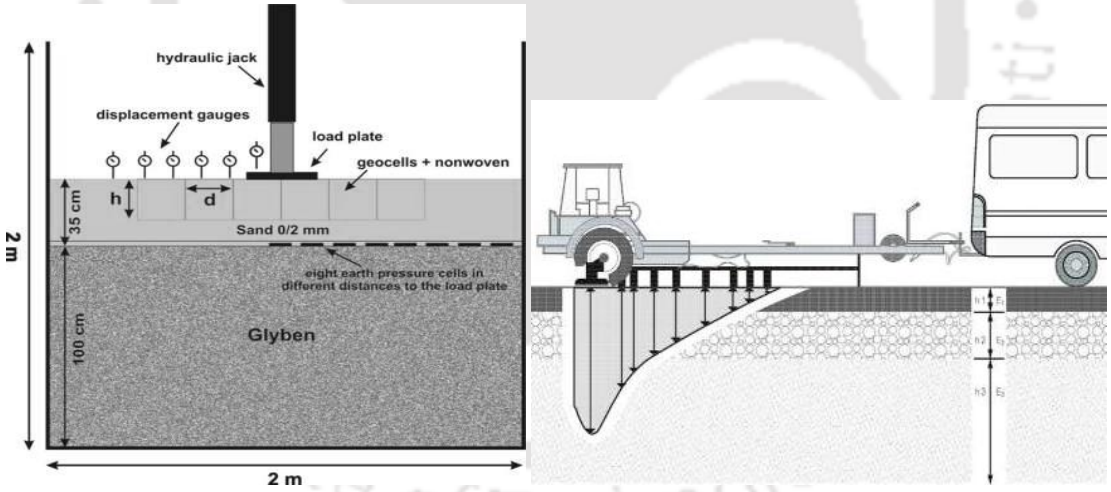

Fig. 2.17 Schematic of laboratory model test set up and in-situ test conducted by Emersleben and Mayer (2008)

Yoon et al. (2008) used 'Tire-cell' to reinforce the foundation system as shown in Fig. 2.18. The tire-cells were made of waste tire treads. The effects of cell-size, relative density of sand, the depth, and the number of reinforcement layers were considered in the investigation. The improvement in bearing capacity was found in the range of 3.2-3.4.

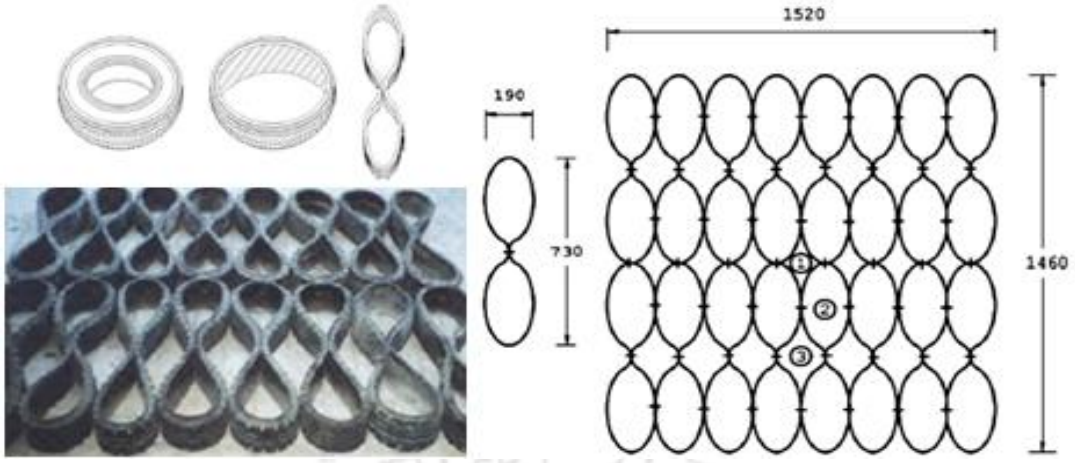

Fig. 2.18 Tire cells used by Yoon et al. (2008)

Sireesh et al. (2009b) investigated the benefits of providing the geocell-sand mattress in a foundation system having a void in the clay (c_u = 10 kPa) subgrade. The schematic foundation configuration is presented in Fig. 2.19. Substantial improvement in bearing capacity with increase in geocell-height and density of the in-filled soil were reported. It was found that the influence of the void became negligible having the geocells of height greater than 1.8*D*.

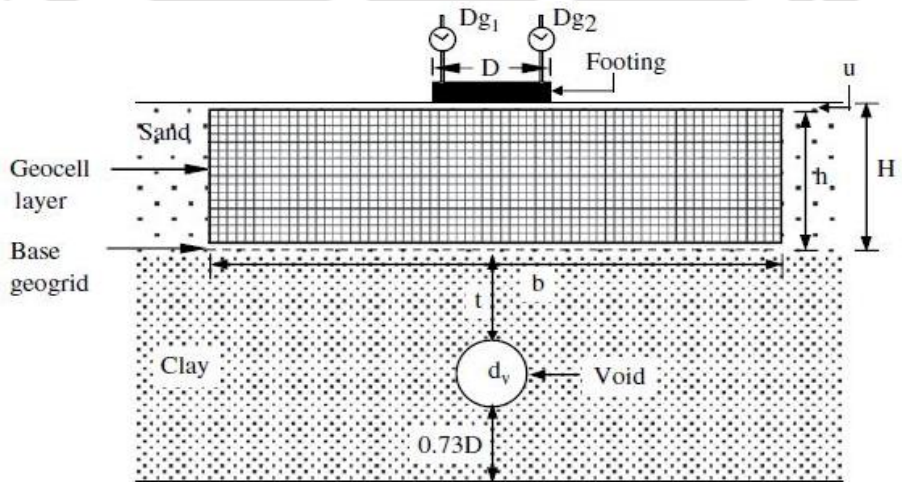

Fig. 2.19 Geometry of model tests used by Sireesh et al. (2009b)

Zhang et al. (2010) proposed a calculation method for the bearing capacity of geocell-reinforced foundations considering the lateral resistance, vertical stress dispersion, and membrane effect. The mechanisms defined are shown in Fig. 2.20.

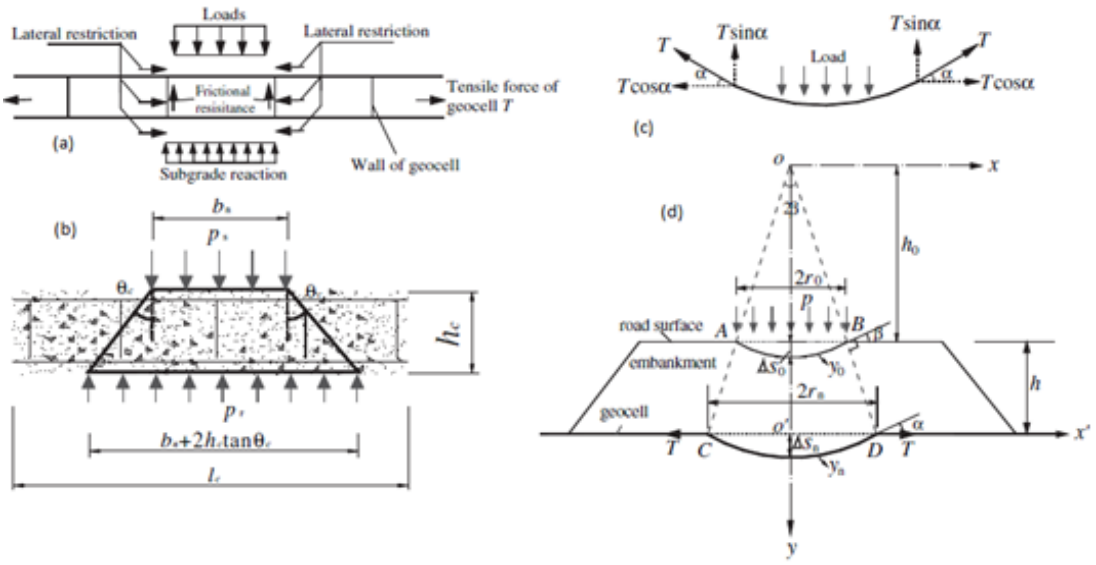

Fig. 2.20 Proposed bearing capacity calculation mechanisms (after Zhang et al. 2010)

Tafreshi and Dawson (2010) performed a comparative study on strip footings supported by geocell and geotextile-reinforced sand. About 3-fold improvements in bearing capacity was achieved. Besides, about 75% and 64% reduction in settlement for the geocell and geotextile reinforcements, respectively, were also reported.

Tanyu et al. (2013) has shown that geocells can reduce the plastic deflection of a working platforms by 30-50%; while, about 40-50% improvement in sub base resilient modulus and about 2 times improvement in subgrade reaction was reported.

Indraratna et al. (2014) reported that geocells influenced the sub-ballast behavior under cyclic loading. The effect is pronounced at low confining pressure under high frequency of loading.

2.4 CRITICAL APPRAISAL OF LITERATURE REVIEW

In general, use of reinforcements in any type indicated significant improvement in bearing capacity as compared to unreinforced cases. The reinforcing mechanism for planar reinforcement was defined as ‘membrane action’, dependent on the tensile strength, interface properties, the geometry of the reinforcement and the

strain generation at the reinforcement level (Guido et al., 1986; Love et al., 1987). The results reported have indicated that reinforcements with larger aperture size, such as geogrids, are better in load bearing than the geotextiles (Guido et al. 1986). Studies inferred that reinforcements placed beyond 2*D* (where '*D*' is the footing diameter) from footing bottom are not much effective; while, optimum width of the reinforcement was found as 6-8*D* (Fragaszy and Lawton, 1984; Omar et al., 1993; Huang and Tatsuoka, 1990; Sitharam and Sireesh, 2008). Researches' are revealed that improvement in bearing capacity, in the range of 2-4 folds, depends on relative stiffness of the fill-material as well as subgrade conditions. In general, soft clay subgrade having c_u < 20 kPa (mostly in the range of 3-10 kPa) or subgrades having loose to medium dense sand (D_r < 70%) were considered in the studies to investigate the reinforcement effects.

The studies with geocell-reinforcement proved to be better alternative to other traditional soil-strengthening techniques, in terms of improved bearing capacity and deformation characteristics, ease of construction and application, economy and environmental-perspective (Robertson and Gilchrist, 1987; Paul, 1988; Hendricker et al., 1998; Palmeira et al., 2008). Higher improvements, as compared to the planar or randomly oriented reinforcement, were noticed for geocell reinforcement. In general, about 6-8 fold improvements in bearing capacity and about 30-50% reduction in settlement were reported. It was observed that performance of the foundation systems increases with geocell height and width. However, the improvement was marginal for $h > 1.5D$ and $b > 6D$. The performance was decreased with increase in geocell-pocket size (d). The optimum placement depth (u) of the geocell-mattress was found to be 0.1-0.3*D* below the footing. Similarly as the planar reinforced foundations, mostly

softer clay subgrade having c_u in the range of 3-15 kPa and loose to medium dense sand having relative density less than 70% were considered for geocell-systems.

A wide range of research has been reviewed on planar and geocell reinforced soil with various types of foundation configurations. The effects of various parameters including relative density of the filled materials are examined in detail by many researchers. Most of researches, reported so far on reinforced clay foundations, are focused on improving the 'soft soil' (c_u < 15 kPa) by varying parameters such as reinforcement-geometry, placement depth, and filled materials etc. However, as per the review of literature, it is yet to be investigated on the ground of varying subgrade strength, specially when the clay is considered. Further, in practice, situations may arise where reasonably strong soil may also fail to meet the design requirements. Thus, owing to difficulties in choosing and understanding the methods of analysis and design under such situations, the behavior of reinforced soil should be investigated for varying subgrades.

2.5 OBJECTIVE AND SCOPE OF THE PRESENT STUDY

The present study aimed for developing an understanding of the performance of different geosynthetic-reinforced foundations with clay subgrades of varying strengths. Different foundation systems are considered, in homogeneous and layered configurations overlying a wide range of subsoil strengths, from very soft to stiff, by varying the undrained shear strengths (c_u) of clay. The layered foundations are consisted of unreinforced and reinforced sand layer of varying depths from the footing bottom. Different types and combinations of reinforcement are considered, in the form of planar geogrid, three dimensional geocells and a combination of the both (geocell-geogrid). The obtained results are analyzed to understand the foundation behavior under varying subgrade strength.

The objective of the present study is achieved through several steps in terms of different series of physical model tests of varying foundation configurations. The test series are designed in such a way that the influence of each parameter varied can be evaluated. The followings are the detailed scope of the present study for achieving the objective.

- A series of tests will be performed on homogeneous clay beds of different undrained shear strengths under the circular footing. Test on the dense sand bed at adopted relative density will also be performed in this series. These tests results will be used further in evaluating and analyzing the foundation behavior with unreinforced or reinforced sand layers of varying thickness overlying the clay subgrades of different strengths.
- A series of model tests on unreinforced layered foundations having sand layer of different thickness overlying clay subgrades of varying strengths will be performed. The foundation behavior obtained from this test series will be analyzed with that of corresponding homogeneous responses. The results will be used further test series in evaluating the contribution of the individual reinforcements in foundation performances in line to the parameters varied.
- Foundations with different reinforced-configurations such as geogrid, geocell, and geocell-geogrid, overlying the clay subgrades of varying strengths will be performed in next stage. In reinforced foundation systems, thicknesses of reinforced-soil layers will be varied in similar way as the unreinforced cases to evaluate the reinforcement effects in similar configurations keeping the relative density of sand constant. The parameters such as, placement depth and geometry of the reinforcements will be kept constant, except the reinforced-sand layer thickness. The results obtained from these tests will be compared with the

responses of corresponding homogeneous clay bed and unreinforced layered foundations.

- For the design implication of the study, a regression analysis will be performed to correlate the foundation behaviors, in terms of bearing pressures, with respect to different influencing parameters. In regression models, bearing pressures of different foundation systems will be expressed as the function of the subgrade strength, layer thickness, and levels of footing settlement. A detailed design application of the regression equations will also be illustrated.

2.6 SUMMARY

The chapter presented the brief literature review in context to the present study. Discussions on selected studies on homogeneous, unreinforced, and reinforced layered foundations are presented. Critical appraisal of the literature reviewed was presented highlighting the importance of subgrade strength and need for the study. The chapter is concluded with objective and detailed scope of the present study.

Chapter 3. MATERIALS AND METHODOLOGY

3.1 INTRODUCTION

A methodology of conducting physical model tests, on different foundation configurations with varying subgrades, was adopted to achieve the objective. Tests were performed on foundation systems having different unreinforced and reinforced configurations. The soils used in the experimental program were sand (filling material) and clay (subgrade soil). Different forms of reinforcements, viz. planar geogrid, geocell, and geocell-geogrid (made of a biaxial geogrid), were considered in the study. Details of the test materials and their characterization are presented in this chapter. Besides, preparation of the foundations, planning of experiments, and testing methodology are described in detail.

3.2 MATERIALS USED

A typical geosynthetic-reinforced foundation system adopted for this study is shown in Fig. 3.1. It consist two types of soils: Type-1, the fill-soil and Type-2, the native soil underneath. In practice, geocell pockets are generally filled with granular soil, such as sand or gravel, having better drainage property and reinforcement interaction behavior. The Type-2 soil can be of clay or sand at different state of strength levels. For the present study, clay subgrades (Type-2) were consisted of locally available red soil. The layers above the subgrades and the pockets of the geocells were filled with river sand (Type-1). A biaxial geogrid was used as the planar form of reinforcement, as well as, to prepare the geocell-mattress using bodkin joints (Simac, 1990; Carroll and Curtis, 1990).

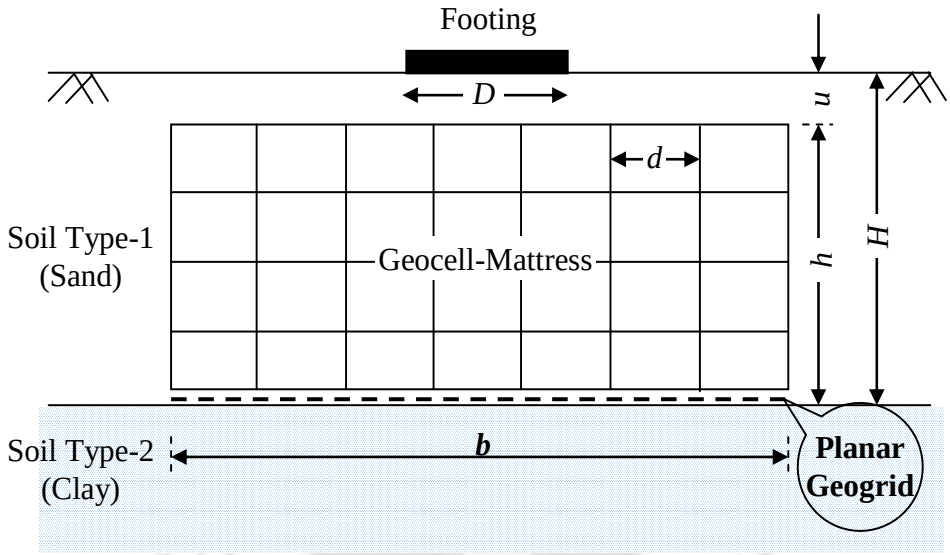

Fig. 3.1 Schematic configuration of geosynthetic-reinforced foundation system

3.2.1 Clay

A locally available clay soil was used to prepare the clay subgrades. Specific gravity (G) of the soil was found as 2.65 according to ASTM D0854-06. Wet sieve (ASTM D6913-04) and hydrometer analysis (ASTM D4221-05) were performed to determine particle size distribution of the clay which is presented in Fig. 3.2. The clay had 70% fines (< 75 micron). The values of liquid and plastic limits were determined as 42% and 21%, respectively (ASTM D4318-05). The maximum dry unit weight and optimum moisture content (OMC) of the soil were determined as 17.31 kN/m^3 and 19.7%, respectively, by standard proctor compaction test (ASTM D698-12). The compaction curve is shown in Fig. 3.3. As per Unified Soil Classification System (USCS; ASTM D2487-11), the soil is classified as clay with low plasticity (*CL*).

For preparing the clay beds with different subgrade strengths, calibration curves were obtained by conducting several trials. The compactive effort, bulk density and water content of the clay for the desired shear strength were estimated before, through several trials, by preparing clay samples in mini-compaction device and a comparatively smaller steel tank of about 40 cm diameter. The clay samples from the tank were collected by the vane shear mould by inserting it into the clay beds, keeping

the bottom hole open to avoid air-locking. The mould was removed from the clay bed by digging the clay around the mould and cut it from the bottom. The shear strength of the collected clay samples were determined in vane shear apparatus along with the bulk density and moisture content. The curves presented in Fig. 3.4 are showing the variation in undrained shear strength (c_u) and bulk unit weight (γ_b) with the corresponding water contents (w).

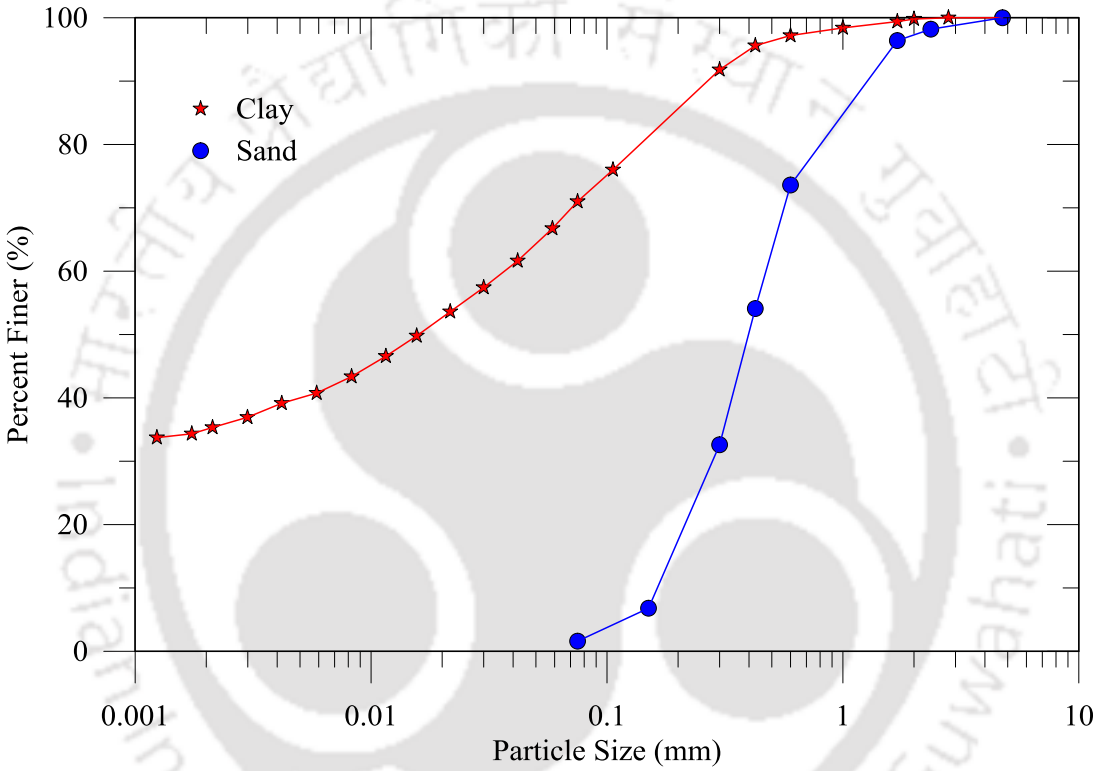

Fig. 3.2 Particle size distribution curves of soils (Clay and Sand)

3.2.2 Sand

A local river sand was used for preparing foundation layers over the clay subgrades and for filling the pockets of the geocell-mattress. Specific gravity (G) of the sand was determined as 2.68 (ASTM D0854-06). Sieve analysis (ASTM D6913-04) was conducted for grain size distribution of the sand that is shown in Fig. 3.2. The coefficient of uniformity (C_u) and coefficient of curvature (C_c) of the sandy soil were evaluated as 3.06 and 0.62, respectively. The maximum ($\gamma_{d,max}$) (ASTM D4253-06) and minimum ($\gamma_{d,min}$) (ASTM D4254-06) dry unit weights of the sand were

determined as 16.43 kN/m^3 and 13.82 kN/m^3, respectively. The sand is classified as poorly graded with letter symbol '*SP*' as per ASTM D2487-11. Relative density (D_r) of the sand was maintained at 80% (γ_d = 15.83 kN/m^3) throughout the test program. The shear strength parameters of sand, corresponding to D_r = 80%, were determined by both direct shear (ASTM D6528-07) and triaxial compression tests (ASTM D2850-07). The responses obtained from standard triaxial compression tests on the dry sand samples are presented in Fig. 3.5. The stress-strain responses obtained from direct shear tests is presented in Fig. 3.6. The peak friction angle (φ) obtained from direct shear and triaxial compression tests were 43° and 40°, respectively. The values of the residual friction angle obtained from direct shear and triaxial compression test are 34° and 28°, respectively. The dilation angle (ψ) as 18° was determined from direct shear test responses, as the peak slope of vertical to horizontal deformation response (Gibson, 1953), as presented in Fig. 3.7.

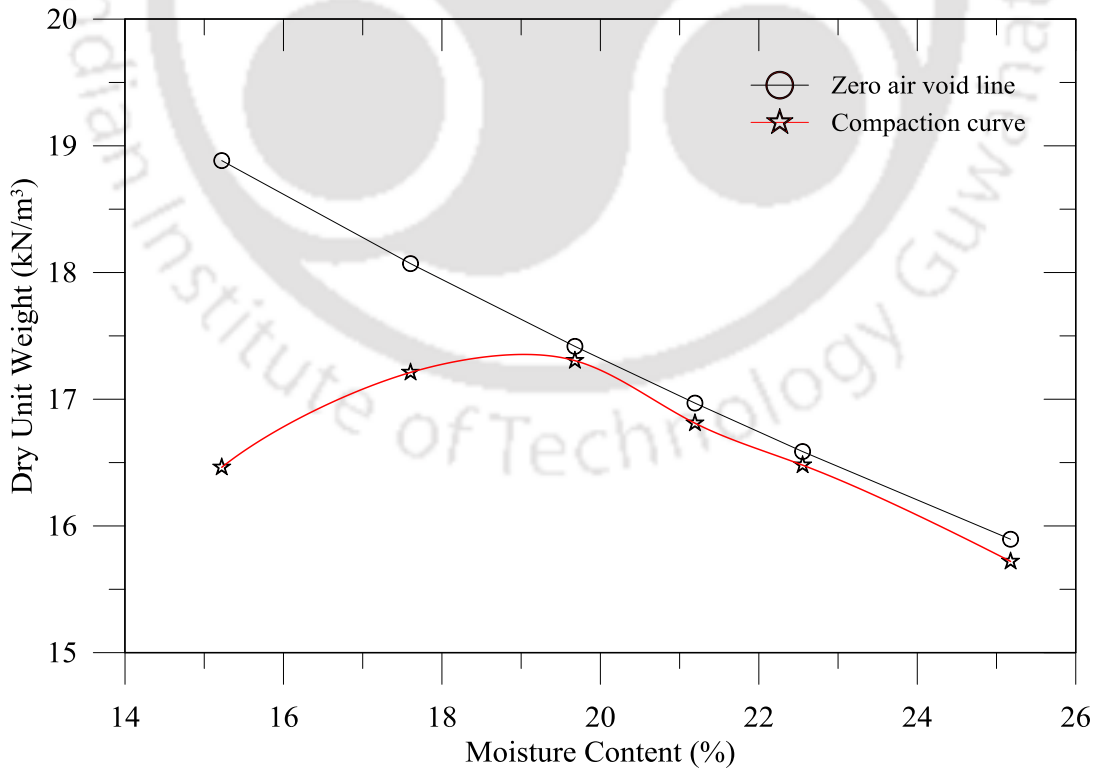

Fig. 3.3 Clay compaction curve

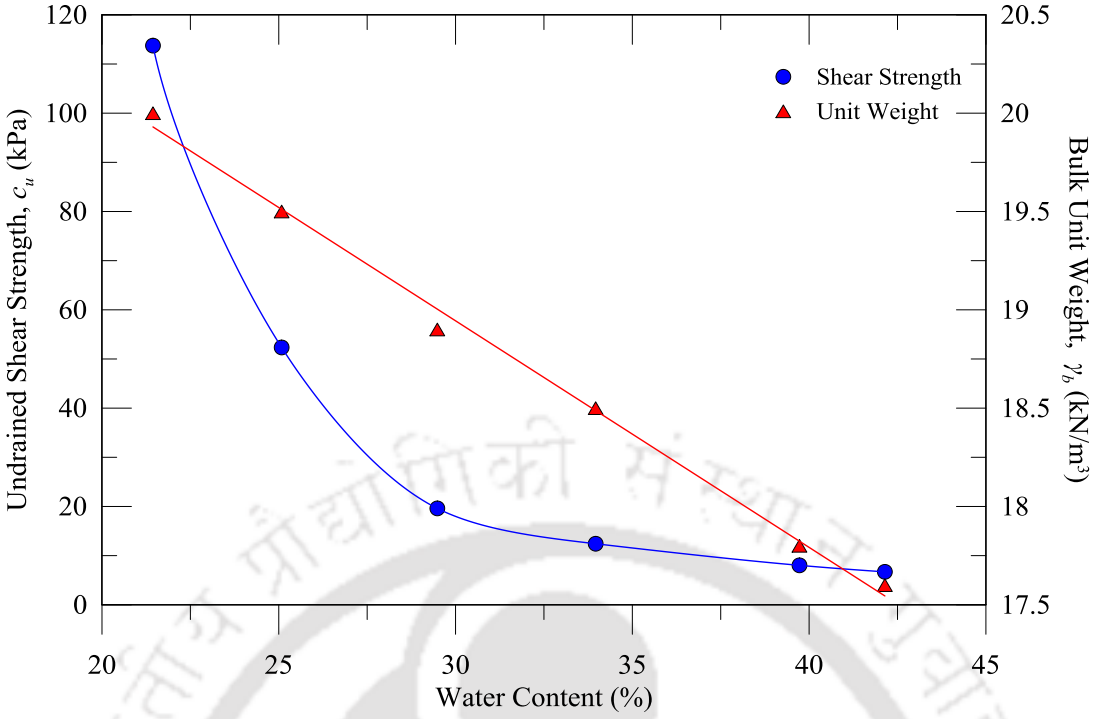

Fig. 3.4 Calibration curves for clay

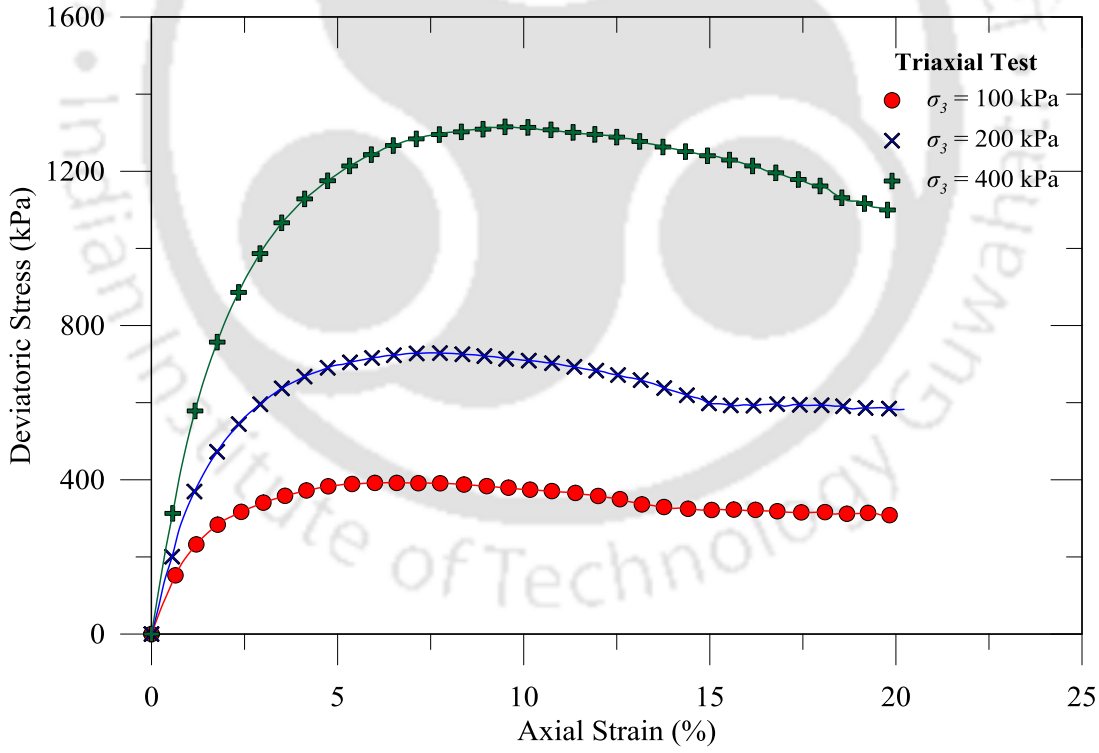

Fig. 3.5 Response of sand (D_r = 80%) in triaxial compression test

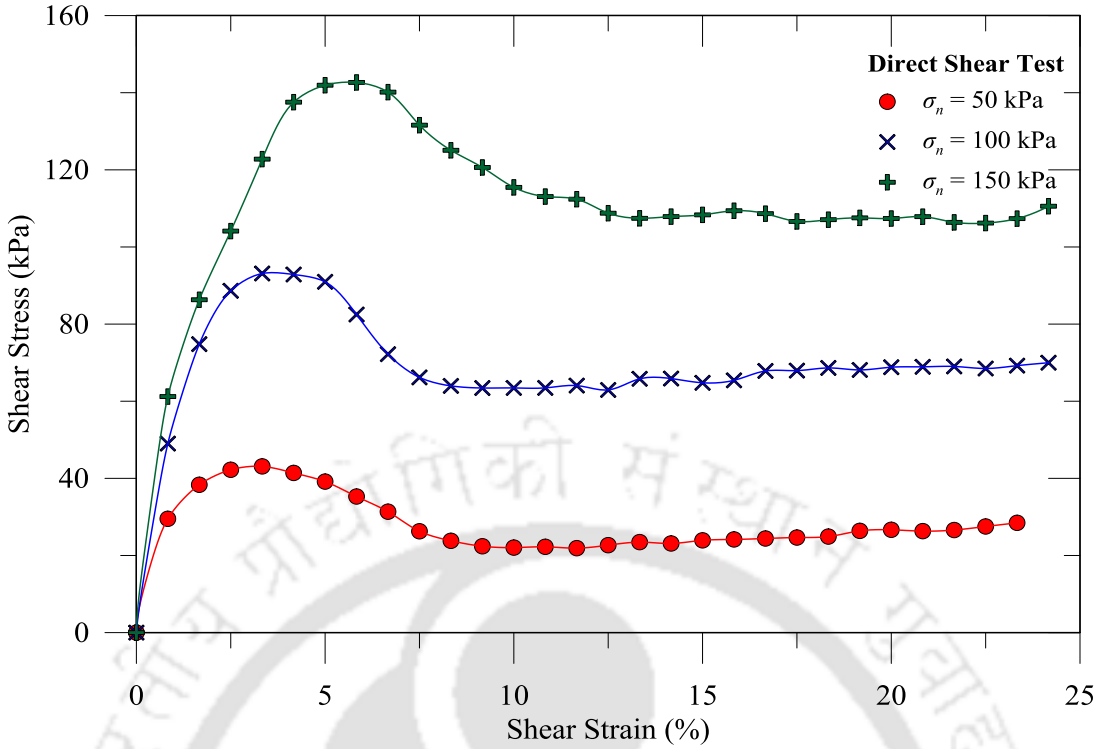

Fig. 3.6 Shear stress-strain response of sand (D_r = 80%) in direct shear test

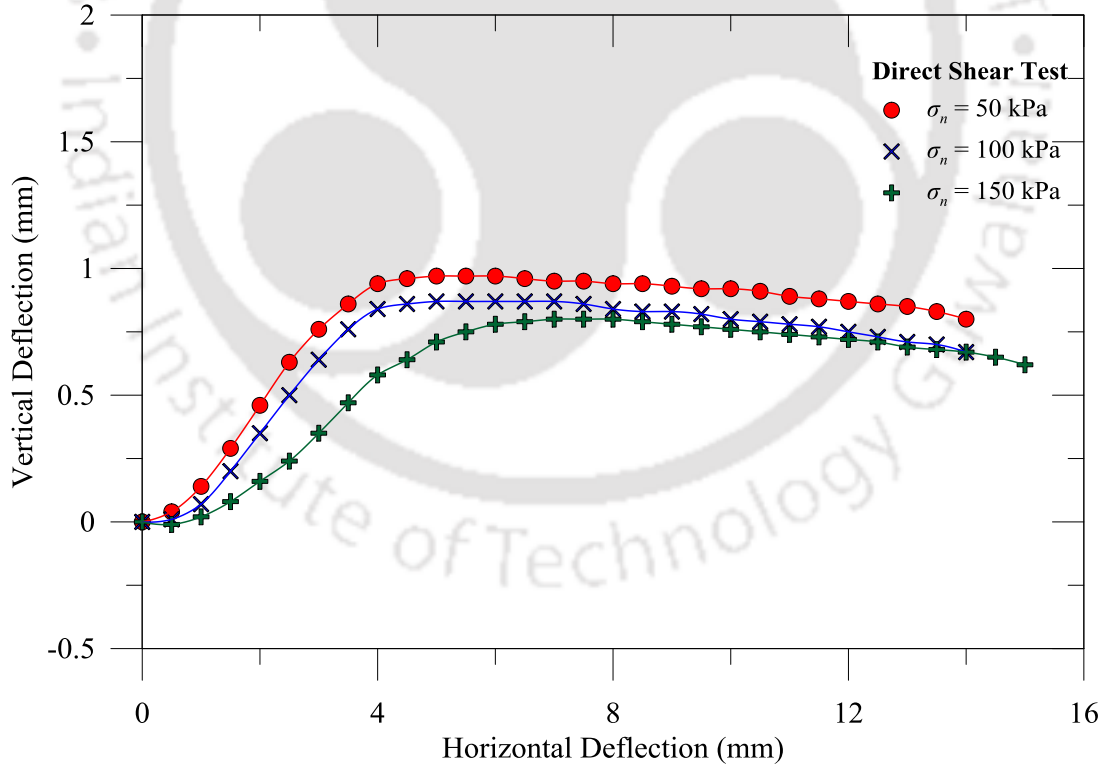

Fig. 3.7 Dilation behavior of sand (D_r = 80%) in direct shear test

3.2.3 Geogrid and Geocell

A biaxial geogrid, made of high density polyethylene (HDPE), having square apertures of 38 mm × 38 mm, was used as planar geogrid and for preparing the geocell-mattress. Tensile strength test was conducted as per ASTM D6637-09 and the response is shown in Fig. 3.8. The maximum tensile strength of the geogrid was obtained as 20 kN/m corresponding to 11% of axial strain.

Geocell preparation

To prepare the geocell-mattress, geogrid pieces were cut from a long roll into required dimensions and assembled in 'Chevron' pattern (Bush et al., 1990) using 'Bodkin' joints (Fig. 3.9). As per the adopted geocell-pocket size (d = 0.8D), thicknesses of the geocell-mattresses (h = 0.53, 1.05, 1.57, and 2.09D) and the tank size (1 m × 1 m), the required dimensions (length and widths) and numbers of the geogrid members were calculated. The targeted numbers of longitudinal and transverse members for the geocell mattress were 10 and 9, respectively, which were constant throughout the study. The lengths of the geogrid members were calculated keeping a clear cover of about 50 mm at each sides of the tank to avoid boundary effects. The length of each longitudinal and transverse members were approximately 912 mm and 1862 mm, respectively; while, the widths of the geogrid cut-pieces were as per the adopted thickness of the geocell-mattress as presented in the Table 3.1.

Geocell-joints were formed by pulling the ribs of the transverse geogrids through the longitudinal geogrid and inserting a dowel through the loop created (Rai, 2010). The bodkin-dowels were 3 mm thick and 6 mm wide plastic strips, cut from low-density polymer sheet. Tensile strength of the bodkin joints was determined as 3.3 kN/m at 9% axial strain (as per ASTM D6637-09) and result obtained is shown in Fig. 3.10. All the materials properties are summarized in Table 3.2

Table 3.1 Average width of the geogrid members

Width of the geogrid members			
$h = 0.53D$	$h = 1.05D$	$h = 1.57D$	$h = 2.09D$
80 mm	158 mm	235 mm	314 mm

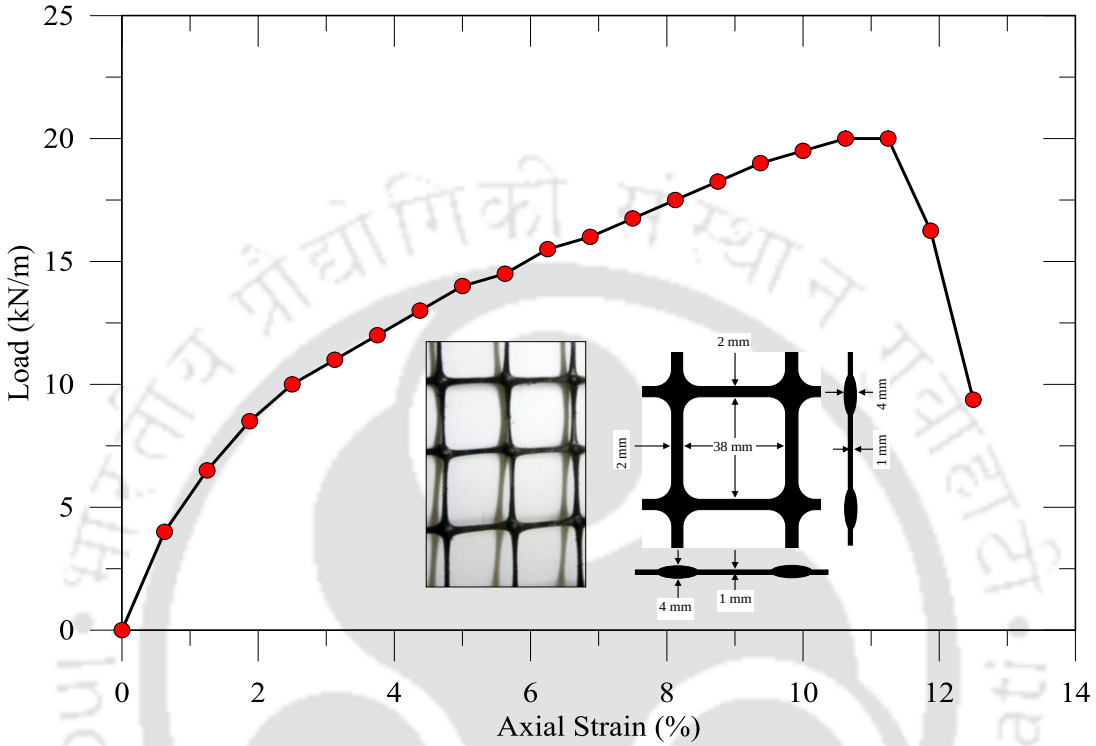

Fig. 3.8 Load-strain behavior of biaxial geogrid

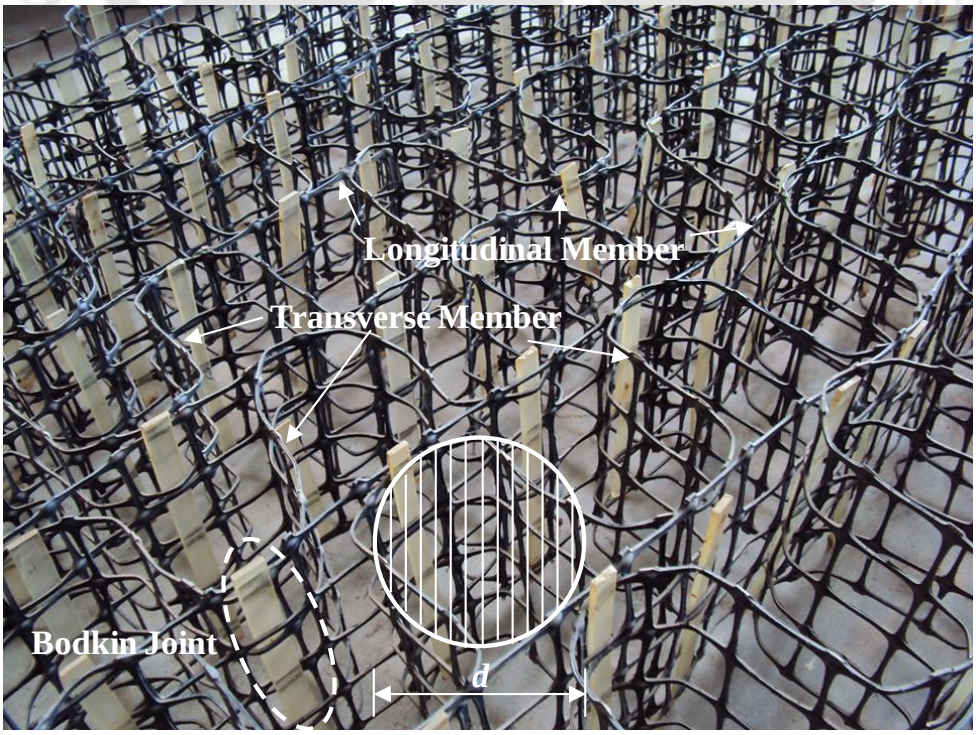

Fig. 3.9 Photograph of typical geocell-mattress in chevron pattern

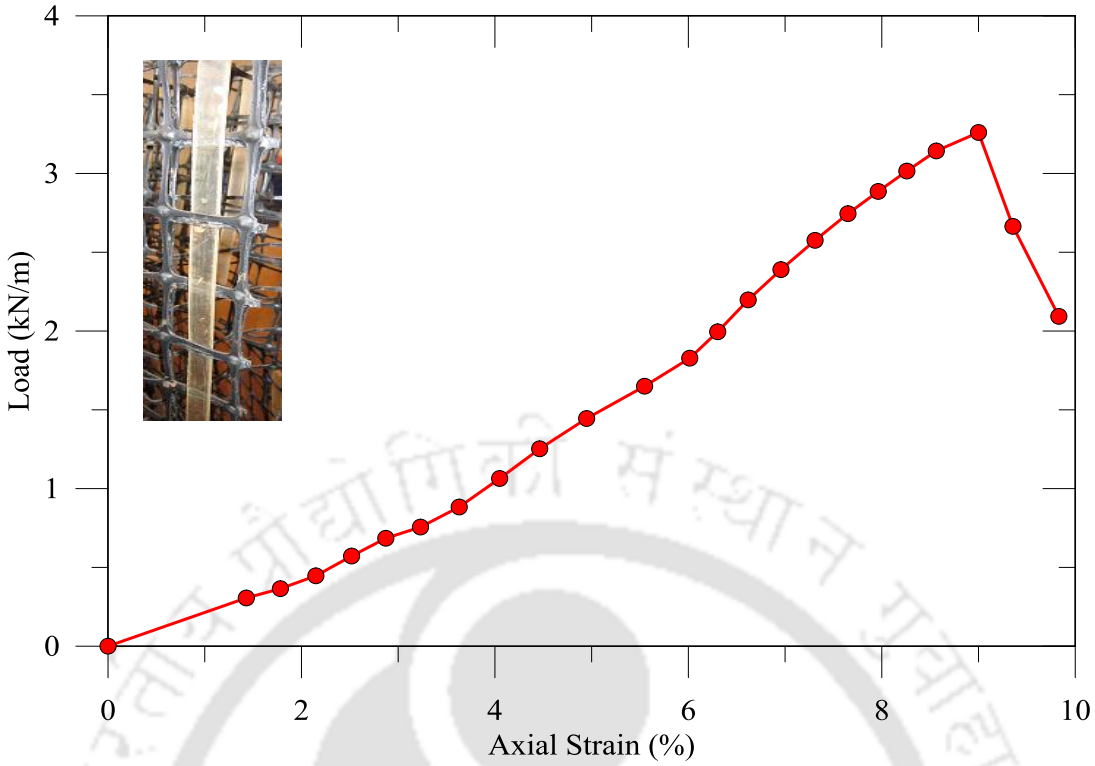

Fig. 3.10 Load-deformation behavior of bodkin joint

Table 3.2 Material properties

Materials	Material Properties		Values
Clay (*CL*)	Specific Gravity (*G*)		2.65
	Liquid Limit (%)		42
	Plastic Limit (%)		21
	Max. unit weight (kN/m^3)		17.31
	OMC (%)		19.7
Sand (*SP*)	Specfic Gravity (*G*)		2.68
	Uniformity Coefficient (C_u)		3.06
	Coefficient of Curvature (C_c)		0.62
	γ_d (kN/m^3)	Maximum	16.43
		Minimum	13.82
	Friction angle (φ°)	Direct Shear Test	43
		Triaxial Test	40
	Dilation angle (ψ°)		18
Geogrid/Geocell	Aperture size (mm)		38 × 38
	Tensile strength (kN/m)	Geogrid	20
		Bodkin Joint	3.3
	Failure strain (%)	Geogrid	11
		Bodkin Joint	9
	Interfacial friction angle (δ_s) (pull-out test; Rai, 2010)		30°

3.3 DETAILS OF TESTING PROGRAM

In the experimental study, tests were conducted on a rigid circular model footing (18 mm thick steel plate) having 150 mm diameter (D) placed on foundation beds of different configurations (homogeneous and layered). Foundation beds were prepared in a steel tank having dimensions of 1 m × 1 m × 1 m. The homogeneous beds were prepared with clay of different undrained shear strengths (c_u) and sand at dense condition (D_r = 80%). Layered foundations were configured with clay subgrades of different strengths overlying by unreinforced and/or reinforced sand of different layer thicknesses (H).

The experimental program was designed under various test series to investigate the influence of different foundation systems. In the study, tests were conducted on different homogeneous and layered configurations (unreinforced and reinforced) of foundations having varying clay subgrades under circular footing, as shown in Table 3.3. In each series, only one parameter was varied keeping the others constant. In the testing program, the subgrade strength (c_u) and layer thicknesses (H) were varied while the other parameters (as shown in Fig. 3.1) were kept constant as per optimum values reported in the literature. The variables in the study, i.e. heights of the geocells (h) were varied as 0.53, 1.05, 1.57, and 2.09D; while, the subgrade clay strengths (c_u) were considered as 7, 15, 30, and 60 kPa.

As per Chummar (1972), for a strip footing of width B in dense sand, the failure wedge is likely to be extended about 3B (maximum) distance on either side of the footing and up to a depth of about 1.1B from the footing bottom. Hence, for present study, the foundation bed width (1.0 m) of 6.67 times the footing diameter (D) can be considered large enough to avoid the boundary effects. The width of the planar geogrid and geocell-mattress were kept constant at 6D according to the reported

optimum range of values (Das and Omar, 1994; Dash et al., 2001a). The 'Chevron' pattern (Fig. 2.15) was adopted for formation of the geocell-mattress (Bush et al., 1990; Dash et al., 2001a; Rai, 2010). The geocell-pocket size was considered as the diameter (d) of an equivalent circular area as shown in Fig. 3.9. It was suggested that for higher performance, the pocket size should be less than the footing size and the footing should, at least, cover a full pocket opening. In this study, the pocket-size of the geocell-mattress was considered as 0.8D which was also adopted by Dash et al. (2001a; 2003b), Sireesh et al. (2007, 2009), Rai (2010). A sand cushion (u) of 0.1D thick was provided in between the footing and geocell-mattress to prevent early buckling in geocell-walls from direct-loading and uniform distribution of footing load (Dash et al., 2001a). Dash (2010) and Pokharel et al. (2010) have observed that the influence of reinforcement in improving bearing capacity is more in case of dense soil condition. Therefore, the sand layer was kept at dense state, i.e. at 80% relative density (D_r) by maintaining the unit weight at 15.83 kN/m^3.

Table 3.3 Details of laboratory model tests

Test Series	Types of Foundation System	Test Parameters		No. of Tests
		Variables	Constants	
A	Homogeneous clay and sand bed	c_u = 7, 15, 30, and 60 kPa D_r = 80% (Sand)	-	5
B	Unreinforced sand layers overlying clay subgrades	c_u = 7, 15, 30, and 60 kPa H/D = 0.63, 1.15, 1.67, 2.19	D_r = 80%	16
C	Sand beds overlying clay subgrades with planar geogrid at the interface	c_u = 7, 15, 30, and 60 kPa H/D = 0.63, 1.15, 1.67, 2.19	D_r = 80% b/D = 6	16
D	Geocell-reinforced sand layers overlying clay subgrades	c_u = 7, 15, 30, and 60 kPa h/D = 0.53, 1.05, 1.57, 2.09	D_r = 80% u = 0.1D, d/D = 0.8, b/D = 6	16
E	Geocell-geogrid reinforced sand layers overlying clay subgrades	c_u = 7, 15, 30 and 60 kPa h/D = 0.53, 1.05, 1.57, 2.09	D_r = 80% u = 0.1D, d/D = 0.8, b/D = 6	16

Total 69 tests were performed in five different test series (series A to E). One homogeneous and four layered configurations were considered in order to evaluate the contribution of each parameter varied. The dimensional parameters, such as sand layer thicknesses (H), height (h) and width (b) of the geocell-mattress, and thickness of the sand cushion (u) are reported in non-dimensional form as H/D, h/D, b/D, and u/D, respectively.

In test series A, responses of the model footing on homogeneous beds of clay having different undrained shear strength (c_u = 7, 15, 30, and 60 kPa) and sand bed at dense state (D_r = 80%) were investigated. Tests on layered foundations having different thicknesses of unreinforced sand overlying the clay subgrades of varying strengths were performed in series B. In this series, thicknesses (H) of unreinforced sand were varied as 0.63, 1.15, 1.67, and 2.19D. In similar layered configurations, the influence of a planar geogrid, placed at sand-clay interface, was investigated in series C. In series D, influence of subgrade strength on the performance of geocell-reinforced foundation systems was investigated. The geocell-heights (h) were varied as 0.53, 1.05, 1.57, and 2.09D keeping other parameters constants as u = 0.1D, b = 6D, d = 0.8D and the 'Chevron' pattern of geocell-formation. The influence of an additional planar geogrid, placed at the bottom of the geocell-sand mattress overlying different clay subgrades, were investigated in series E, keeping other test parameters as in series D.

3.4 TEST DESCRIPTION

3.4.1 Test Set-up and Instrumentation

A photograph of the experimental set up is shown in Fig. 3.11. Foundation beds were prepared in a steel tank having dimensions of 1 m × 1 m × 1 m. The tank walls were braced horizontally and vertically with heavy steel-sections to avoid lateral

deformation, during preparation of the foundation beds and testing. The test tank was provided with a loading frame to facilitate load application. The load was applied through a manually operated hydraulic jack of 100 kN capacity. A pre-calibrated proving ring was used, in between the hydraulic jack and the footing, to measure the magnitude of the load transferred. A ball-bearing was positioned between the proving ring and the footing to ensure the verticality of the applied load.

Fig. 3.11 The photograph of the experimental set up

Responses of the model foundations were monitored at different loading stages by recording the deformations (heave or settlement) at different locations on the foundation surface through eight dial gauges (D_{g1} to D_{g8} shown in Fig. 3.12) of 0.01 mm accuracy. Two dial gauges were placed diagonally opposite to each other over the footing (D_{g4} and D_{g5}) to measure the footing settlement. The other dial

gauges were placed at distances *D*, 2*D*, and 3*D*, from the center and on either side of the footing. The dial gauges were fixed through nut and bolt arrangements to a reference beam which was connected to the loading frame. The spindles of the dial gauges were rested over small plates of Perspex sheet placed on the foundation surface.

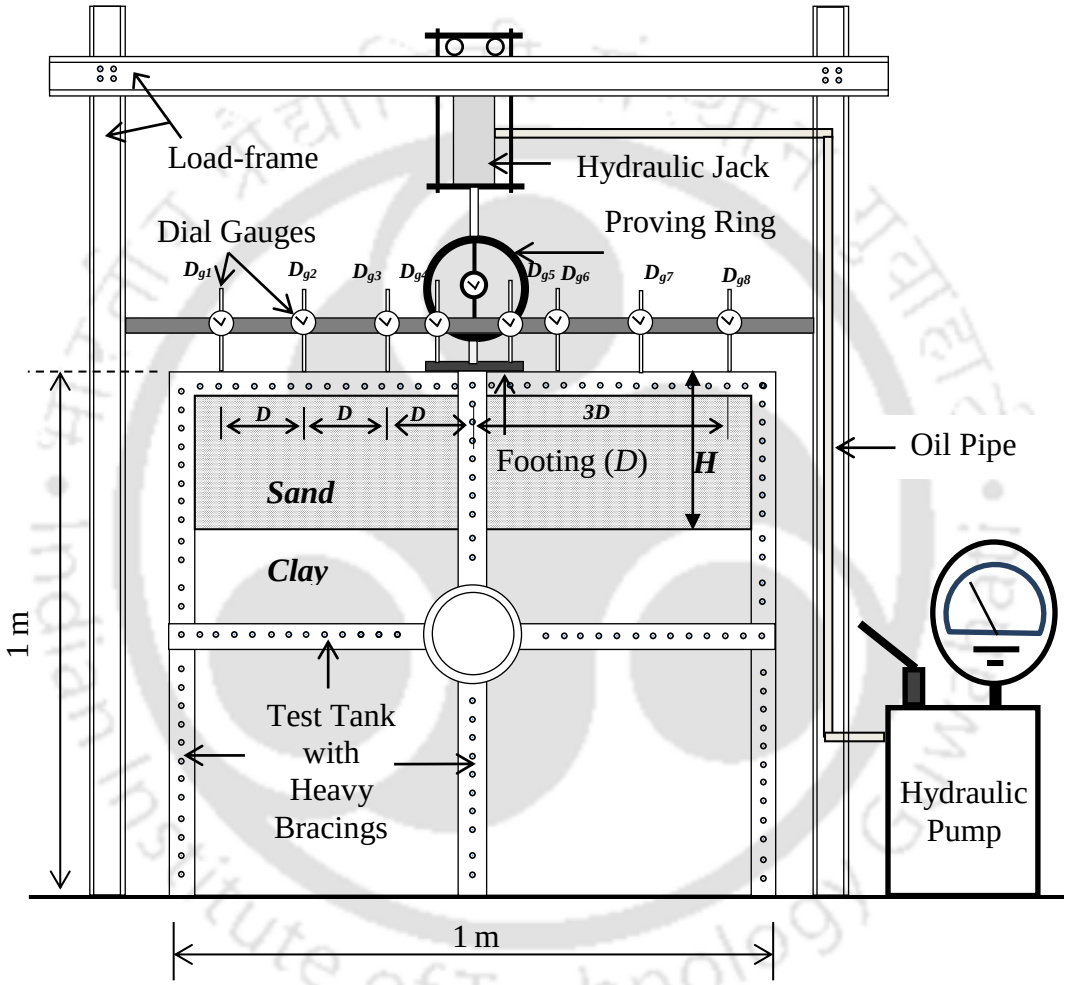

Fig. 3.12 Schematic diagram of the experimental set up

3.4.2 Test Bed Preparation

The foundation beds were prepared in two stages; (1) preparation of clay subgrade and (2) preparation of sand beds (unreinforced and reinforced) over the clay subgrades.

Preparation of clay beds/subgrades

Different clay subgrades of varying strength were prepared in the laboratory with the help of calibration curves presented in Fig. 3.4. Four shear strengths (c_u = 7, 15, 30, and 60 kPa) were selected for the present study. The required water content and bulk densities corresponding to the desired shear strengths were obtained from the calibration curves, as presented in Table 3.4. To prepare a clay bed/subgrade of desired shear strength, the soil was pulverized, air dried, and checked for initial water content. The additional water required for that strength was added (as per the calibration curve) and mixed thoroughly. To achieve moisture equilibrium, the mixed soil was kept in sealed containers for a week before it was used for test-bed preparation. The clay beds of different water content and bulk densities were prepared in the test tank in layers of approximately 50 mm thick by uniform compactive efforts. The soil-layers were compacted by a rammer, dropping from a fixed height over a plywood board placed at the clay surface, to get uniform compaction for entire clay bed. However, the compactive efforts were different (with the change in number of blows) for different clay beds. About 23, 68, 90, and 135 kJ/m^3 of compactive efforts were adopted for clay beds having c_u = 7, 15, 30 and 60 kPa, respectively.

Thus, by controlling water content and maintaining uniform compaction, fairly uniform clay beds/subgrades were prepared (until the desired depth was reached) and maintained throughout the experimental program. In order to verify the clay consistency, samples from different locations of the test beds were collected to check unit weight, moisture content, and undrained shear strength (vane shear test). The variations of these data is presented in Fig. 3.13 which were found to be within a range of ±3%, indicating consistent test conditions.

Table 3.4 Properties of clay beds

Parameters	Undrained Shear Strengths			
	c_u = 7 kPa	c_u = 15 kPa	c_u = 30 kPa	c_u = 60 kPa
Unit Weight (kN/m^3)	17.6	18.8	19.25	19.6
Moisture Content (%)	41	31	27.5	24.5
Degree of Saturation, *S* (%)	100	100	100	99.7

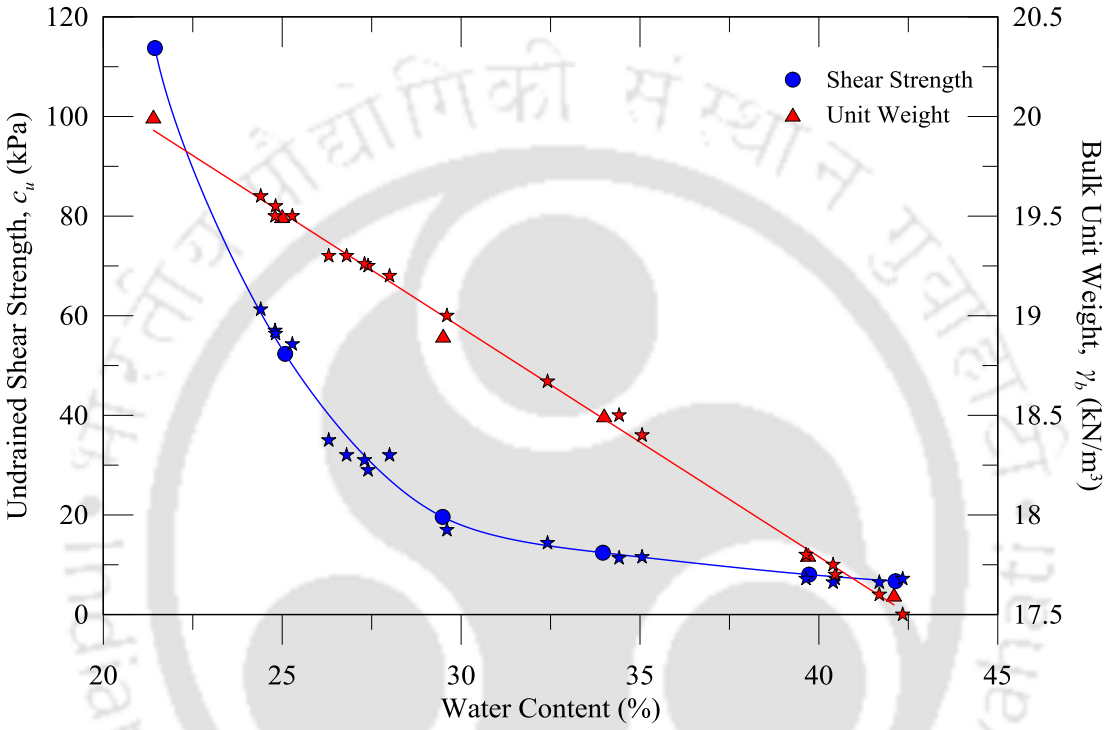

Fig. 3.13 Scattering of shear strength and unit weight of clay with water content

Preparation of sand beds

Sand beds were prepared through pluviation technique. Photograph and schematic diagram of the sand raining device are shown in Fig. 3.14. It is an assembly of a large hopper (sand container) and a long hollow pipe having a 60° inverted cone connected at the bottom. A calibration curve was obtained through several trial tests to establish a relation between the height of fall and the achieved relative density (%). The calibration curve for sand bed preparation is shown in Fig. 3.15. The figure also presents calibration curve for a case when geocell was placed. It can be observed from

the figure that the height of fall for achieving 80% relative density are 300 mm and 400 mm for the case without and with geocell reinforcement.

For the unreinforced layered foundation systems, the clay subgrades were prepared up to the desired level of the test tank and sand pluviation was continued until the full height of the test bed. For the reinforced foundation systems, sand raining was started after placing the reinforcement (geogrid or geocell) directly on the clay subgrade. Uniformity of the sand bed preparation was checked by collecting regular samples in small containers during the preparation. Variation in the relative density of the sand was within a range of ± 2%. Photograph of a prepared test bed is shown in Fig. 3.16.

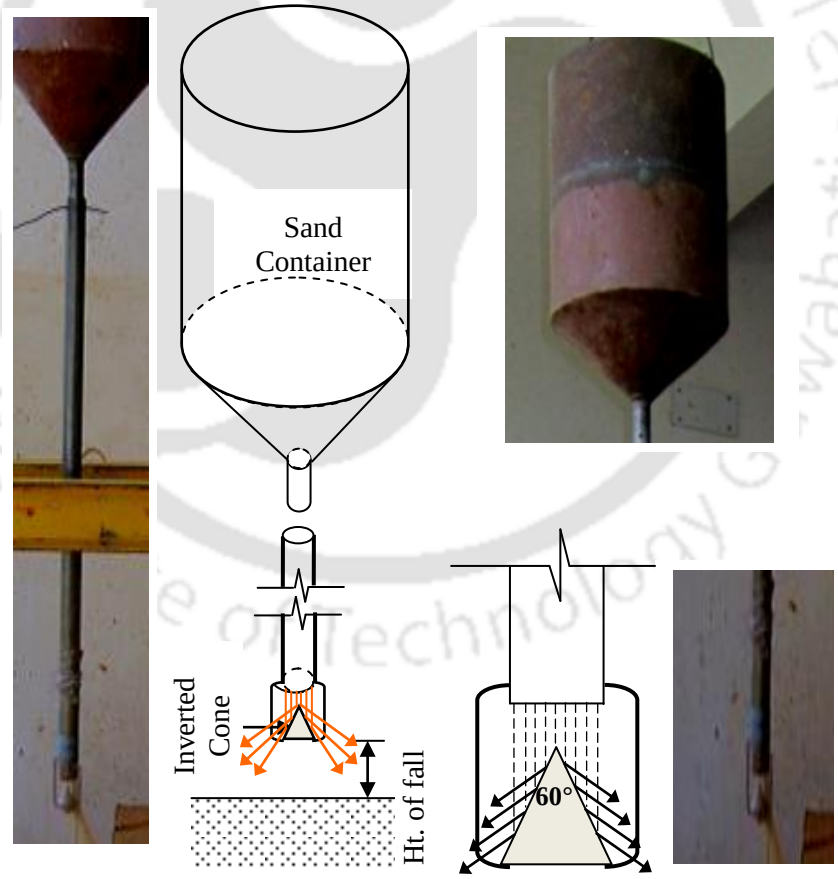

Fig. 3.14 Photograph and schematic diagram of the sand pouring device

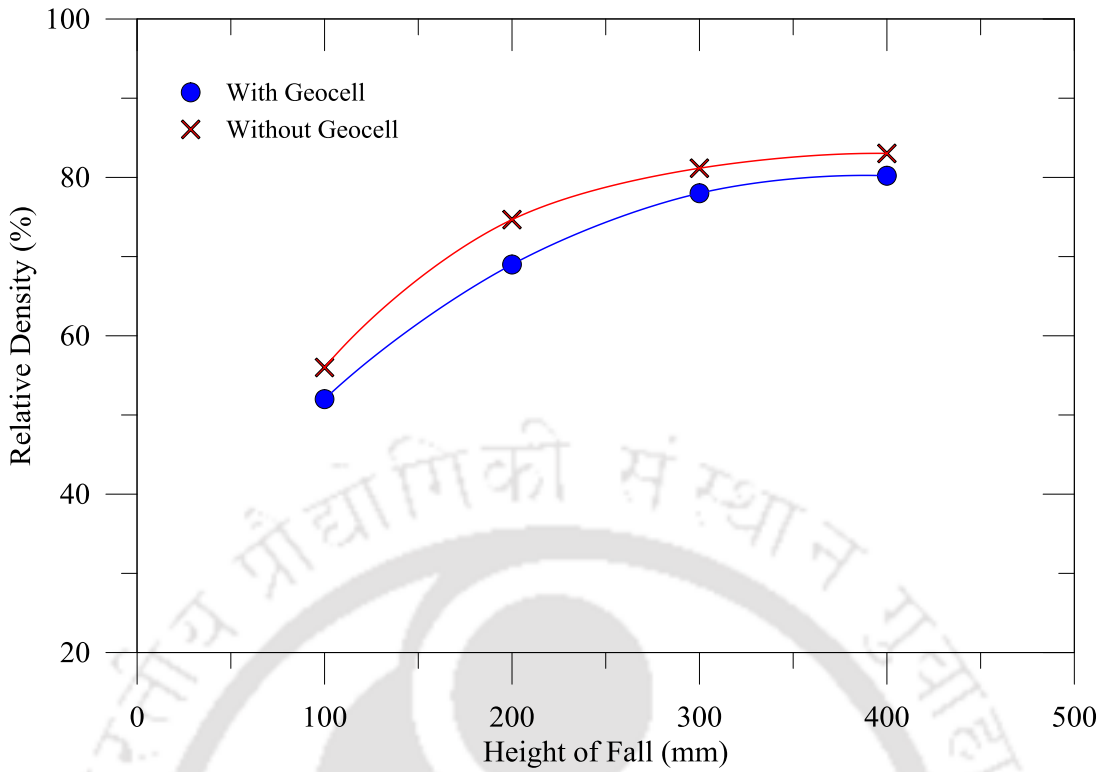

Fig. 3.15 Calibration curve for sand pluviation

Fig. 3.16 Photograph of the prepared test bed

3.4.3 Test Procedure

Tests were conducted using a rigid circular model footing placed. The bottom of the footing was roughened by applying a thin layer of sand with epoxy glue. After preparing the foundation beds to its full height, the footing was placed at the center of the leveled surface. The loading arrangement was suitably placed along the center line of the footing. The dial gauges were positioned at the desired locations; at distances *D*, 2*D*, and 3*D* from the center and on either side of the footing (Fig. 3.12). The footing was loaded (pushed into the soil) with the hydraulic jack, at a rate of approximately 3 mm/minute, up to 36 mm settlement (24% of *D*). The comparatively faster rate of loading was considered to simulate the undrained condition in saturated clay (Dash et al., 2003b; Sitharam et al., 2005). During loading, deformations from the dial gauges and load in the proving ring were recorded at different intervals of footing settlements.

3.5 SUMMARY

The chapter presented details of materials used in the study, i.e. clay, sand and the biaxial geogrid, and their characterization with the methodology adopted. The test set up was described along with the preparation of foundation beds (clay beds/subgrades and unreinforced/reinforced sand bed/layer). Details of test parameters adopted and planning of experimental program are explained. The test methodology followed was presented in brief. Further chapters present the results obtained from various tests conducted under different series.

Chapter 4. UNREINFORCED FOUNDATIONS

4.1 INTRODUCTION

Responses of unreinforced foundations, model tests conducted in test series A and B, are presented in this chapter. In series A, responses of homogeneous foundations of clay of different undrained shear strengths (c_u = 7, 15, 30, and 60 kPa) and sand at dense state (D_r = 80%) were investigated. In series B, tests were conducted on layered foundations having layers of unreinforced sand (D_r = 80%) of varying thickness (H = 0.63, 1.15, 1.67, and 2.19D) overlying clay subgrades of different strengths. The test series details are presented in Table 4.1. Model test under test series A were repeated to confirm the repeatability of testing.

Table 4.1 Details of laboratory model tests: Test series A and B

Test Series	Foundation systems	Test parameters		No. of Tests
		Variables	Constants	
A	Homogeneous clay and sand bed	c_u = 7, 15, 30, 60 kPa D_r = 80% (Sand)	-	5 (+ 5 R)
B	Unreinforced sand layers overlying clay subgrades	c_u = 7, 15, 30, 60 kPa H/D = 0.63, 1.15, 1.67, 2.19	D_r = 80%	16

Results are discussed in terms of bearing pressure and surface deformations (δ) with respect to footing settlements (s). Parameters, such as footing settlement, sand layers thickness (H), and surface deformations are non-dimensionalised with footing diameter (D) and presented as s/D (%), H/D, and δ/D (%), respectively. Further, a bearing pressure improvement factor, I_{fs}, is introduced to discuss the performance of the layered foundations with respect to corresponding homogeneous clay beds.

4.2 HOMOGENEOUS FOUNDATIONS (CLAY AND SAND)

In series A, tests were performed on homogeneous foundations of clay having different undrained shear strengths (c_u = 7, 15, 30, and 60 kPa) and sand at dense state (D_r = 80%). The schematic of foundation configuration is shown in Fig. 4.1.

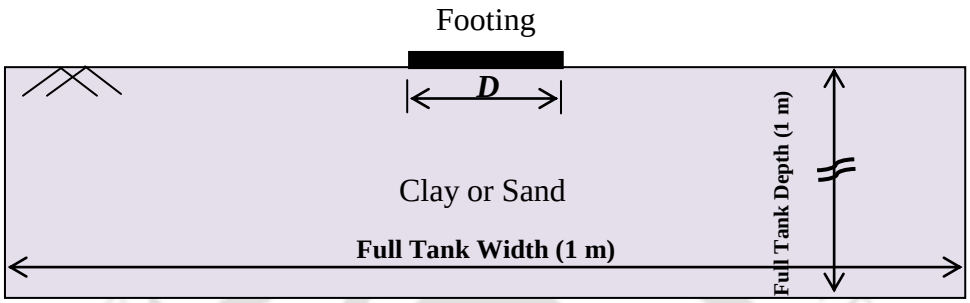

Fig. 4.1 Schematic of homogeneous foundation configuration

Bearing pressure-footing settlement responses of homogeneous clay foundations of different undrained shear strengths (c_u), ranging from 7 to 60 kPa, are presented in Fig. 4.2. In general, higher pressure-settlement responses were obtained for clay beds with higher 'c_u' values. It can be noticed that the variation in bearing pressures with footing settlements were non-linear and none of the four clay bed response curves showed peak values within the range of settlements tested (up to *s/D* = 24%). For instance, at *s/D* = 2%, the bearing pressure for very soft clay bed (c_u = 7 kPa) is 17.5 kPa; whereas, it is 84 kPa for stiff clay (c_u = 60 kPa). The corresponding pressure values at *s/D* = 12% were about 31 and 196 kPa, respectively. However, the maximum bearing pressure of about 31.4 kPa for c_u = 7 kPa and about 245 kPa for c_u = 60 kPa can be noted at *s/D* = 24% from the response curves.

The response of the homogeneous sand bed (D_r = 80%) is also presented in Fig. 4.2. It is seen that the bearing pressure of the sand bed increased to about 175 kPa (at *s/D* = 18%) and then it became almost constant with footing settlement. In comparison with the homogeneous clay bed responses, it is found that clay up to c_u = 30 kPa depicted a softer response (less bearing pressure) than that of the sand bed.

Model tests on homogeneous clay and sand bed were repeated in order to verify the repeatability of the test conditions. The repeated test data are presented in Fig. 4.2 in dotted lines. The figure shows close match between the results of the repeated tests. This indicates the uniform test conditions were achieved during experiments.

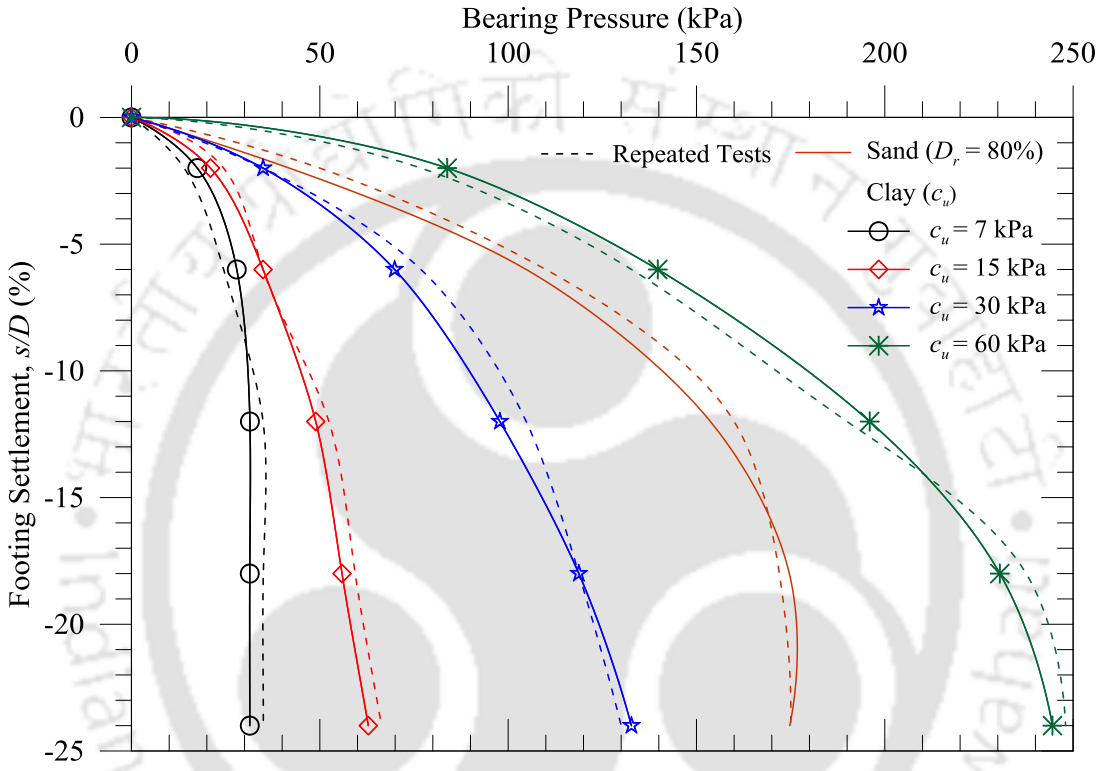

Fig. 4.2 Pressure-settlement responses of homogeneous beds: Clay and Sand

In Fig. 4.3, a typical surface deformation profile of homogeneous bed (c_u = 15 kPa) at different levels of footing settlements (*s*/*D*) is presented. The distance from the footing center '*x*' is expressed in non-dimensional form as *x*/*D*. The surface settlement and heave are differentiated with '-' and '+' signs, respectively. It can be noticed that the surface deformations were mostly pronounced around the footing center (at $x = D$); while it was reduced as the distances increased (at $x = 2D$ and $3D$).

Average surface deformations at $x = D$ from the footing center (left and right side of the footing) are presented in Fig. 4.4. Though not very consistent with the clay strength, the variations are showing predominantly heaving for the clay beds. The

pronounced heaving is attributed to the undrained behavior of the saturated clay which was generated with the faster rate of loading. Deformation response of the sand bed, presented in dotted lines in Fig. 4.4, indicated an initial settlement (up to $s/D \approx$ 15%) followed by heaving. The maximum settlement ($-\delta/D$) was about 0.15% at s/D = 6% and maximum heaving ($+\delta/D$) was about 0.6% at s/D = 24%. The behavior is attributed with the dilation of dense sand. However, away from the footing center ($x \geq 2D$), marginal deformations were seen.

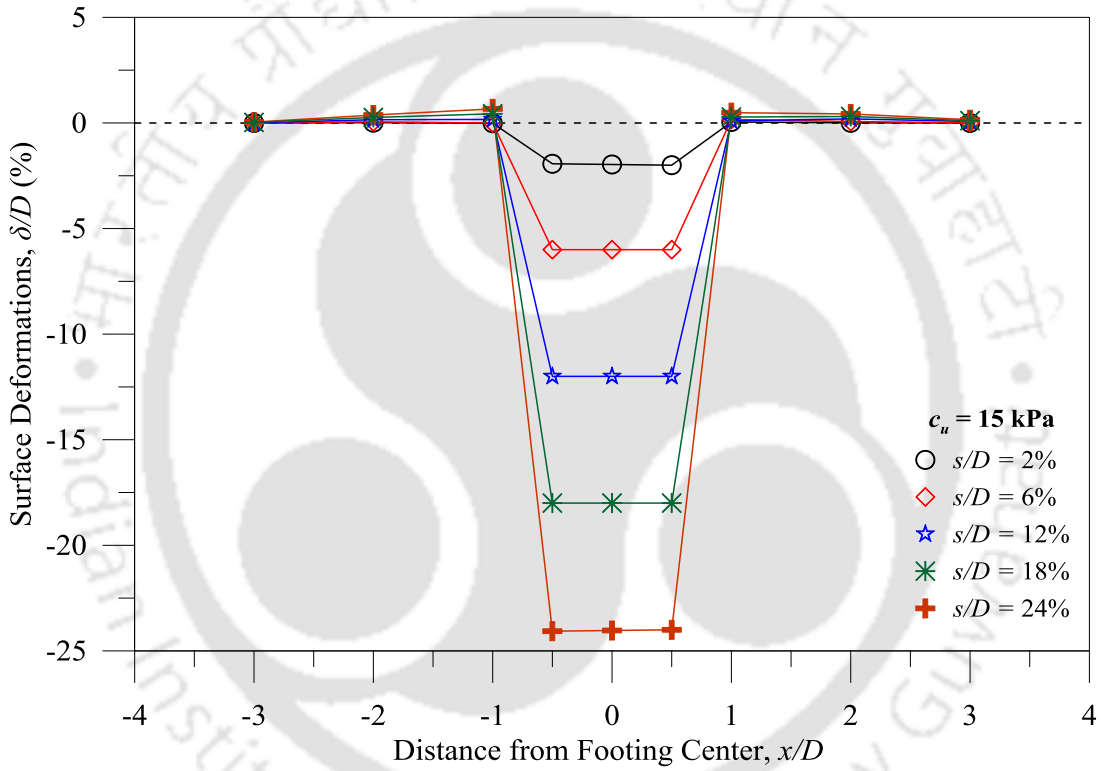

Fig. 4.3 Surface deformation profile at different s/D for c_u = 15 kPa

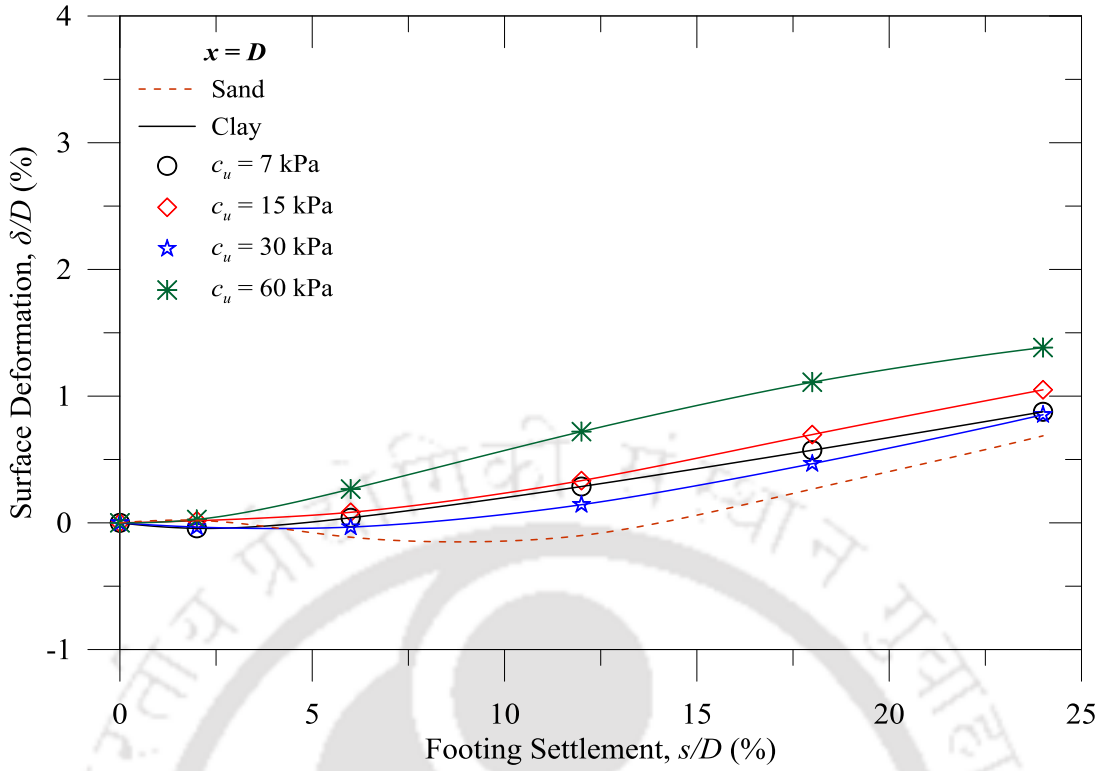

Fig. 4.4 Variation of surface deformations at $x = D$ for homogeneous beds

A comparison of theoretical ultimate bearing pressure, as per $q_u = 5.14\ c_u$ (Meyerhof, 1951) with the maximum bearing pressures obtained from the experiments is presented in Table 4.2. The differences are in the range of 13-21% with respect to the theoretical values. In this regard, it may be noted that the ultimate bearing capacity were not attained during the experiments, but it was continued up to 24% of *s/D*.

Table 4.2 Comparison of theoretical and experimental bearing pressures

Undrained Shear Strength, c_u (kPa)	Theoretical Ultimate Bearing Pressure (kPa) ($q_u = 5.14\ c_u$)	Observed Maximum Bearing Pressure (kPa) (at *s/D* = 24%)	% Difference (w.r.t. $q_u = 5.14\ c_u$)
7	35.98	31.4	12.73
15	77.1	62.9	18.42
30	154.2	132.7	13.94
60	308.4	244.5	20.72

4.3 UNREINFORCED LAYERED FOUNDATIONS (SAND OVER CLAY)

Model tests on layered foundations having varying thicknesses of unreinforced sand (H = 0.63, 1.15, 1.67, and 2.19D) overlying clay subgrades of different strengths were performed in series B. The schematic test configuration is shown in Fig. 4.5.

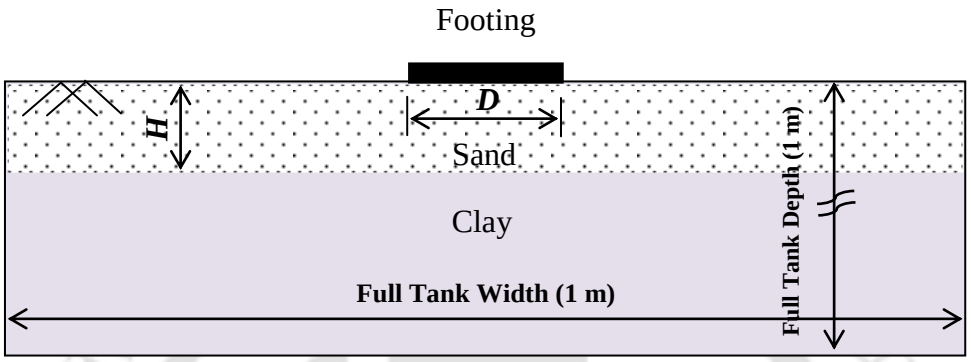

Fig. 4.5 Schematic of unreinforced layered foundation configurations

The pressure-settlement responses of the layered foundations of varying sand layer thickness are presented in Fig. 4.6 to Fig. 4.8 for different clay subgrades (c_u = 7, 15, and 30 kPa). In general, the figures are indicating significant improvement in bearing pressures as compared to corresponding homogeneous clay beds. In Fig. 4.6, increase in bearing pressures from 31 to 56 kPa can be noticed at s/D = 24% for clay subgrade of 7 kPa (c_u), with a 0.63D thick sand layer. Similar improvements in bearing pressures are also observed for c_u = 15 and 30 kPa (Fig. 4.7 and Fig. 4.8, respectively). Besides, higher pressure values were noticed with increase in layer thicknesses (H). Bearing pressures were increased from 56 to 168 kPa with an increase in thickness (H) from 0.63 to 2.19D, for c_u = 7 kPa (at s/D = 24%). At similar thickness variation, the increase in bearing pressures are about 140 to 168 kPa and 161 to 217 kPa, for c_u = 15 and 30 kPa, respectively. However, reduction in improvement rate was noticed beyond a layer thickness H of 1.67D. In Fig. 4.6, for c_u = 7 kPa, bearing pressure increased from 161 to 168 kPa for an increase in H from

1.67 to 2.19*D*; whereas, the increase was in the range of 56 to 161 kPa for the *H* variation from 0.63 to 1.67*D* (at *s/D* = 24%).

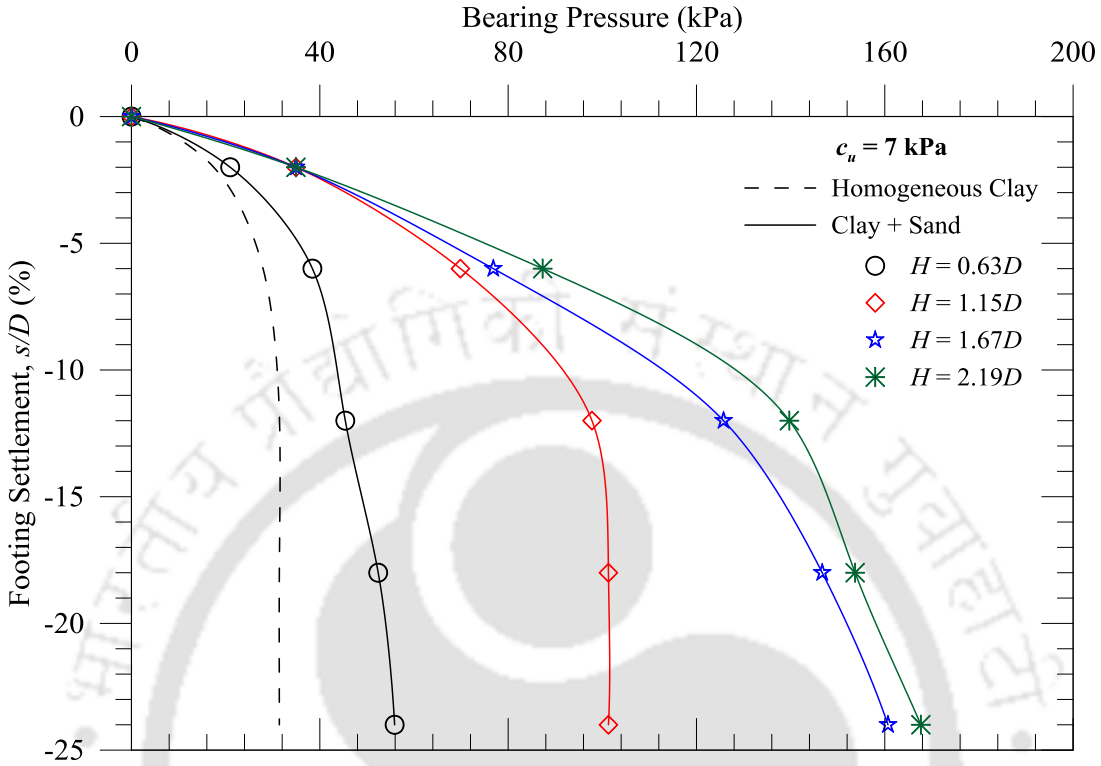

Fig. 4.6 Pressure-settlement response of unreinforced foundations: c_u = 7 kPa

Similar variations in foundation performances were also observed for subgrades having c_u = 15 and 30 kPa, in Fig. 4.7 and Fig. 4.8, respectively. In the figures, the maximum bearing pressures of the corresponding foundations are at *H* = 1.67*D*. Besides, in Fig. 4.8, a peck bearing pressure of about 238 kPa at *s/D* = 18% level of settlement can be noticed for c_u = 30 kPa. From the observations, the optimum thickness for the layered configuration can be considered as *H* = 1.67*D* which could derive maximum contribution from the clay subgrade and the overlying sand layer.

Responses of unreinforced foundations on stiff clay (c_u = 60 kPa) are presented in Fig. 4.9. It can be seen that the responses are very much similar irrespective of sand layer thickness variations. A minor difference was noted at *H* = 0.63*D* with a maximum bearing pressure of 203 kPa. However, beyond *H* = 1.15*D*,

the responses remained almost unchanged with maximum bearing pressure of about 189 kPa. The increased bearing pressure with H of 0.63D is the effect of additional support derived from the underlying stiff clay. For a relatively thin layer of sand ($\leq D$), such as 0.63D, the failure surface extended to the underlying stiff clay subgrade which provided higher resistance. Whereas, for the thick layers ($> D$), the failure surface develops within the sand layer and the layered responses were dominated by the sand behavior. Thus, it can be noticed that with a relatively higher magnitude of bearing pressure (~190 kPa), the pressure-settlement responses for $H \geq 1.15D$ are closer to that of the homogeneous dense sand, in which case the maximum bearing pressure observed as about 175 kPa. This is the typical foundation behavior with softer layer overlying stiffer subgrade as reported by Meyerhof (1974).

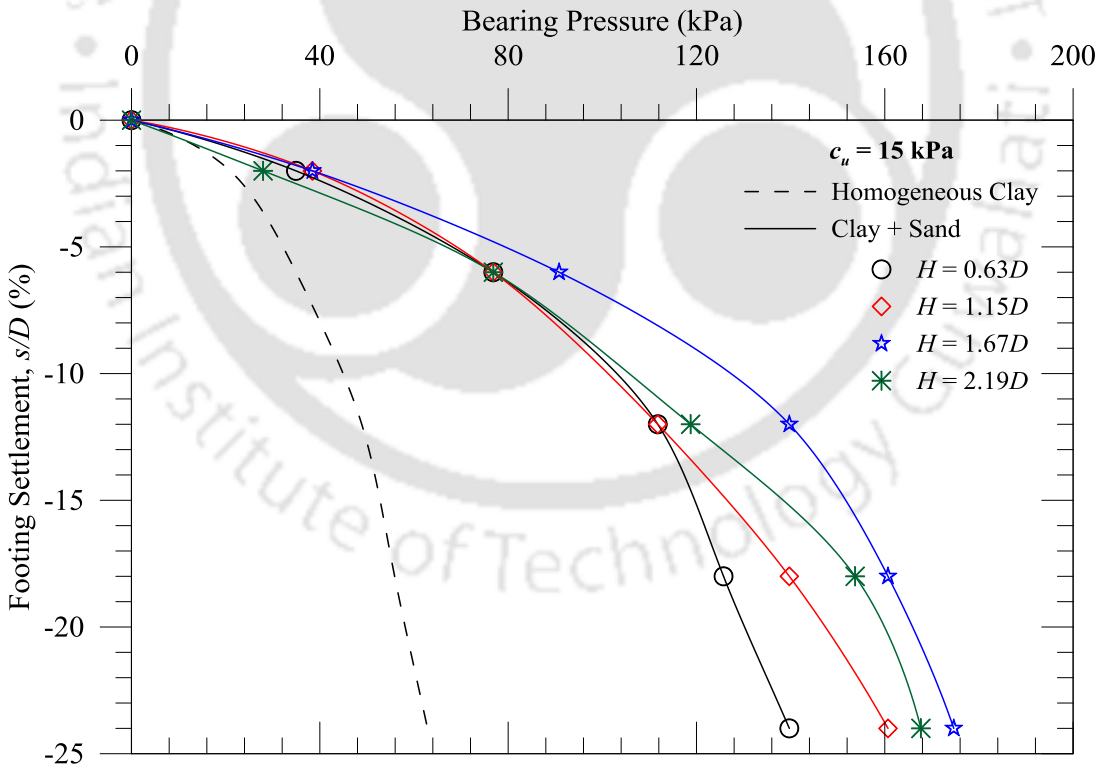

Fig. 4.7 Pressure-settlement response of unreinforced foundations: c_u = 15 kPa

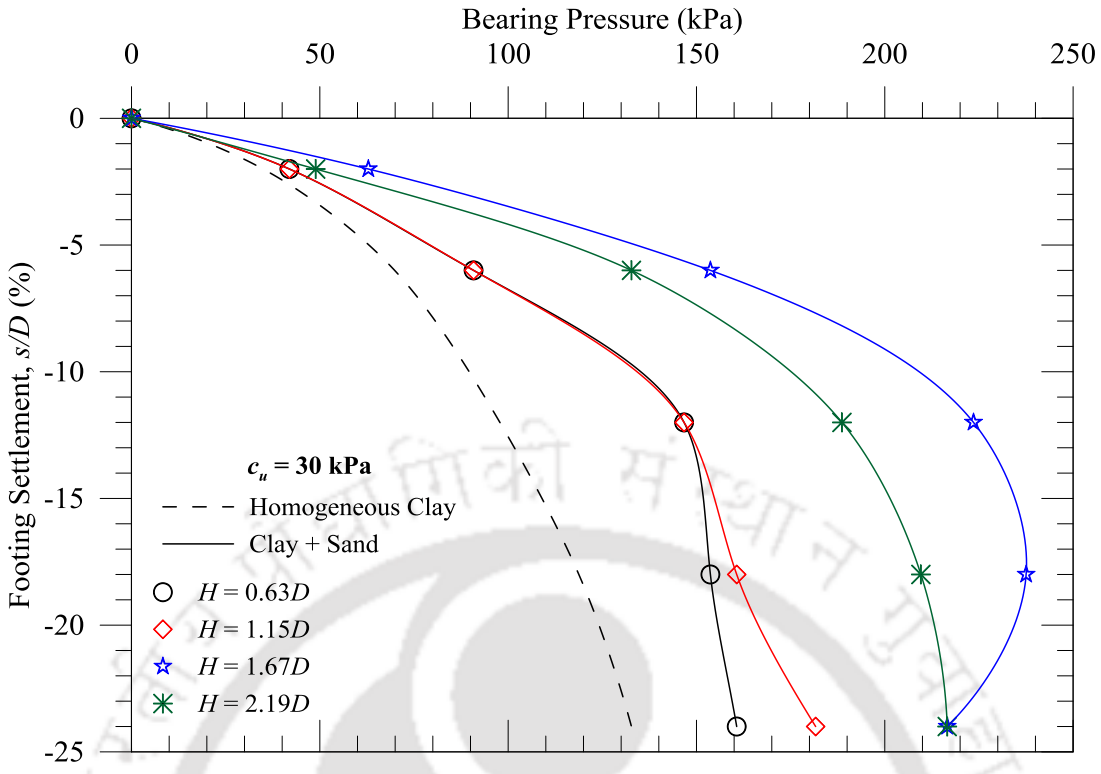

Fig. 4.8 Pressure-settlement response of unreinforced foundations: c_u = 30 kPa

***Bearing Pressure Ratio* (*Improvement Factors*)**

The behaviors of layered foundations are further analyzed in terms of improvement factor, I_{fs}. It is defined as the ratio of bearing pressure of the layered foundation (q_s) to that of the corresponding homogeneous clay bed (q_c), at similar levels of footing settlement (s/D), as shown in Eq. 4.1.

$$I_{fs} = \left(\frac{q_s}{q_c}\right)_{\text{[at same } s/D \text{ level]}} \quad (4.1)$$

The improvement factors for layered systems are presented in Table 4.3. The I_{fs} values for softer subgrades ($c_u \leq 30$ kPa) are ranging from 1.2 to 5.34, signifying considerable improvements as compared to corresponding homogeneous clay beds. Variations in improvement factors with footing settlement, for different layered configurations having the clay subgrade of 7 kPa are presented in Fig. 4.10.

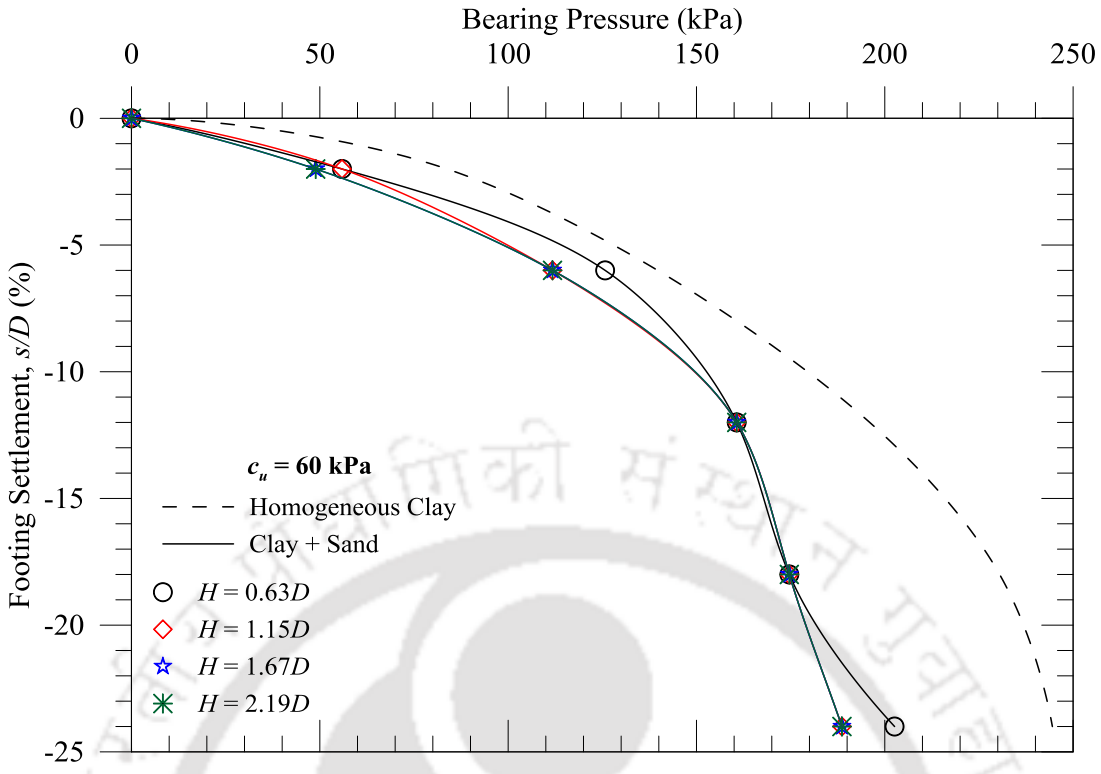

Fig. 4.9 Pressure-settlement response of unreinforced foundations: c_u = 60 kPa

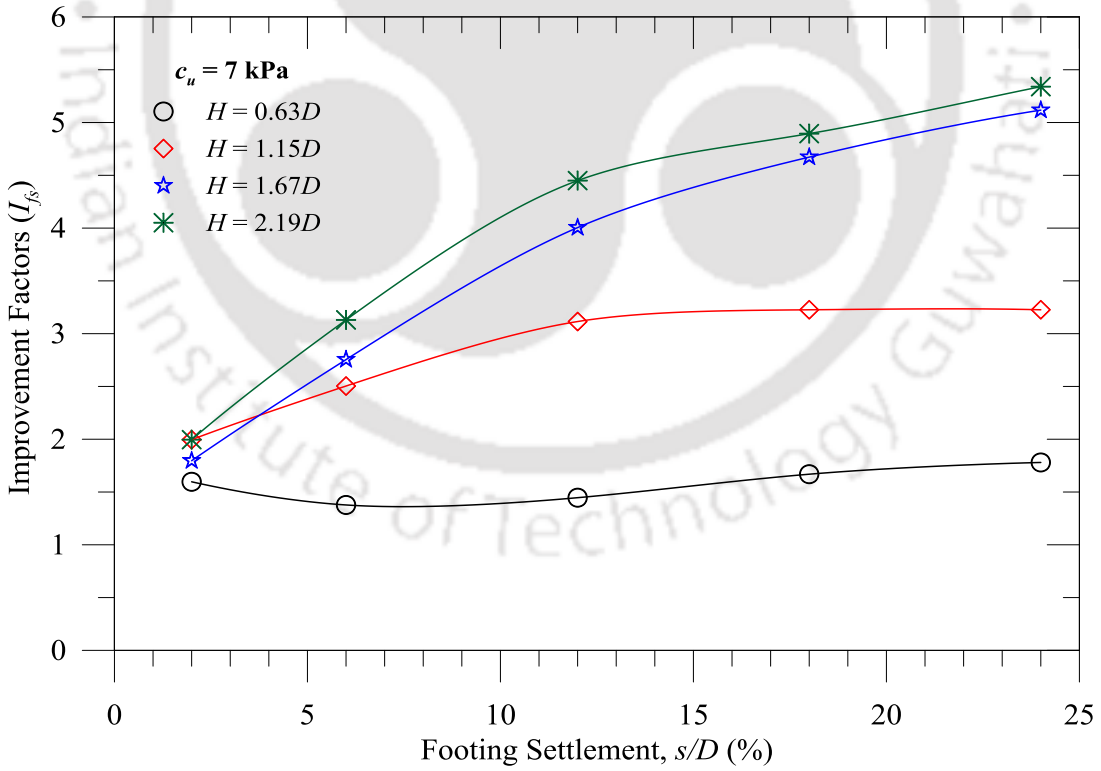

Fig. 4.10 Variation of improvement factors, I_{fs}, for varying H/D for c_u = 7 kPa

Table 4.3 Summary of bearing pressure improvement factor (I_{fs})

Settlements (s/D)	Layer Thickness (H/D)	Bearing Pressure Improvement Factor (I_{fs})			
		c_u = 7 kPa	c_u = 15 kPa	c_u = 30 kPa	c_u = 60 kPa
2%	0.63	1.20	1.66	1.20	0.67
	1.15	2.00	1.83	1.20	0.67
	1.67	2.00	1.83	1.80	0.58
	2.19	2.00	1.33	1.40	0.58
6%	0.63	1.38	2.20	1.30	0.90
	1.15	2.50	2.20	1.30	0.80
	1.67	2.75	2.60	2.20	0.80
	2.19	3.13	2.20	1.90	0.80
12%	0.63	1.45	2.29	1.50	0.82
	1.15	3.11	2.29	1.50	0.82
	1.67	4.00	2.86	2.29	0.82
	2.19	4.45	2.43	1.93	0.82
18%	0.63	1.67	2.25	1.29	0.76
	1.15	3.23	2.50	1.35	0.76
	1.67	4.67	2.87	2.00	0.76
	2.19	4.89	2.75	1.76	0.76
24%	0.63	1.78	2.22	1.21	0.83
	1.15	3.23	2.55	1.37	0.77
	1.67	5.12	2.78	1.63	0.77
	2.19	5.34	2.67	1.63	0.77

It is observed that the foundation performances, in terms of bearing pressure improvement factors, are enhanced with increase in layer thickness (H) and footing settlement (s/D) (Table 4.3). The improvement is significantly high for the very soft clay subgrade (c_u = 7 kPa). In this case, the I_{fs} varied from 1.78 to 5.34 for an increase in layer thickness (H) from 0.63 to 2.19D (at s/D = 24%). At similar conditions, the I_{fs} for the subgrades having c_u = 15 and 30 kPa are found to be varied as 2.22 to 2.67 and 1.21 to 1.63, respectively. However, beyond a sand layer thickness H of 1.15D and a settlement level of $s/D \geq 12\%$, the rate of improvements (I_{fs}) were reduced which is represented by flatter slopes (Fig. 4.10). This could be attributed to the punching of

sand layer into the softer subgrades which increases the influence of softer clay underneath. Besides, the local shear and squeezing out of the sand layer from the footing bottom resulted in localized footing settlement which leads to reduction in the overall performance improvement.

For the layered systems on c_u = 60 kPa, foundation performances were reduced as compared to the corresponding homogeneous clay bed which is the typical response of softer sand layer over the stiff clay subgrade. The variations of improvement factors with footing settlement, for different layered configurations overlying the stiff clay subgrade, are depicted in Fig. 4.11. In this case, the improvement factors are in the range of 0.58 to 0.90 (Table 4.3). Besides, it can be noticed that the improvement factors are almost remain the same for $H > 0.63D$. It is attributed to the relatively soft sand column failure by shear and squeezing out of sand layer due to very high restraint offered by the stiff clay subgrade against the footing penetration. The effect could be seen in terms of I_{fs} which was less than unity (< 1.0).

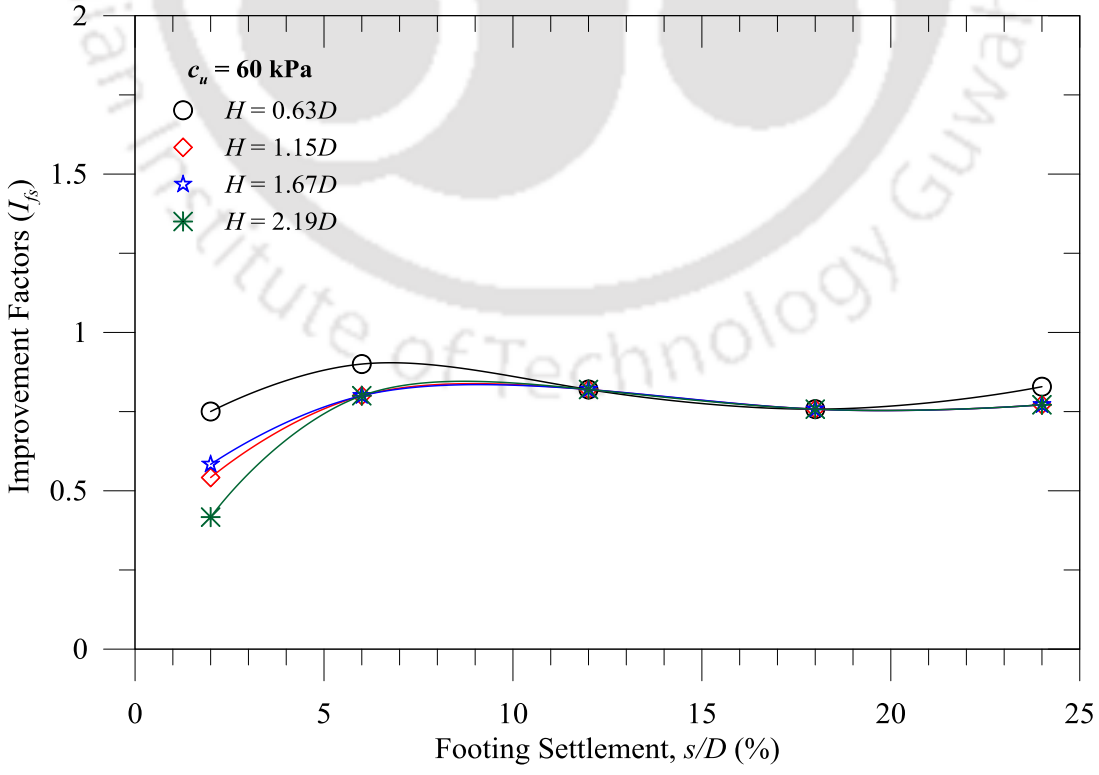

Fig. 4.11 Variation in improvement factors, I_{fs}, for varying H/D for c_u = 60 kPa

In Fig. 4.12, the effect of layer thicknesses (H) is presented, in the form of typical variations in improvement factors (I_{fs}), at the maximum level of footing settlements (s/D = 24%). In general, for softer subgrades ($c_u \leq 30$ kPa), the improvement factors were increased with increase in layer thickness up to about 1.67D. In the figure, the maximum values of I_{fs} can be noted as 5.34, 2.67, and 1.63 for the subgrades having c_u = 7, 15, and 30 kPa, respectively, at 2.19D. Whereas, for the stiff subgrade of 60 kPa, the responses were almost constant irrespective of layer thickness variation and ranged between 0.77-0.83.

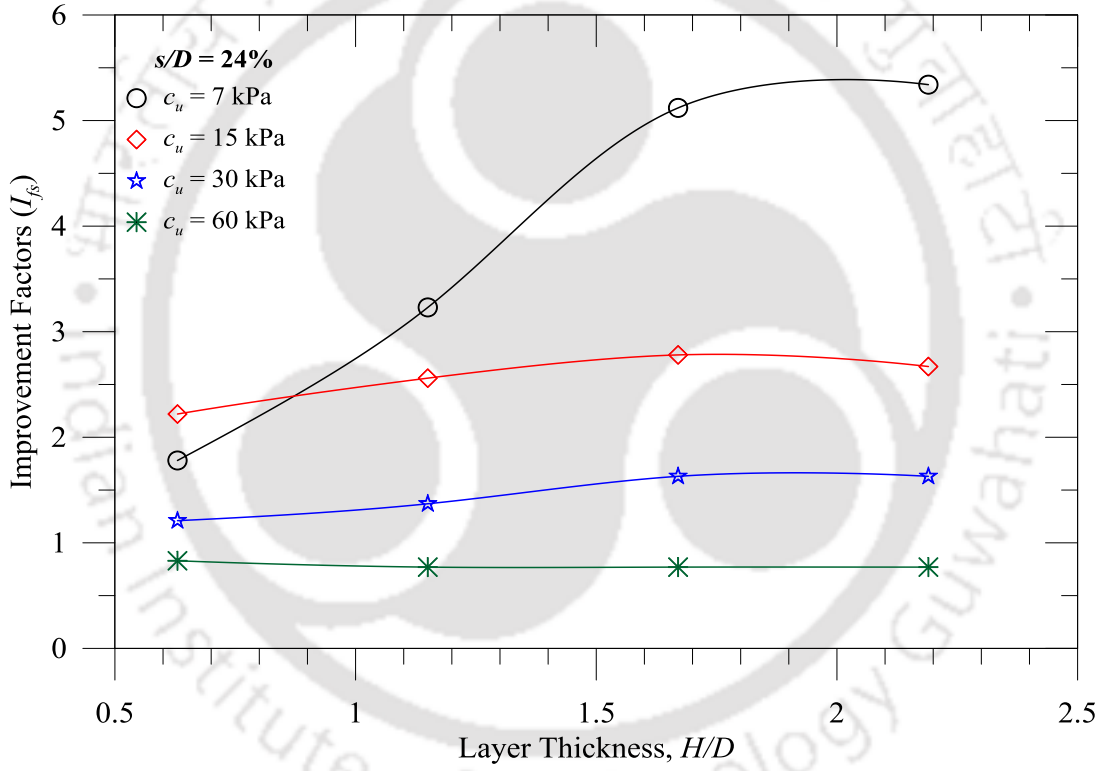

Fig. 4.12 Variation of I_{fs} with layer thickness (H) for different c_u at s/D = 24%

The influence of different subgrades (c_u), in terms of improvement factors (I_{fs}), on overall foundation performance is presented in Fig. 4.13, for H = 2.19D. In general, a decreasing trend in improvement factors with increasing subgrade strength can be noticed. This was significantly very high at higher level of settlement, such as s/D = 24%. At s/D = 24%, the I_{fs} decreased from 5.34 to 0.77 for an increase in c_u from 7 to

60 kPa. In this regard, it should be mentioned here that the decreasing trend is in terms of improvement factors only; however, the corresponding bearing pressures were still increasing with the subgrade strengths.

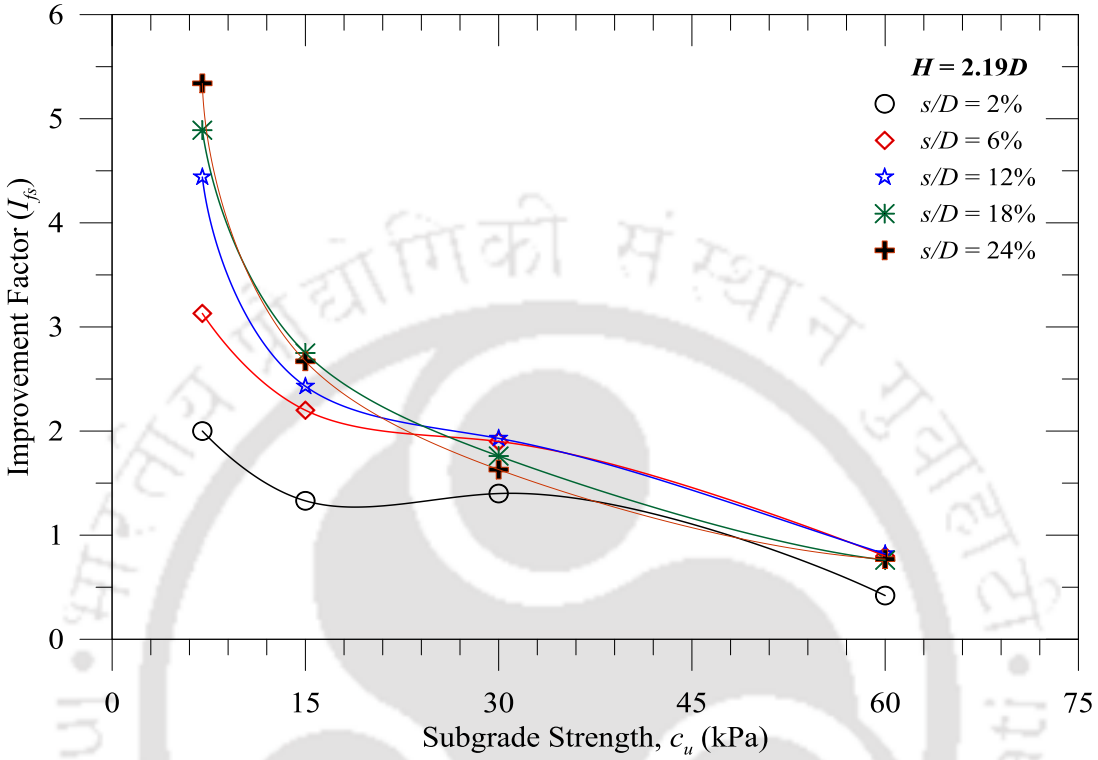

Fig. 4.13 Variation of I_{fs} for different c_u and s/D at H = 2.19D

A typical variation in surface deformations is presented in Fig. 4.14, for c_u = 7 kPa at H = 0.63D. In Fig. 4.14 and in general, similar symmetrical deformation at both the sides of the footing (left and right) was observed. In Fig. 4.15 a comparison of average surface deformation (at x = D, 2D, and 3D) of the homogeneous and layered (H = 0.63D) foundations are presented for c_u = 7 kPa. It is observed that the surface heaving was reduced for the layered foundations as compared to the homogeneous clay beds. However, the deformation profiles were dependent on subgrade strength (c_u) as presented in Fig. 4.16. Surface deformations at H = 0.63D are almost in the same order for $c_u \leq$ 30 kPa; while, the foundations on stiff clay subgrade (c_u = 60 kPa) were mostly undergone surface heaving as presented in Fig.

4.17. The behavior is attributed to sand column failure by squeezing which enhanced the heaving at foundation surface.

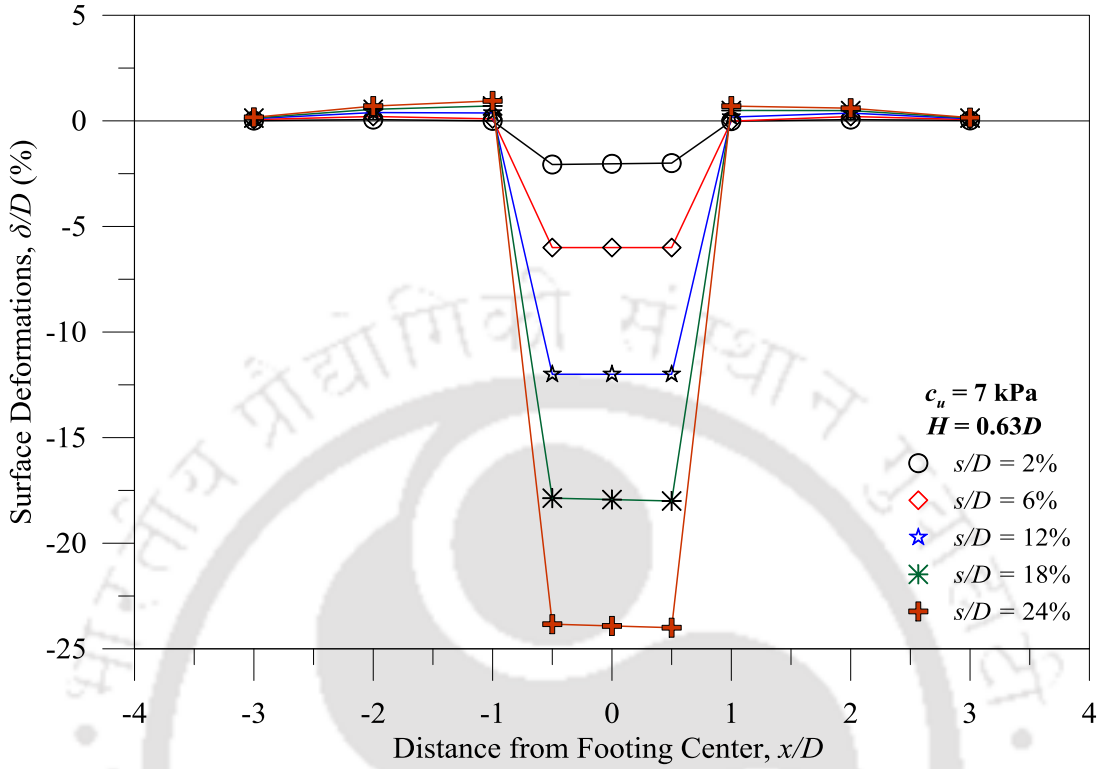

Fig. 4.14 Surface deformation profile of layered foundation; c_u = 7 kPa (H = 0.63D)

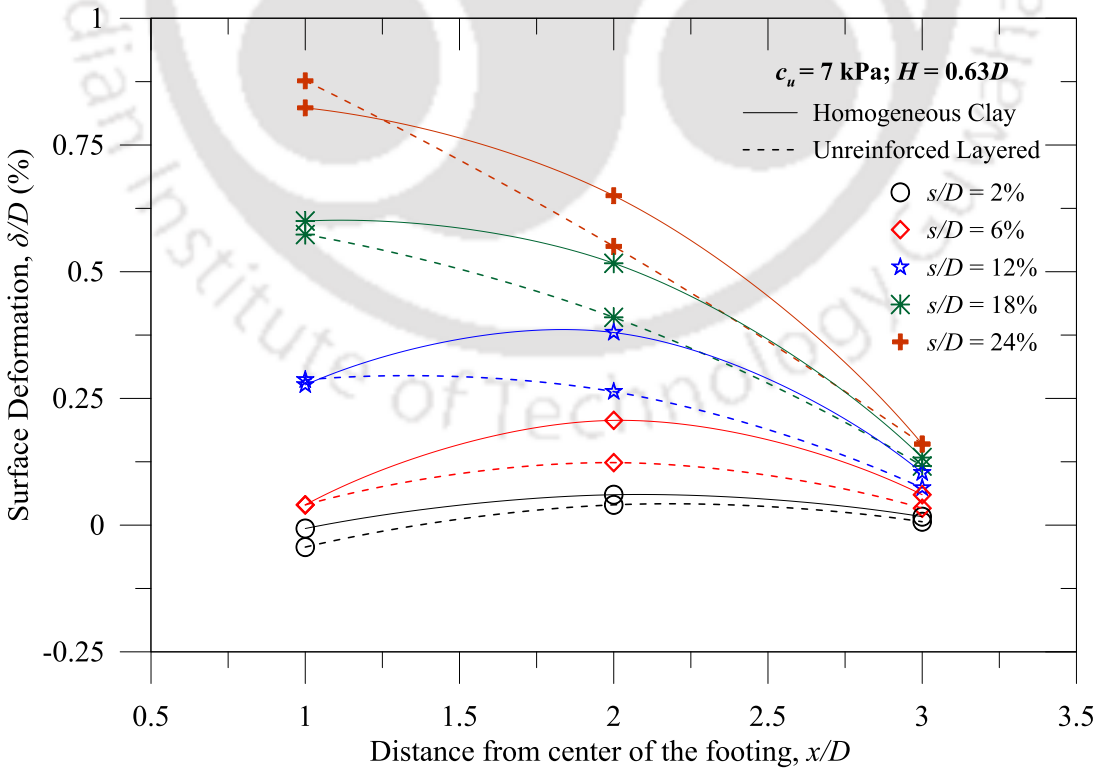

Fig. 4.15 Variation of δ/D with s/D for homogeneous and layered foundation (H = 0.63D) with c_u = 7 kPa

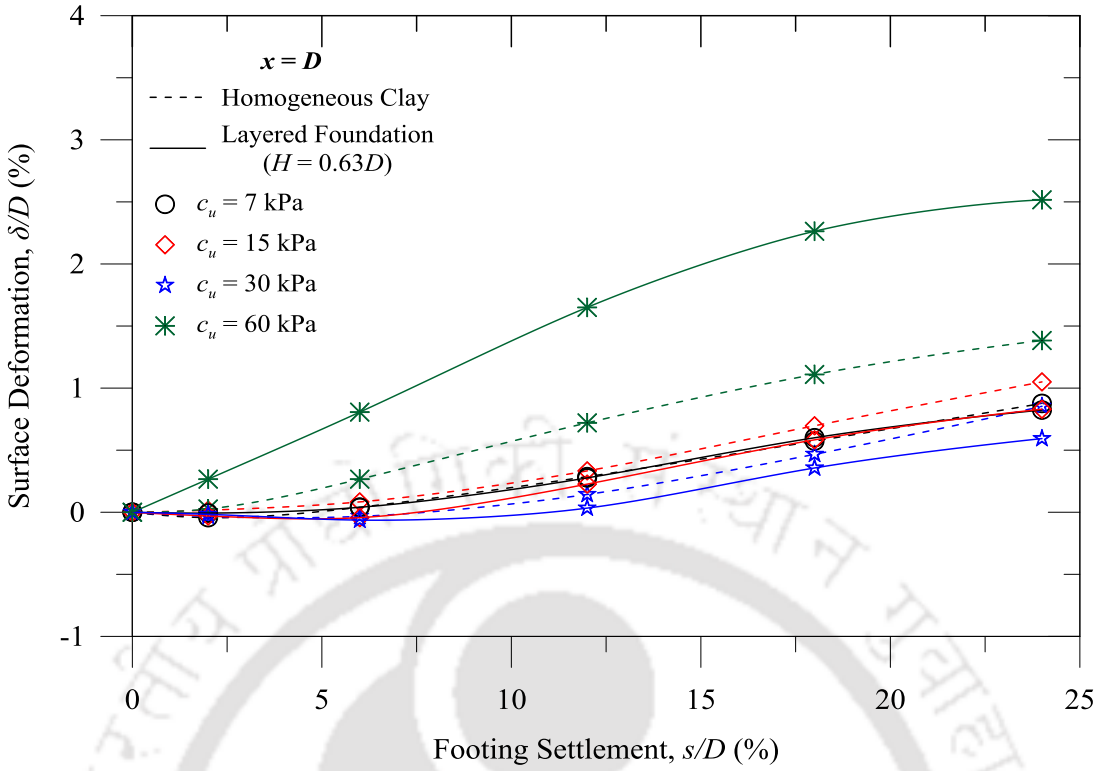

Fig. 4.16 Variation of δ/D with s/D at $x = D$ for homogeneous clay and layered foundations ($H = 0.63D$)

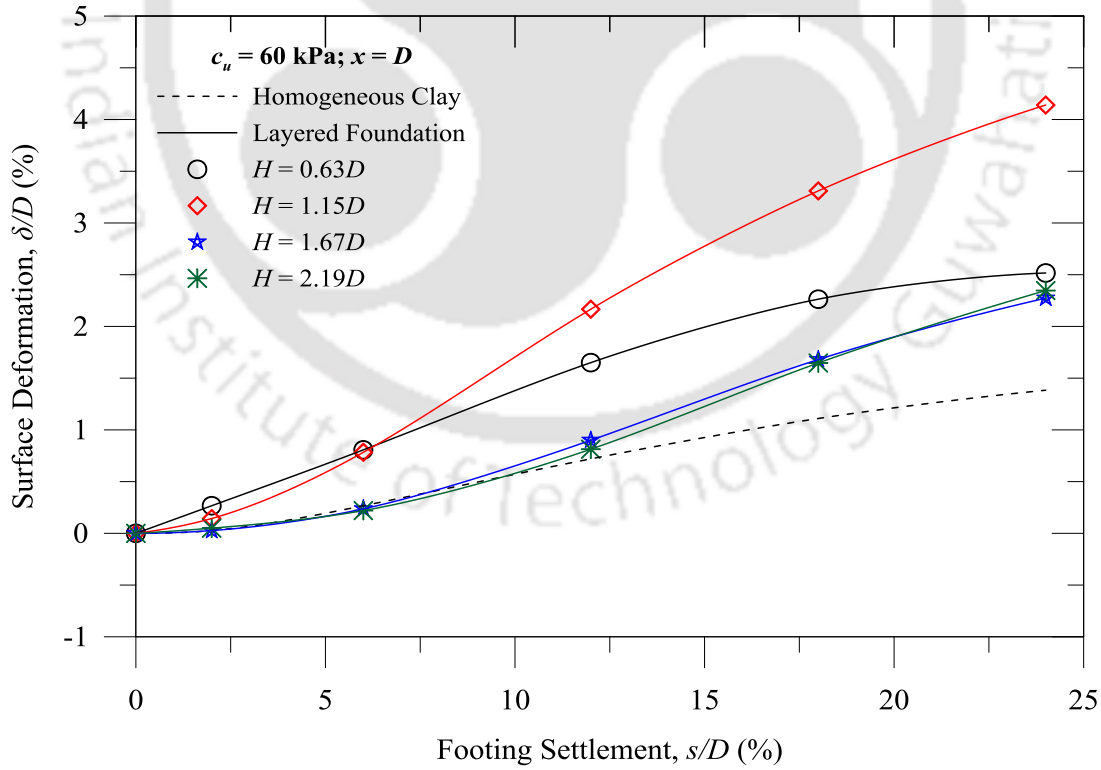

Fig. 4.17 Variation of δ/D with s/D at $x = D$ for varying H/D for $c_u = 60$ kPa

A comparision of experimentally obtained foundation responses with the theoretical approach proposed by Meyerhof (1974) and Meyerhof and Hanna (1978) is presented in Fig. 4.18 and Fig. 4.19. The ultimate bearing capacity of layered foundations having a sand layer overlying relatively soft and stiff clay subgrade, respectively, are estimated by eq. 4.2 and 4.3, respectively.

$$q_u = (1+0.2(B/L))5.14c_u + \gamma_1 H^2 (1+B/L)(1+2D_f/H)(K_s \tan\varphi/B) + \gamma_1 D_f \leq q_t \quad (4.2)$$

$$q_u = q_t + (q_b - q_t)(1 - H/H_t)^2 \quad (4.3)$$

where, B/L is the width to length of the footing, c_u is undrained shear strength of the clay, γ_1, H, φ and D_f are the density, thickness, internal friction angle of overlying sand layer and depth of footing from ground surface, respectively, ultimate bearing capacity of surface footing rested over homogeneous beds of sand and clay is given by q_t and q_b, respectively. The K_s is the coefficient of punching shear.

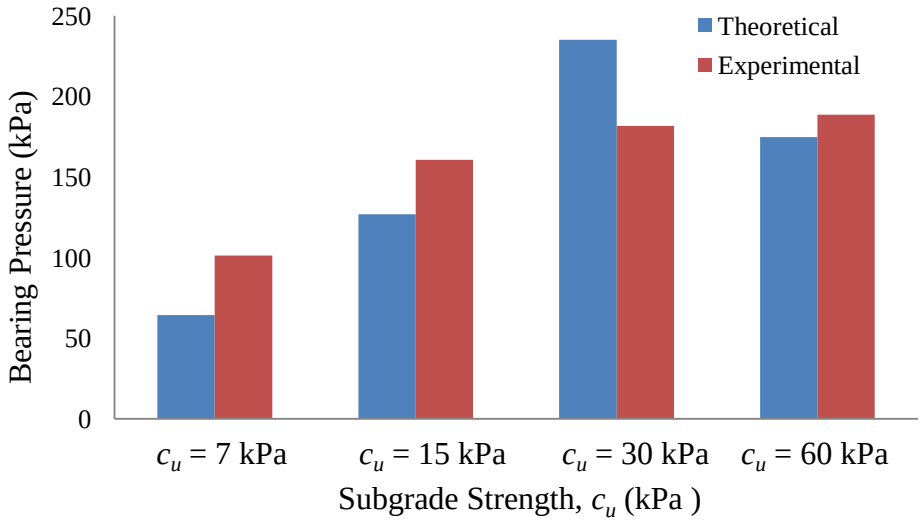

Fig. 4.18 Comparison of theoretical ultimate and experimental maximum bearing pressure for different clay subgrades for $H = 1.15D$

In present analysis, the q_t and q_b are considered as the experimentally obtained maximum bearing pressures for the homogeneous sand and clay beds, respectively. In Fig. 4.18, considerably good agreement can be noticed between the experimental and

the theoretical values (at H = 1.15D; c_u = 15 kPa). In case of sand overlying the stiff clay subgrade, the comparison presented in Fig. 4.19 presenting an excellent agreement between the theoretical and experimental values at H = 1.15D.

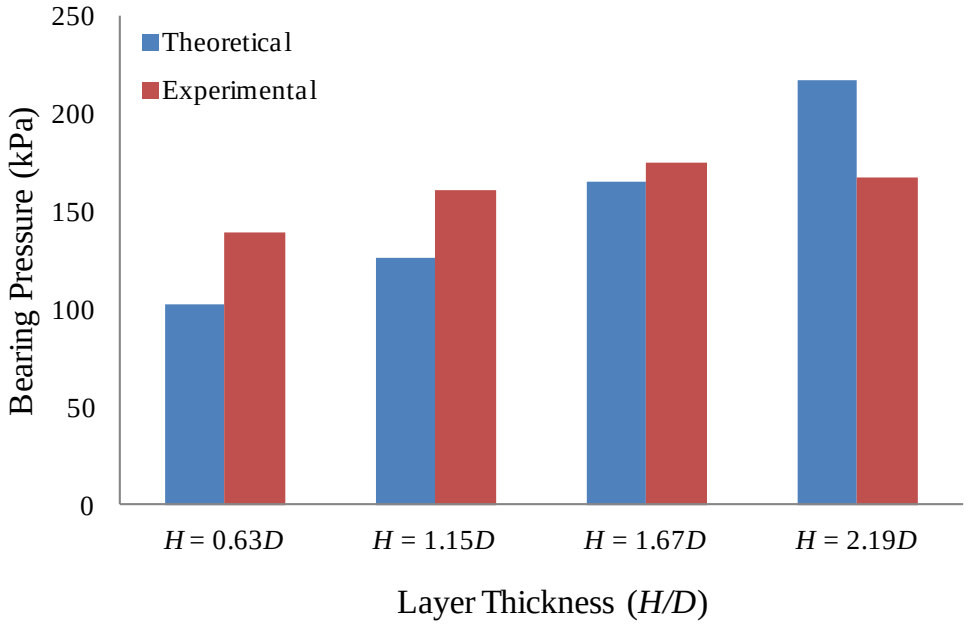

Fig. 4.19 Comparison of theoretical ultimate and experimental maximum bearing pressure for different layer thicknesses of sand overlying clay subgrade of c_u = 60 kPa

Visual inspection of the physical deformations of the subgrades was performed after each test. After careful removal of sand layer, a circular bowl-shaped depression, having a larger diameter than the footing, was noticed just under the footing. The Fig. 4.20a shows such depression observed at the end of a test with very soft clay subgrade (c_u = 7 kPa) overlain by a sand layer of thickness 0.63D. A maximum depression of about 30 mm was found in this case. It can be inferred that during loading, a truncated pyramidal sand column was formed in between the footing and the clay subgrades (Fig. 4.20b) through which load was transferred. The depressions were resulted due to such penetrations of the sand columns on the subgrade. Similar depression formations were also discussed by Meyerhof (1974). The D' indicated in Fig. 4.20b is the diameter of the impression of the depression

region generated through the sand column penetration. The formation and penetration of truncated pyramidal sand column was depended on layer thickness and subgrade strength. It was observed that the D' was more than D for the softer subgrades (c_u < 30 kPa) with layer thicknesses $H \leq 1.15D$. In the stiffer soil overlying softer subgrades configuration, a punching shear failure can be anticipated. However, $D' < D$ was noticed for the thicker layers and stiffer subgrades, where the failure surfaces are expected to develop within the sand layer resembling general shear failure.

It was observed that the depth of the depressions was reduced with the increase in subgrade strength and sand layer thickness. It can be attributed to the increased restraint against the footing settlement by the stiffer subgrades and higher load distribution through the thicker sand layers, respectively. For very soft clay, such as 7 kPa, the resistance from the subgrade against the transmitted footing load was not significant. Hence, the sand column could easily penetrate through the subgrade and the depressions were very prominent. For the stiff clay subgrade, such as c_u = 60 kPa, depressions were not prominent even at $H = 0.63D$. However, significant heaving was observed on the sand surface for the stiff clay subgrades when the thickness of the sand layer was more than the diameter of the footing, i.e. $H \geq 1.15D$. The post-test exhumed stiff clay layer however did not exhibit any visible deformation. Hence it is hypothesised that the upper sand layer has failed in general shear mode (Jumikis, 1961; Selig and McKee, 1961; Vesic, 1973) due to the high restrained footing settlement and affected as enhanced surface heaving.

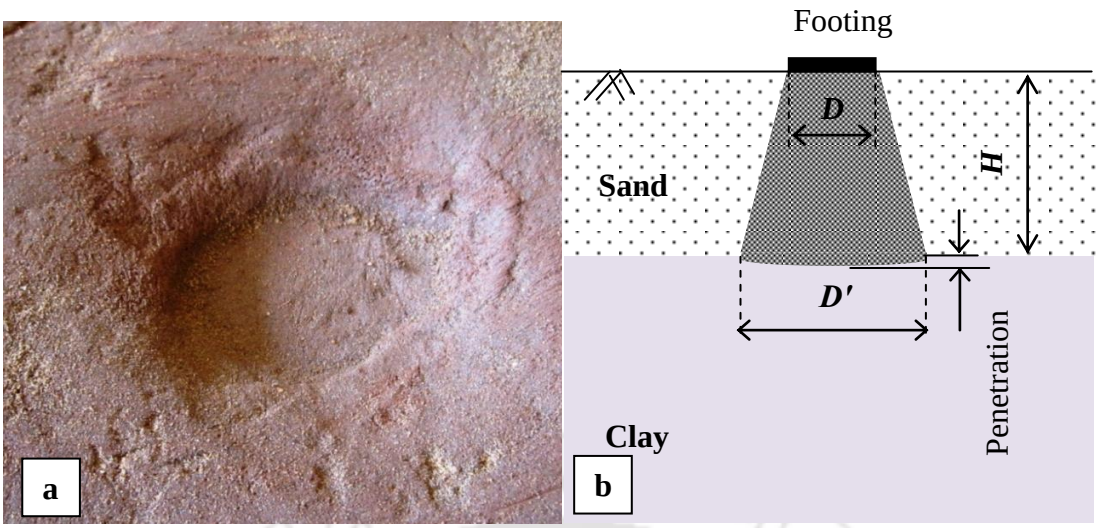

Fig. 4.20 Formation of sand-column and a typical subgrade penetration for layered foundation (c_u = 7 kPa; H = 0.63D)

4.4 SUMMARY

This chapter presented the responses of model tests performed in series A and B, on homogeneous and layered foundations, respectively. In series A, responses of the model footing on homogeneous beds of clay (c_u = 7, 15, 30, and 60 kPa) and sand (D_r = 80%) were investigated. The sand bed depicted stiffer pressure-settlement response compared to that of clay beds having c_u up to 30 kPa.

The responses of sand layered-foundations of different configurations (H = 0.63, 1.15, 1.67, and 2.19D) were investigated in series B. Significant improvement in bearing pressure was observed for softer clay subgrades ($c_u \leq$ 30 kPa); while, performances were reduced for stiff clay subgrade (c_u = 60 kPa), as compared to corresponding homogeneous clay beds. For softer subgrades, bearing pressures were observed to be increased with sand-layer thickness; however, improvements were reduced for $H >$ 1.67D of unreinforced sand. The improvements in terms of bearing pressure ratios were decreased with subgrade strengths. A maximum of about 5.6-fold improvement in bearing pressure was observed for 7 kPa (c_u) clay subgrades.

Chapter 5. GEOGRID REINFORCED FOUNDATIONS

5.1 INTRODUCTION

Behavior of layered foundations having a planar geogrid at the sand-clay interface, investigated in test series C, is presented in this chapter. The foundation configurations were kept similar to that in series B, except placing a planar geogrid of width '*b*', at the two layers interface. Schematic of the test configuration is presented in Fig. 5.1. Details of the test series C are presented in Table 5.1.

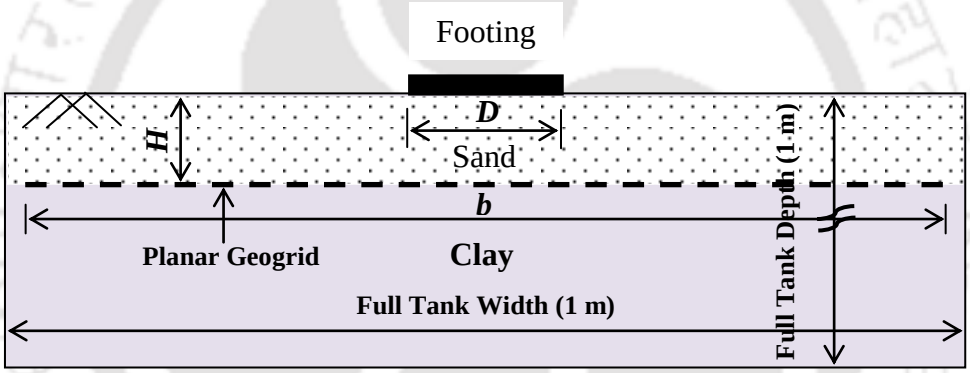

Fig. 5.1 Schematic configuration of geogrid reinforced layered foundations

Table 5.1 Detail of the test series C

Test Series	Foundation system	Test parameters		No. of Tests
		Variables	Constants	
C	Sand bed overlying clay subgrade with planar geogrid at the interface	c_u = 7, 15, 30, 60 kPa H/D = 0.63, 1.15, 1.67, 2.19	D_r = 80% b/D = 6	16

5.2 TEST RESULTS

In test series C, the sand layer thicknesses (H) were varied as 0.63, 1.15, 1.67, and 2.19D overlying the clay subgrades of different undrained shear strengths (c_u = 7, 15, 30, and 60 kPa). The pressure-settlement responses of geogrid-reinforced

foundations are presented in Fig. 5.2 to Fig. 5.5, for foundation systems with different c_u. Response of the corresponding homogeneous clay bed (series A) is also provided in each figure. For clay subgrages with $c_u \leq 30$ kPa, geogrid-reinforced foundations showed significantly higher pressure-settlement responses as compared to corresponding homogeneous clay beds. For example, in Fig. 5.2 for very soft clay subgrade (c_u = 7 kPa), the maximum bearing pressure for reinforced system at s/D = 24% is 175 kPa (at H = 2.19D); while the corresponding value for the homogeneous clay bed was 31 kPa. In general, it is seen that bearing pressures were enhanced with footing settlements. For c_u = 7 kPa and H = 2.19D (in Fig. 5.2), the bearing pressure at s/D = 12% is 143 kPa, which has increased to 175 kPa at s/D = 24%.

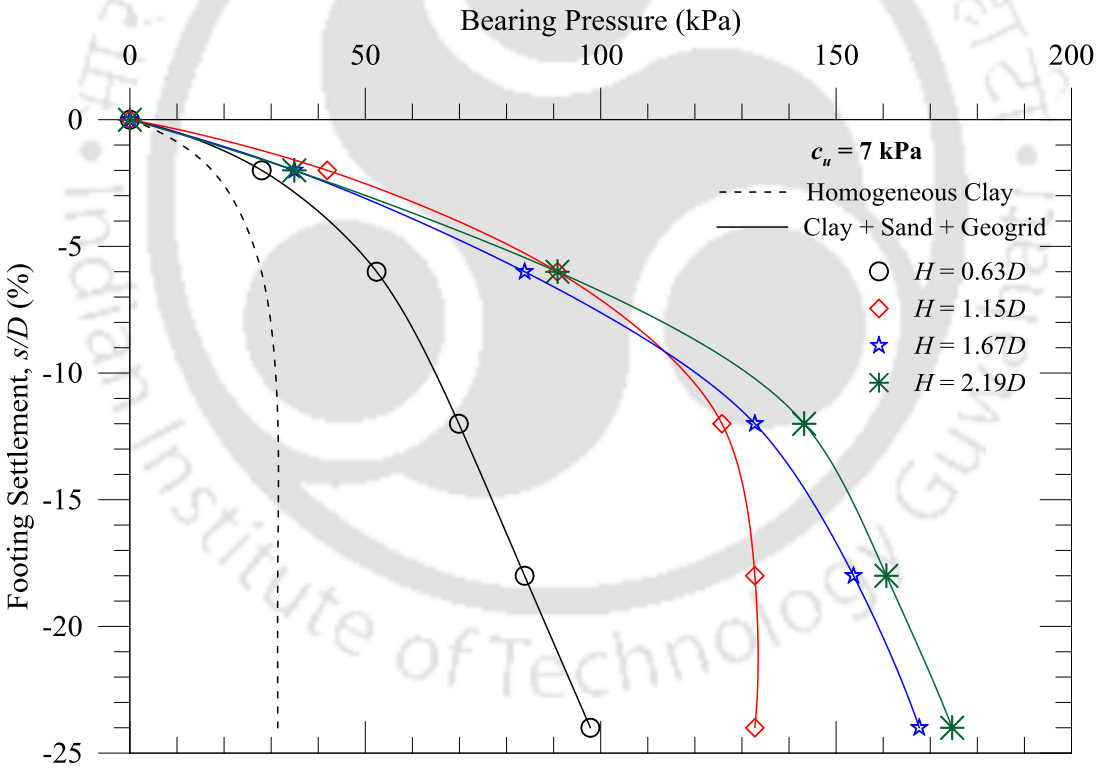

Fig. 5.2 Pressure-settlement responses of geogrid-reinforced foundations: c_u = 7 kPa

Responses of comparatively stiffer subgrades of 15 and 30 kPa (c_u) are shown in Fig. 5.3 and Fig. 5.4, respectively. It can be noticed that the improvement in bearing pressure are not consistent with respect to layer thickness (H) at all settlement levels

(*s/D*). In Fig. 5.3, for c_u = 15 kPa, bearing pressures were increased with layer thickness up to H = 1.67D for the range of footing settlement, *s/D* = 12-24%; while, for H = 2.19D, a reduced pressure-settlement response was observed compared to H = 1.67D. A similar trend of pressure-settlement responses was also noticed for c_u = 30 kPa in Fig. 5.4. In the case of stiff clay subgrade (c_u = 60 kPa), the reinforced beds showed higher performance up to $H \leq 1.15D$ (compared to the homogenous bed), for *s/D* in the range 2-18% as shown in Fig. 5.5.

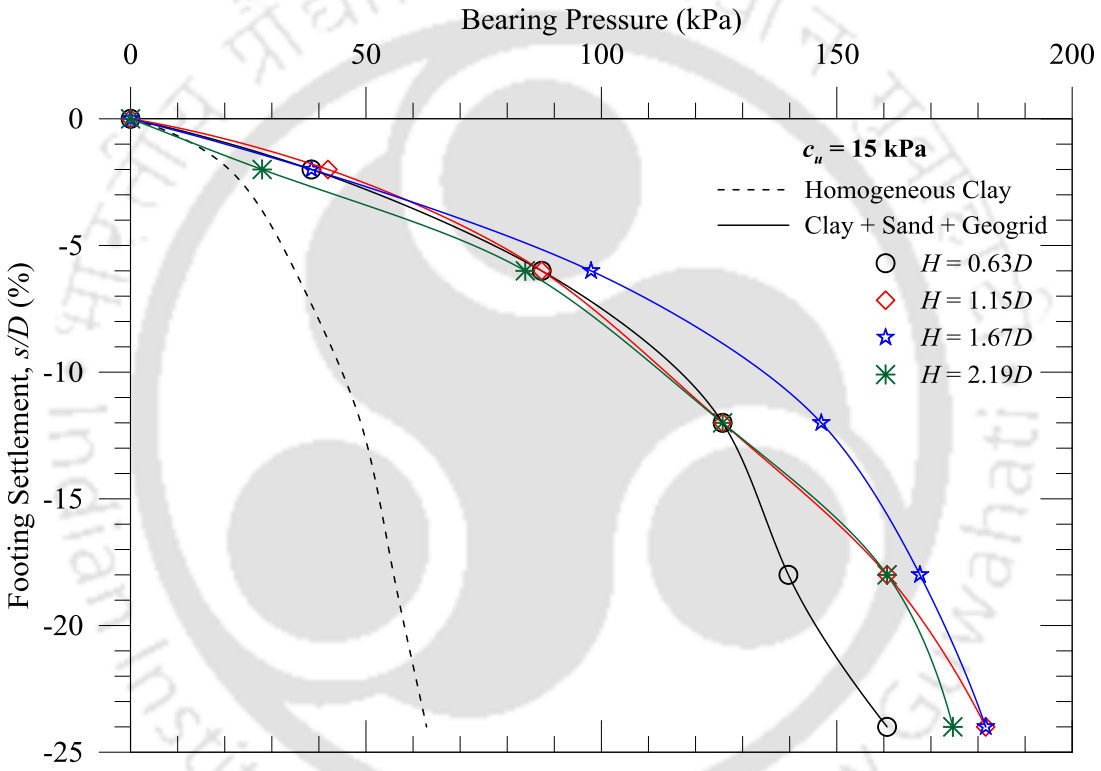

Fig. 5.3 Pressure-settlement responses of geogrid-reinforced foundations: c_u = 15 kPa

A bearing pressure improvement factor, I_{fsg}, is defined as Eq. 5.1 to evaluate the improvements in bearing pressure with geogrid reinforcement. It is the ratio of the bearing pressure of geogrid reinforced foundation (q_{sg}) to the bearing pressure of corresponding homogeneous clay bed (q_c), at similar footing settlement level (*s/D*).

$$(I_{fsg}) = \left(\frac{q_{sg}}{q_c}\right)_{\text{[at same } s/D \text{ level]}} \quad (5.1)$$

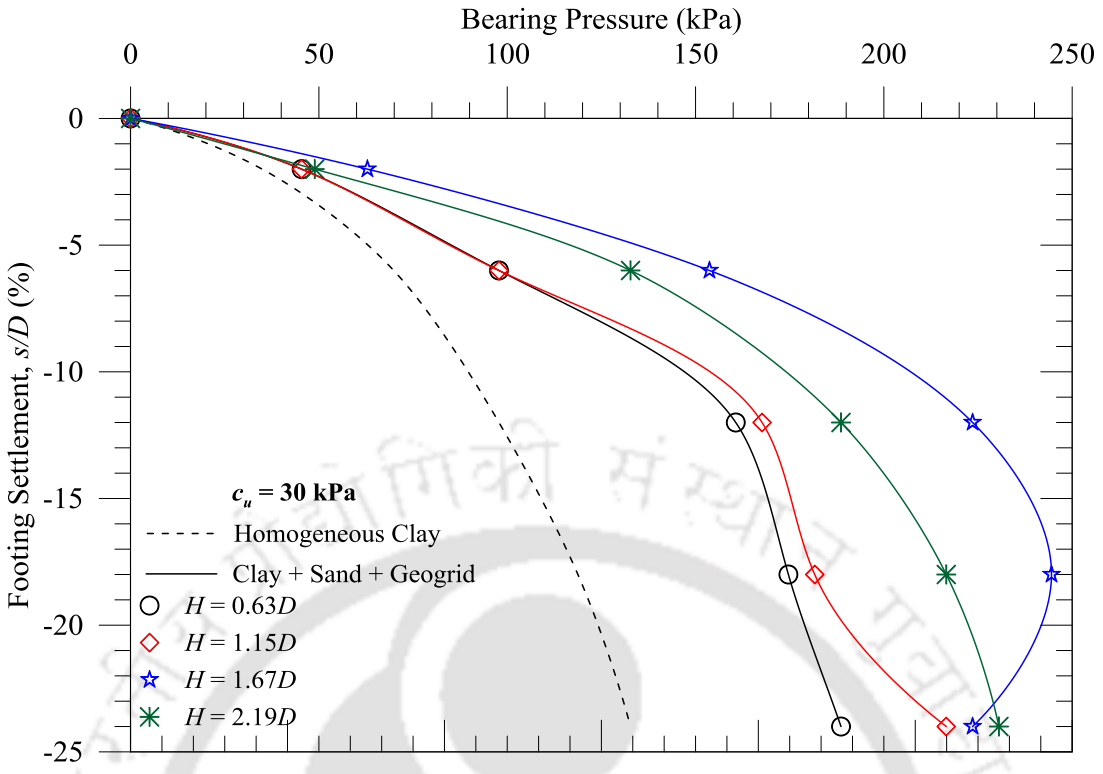

Fig. 5.4 Pressure-settlement responses of geogrid-reinforced foundations: c_u = 30 kPa

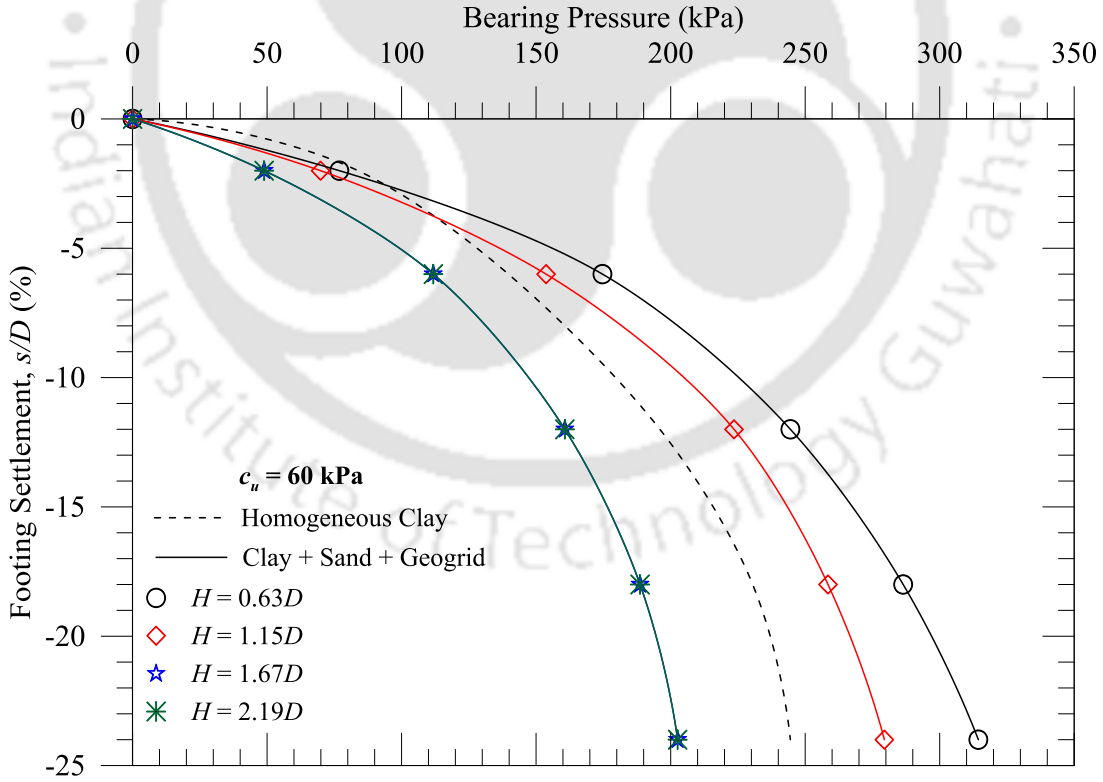

Fig. 5.5 Pressure-settlement responses of geogrid-reinforced foundations: c_u = 60 kPa

The contribution of the interface-geogrid, with respect to the unreinforced layered foundations, is quantified as I_{fg}. It is defined as Eq. 5.2, as the ratio of q_{sg} to the

bearing pressure of unreinforced sand-layered foundations (q_s) at similar levels of *s/D*. The improvement factors are summarized in Table 5.2.

$$(I_{fg}) = (\frac{q_{sg}}{q_s}) \text{ [at same } s/D \text{ level]} \quad (5.2)$$

Table 5.2 Summary of bearing pressure improvement factors

Footing Settlements (*s/D*)	Layer Thickness (*H/D*)	Bearing Pressure Improvement Factor							
		c_u = 7 kPa		c_u = 15 kPa		c_u = 30 kPa		c_u = 60 kPa	
		I_{fsg}	I_{fg}	I_{fsg}	I_{fg}	I_{fsg}	I_{fg}	I_{fsg}	I_{fg}
2%	0.63	1.60	1.33	1.83	1.10	1.30	1.08	0.92	1.38
	1.15	2.40	1.20	2.00	1.09	1.30	1.08	0.83	1.25
	1.67	2.00	1.00	1.83	1.00	1.80	1.00	0.58	1.00
	2.19	2.00	1.00	1.33	1.00	1.40	1.00	0.58	1.00
6%	0.63	1.88	1.36	2.50	1.14	1.40	1.08	1.25	1.39
	1.15	3.26	1.30	2.50	1.14	1.40	1.08	1.10	1.38
	1.67	3.00	1.09	2.80	1.08	2.20	1.00	0.80	1.00
	2.19	3.26	1.04	2.40	1.09	1.90	1.00	0.80	1.00
12%	0.63	2.22	1.54	2.57	1.13	1.64	1.10	1.25	1.52
	1.15	4.00	1.29	2.57	1.13	1.71	1.14	1.14	1.39
	1.67	4.23	1.06	3.00	1.05	2.29	1.00	0.82	1.00
	2.19	4.56	1.03	2.57	1.06	1.93	1.00	0.82	1.00
18%	0.63	2.67	1.60	2.50	1.11	1.47	1.14	1.24	1.64
	1.15	4.23	1.31	2.87	1.15	1.53	1.13	1.12	1.48
	1.67	4.89	1.05	3.00	1.04	2.06	1.03	0.82	1.08
	2.19	5.12	1.05	2.87	1.05	1.82	1.03	0.82	1.08
24%	0.63	3.11	1.75	2.55	1.15	1.42	1.17	1.29	1.55
	1.15	4.23	1.31	2.89	1.13	1.63	1.19	1.14	1.48
	1.67	5.34	1.04	2.89	1.04	1.68	1.03	0.83	1.07
	2.19	5.56	1.04	2.78	1.04	1.74	1.06	0.83	1.07

A typical surface deformation profile of the geogrid-reinforced foundation, for c_u = 7 kPa (at H = 0.63D), is presented in Fig. 5.6. In general, the surface deformations were mostly observed at distance x = D and 2D from footing center; while, it was negligible at x = 3D. It can be noticed that the variations of the deformations were not very consistent with respect to different influencing parameters, such as footing settlement, layer thickness, and the subgrade strengths. However, the observations

provide a general pattern of deformation. The detailed discussions on test results, in analyzing influences of different parameters on the foundation behavior, are presented in the following sections.

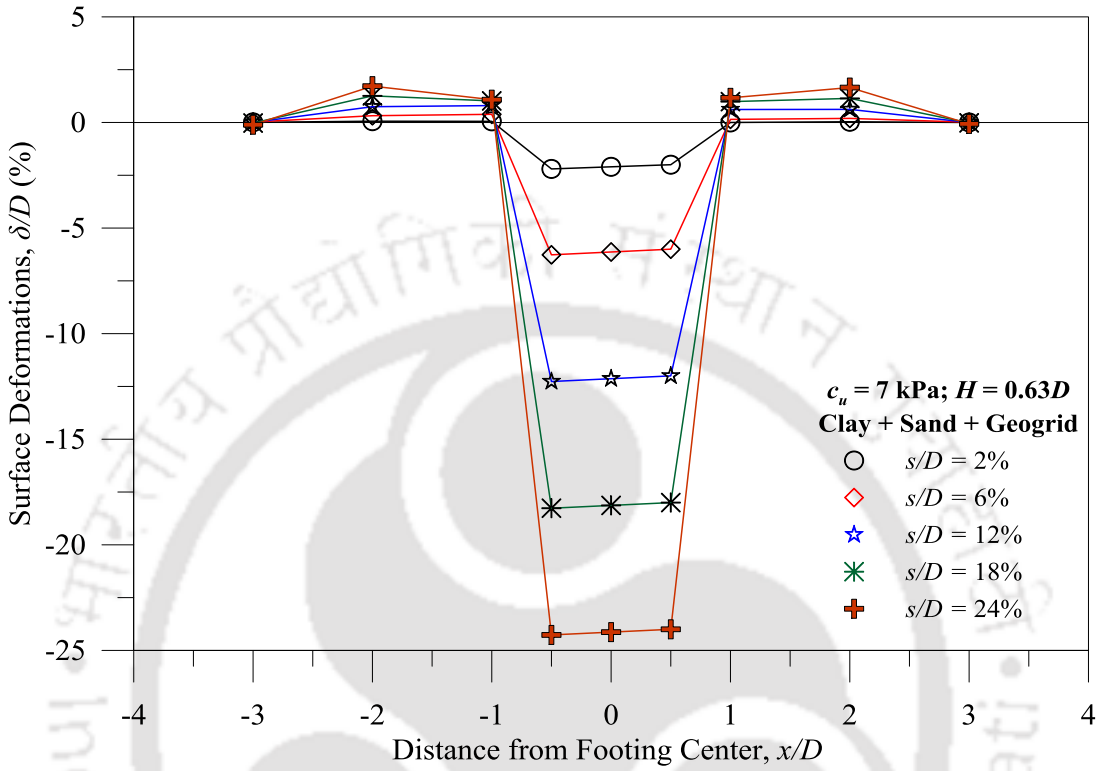

Fig. 5.6 Surface deformation profile for geogrid reinforced foundations: c_u = 7 kPa (H = 0.63D)

5.3 DISCUSSIONS ON TEST RESULTS

Pressure-settlement responses, presented in Fig. 5.2 to Fig. 5.5, indicated that the foundation performances were largely influenced by footing settlements (s/D), layer thicknesses (H), and subgrade strengths (c_u). The following sections provide detailed discussions on the effects of these parameters.

5.3.1 Effect of Footing Settlement (*s/D*)

In Fig. 5.2 to Fig. 5.5, it is noticed that the bearing pressures were increased with the footing settlement. For instance, in Fig. 5.3 (c_u = 15 kPa), bearing pressure is increased from 126 to 175 kPa, for the variation in footing settlement from 12 to 24%

of *s/D* (at $H = 2.19D$). Similarly, for c_u = 30 and 60 kPa, the variation in bearing pressures were about 189 to 231 kPa and 161 to 203 kPa, respectively, for similar foundation configurations (Fig. 5.4 and Fig. 5.5, respectively).

A typical comparison of pressure-settlement responses of unreinforced and geogrid-reinforced foundations is presented in Fig. 5.7, for c_u = 7 kPa. Significant improvement in bearing pressures can be seen with geogrid-reinforced systems as compared to the corresponding unreinforced systems (series A and B). Greater improvement in bearing pressure was noticed at higher settlement levels. At $H = 0.63D$ and *s/D* = 6%, about 1.4 times higher bearing pressure is seen for the geogrid-reinforced system (~52 kPa), as compared to the corresponding value of unreinforced layered system (~38 kPa). In similar layered configuration, the variation in bearing pressures of the unreinforced system was 45 to 56 kPa, in the settlement range 12-24% of *s/D*; while, the corresponding values for geogrid reinforced foundation was about 70 to 98 kPa, respectively. This show about 1.55 and 1.75 times improvement in bearing pressures at 12% and 24% settlement levels. Similar improvements can also be noticed for comparatively stiffer subgrades ($c_u \geq 15$ kPa); however, the improvements were reduced with increase in layer thickness (H) and subgrade strengths (c_u).

Variation of improvement factors, I_{fsg} and I_{fg}, with footing settlements are presented in Fig. 5.8, for c_u = 7 kPa. The contribution of geogrid reinforcement, as compared to the corresponding unreinforced systems, is defined as I_{fg} (Eq. 5.2). It is seen that both the improvement factors are increased with footing settlements. However, for $H > 0.63D$, reduction in the rate of bearing pressure improvements, I_{fsg}, indicated by a flatter slope, is observed at $s/D \geq 12\%$. The reduction was due to punching of the sand column into the subgrade and squeezing out of the sand layer from the footing bottom. Thus, the footing had undergone localized settlement without generating sufficient

strain for the membrane resistance at the interface-geogrid. The effect could be seen in terms of I_{fg} which approached to unity (I_{fg} ~ 1) indicating insufficient or no contribution.

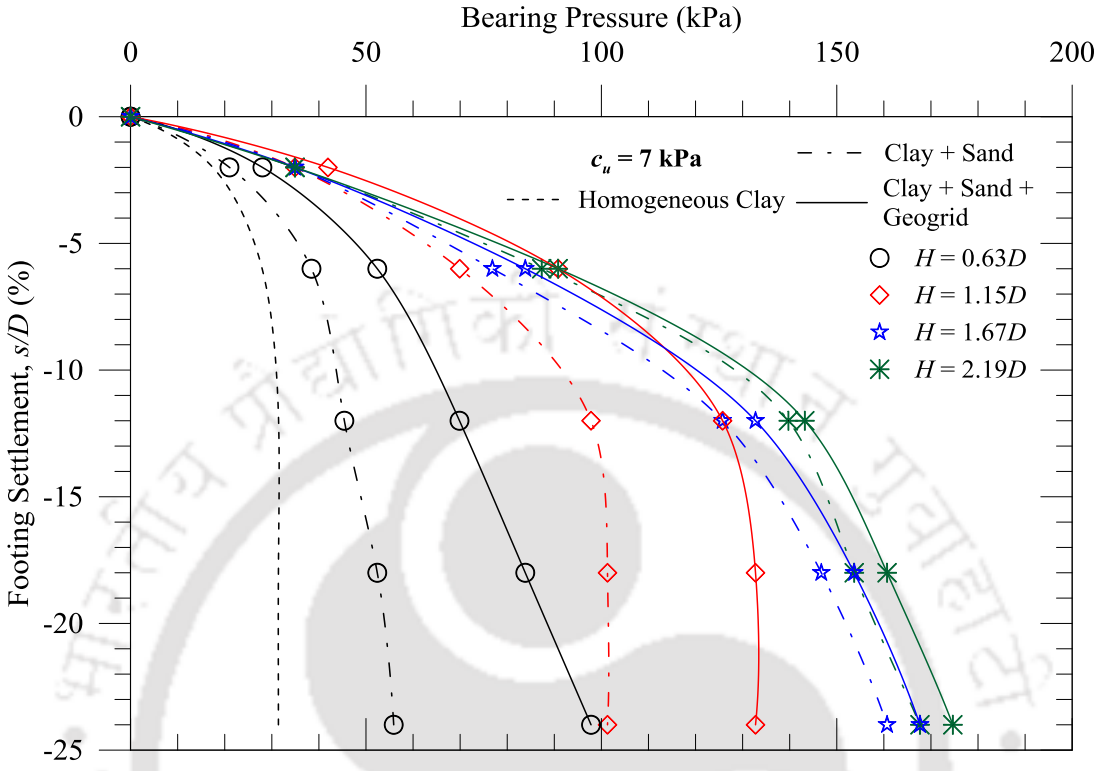

Fig. 5.7 Comparison of pressure-settlement responses: unreinforced and geogrid-reinforced foundations with c_u = 7 kPa

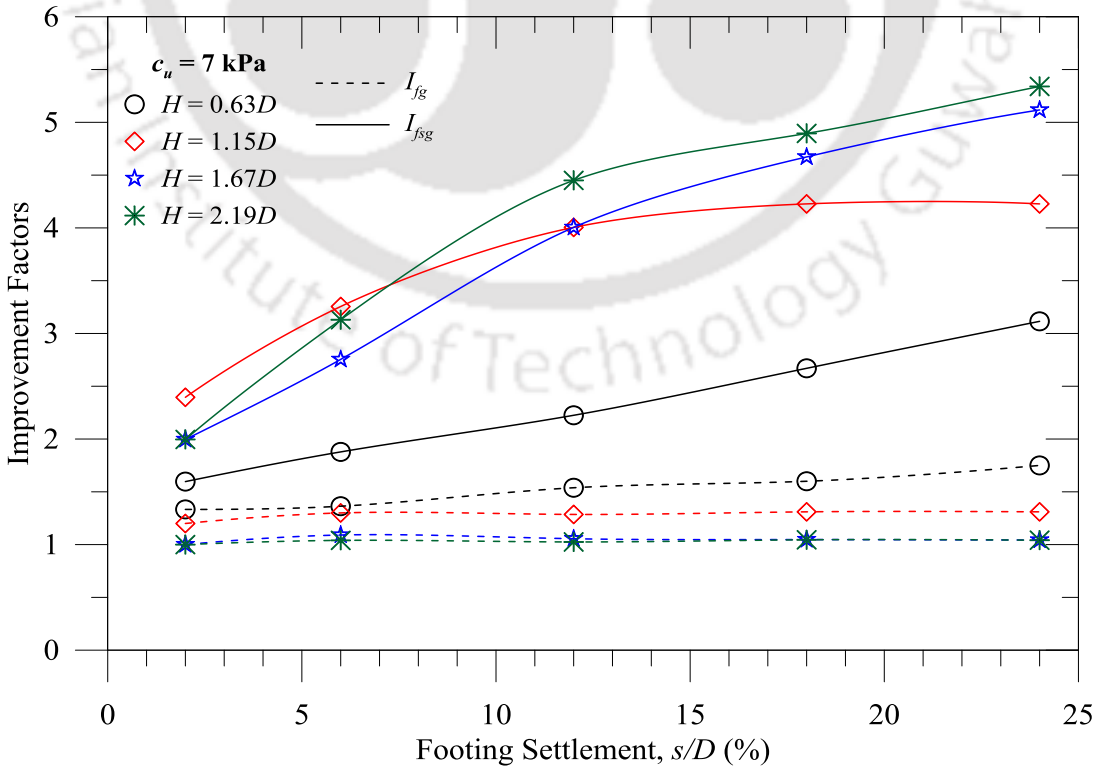

Fig. 5.8 Variation of I_{fsg} and I_{fg} with *s/D* at different *H/D* for c_u = 7 kPa

In Fig. 5.9, typical surface deformation variations at x = D, 2D, and 3D are presented for unreinforced and geogrid reinforced foundations with different levels of footing settlements for c_u = 7 kPa (at H = 0.63D). The deformation response of corresponding homogeneous bed is also presented for comparison. The responses, though not very consistent with respect to distance from footing center, depicted mostly heaving on foundation surface at x = D and 2D and enhanced with increase in footing settlements. However, at x = 3D, variation in surface deformation was negligible with respect to foundation configurations. Marginal surface settlement (± 0.2% of δ/D) at x = 3D can be noticed in Fig. 5.9, for geogrid-reinforced foundation. It is attributed to the movement of interfacial sand layer, being interlocked in geogrid, towards footing center upon load. This was reflected as slight settlements at the foundation surface at x = 3D and enhanced heaving around the footing (x = D and 2D) with the increase in footing settlement levels (s/D).

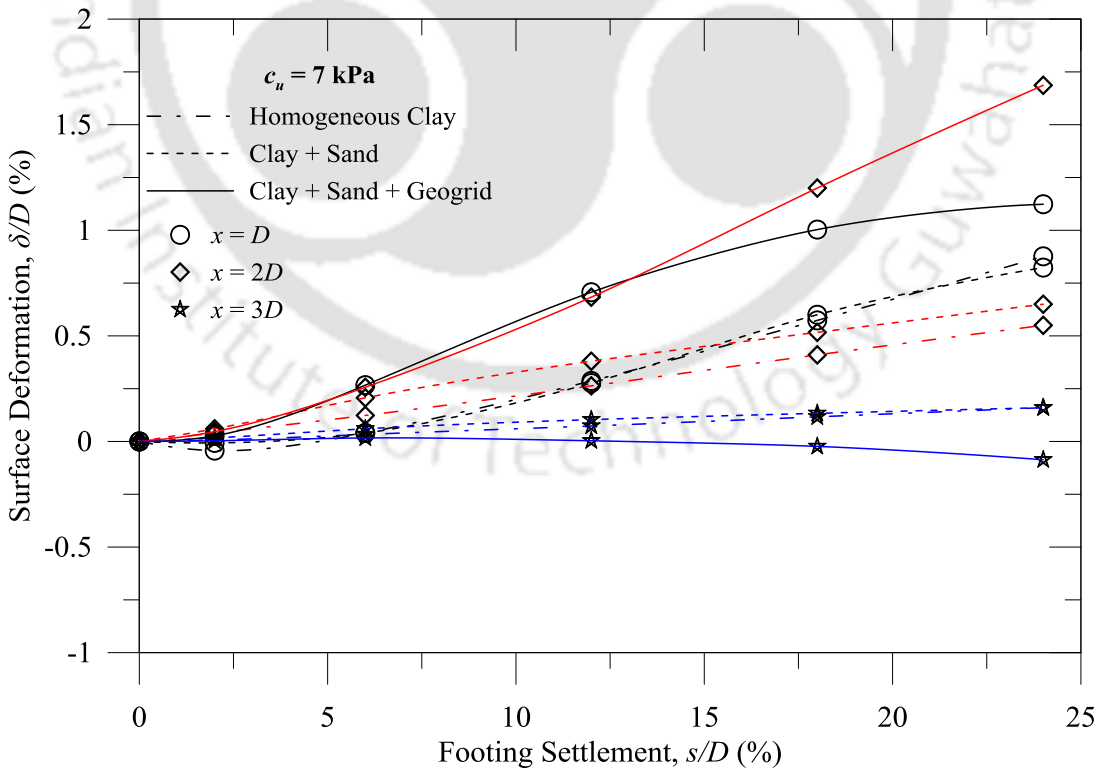

Fig. 5.9 Variation of δ/D with s/D at x = D, 2D, and 3D for c_u = 7 kPa (H = 0.63D)

Improved performances in bearing pressures with increase in footing settlements, for reinforced foundations, are attributed to the 'membrane resistance' mobilized along the planar geogrid (Giroud and Noiray, 1981; Love et al., 1987). It can be defined as the transverse resistance of '2*T*sin*α*', developed through the planar geogrid due to soil-geosynthetic interfacial resistance '*T*', when the geogrid deflects at an angle '*α*', as shown in Fig. 5.10. The deflection angle, *α*, is expected to increase with the footing settlement which further contributes to the enhanced membrane resistance. Though, no deformation measurements regarding this were available in the present test program, post-test exhumations indicated visible deformations of clay subgrades. Besides, impressions of geogrid apertures were observed on the clay subgrade, indicating that interlocking took place during footing settlement through the clay subgrade. Similar deformation observations at the interface and interlocking aspects were also reported by Love et al. (1987).

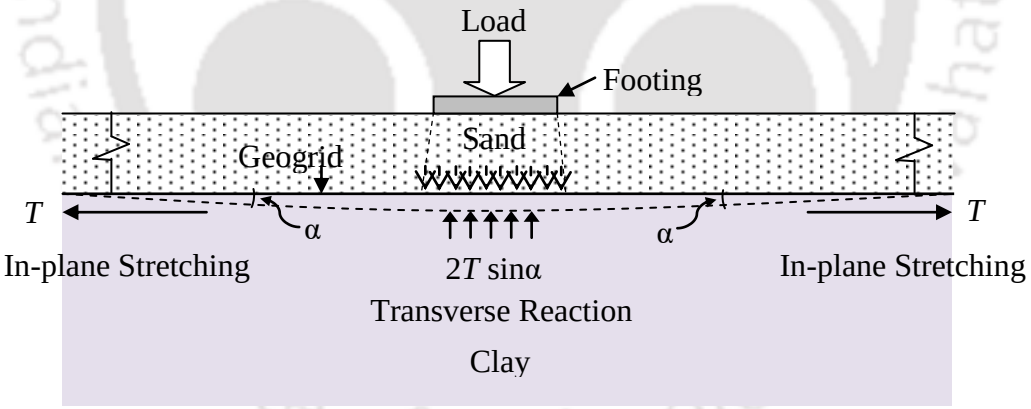

Fig. 5.10 Membrane action of planar geogrid

5.3.2 Effect of Layer Thickness (H)

The responses shown in Fig. 5.2 to Fig. 5.5 and Fig. 5.7 have indicated that the sand layer thicknesses (*H*), in the range of 0.63*D* to 2.19*D*, significantly affected the foundation behavior at a given footing settlement. For instance, in Fig. 5.7 for c_u = 7 kPa, bearing pressures at *s/D* = 12% are enhanced from 70 kPa to 126, 133, and 143

kPa for the layer thickness (*H/D*) variation from 0.63 to 1.15, 1.67, and 2.19, respectively. In this case bearing pressures were improved with increase in *H/D* values. However, this is not true at the other settlement levels (such as *s/D* = 2% and 6%) and for other subgrades (c_u = 15 and 30 kPa). For comparatively stiffer subgrades (c_u = 15 and 30 kPa), a reduction in the rate of improvement can be observed for thicker layers ($H \geq 1.67D$) (Fig. 5.3 and Fig. 5.4). Reduction in pressure values were also noticed for the stiff clay subgrade (c_u = 60 kPa) for $H \geq 1.15D$ (Fig. 5.5). This can be attributed to the insufficient strain generated at the geogrid interface to derive the membrane resistance which can be the result of the followings: squeezing out of sand from footing bottom and the reduction in pressure intensity with increased layer thickness.

The improvement factors (I_{fsg} and I_{fg}), summarized in Table 5.2, indicate that I_{fsg} for different subgrades are in the range of 0.76-5.56. Variations in improvement factors, I_{fsg} and I_{fg}, with change in layer thickness for different subgrades, at two different levels of footing settlement (s/*D* = 12 and 24%), are presented in Fig. 5.11. The figure depicts that the layer thickness is significantly influencing the improvement for very soft subgrade (c_u = 7 kPa); while, the effect is marginal for other stiffer subgrades. For very stiff subgrade, c_u = 60 kPa, increase in layer thickness showed a negative effect. The improvement factor I_{fg} (q_{sg} / q_s), showing the geogrid-contribution, is also depicted a decreasing trend with increase in layer thickness. The I_{fg} is found in the range of 1.0-1.75 (Table 5.2). The I_{fg} values approached 1.0 indicating no geogrid contribution, beyond a thickness of 1.67*D*. This behaviour can be inferred due to the fact that, as geogrid placement depth increases the reinforcement effect decreases (Guido et al., 1986; Mandal and Sah, 1992; Khing et al., 1994). Further, as typical foundation systems show significant depth of about 1 to 1.5 times diameter (or width) of the

footing (Terzaghi, 1943; Meyerhof, 1974; Terzaghi et al., 1996), geogrid placed at a depth beyond 1.67*D* showed practically no contribution.

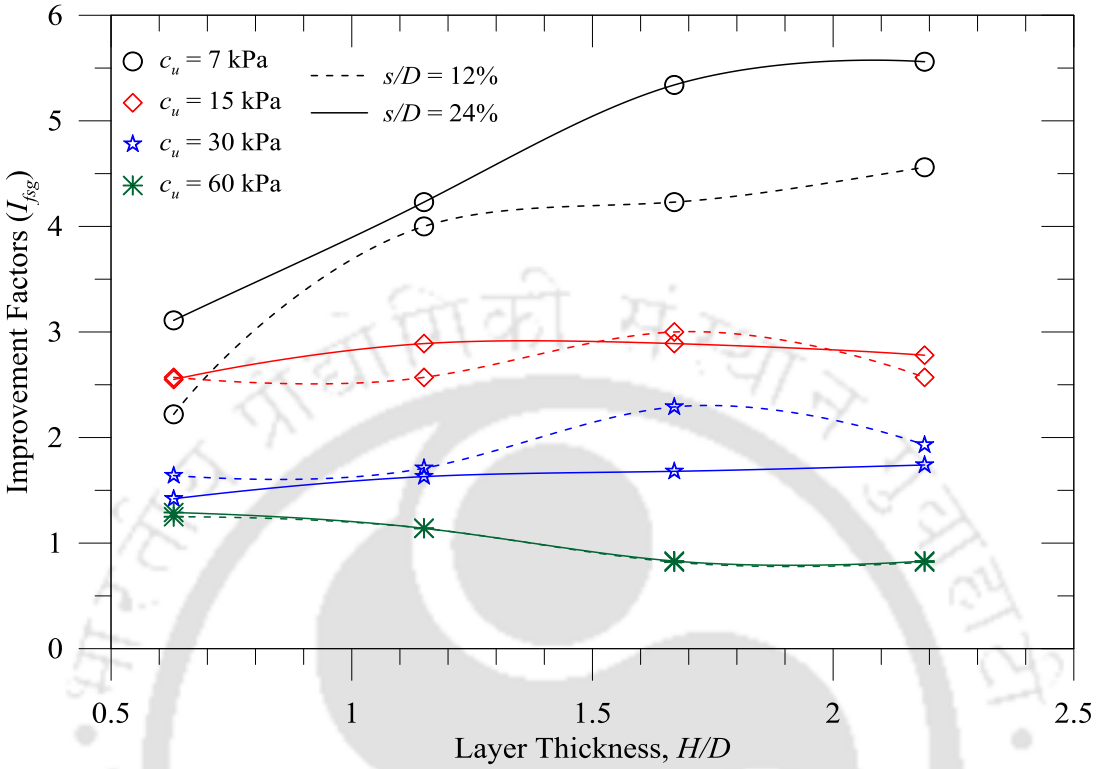

Fig. 5.11 Effect of layer thickness (*H*) in terms of I_{fsg} at s/*D* = 12 and 24%

Typical average surface deformations, at *x* = *D* and 2*D* are presented in Fig. 5.12 and Fig. 5.13, respectively, for different layered configurations (*H* = 0.63, 1.15, 1.67, and 2.19*D*, for c_u = 7 kPa), at different levels of footing settlements (s/*D* = 6, 12, and 24%). The deformation profiles of corresponding unreinforced foundations are also included in the figures. Though the responses are not very consistent with the sand-layer thickness variations, however, mostly heaving was observed at the foundation surface as compared to unreinforced systems. It is due to the combined effect of undrained behavior of saturated clay and dilation of the dense sand. Besides, it has been further enhanced due to sand-squeezing and centrally-loaded flexible plate like behavior of the planar geogrid. Marginal variations in deformation, for unreinforced and geogrid reinforced foundations, can be noticed at *x* = *D* for *H* = 2.19*D*; while, at *x* =

2*D*, the variation was negligible for $H \geq 1.67D$. This observation is also indicates the reduction in geogrid effect with increase in layer thickness.

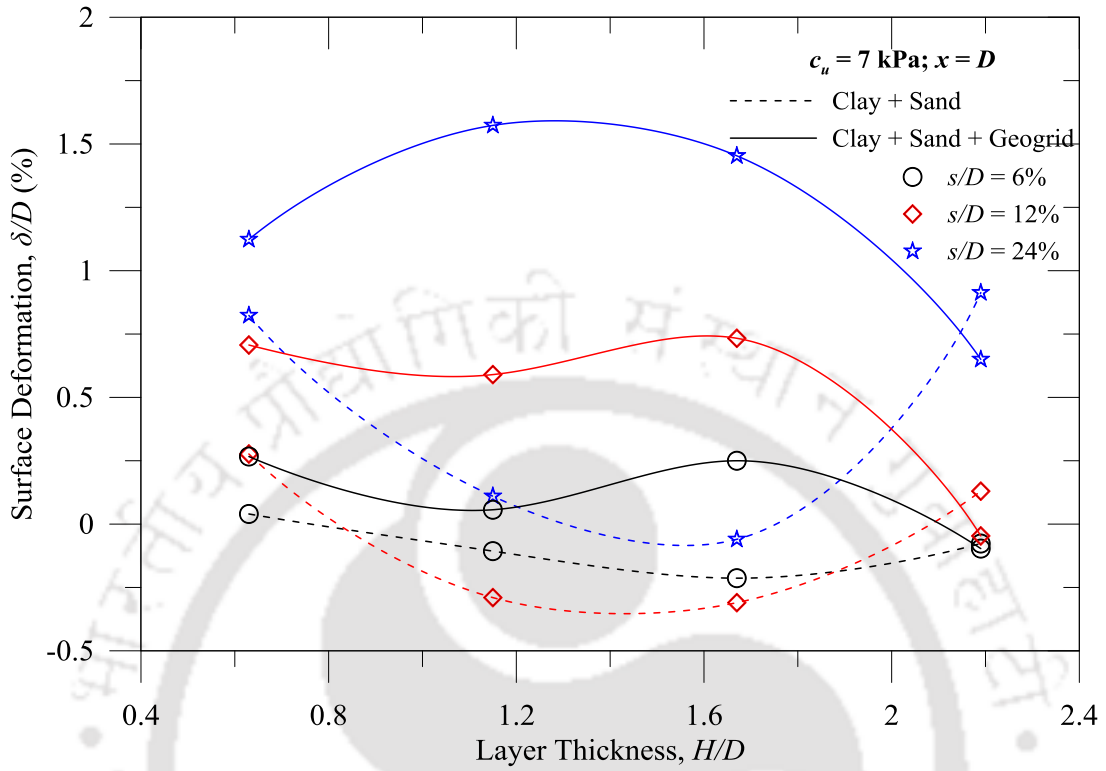

Fig. 5.12 Typical variation of surface deformation at $x = D$ for different geogrid-reinforced foundations with c_u = 7 kPa at s/D = 6, 12, and 24%

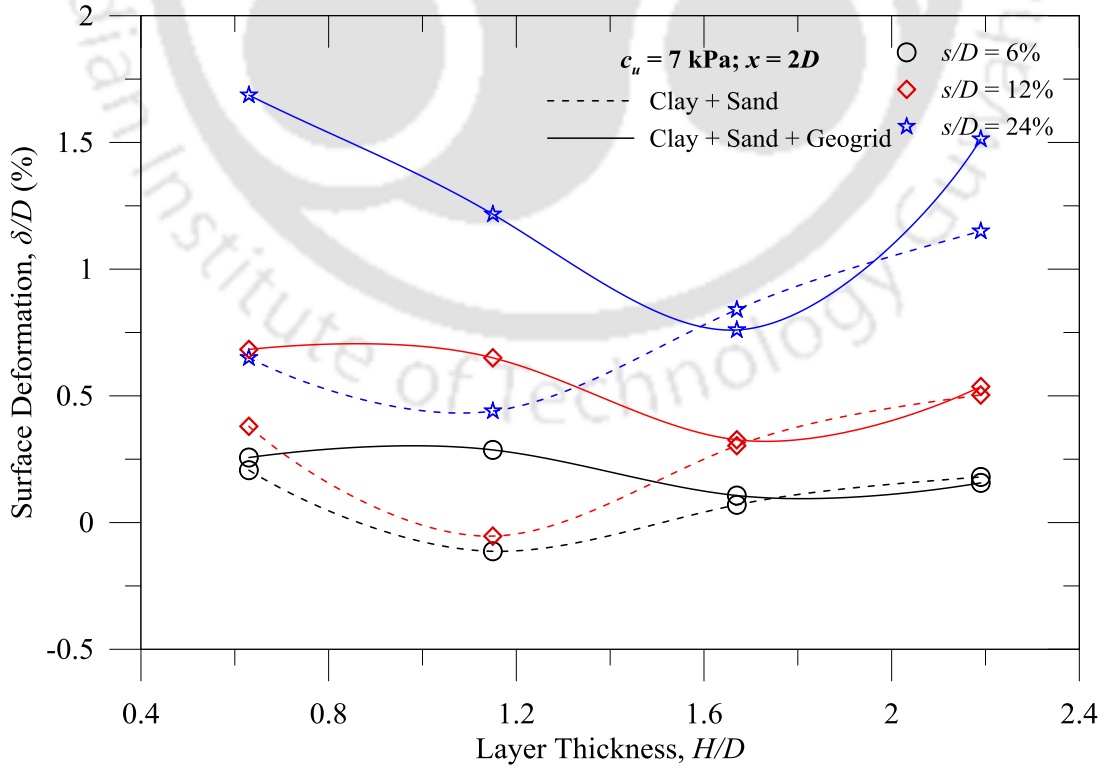

Fig. 5.13 Typical variation of surface deformation at $x = 2D$ for different geogrid-reinforced foundations with c_u = 7 kPa at s/D = 6, 12, and 24%

5.3.3 Effect of Subgrade Strength (c_u)

Pressure-settlement responses of the unreinforced and geogrid-reinforced layered foundations, at $H = 0.63D$ with different subgrades (c_u), are presented in Fig. 5.14. For all the clay subgrades, geogrid-reinforced foundations showed higher bearing pressures compared to the corresponding unreinforced layered systems. The bearing pressure of unreinforced layered foundations are about 45, 112, 147, and 161 kPa for c_u = 7, 15, 30, and 60 kPa, respectively, at s/D = 12%. The bearing pressures with the geogrid reinforcement, at similar settlement level and subgrade variations are increased to 70, 126, 161, and 245 kPa.

The pressure-settlement responses of homogeneous, unreinforced, and geogrid reinforced layered foundations, for c_u = 7 and 60 kPa (at $H = 0.63D$), are compared in Fig. 5.15. Considerably higher improvement in bearing pressures can be observed for the geogrid reinforced foundations as compared to corresponding homogeneous and unreinforced layered foundations. Variation in bearing pressures of about 31, 45, and 70 kPa, for the homogeneous, unreinforced, and geogrid-reinforced foundations, respectively, can be noted for c_u = 7 kPa (at s/D = 12%). The variations for c_u = 60 kPa, in similar foundation configurations and settlement level, are about 196, 161, and 245 kPa. It is observed that the planar geogrid is mostly effective in softer clay subgrades ($c_u \leq$ 15 kPa) and shorter layer thicknesses ($H \leq 1.15D$). The effectiveness of planar geogrid was gradually decreased with subgrade strengths (c_u) which could be seen through I_{fsg}. The improvement factor, I_{fsg}, is found in the range of 1.33-5.56 for $c_u \leq$ 15 kPa; while, for comparatively stiffer subgrades ($c_u \geq$ 30 kPa), it is in the range of 0.58-2.29 (Table 5.2). The I_{fsg} values less than unity were observed for c_u = 60 kPa at low settlement levels and for higher layer thicknesses ($H/D \geq 1.67$). It was due to obvious

reasons of relatively softer sandy soil overlying the stiff clay subgrade and insufficient membrane resistance under such conditions.

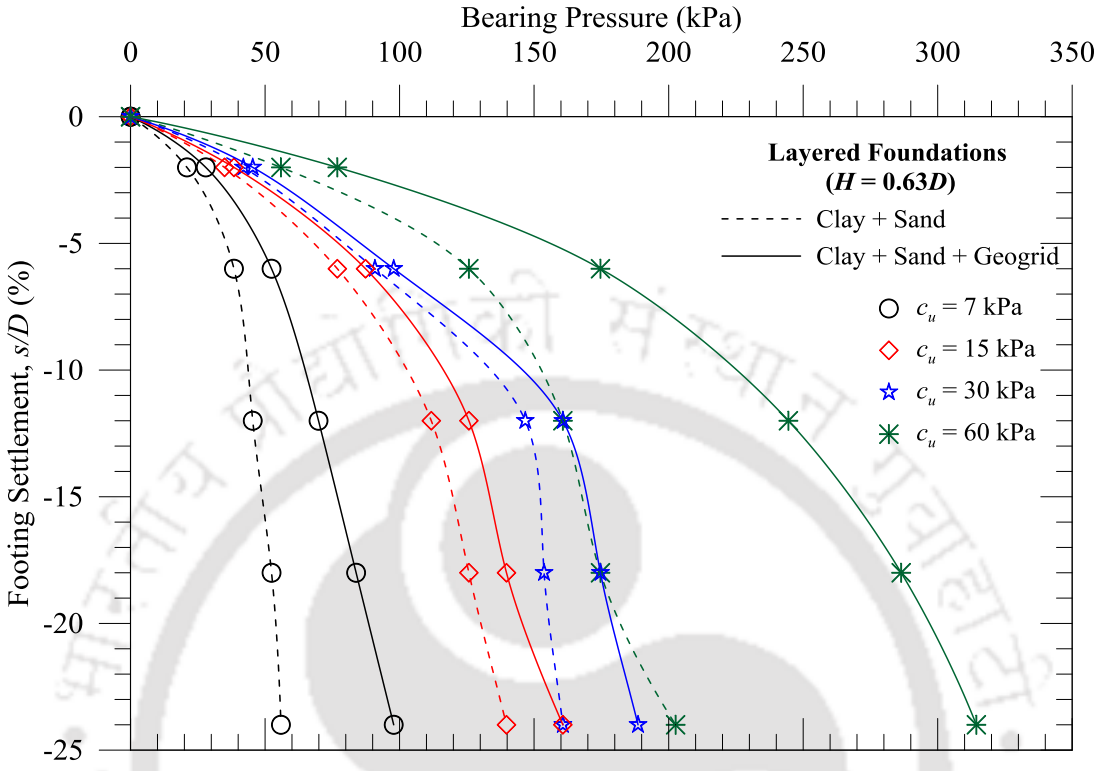

Fig. 5.14 Responses of geogrid-reinforced foundations for different c_u at H = 0.63D

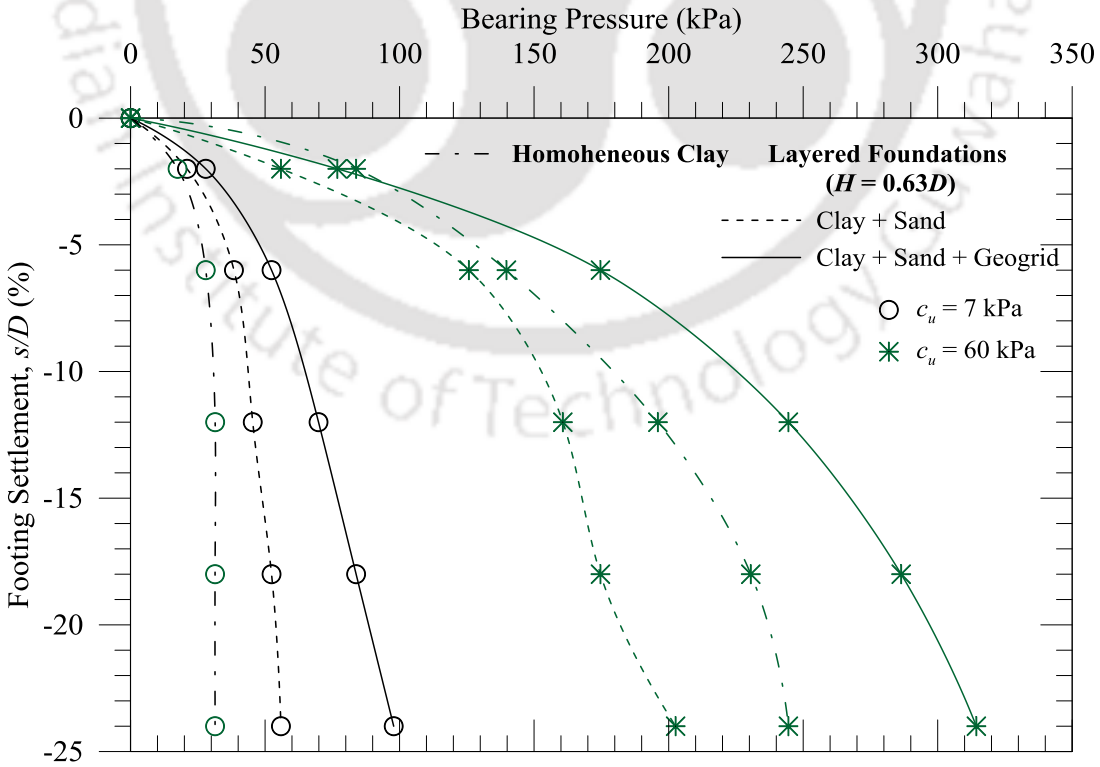

Fig. 5.15 Responses of homogeneous, unreinforced, and geogrid-reinforced foundations for c_u = 7 and 60 kPa at H = 0.63D

Variation of I_{fsg} is presented in Fig. 5.16, for different foundation configurations (H = 0.63 to 2.19D) overlying varying subgrades (c_u = 7 to 60 kPa), at two different levels of footing settlements (s/D = 12 and 24%). The decreasing trend in improvement factor with increasing c_u can be noticed which is irrespective of layer thickness variations.

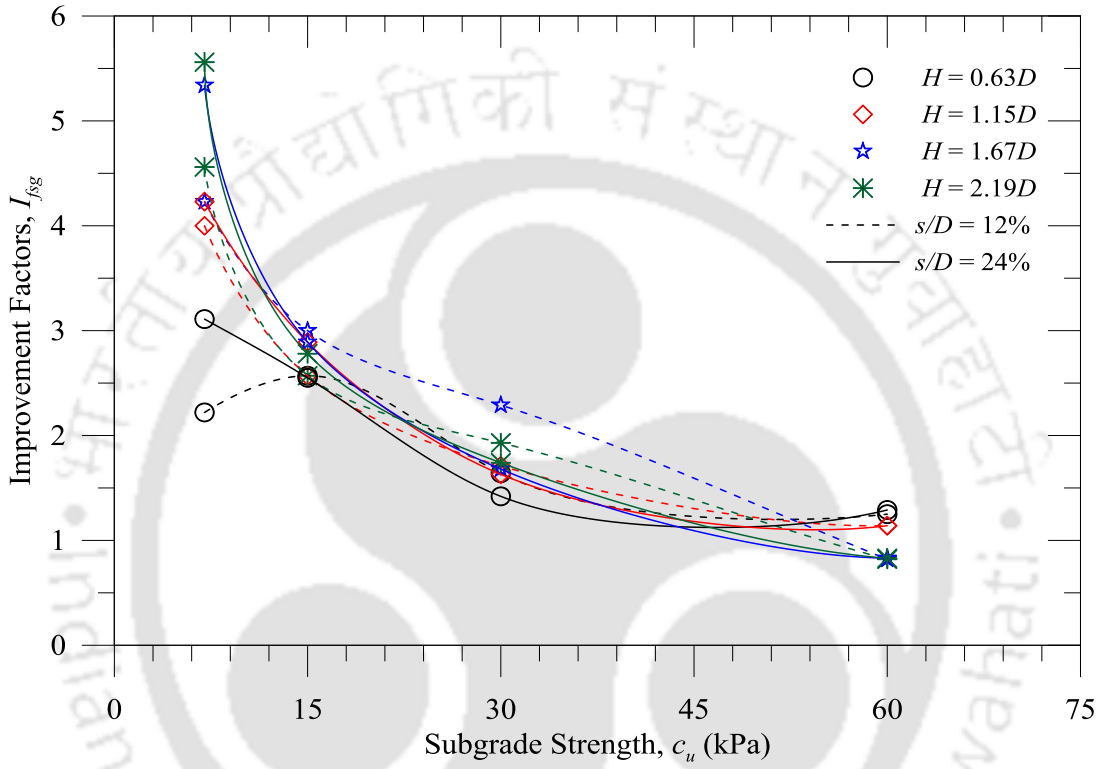

Fig. 5.16 Variation in I_{fsg} for varying c_u and H/D at s/D = 12 and 24%

The variation of I_{fg} (= q_{sg} / q_s), corresponding to similar foundation configurations, is presented in Fig. 5.17. In Fig. 5.17 (also in Table 5.2), comparatively higher contribution of geogrid, in terms of I_{fg}, can be found for c_u = 60 kPa (for $H \leq$ 1.15D). In this layer configuration, the I_{fg} is in the range of 1.25-1.64 for c_u = 60 kPa as compared to 1.2-1.6, 1.09-1.15, and 1.08-1.19 for c_u = 7, 15, and 30 kPa, respectively. This anomaly in general trend is due to the definition of I_{fg}, wherein, it is evaluated with respect to the bearing pressure of unreinforced layered foundations (q_s). In unreinforced layered configurations, the bearing pressures for c_u = 60 kPa were reduced as compared to homogeneous clay bed ($q_s < q_c$) due to relatively softer sandy layer was replaced the

stiff clay layer. However, with planar geogrid, higher bearing pressures were obtained compared to corresponding homogeneous clay bed ($q_{sg} > q_c$) and unreinforced layered foundations ($q_{sg} > q_s$). Therefore, the I_{fg} (i.e. q_{sg} / q_s) is magnified for 60 kPa (as $q_c > q_s$), compared to the other subgrades ($c_u \leq 30$ kPa).

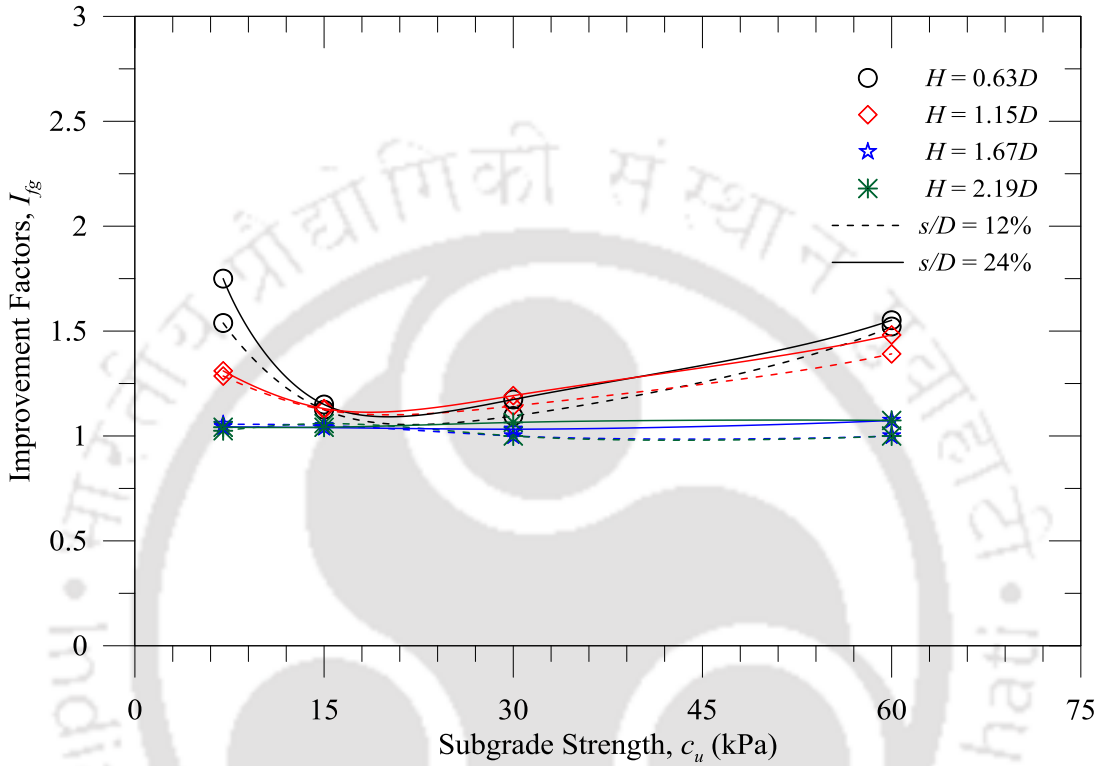

Fig. 5.17 Variation in I_{fg} for varying c_u and H/D at s/D = 12 and 24%

Typical surface deformations at D and $2D$ distances from footing centre are presented in Fig. 5.18 and Fig. 5.19, respectively, for unreinforced and geogrid-reinforced layered systems at $H = 0.63D$ with varying subgrades (c_u) and different s/D levels (6, 12, and 24%). It can be noticed that, for geogrid reinforced systems, heaving was pronounced at $x = D$, irrespective of subgrade strengths (c_u); while, in some instances, it is reduced at $x = 2D$, as compared to unreinforced layered cases. The surface deformations of geogrid reinforced foundations were predominantly influenced by the plate like deformation of the geogrid (membrane action). During loading, sand particles were interlocked within the geogrid apertures and pulled towards the footing center. This affected as settlement at foundation surface away from the footing center (x

= 2*D*) and enhanced heaving around the footing (*x* = *D*). The surface heaving at *x* = *D* was further enhanced by the higher sand-squeezing from footing bottom due to greater penetration resistance provided by the interface-geogrid.

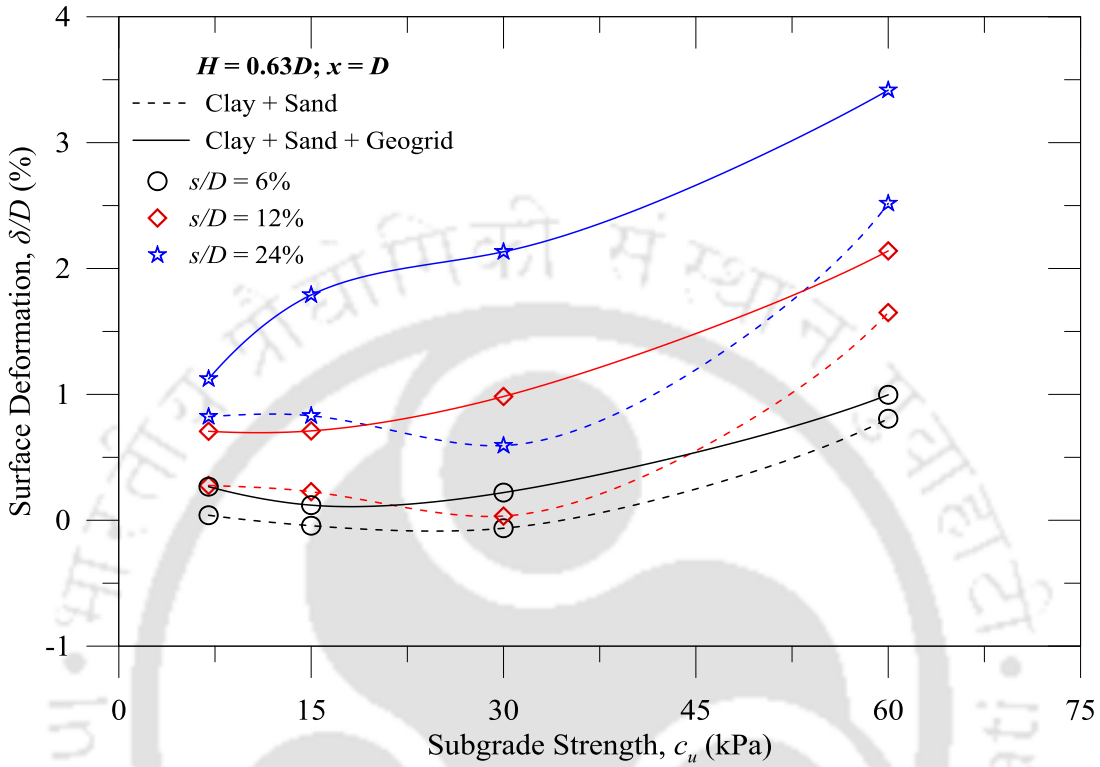

Fig. 5.18 Surface deformation at *x* = *D* for varying subgrade (*H* = 0.63*D*)

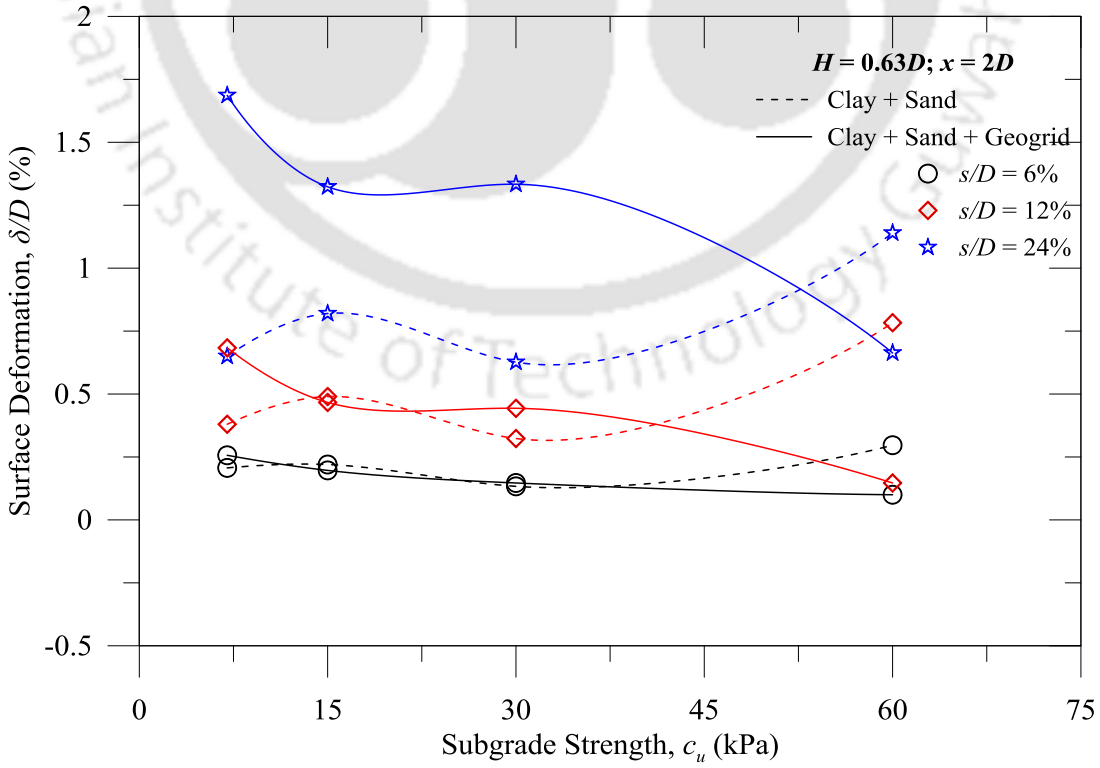

Fig. 5.19 Surface deformation at *x* = 2*D* for varying subgrade (*H* = 0.63*D*)

A comparison of experimental observations and theoretical analysis is presented in Fig. 5.21 and Fig. 5.20 for H = 0.63D and c_u = 7 kPa, respectively. The theoretical approaches proposed by Giroud and Noiray (1981), Love et al. (1987) and Burd (1995) were considered for the analysis. However, in present study, observations related to membrane action were not available and hence, these parameters are assumed as per literature. The figures are presented considerably good agreement between the experimental observations and theoretical analysis. The theoretical bearing capacities are evaluated as per eq. 5.3.

$$q = (\pi + 2)\, c_u \frac{B'}{B} + \frac{(3T \sin \Psi)}{B} \tag{5.3}$$

where, B' = width of the rough footing on the clay surface,

B = footing width,

T = tensile strength of the geogrid,

Ψ = deformation angle for geogrid at clay surface.

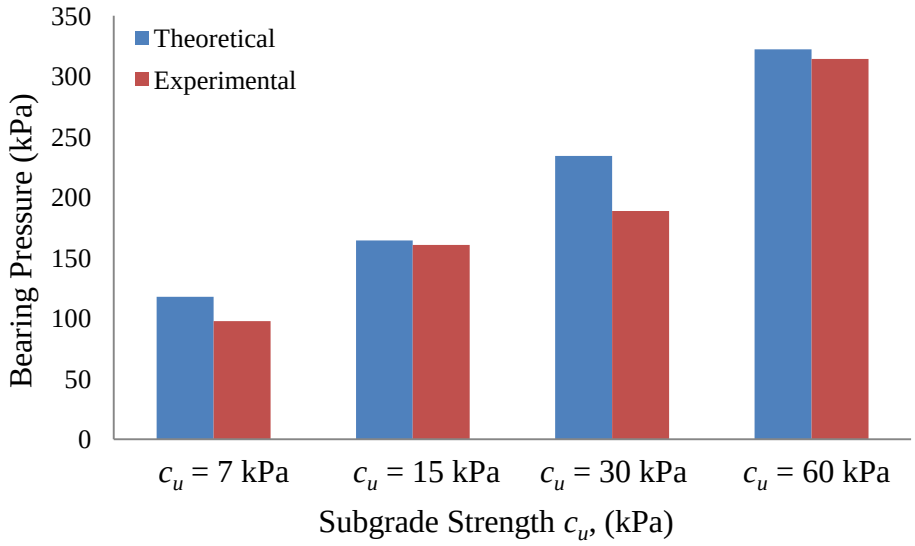

Fig. 5.20 Comparison of theoretical and experimental maximum bearing pressure for geogrid reinforced foundations overlying different clay subgrades at H = 0.63D

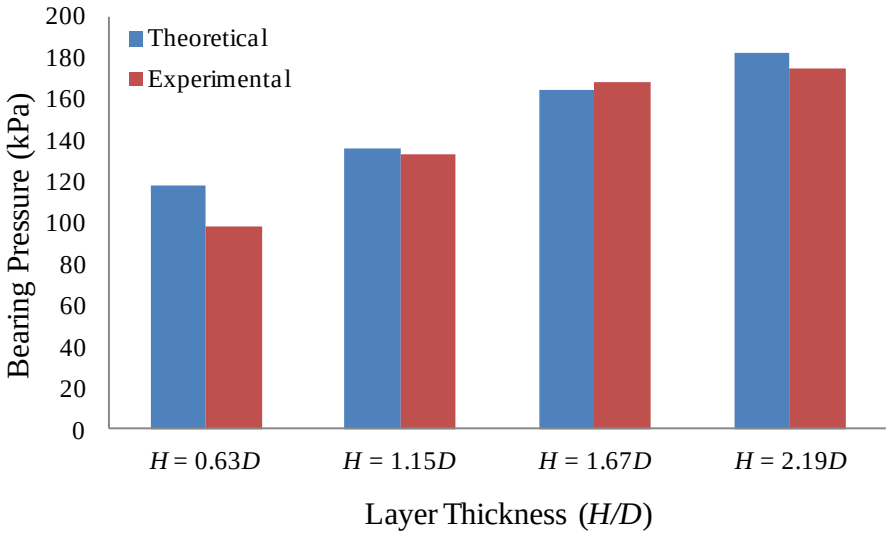

Fig. 5.21 Comparison of theoretical and experimental maximum bearing pressure for different geogrid reinforced foundations overlying clay subgrade for c_u = 7 kPa

5.4 POST EXPERIMENTAL OBSERVATIONS

Visual inspection was made after each experiment by post-test exhumation up to *H*, to study the physical deformations of the clay subgrades. Fig. 5.22 shows such visual observation for clay subgrade of c_u = 7 kPa at $H = 0.63D$, for unreinforced and geogrid-reinforced layered foundations. In unreinforced cases, circular bowl-shaped depressions, having diameter larger than the footing (Fig. 5.22a) were observed which were resulted from the sand-column penetration on the clay subgrades. In geogrid-reinforced cases, similar circular bowl-shaped depressions, accompanied by impressions of geogrid apertures were observed (Fig. 5.22b). The geogrid-impressions are signifying the soil-geogrid interlocking. In geogrid reinforced case, the depths of the depressions were reduced and the diameters of the depressions were further increased, as compared to unreinforced cases. This signifies the higher load distribution to larger area on the clay subgrade, through the interface-geogrid. The reduction in depression-depths and increase in depression-diameters were noticed as the subgrade strength and layer thicknesses were increased.

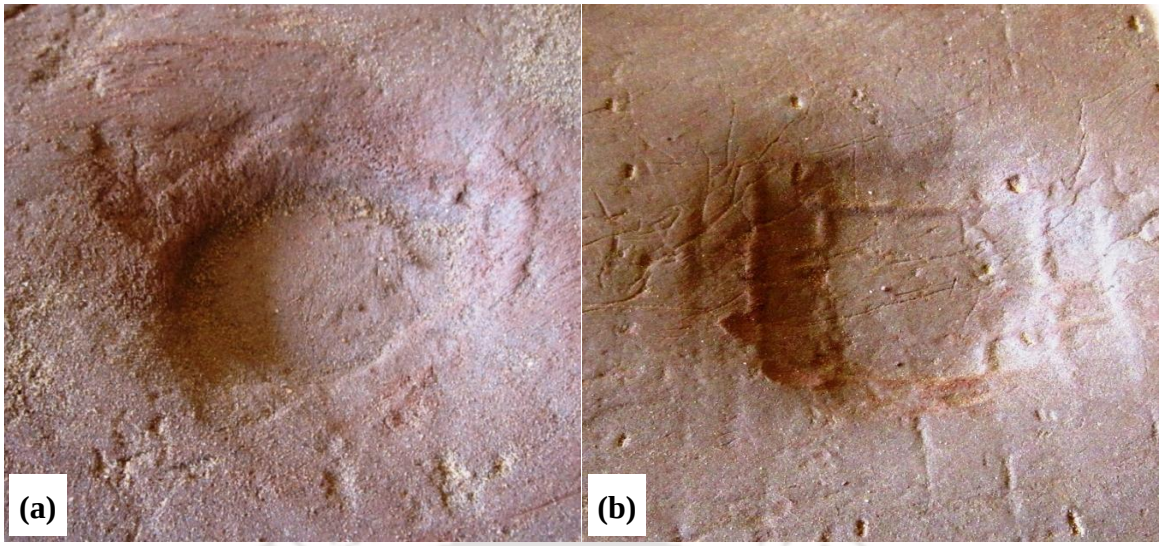

Fig. 5.22 Subgrade deformation for (a) unreinforced and (b) geogrid-reinforced foundations (c_u = 7 kPa with H = 0.63D)

5.5 SUMMARY

Foundation responses investigated in series C, with a geogrid of width 'b' placed at sand-clay interface, are presented in this chapter. Considerable improvements in pressure-settlement responses were noticed as compared to the corresponding unreinforced foundations. The beneficial effect of geogrid reinforcement is attributed to the 'membrane resistance' due to mobilized strain (or deformations). The improvements in bearing pressures were decreased with increase in subgrade strengths and layer thickness. A maximum of 5.6-fold improvement (I_{fsg}) over the corresponding homogeneous clay bed was observed for c_u = 7 kPa; while that of for the stiff clay of 60 kPa was found as about 1.29. The maximum contribution of geogrid, in terms of I_{fg}, was about 1.75-fold over the similar unreinforced layered configuration on c_u = 7 kPa. The influence of the geogrid was significant even for c_u = 60 kPa (for $H \leq 1.15D$) in which case the I_{fg} was in the range of 1.25-1.64. However, it is seen that the interfacial-geogrid can be beneficial up to a sand layer thickness of 1.67D, over the softer clay subgrades.

Chapter 6. GEOCELL REINFORCED FOUNDATIONS

6.1 INTRODUCTION

Behaviour of geocell-reinforced foundations, investigated under series D, is presented in this chapter. Schematic diagram of the foundation configuration considered in this series is shown in Fig. 6.1. Geocell mattress of width '*b*' and height '*h*' with pocket size '*d*' was placed on clay subgrades. The heights of the geocells (*h*) were selected in such a way that combining with the sand cushion thickness (u = 0.1D), the total thickness of the geocell-sand layer will be the '*H*' that was considered in the series B and C (i.e., $H = h + u$). Details of the test series are presented in Table 6.1. The heights of geocell-mattress (*h*) were varied as 0.53, 1.05, 1.57, and 2.09*D*. Parameters, such as size of geocell-pockets (d = 0.8D), geometry of geocell-mattress ($b = l$ = 6D) and relative density of sand (D_r = 80%) were kept constant.

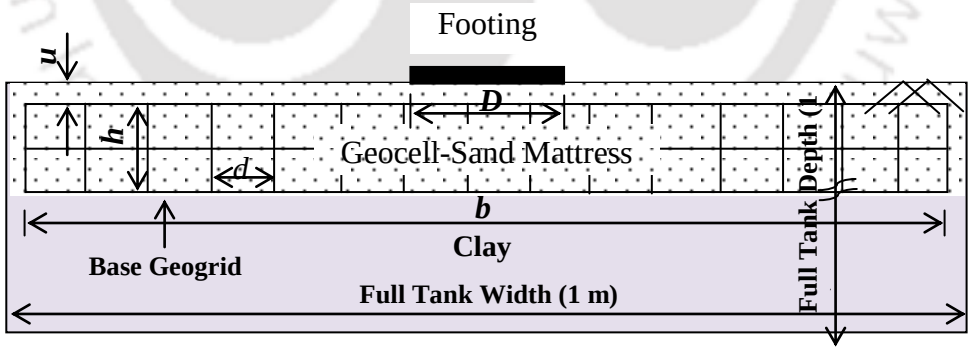

Fig. 6.1 Schematic of geocell-reinforced foundations followed in series D

Table 6.1 Details of the test series D

Test Series	Foundation System	Test parameters		No. of Tests
		Variables	Constants	
D	Geocell-reinforced sand overlying clay subgrades	c_u = 7, 15, 30, 60 kPa h/D = 0.53, 1.05, 1.57, 2.09	D_r = 80% u = 0.1D, d/D = 0.8, b/D = 6	16

6.2 TEST RESULTS

The pressure-settlement responses of geocell-reinforced foundations on different clay subgrades (c_u = 7, 15, 30, and 60 kPa), are presented in Fig. 6.2 to Fig. 6.5. The figures also present the corresponding homogeneous clay beds' responses that were obtained in series A. In general, significantly high bearing pressures were observed for geocell-reinforced foundations as compared to corresponding homogeneous clay beds at similar settlement levels. Maximum bearing pressures of about 363, 377, 398, and 559 kPa (at H = 2.19D and s/D = 24%) can be noted for geocell-reinforced foundations with c_u = 7, 15, 30, and 60 kPa, respectively. The corresponding bearing pressures for homogeneous clay beds were 31, 63, 133, and 245 kPa, respectively.

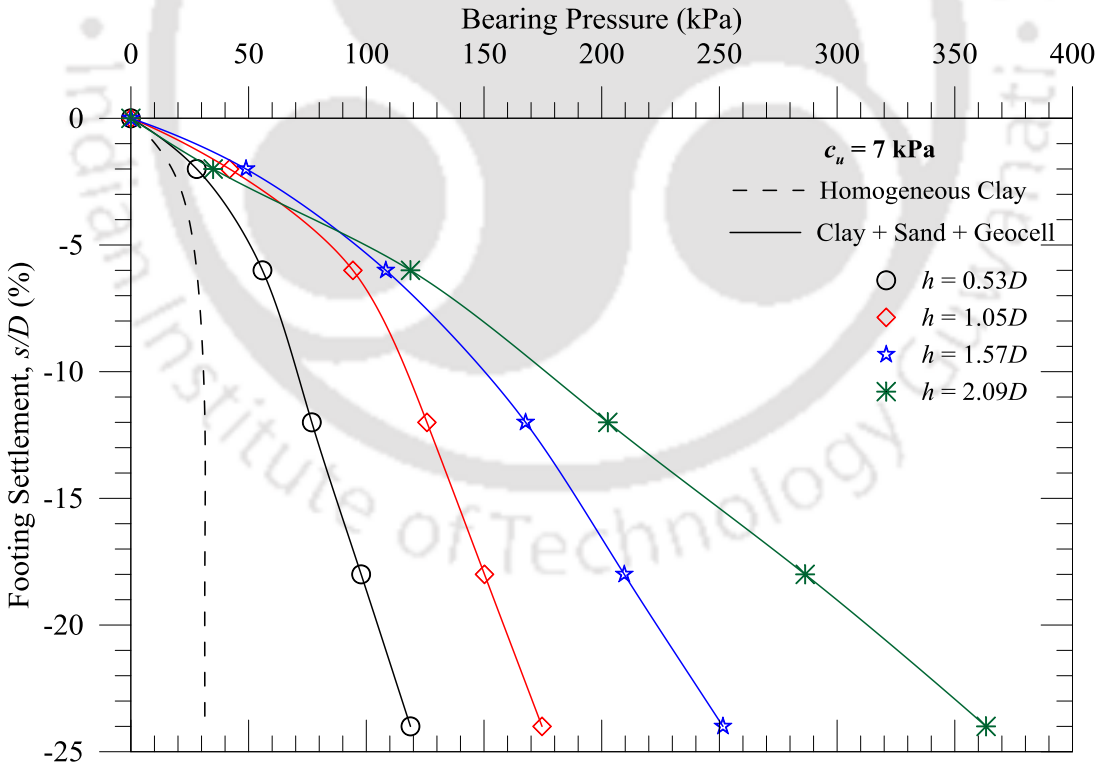

Fig. 6.2 Pressure-settlement responses of geocell-reinforced foundations: c_u = 7 kPa

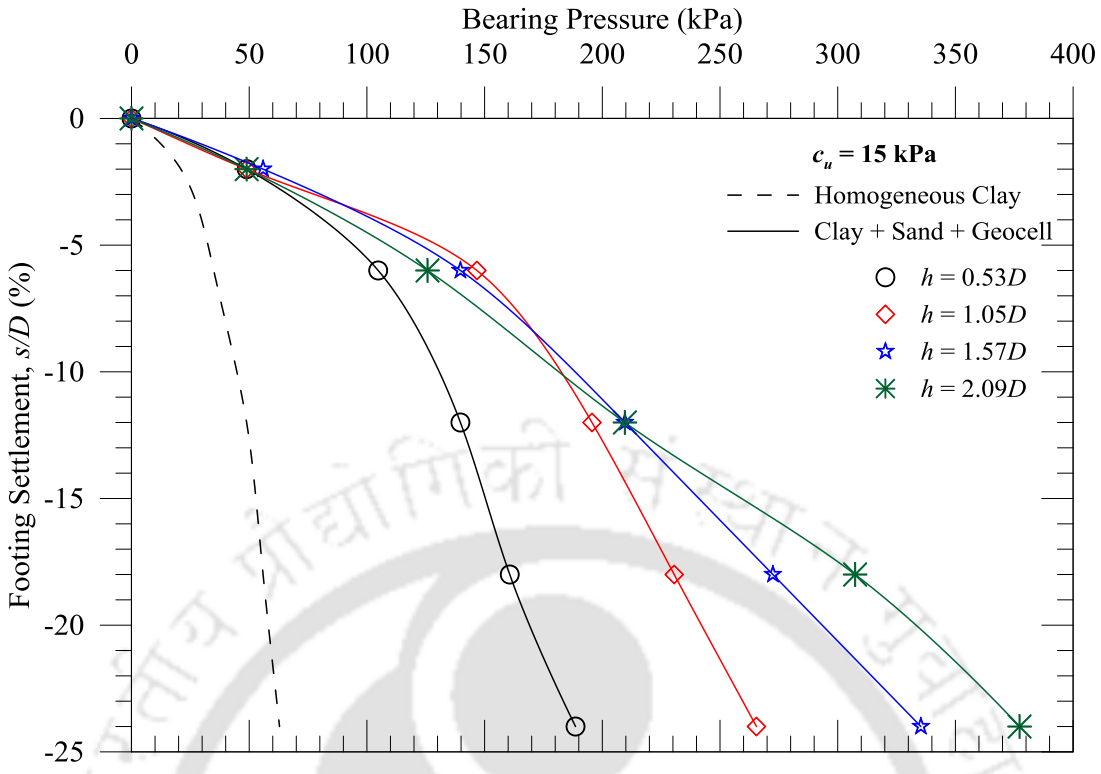

Fig. 6.3 Pressure-settlement responses of geocell-reinforced foundations: c_u = 15 kPa

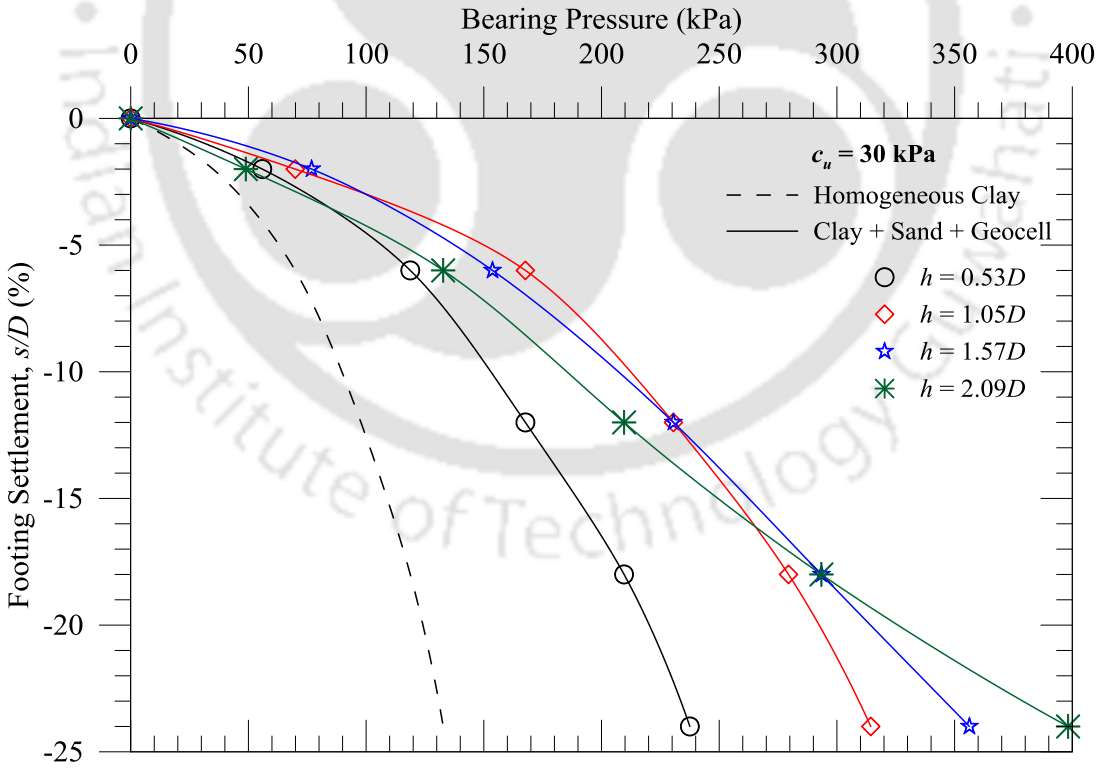

Fig. 6.4 Pressure-settlement responses of geocell-reinforced foundations: c_u = 30 kPa

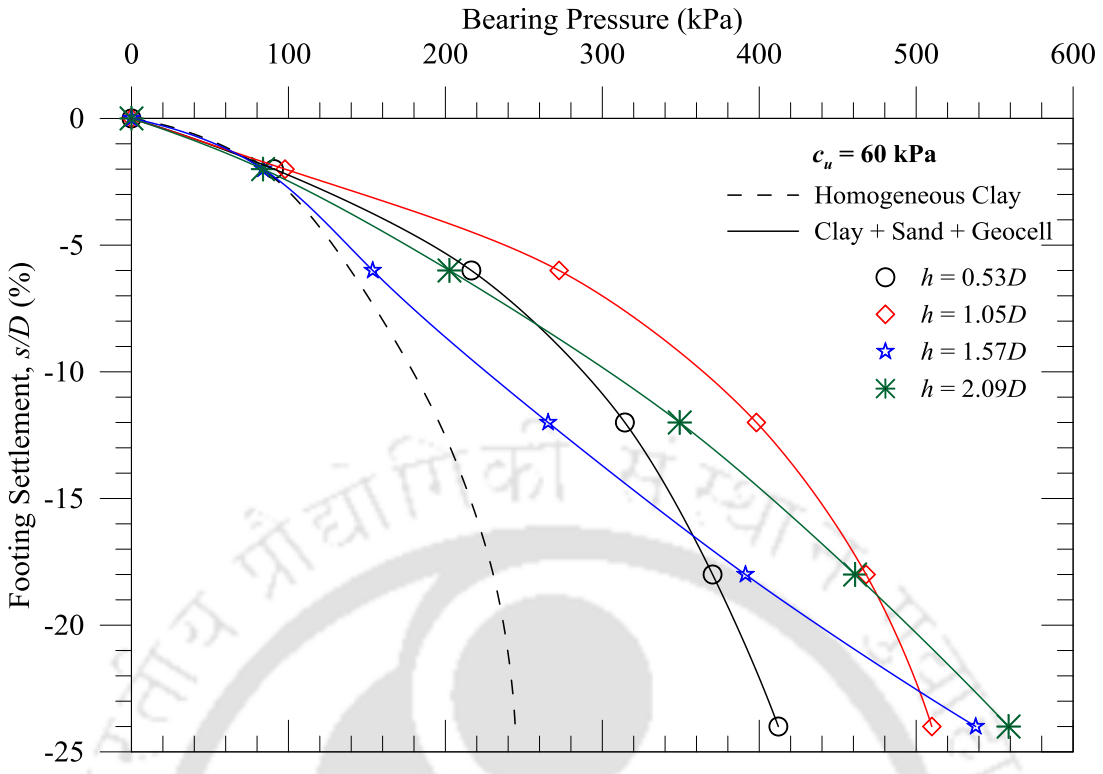

Fig. 6.5 Pressure-settlement responses of geocell-reinforced foundations: c_u = 60 kPa

It is seen that the bearing pressures are increased non-linearly with footing settlement (*s/D*). In Fig. 6.2, for c_u = 7 kPa and h = 0.53D, the bearing pressure variations are about 28, 56, 77, 98, and 119 kPa with *s/D* of 2, 6, 12, 18, and 24%, respectively. In general, bearing pressures are increased with layer thickness up to H = 1.15D for all the subgrades. However, the increase in bearing pressures is not consistent with the variation in geocell-heights for $h \geq 1.57D$ on comparatively stiffer subgrades (c_u > 7 kPa).

A typical surface deformation profile for geocell-reinforced foundations, with 0.63D thick geocell-reinforced sand layer (H) overlying clay subgrade of c_u = 7 kPa, is shown in Fig. 6.6. Considerable surface settlement around the footing center (x = D) and heaving away from the footing center (x = 2D and 3D) can be noticed from the figure. In general, as compared to unreinforced and/or geogrid reinforced foundations,

surface heaving was reduced at $x = D$ from footing center for geocell-reinforced systems; while, it was comparatively higher at $x = 2D$ and $3D$.

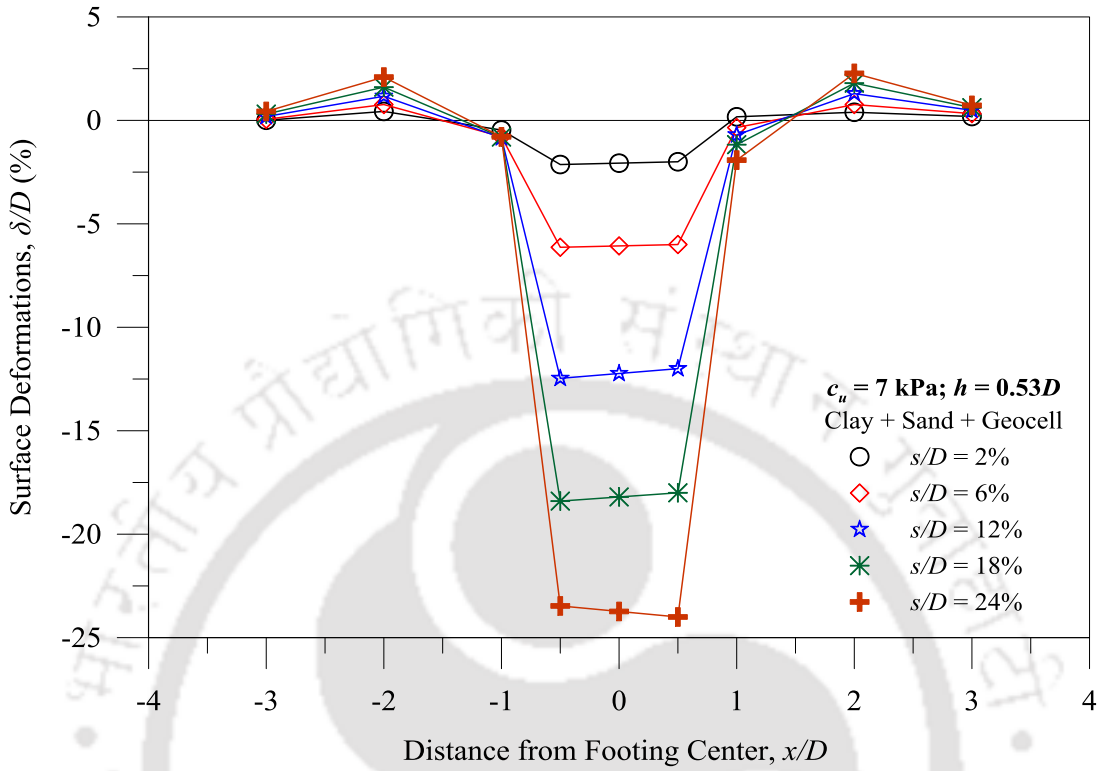

Fig. 6.6 Surface deformation profile of geocell-reinforced foundations (c_u = 7 kPa and $H = 0.63D$)

Variations of bearing pressures are further analyzed in terms of bearing pressure improvement factor, I_{fsgc}. It is defined as the ratio of two bearing pressures: the bearing pressure of geocell reinforced foundations (q_{sgc}) to the bearing pressure of corresponding homogeneous clay beds (q_c) at similar *s/D* level, as defined in Eq. 6.1.

$$(I_{fsgc}) = \left(\frac{q_{sgc}}{q_c}\right)_{\text{[at same } s/D \text{ level]}} \quad (6.1)$$

The contribution of the geocell-reinforcement is quantified as I_{fgc}, defined as the ratio of q_{sgc} to q_s (unreinforced sand-layered foundations) at similar level of *s/D* (Eq. 6.2). The improvement factors are summarized in Table 6.2.

$$(I_{fgc}) = \left(\frac{q_{sgc}}{q_s}\right)_{\text{[at same } s/D \text{ level]}} \quad (6.2)$$

Table 6.2 Summary of bearing pressure improvement factors

Footing Settlements (*s/D*)	Geocell Height (*h/D*)	Bearing Pressure Improvement Factor							
		c_u = 7 kPa		c_u = 15 kPa		c_u = 30 kPa		c_u = 60 kPa	
		I_{fsgc}	I_{fgc}	I_{fsgc}	I_{fgc}	I_{fsgc}	I_{fgc}	I_{fsgc}	I_{fgc}
2%	0.53	1.60	1.33	2.33	1.40	1.60	1.33	1.08	1.63
	1.05	2.40	1.20	2.33	1.27	2.00	1.67	1.17	1.75
	1.57	2.79	1.40	2.66	1.45	2.20	1.22	1.00	1.71
	2.09	2.00	1.00	2.33	1.75	1.40	1.00	1.00	1.71
6%	0.53	2.00	1.45	3.00	1.36	1.70	1.31	1.55	1.72
	1.05	3.38	1.35	4.20	1.91	2.40	1.85	1.95	2.44
	1.57	3.88	1.41	4.00	1.54	2.20	1.00	1.10	1.38
	2.09	4.26	1.36	3.60	1.64	1.90	1.00	1.45	1.81
12%	0.53	2.45	1.69	2.86	1.25	1.71	1.14	1.60	1.96
	1.05	4.00	1.29	4.00	1.75	2.36	1.57	2.03	2.48
	1.57	5.34	1.33	4.29	1.50	2.36	1.03	1.35	1.65
	2.09	6.45	1.45	4.29	1.76	2.14	1.11	1.78	2.17
18%	0.53	3.11	1.87	2.87	1.28	1.76	1.36	1.61	2.12
	1.05	4.78	1.48	4.12	1.65	2.35	1.74	2.03	2.68
	1.57	6.67	1.43	4.87	1.70	2.47	1.24	1.70	2.24
	2.09	9.12	1.86	5.50	2.00	2.47	1.40	2.00	2.64
24%	0.53	3.78	2.13	3.00	1.35	1.79	1.48	1.69	2.03
	1.05	5.56	1.72	4.22	1.65	2.37	1.73	2.09	2.70
	1.57	8.01	1.57	5.33	1.92	2.68	1.65	2.20	2.85
	2.09	11.57	2.17	6.00	2.25	3.00	1.84	2.29	2.96

6.3 DISCUSSIONS ON TEST RESULTS

The effect of footing settlement (*s/D*), geocell-height (*h*), and subgrade strengths (c_u), on the performance of geocell-reinforced foundation systems, are discussed in following sections.

6.3.1 Effect of Footing Settlement (*s/D*)

A typical comparison of pressure-settlement responses of unreinforced and geocell-reinforced foundation systems, for c_u = 7 kPa, is presented in Fig. 6.7. Higher

bearing pressures at larger footing settlements can be noticed. The geocell-reinforced bearing pressure is increased from 77 to 119 kPa, for the footing settlement (*s/D*) variation from 12 to 24% (at H = 0.63D). In similar foundation configurations, the variation of bearing pressures for unreinforced foundations was from 45 to 56 kPa. This indicates considerably high improvement in pressure values, for geocell-reinforced foundation systems as compared to unreinforced cases. Besides, it is seen that this improvement was increased with increasing settlement levels.

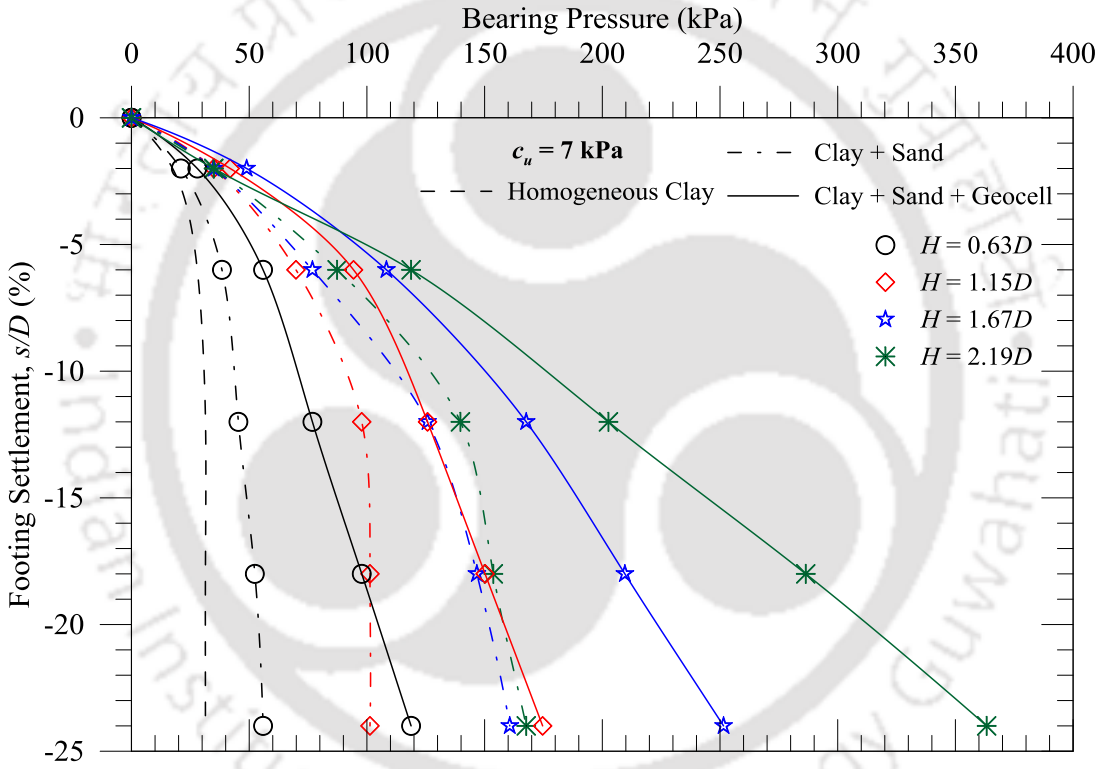

Fig. 6.7 Response of unreinforced and geocell-reinforced foundations: c_u = 7 kPa

The improvement in bearing pressures, with respect to corresponding homogeneous clay beds, is evaluated in terms of I_{fsgc}. Variations of improvement factors, I_{fsgc}, with footing settlement, for different layered configurations on very soft clay subgrade (c_u = 7 kPa), are presented in Fig. 6.8. The figure also shows the improvement factors, I_{fs}, obtained for the unreinforced layered configurations tested under series B. It can be observed that the improvement factors, I_{fsgc} and I_{fs}, are

increased with increasing footing settlement. Variation of I_{fsgc} as 3.38 to 5.56 can be noted with footing settlement (s/D) in the range of 6-24%, for c_u = 7 kPa at H = 1.15D; while, the corresponding variation in I_{fs} is 1.35 to 1.72. A very high improvement factor of 11.6 is observed for c_u = 7 kPa, for the thickest geocell-mattress of h = 2.09D (H = 2.19D), at the largest settlement level tested (s/D = 24%).

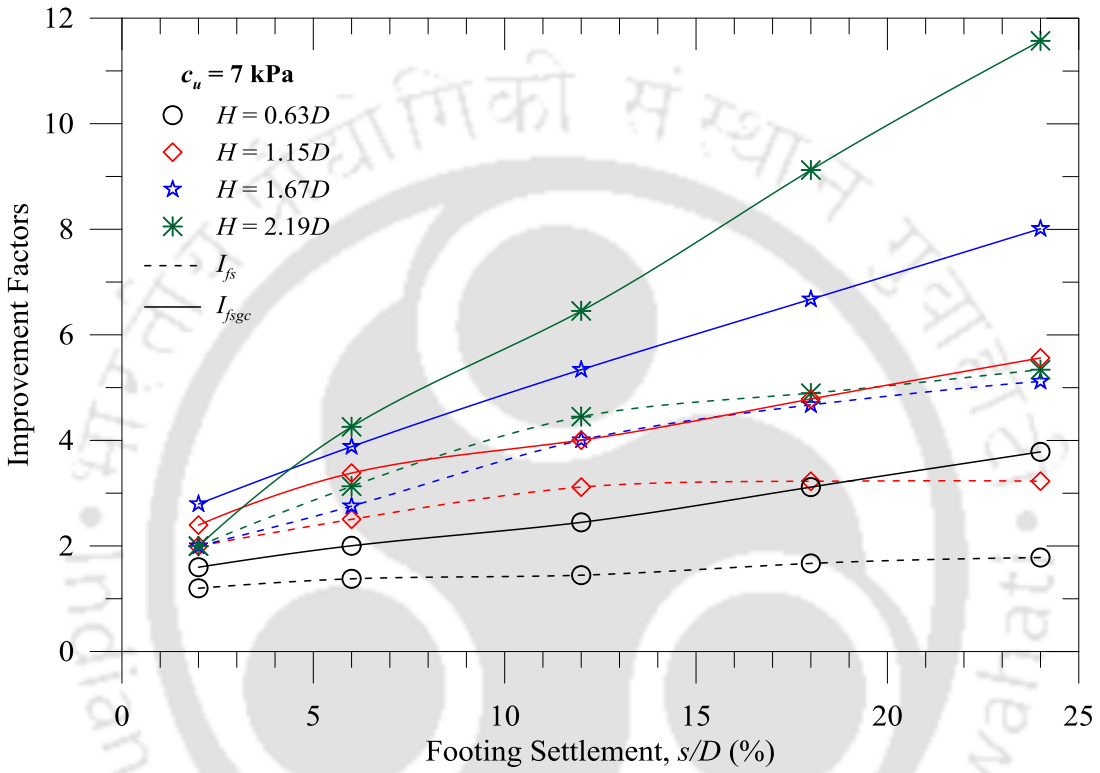

Fig. 6.8 Variation of I_{fs} and I_{fsgc} with s/D for c_u = 7 kPa.

This higher improvement in bearing pressure responses is contributed by the geocell reinforcement. To evaluate the geocell contribution, I_{fgc} (= I_{fsgc} / I_{fs} = q_{sgc} / q_s; Eq. 6.2) are evaluated and summarized in Table 6.2. Variations of I_{fgc} with footing settlement for different subgrades (c_u = 7, 15, 30, and 60 kPa) are presented in Fig. 6.9, for two different layer thicknesses, such as H = 0.63 and 1.15D. It can be noticed that the variation of I_{fgc}, in Fig. 6.9 and Table 6.2, is not very consistent for all subgrades and for the layer thickness variations. However, in most of the cases, it was found increasing with settlement, showing more geocell contribution at higher strain.

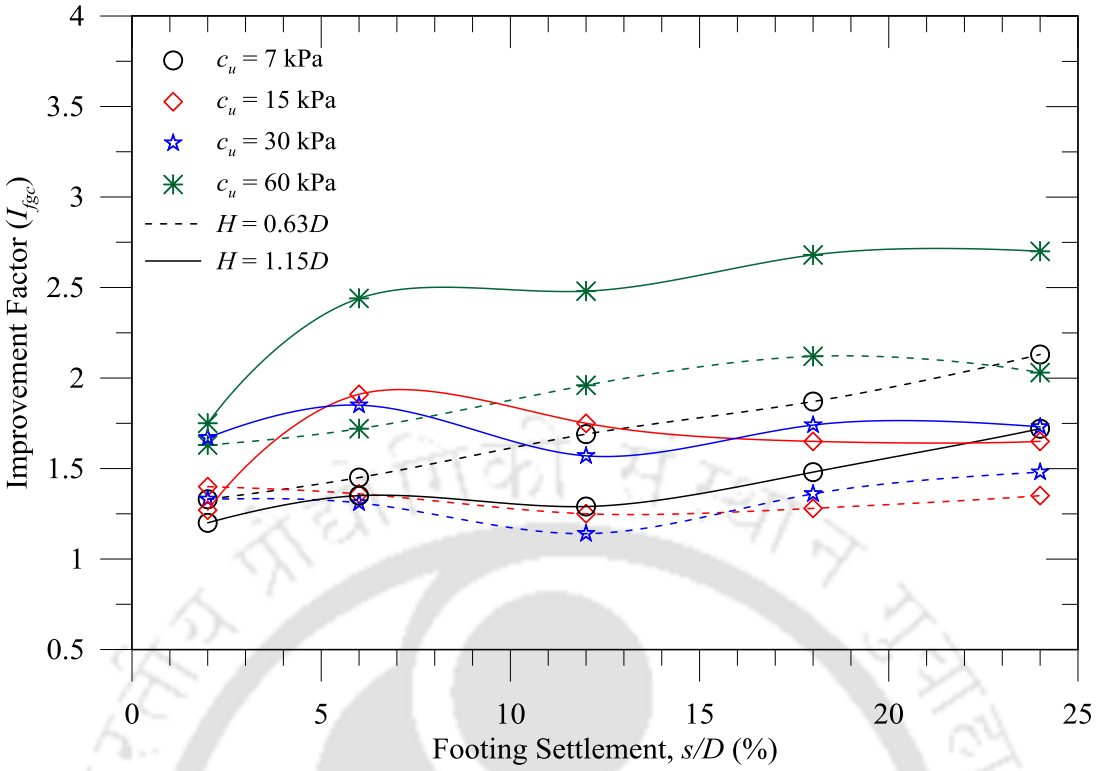

Fig. 6.9 Variation of I_{fgc} with s/D for different c_u at H = 0.63 and 1.15D

The geocell contribution in higher bearing pressures is attributed to two geocell-mechanisms: 1) confinement of in-filled sand within the geocells, and 2) distribution of footing load to deeper zones and larger area. The geocell pockets, owing to three-dimensional configuration, cease the lateral squeezing of sand and hence, increase the density of the fill soil leading to increased performance (confinement). In addition, the strain mobilized interfacial friction along the geocell-walls gives additional resistance against the footing loads, as shown in Fig. 6.10. Simultaneously, the geocell-walls intercept the potential shear planes of the in-filled sand and force to go deeper and wider into the soil underneath, as shown schematically in Fig. 6.11.

In case of increase in footing settlement, the interfacial resistance through the geocell-wall provides enhanced resistance against the possible downward movement of the geocell-mattress. Further, with geocell-height, the increased number of bodkin

joints and the interfacial resistances through the enhanced surface area improves the stiffness of the geocell-sand mattress. Combining the above, the sand-filled geocell-mattress behaves as a semi-rigid slab which can carry and redistribute high load uniformly with lesser intensity to the underlying subgrades. Similar reinforcing mechanisms of geocell contributions were also reported by Dash et al. (2001a, 2003a, 2007), Latha et al. (2009), Wesseloo et al. (2009), Pokharel et al. (2010), and Tafreshi and Dawson (2010).

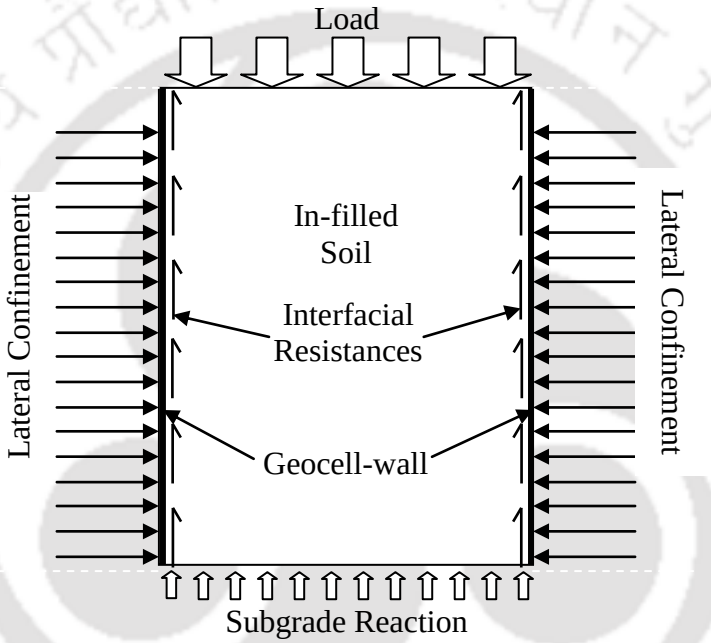

Fig. 6.10 Confinement and interfacial resistance though geocell-walls

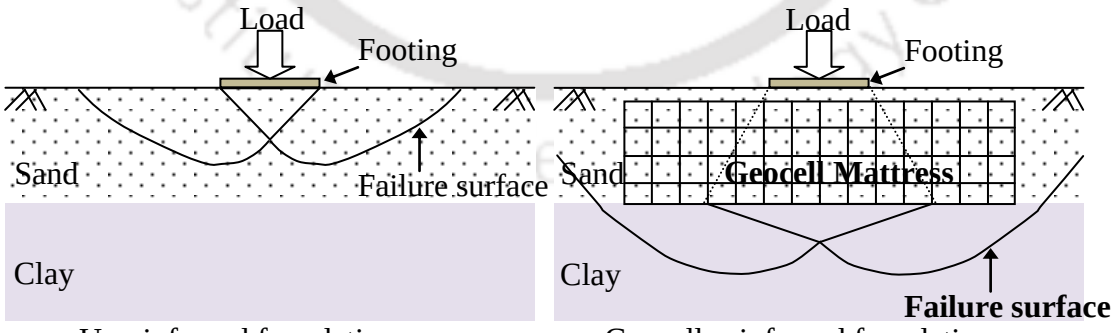

Unreinforced foundation Geocell-reinforced foundation

Fig. 6.11 Interception of potential failure plane and load redistribution

A typical variation of surface deformation with footing settlement is shown in Fig. 6.12, for different foundation systems overlying clay subgrade of 7 kPa (c_u) at H

= 0.63*D*. It can be noticed that as compared to the unreinforced foundations, the geocell-reinforced system has shown higher settlement at $x = D$ and more heaving at $x = 2D$ and $3D$. Such deformation profile is attributed to the deep beam action of geocell mattress (Dash et al., 2001a) which undergone sagging (causing settlement) around the footing center and hogging (causing heaving) away from the loading. However, the magnitude of deformations is dependent on thickness of geocell mattress (h) and the strengths of the underlying subgrades (c_u).

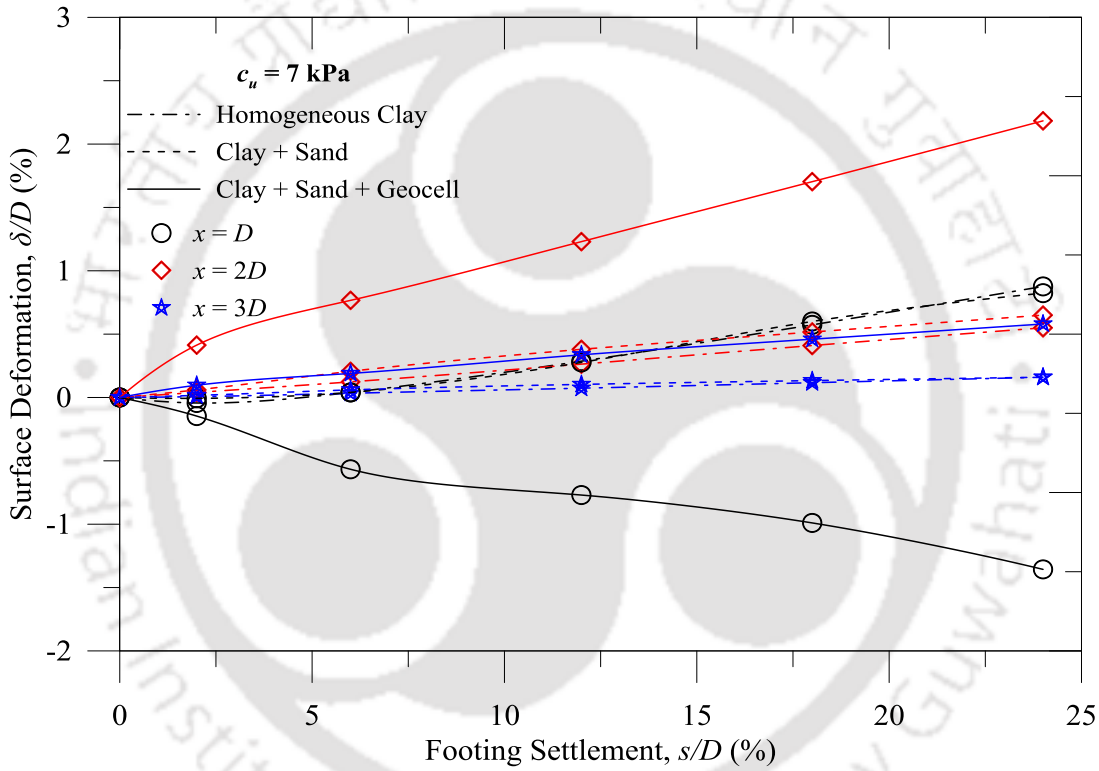

Fig. 6.12 Variation of δ/D with s/D at $x = D$, $2D$, and $3D$ for c_u = 7 kPa ($H = 0.63D$)

6.3.2 Effect of Geocell-Height (h)

Significant influence of geocell height (h) in improvement of bearing pressure is noticed in Fig. 6.2 to Fig. 6.5, for all clay subgrades. In Fig. 6.7, higher performance of geocell-reinforced foundations compared to unreinforced layered foundations on the clay subgrade having c_u = 7 kPa, for different layer thicknesses (H) was observed. The bearing pressure is increased from 119 to 363 kPa for the geocell-thickness (h) variation from 0.53 to 2.09*D*, at s/D = 24% (for c_u = 7 kPa). In general,

the bearing pressure is found to have increased with increase in thickness of geocell-sand mattress (H) from 0.63 to 1.15D. However, improvements in bearing pressure did not follow consistent increasing trend in relation to height of geocells at different settlement levels, for all the subgrades.

In Fig. 6.13, variation in bearing pressure for different subgrades, having varying geocell-heights, are presented (at s/D = 12%). The corresponding responses of unreinforced layered foundations are also shown in that figure. The variation in bearing pressure for clay subgrade having c_u = 15 kPa is as 140, 196, 210, and 210 kPa, for the variation in geocell-height as 0.53, 1.05, 1.57, and 2.09D, respectively. Similarly, for 30 kPa (c_u) subgrade, such variation was noted as about 168, 231, 231, and 210 kPa, respectively; while the variation is about 314, 398, 265, and 349 kPa, respectively, for c_u = 60 kPa. Similar relative bearing pressures at different layer thicknesses could be seen for unreinforced systems. The results indicate the most effective geocell height (h) is 1.05D (H = 1.15D) for all subgrades.

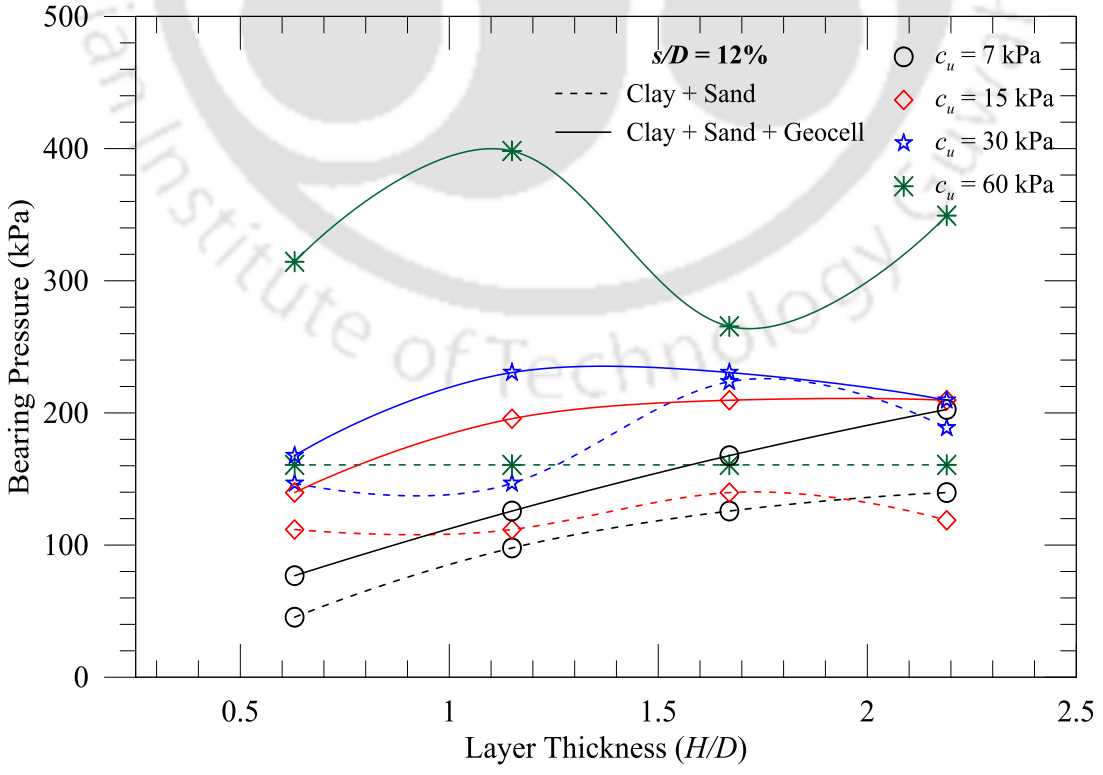

Fig. 6.13 Variation of bearing pressure for different H/D and c_u at s/D = 12%

The deviation, in improvement trend with geocell-height, is attributed to the initiation of reinforcing mechanism which requires certain levels of footing settlement (s/D ~ 6%), depending of subgrade strengths (c_u). For thicker geocells (h > 1.05D), buckling in geocell-walls has dominated the performance of geocell-reinforced foundations on comparatively stiffer subgrades (c_u > 15 kPa). The thicker and stiffer geocell-sand mattress ($H \geq 1.67D$), owing to their structural stiffness (due to more bodkin joints per unit plan area), absorbs most of the incoming load and transfer less to the underlying subgrade. This, in turn, increases stress concentration on the sand cushion provided in between the footing and the geocell-mattress. Upon squeezing of sand cushion from the footing bottom, the footing load directly comes on the geocell-mattress. This leads geocell-walls (first array of geogrid apertures) to get buckled with excessive stress just under the footing. The buckling in geocell-walls resulted in localized footing settlement and simultaneously, reduces the performance of the foundation system. Further, having same heights (h), the intensity of stress concentration on the geocell-walls is depended on the subgrade stiffness (c_u). The stiffer subgrades provide higher resistance against the possible bending and/or subgrade penetrations which increases the intensity of stress concentration on the top of the geocell-sand mattress and probability of higher buckling. A photograph of the buckled geocell-wall is presented in Fig. 6.14 which was obtained from an experiment with c_u = 60 kPa (h = 1.05D). However, it is noticed that after certain level of footing settlement, the thicker ($h \geq 1.57D$) geocell-foundations could overcome the buckling effect and enhances the overall performance. It is attributed to the continuity of the interconnected geocell-system which restricted the localized buckling. Hence, the bearing pressure increases which was seen after about 12, 18, and 24% of s/D, for the subgrades having c_u = 15, 30, and 60 kPa, respectively.

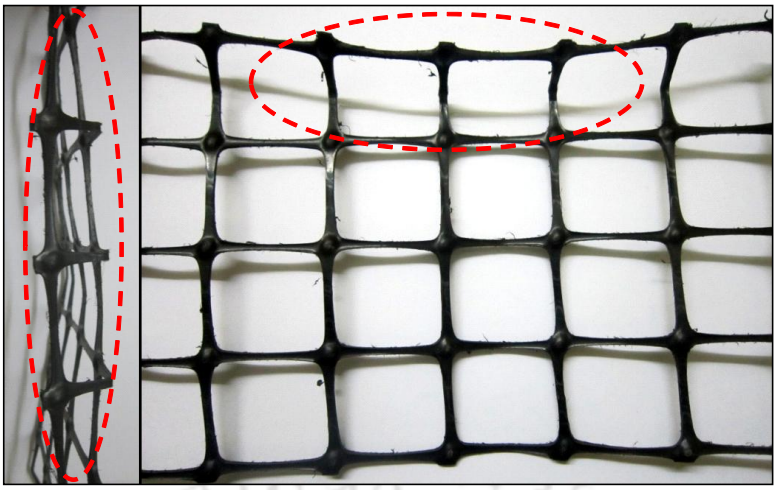

Fig. 6.14 The "buckling" in geocell-wall

Fig. 6.15 presents the effect of layer thickness on the bearing pressure improvement factors, I_{fs} and I_{fsgc}, at s/D = 12%. The effect of layer thickness is very significant, in both the unreinforced and geocell-reinforced systems, for very soft clay subgrade (c_u = 7 kPa). The I_{fsgc} is varied from 2.45 to about 6.45 for an increase in the geocell-reinforced sand layer thickness (H) from 0.63 to 2.19D. A similar trend was observed for the unreinforced case (I_{fs}) as well. However, it can be seen that the rate of increase in improvement factor, I_{fs}, was decreased for the subgrades having sand layer thickness $H \geq 1.67D$. The reduction in improvement rate was the effect of local shear failure and squeezing out of the sand column from the footing bottom. This reduction in improvement rate was not very significant in the case geocell reinforcement, in terms of I_{fsgc}. This was because the geocell walls arrest the squeezing of the sand by intercepting shear planes and confines the sand within its pockets. Similar observations have also been reported by Dash et al. (2001a). However, the reduction in I_{fsgc}, beyond 1.67D, is due to the effect of buckling of geocell walls and squeezing out the sand cushion from the footing bottom, as discussed earlier. A similar observation was also reported by Mandal and Gupta

(1994), Dash et al. (2003b), Sireesh et al. (2009a), Tafreshi and Dawson (2010), where the optimum '*h*' was found within a range of 1.5-2.0 times '*D*'.

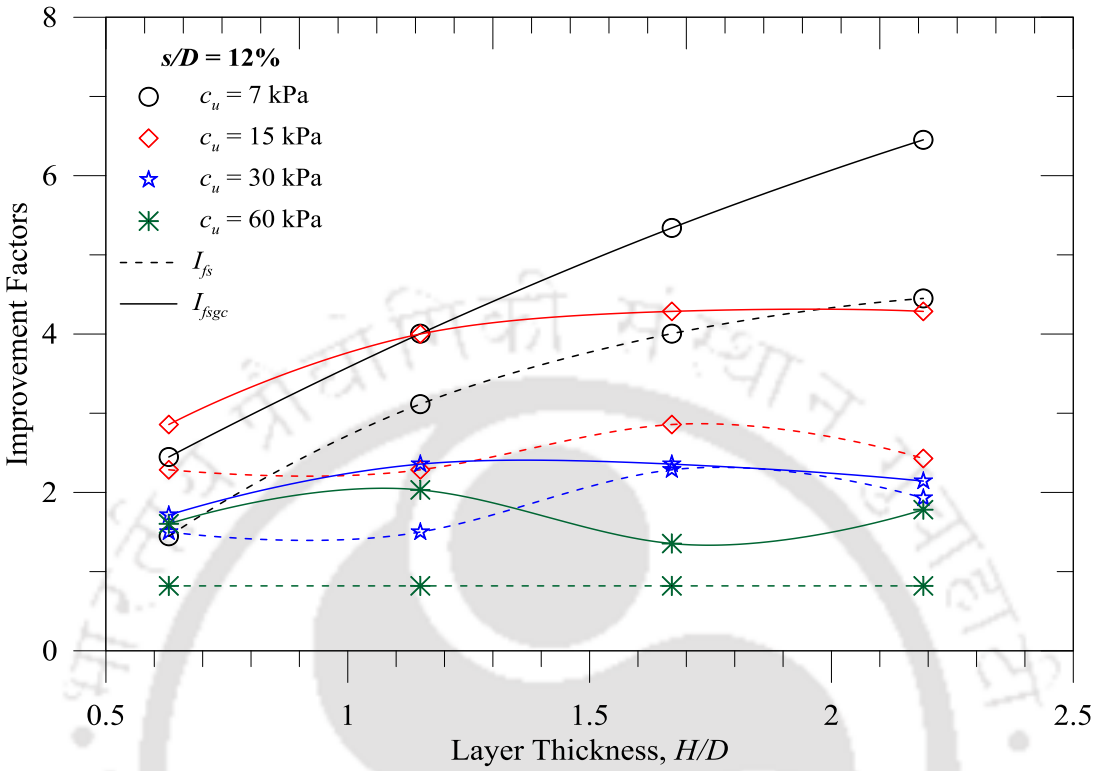

Fig. 6.15 Variation in I_{fs} and I_{fsgc} with H/D at s/D = 12% for different c_u

The average surface deformations at $x = D$ and $2D$, presented in Fig. 6.16 and Fig. 6.17, respectively, are showing the effect of layer thickness overlying the clay subgrade of 7 kPa. Mostly, surface settlement can be observed at $x = D$ from footing center. It indicates that the geocell reinforcement has prevented the shear failure of sand and behaved as a coherent body which deformed like a centrally loaded slab. It is also in agreement with the findings of Dash et al. (2001a) in which case it was attributed as deep beam action for the thicker geocells. The deformation for shorter geocells ($h \leq 1.05D$) were more as compared to that of thicker geocells ($h \geq 1.57D$) due to its less structural rigidity and thus, were prone to collapse upon footing load. On exhumation the sand layer, the clay subgrade was found settled under the loaded area with heave in the adjacent region indicating that it has undergone shear failure.

Hence, around the footing, the foundation surface undergone settlements; whereas, the hogging deformation away from the footing center (x = 2D) affected as heaving.

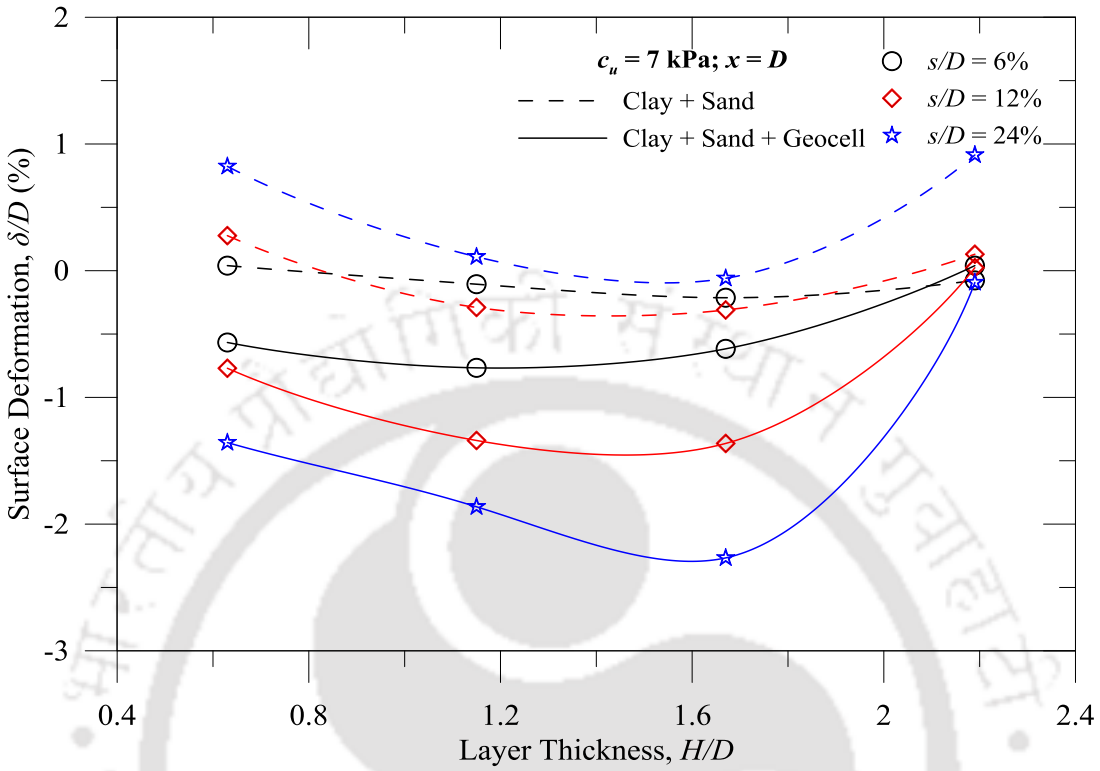

Fig. 6.16 Variation of δ/D with H/D for geocell-reinforced foundations at x = D

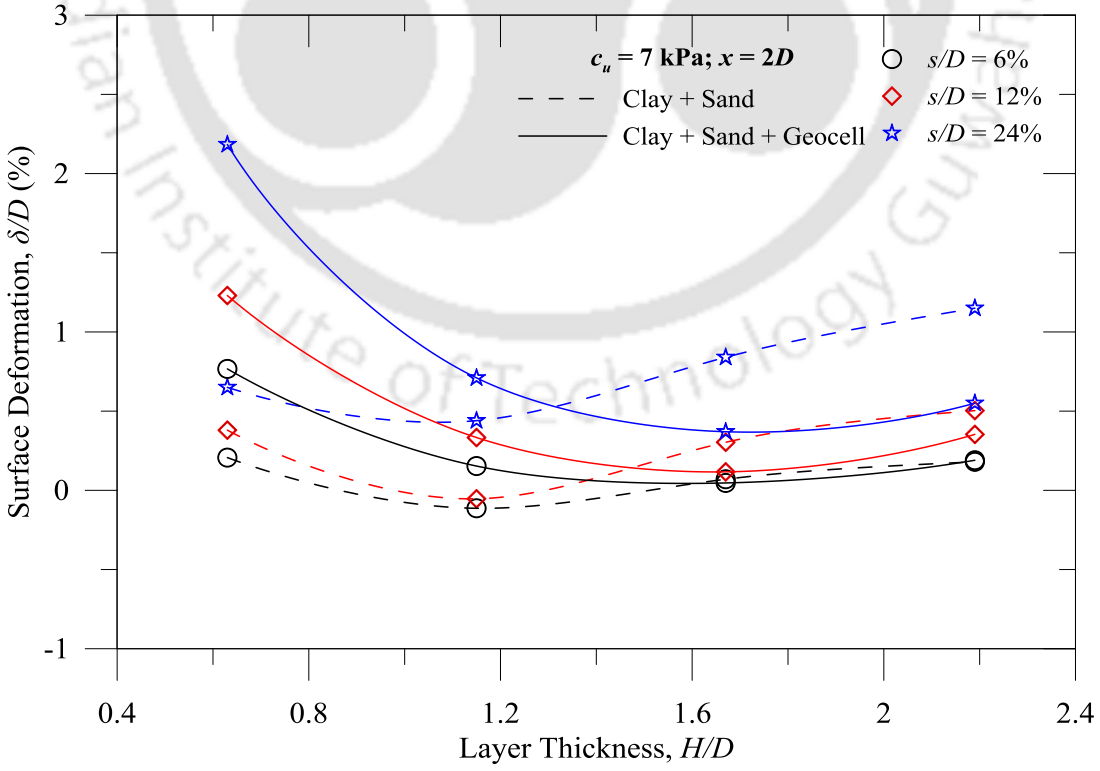

Fig. 6.17 Variation of δ/D with H/D for geocell-reinforced foundations at x = 2D

6.3.3 Effect of Subgrade Strength (c_u)

The pressure-settlement responses showing the influence of subgrade strength on the performance of geocell-reinforced foundations are presented in Fig. 6.18. In the figure, the responses are compared with the responses of the corresponding unreinforced layered foundations (test series B). Substantial improvements, with higher bearing pressures for stiffer subgrades, can be noticed in the figure. The bearing pressures at H = 0.63D and s/D = 24% are 56, 140, 161, and 203 kPa for unreinforced layered systems, having c_u = 7, 15, 30, and 60 kPa; while bearing pressures were increased to about 119, 189, 238, and 413 kPa, respectively, with geocell reinforcement. Similar improvements can also be noted for foundations having geocell-heights as h = 1.05, 1.57, and 2.09D. The change in bearing pressures for the unreinforced and geocell-reinforced foundations for the above configurations are about 175 to 510 kPa, 252 to 538 kPa, and 363 to 559 kPa, respectively, for the variation in c_u from 7 to 60 kPa. The higher bearing pressure is attributed to the semi-rigid slab like structure that offered greater subgrade support on stiffer subgrades.

The effect of subgrade strength (c_u) on the variation of improvement factors for unreinforced and geocell-reinforced foundation systems (I_{fs} and I_{fsgc}) at different settlement levels (s/D) is presented in Fig. 6.19, for H = 1.15D. In general, a decrease in improvement factors with increase in subgrade strengths can be seen, depending on layer thickness (H/D) and level of footing settlements (s/D). The decreasing trend is significantly prominent for thicker geocells (h > 1.05D; Table 6.2) at a higher level of settlements ($s/D \geq$ 12%). For an unreinforced layered foundation with H = 1.15D at s/D = 12%, the improvement factor I_{fs} is decreased from 3.11 to 0.82 as the subgrade strength (c_u) increased from 7 to 60 kPa (Fig. 6.19); while, in similar subgrade variation with H = 2.19D at s/D = 24%, the improvement factor (I_{fs}) decreased from

5.34 to 0.77 (Table 4.2). In geocell-systems, for c_u variations from 7 to 60 kPa, the I_{fsgc} is changed from 4.0 to 2.03 for s/D = 12% and h = 1.05D; while, at s/D = 24% and h = 2.09D, the variation is about 11.57 to 2.29, respectively (Table 6.2).

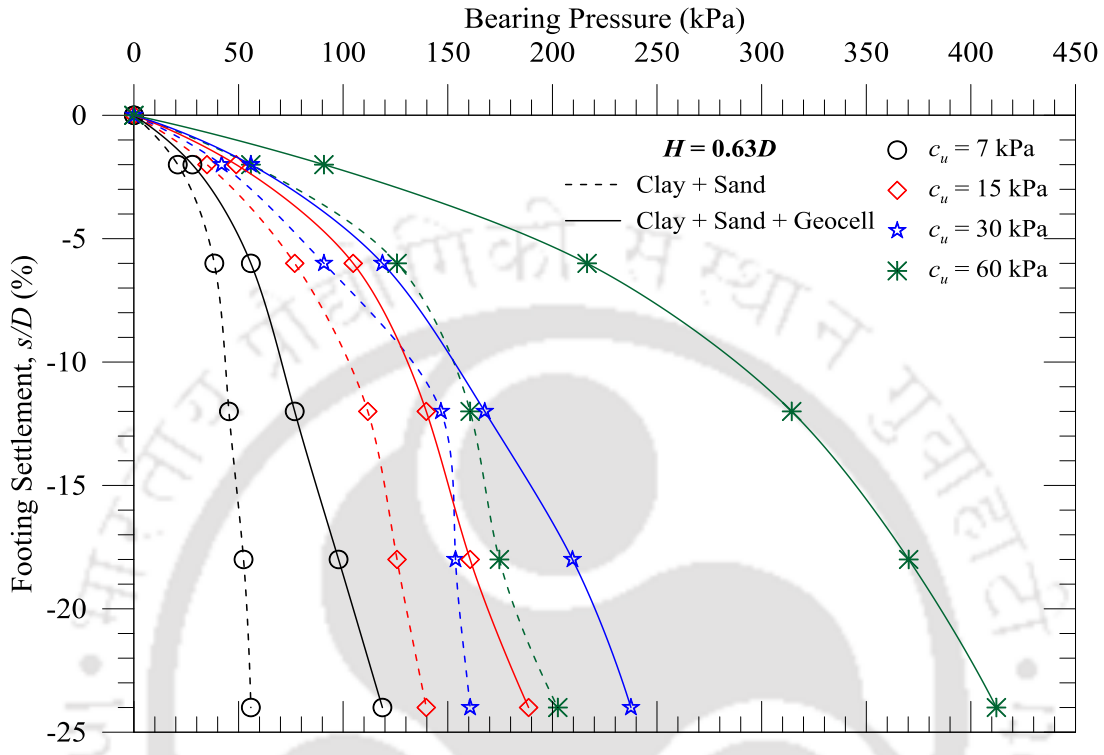

Fig. 6.18 Pressure-settlement response of geocell-reinforced foundations at H = 0.63D

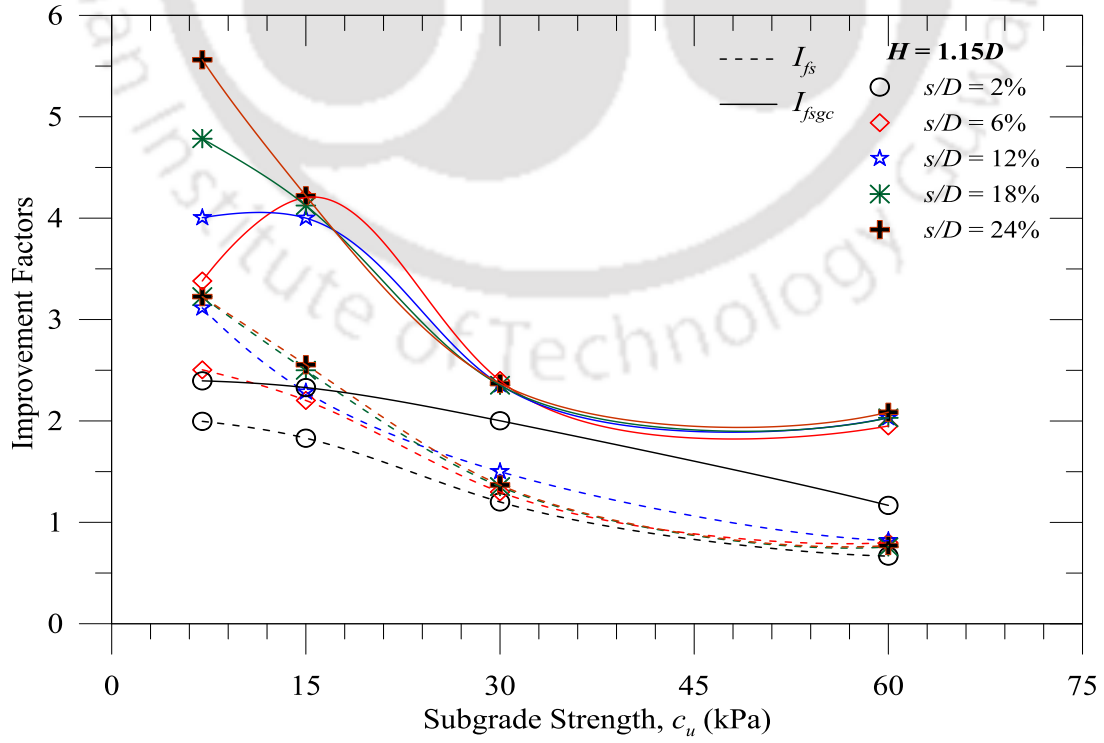

Fig. 6.19 Effect of c_u on I_{fs} and I_{fsgc} at H = 1.15D for different settlement levels (s/D)

Variations in improvement factors (I_{fs} and I_{fsgc}) for different subgrades (c_u) with varying layer thicknesses (H/D) are presented in Fig. 6.20 (at 12% of s/D). It is observed that the improvement factors are decreased with the increase in subgrade strength. At H = 2.19D, the improvement factor I_{fs} (dotted lines) is varied from 4.45 to 0.82 as the subgrade strength (c_u) increased from 7 to 60 kPa; while, with geocell reinforcement in similar condition, the I_{fsgc} variation is 6.45 to 1.78. However, at H = 0.63D, for both the foundation systems, the improvement factors (I_{fs} and I_{fsgc}) were greater for the subgrade having c_u = 15 kPa. The improvement factor, I_{fs}, was found as 2.29 compared to 1.45 (for c_u = 7 kPa), 1.5 (for c_u = 30 kPa), and 0.82 (for c_u = 60 kPa). Similarly, for 15 kPa the I_{fsgc} was 2.86 compared to 2.45, 1.71, and 1.60, for c_u = 7, 30, and 60 kPa, respectively.

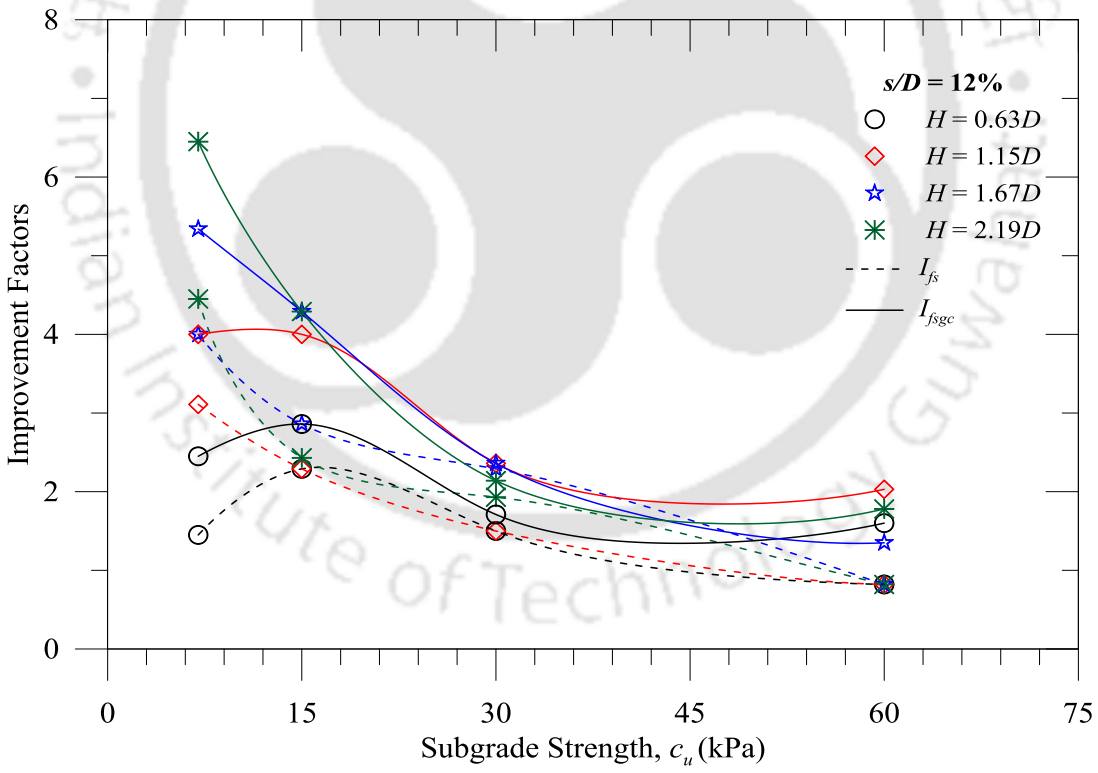

Fig. 6.20 Variation of I_{fs} and I_{fsgc} with c_u for different H/D at s/D = 12%

The contribution of geocell-reinforcement in bearing pressure improvements is quantified as I_{fgc}, as the ratio of two improvement factors, I_{fsgc} and I_{fs} (Eq. 6.2). The variation in the reinforcement contributions in terms of improvement factors, I_{fgc} and

I_{fg} (geogrid; Eq. 5.2), with subgrade strength (c_u) at different levels of footing settlement is shown in Fig. 6.21 (at H = 1.15D). It is seen that irrespective of footing settlements, the geocell and geogrid have contributed mostly for clay subgrade having c_u = 60 kPa. It is attributed to the definition of the improvement factor, I_{fgc}, which is compared with unreinforced systems. In unreinforced case, the bearing pressures for 60 kPa subgrade were reduced as compared to corresponding homogeneous clay beds. Hence, the improvement factors, I_{fgc}, are magnified for c_u = 60 kPa (as explained for the case of geogrid reinforced systems in Chapter 5). The geocell contributions for different subgrades at 12% of s/D are 1.29, 1.75, 1.57, and 2.48 (I_{fgc}), for c_u = 7, 15, 30, and 60 kPa, respectively (at H = 1.15D); whereas, in similar situations, for geogrid it was 1.31, 1.15, 1.13, and 1.48, respectively (I_{fg}).

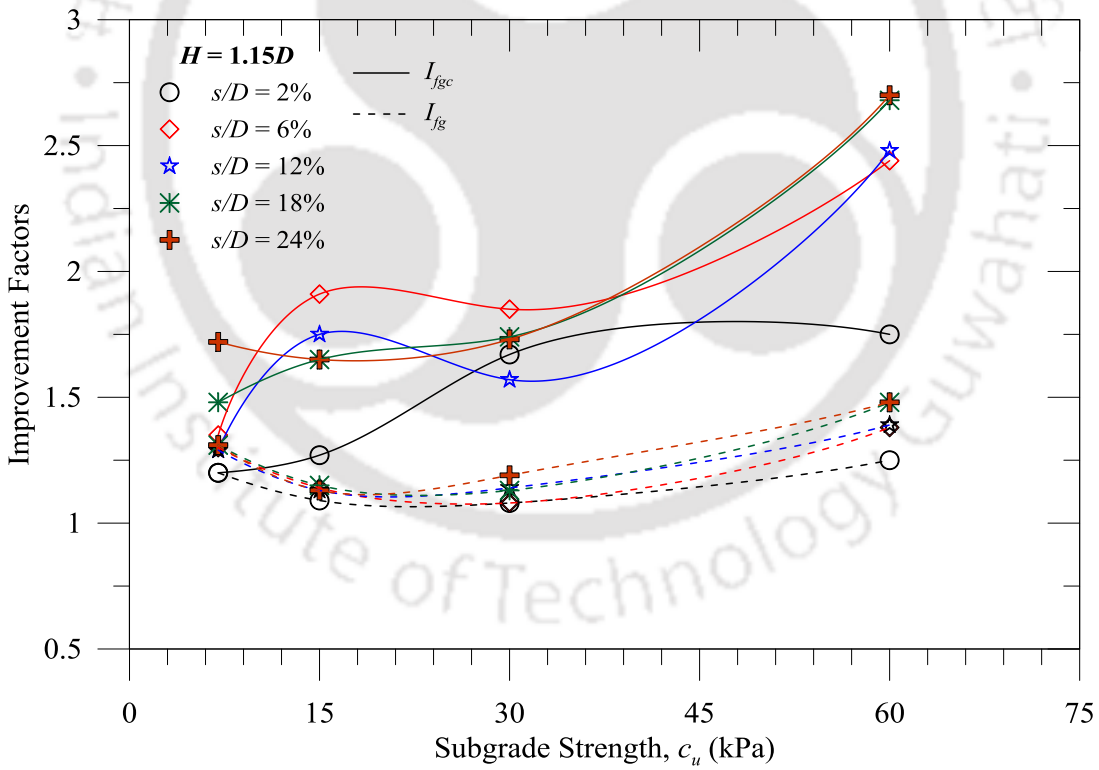

Fig. 6.21 Variation of I_{fgc} and I_{fg} with c_u at H = 1.15D for different s/D

In Fig. 6.22 and Fig. 6.23, surface deformations at x = D and 2D from the center of the footing are presented for different subgrades (at H = 0.63D). It can be

observed that surface heaving is significantly reduced at $x = D$ irrespective of subgrade strengths; while, it was enhanced at $x = 2D$. It is attributed to the semi-rigid slab-like behavior of the geocell-sand mattress which is having a sagging deformation around the footing center and hogging deformations away from the footing center, as discussed earlier. However, the encapsulation of in-filled sand from squeezing out also reduces the surface heaving to a great extent. An irregular footing-tilting is observed for the geocell-reinforced foundations. The rotation of the footing is the result of non-uniform loading-geometry on the geocell-walls. In the study, footing size was adopted as $0.8D$ placed on the geocell-mattress which was assembled in chevron pattern. The loading alignment was in such a way that it can cover the central geocell-pocket. Hence, the footing load was asymmetrically distributed over geocell-walls which affected as non-uniform sand-squeezing and irregular buckling in geocell-walls. The effect was further enhanced due to breakage of the bodkin-dowels just under the footing which resulted in abrupt change in surface deformations.

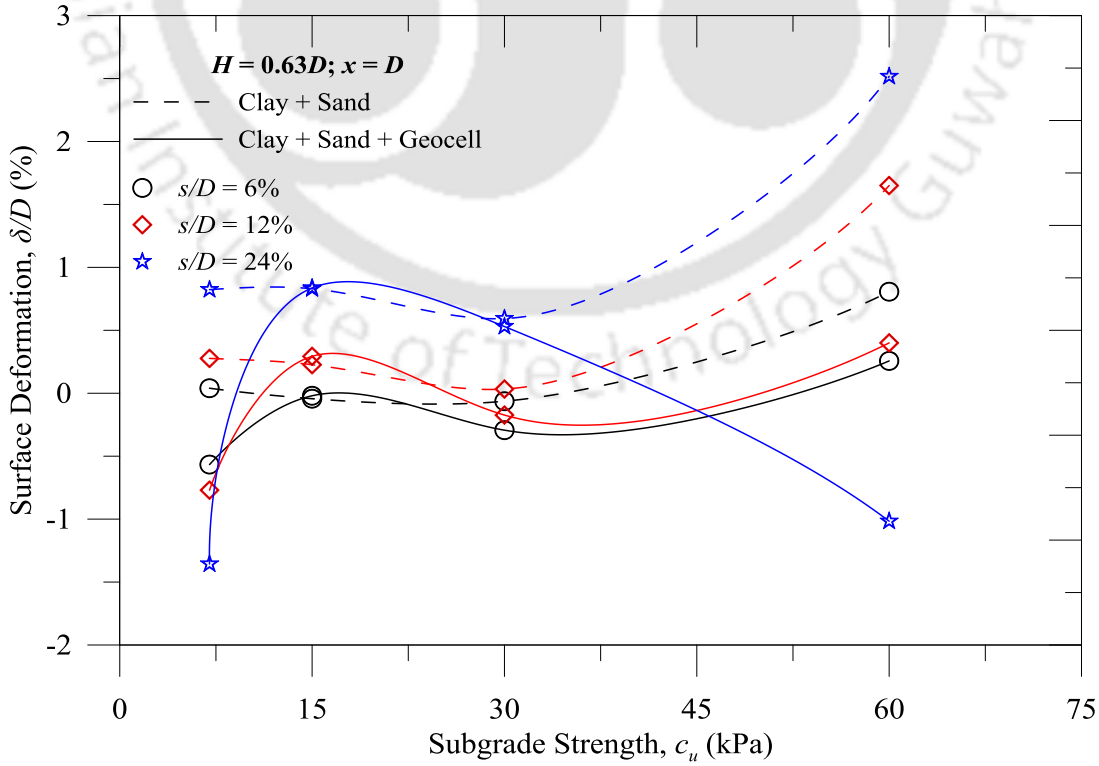

Fig. 6.22 Variation of δ/D at $x = D$ at different s/D with c_u ($H = 0.63D$)

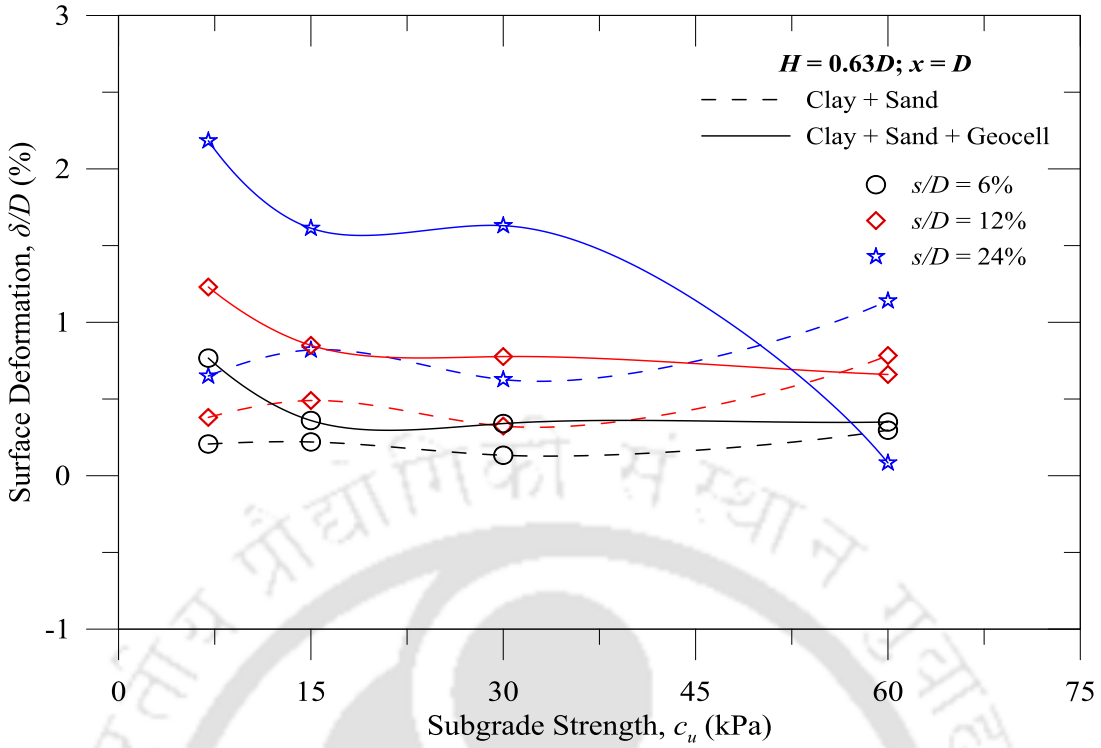

Fig. 6.23 Variation of δ/D at x = 2D at different s/D with c_u (H = 0.63D)

The experimental results are analyzed in terms of theoretical approaches proposed by Rajagopal et al. (1999,) Latha et al. (2006, 2008, 2009). In first stage of analyses, the additional stiffness of the geocell-reinforced layer is considered as the apparent cohesion (c_r) induced through the geocell-wall (Henkel and Gilbert, 1952; Bathurst and Karpurapu, 1993). In second step, the geocell-reinforced sand layer is replaced by equivalent stiffness of soil layer considering the apparent cohesion and friction angle of the sand and analyzed as layered foundation similar as presented in section 4.4. The apparent cohesion, c_r, and the increase in confinement, $\Delta\sigma_3$, were determined through eq. 6.3 and 6.4, respectively.

$$c_r = \frac{\Delta\sigma_3}{2}\sqrt{k_p} \tag{6.3}$$

$$\Delta\sigma_3 = \frac{2M}{d_0}\left[\frac{1-\sqrt{(1-\varepsilon_a)}}{1-\varepsilon_a}\right] \tag{6.4}$$

In the above equations, ε_a is the axial strain in geocell, d_o is initial geocell-pocket diameter (0.8D) and M is the average secant modulus corresponding the axial strain in geocell wall which is considered as 200 kN/m. In Fig. 6.24 and Fig. 6.25,

typical comparison of theoretical and experimental bearing pressures (at s/D = 12%) are presented for c_u = 30 and H = 1.15D, respectively, for different layered configurations. An area correction factor of 0.05 was considered for the interface effect in confinements. The comparison presents a reasonably good agreement. The differences in bearing pressures can be noticed which may be attributed to the buckling of geocell-walls and squeezing out of sand which could not be considered in analysis.

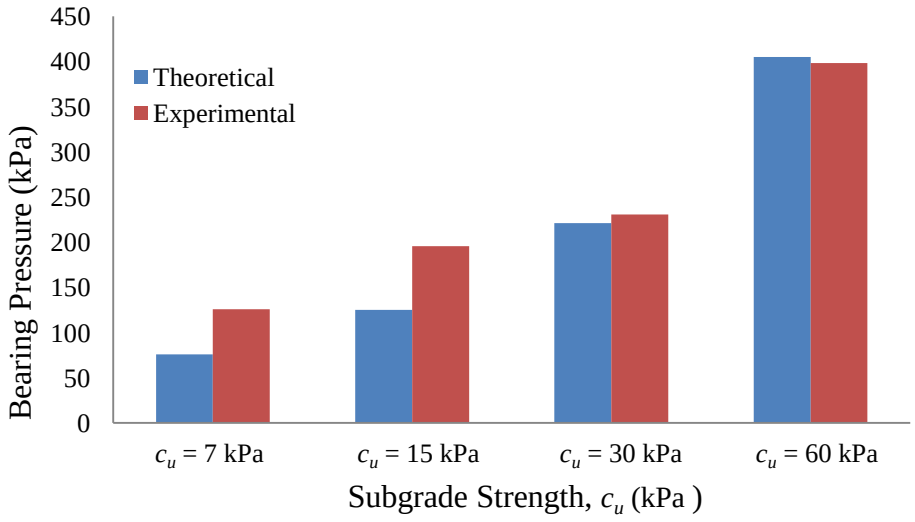

Fig. 6.24 Comparison of theoretical and experimental maximum bearing pressure for different geocell-reinforced foundations for H = 1.15D kPa at s/D = 12%

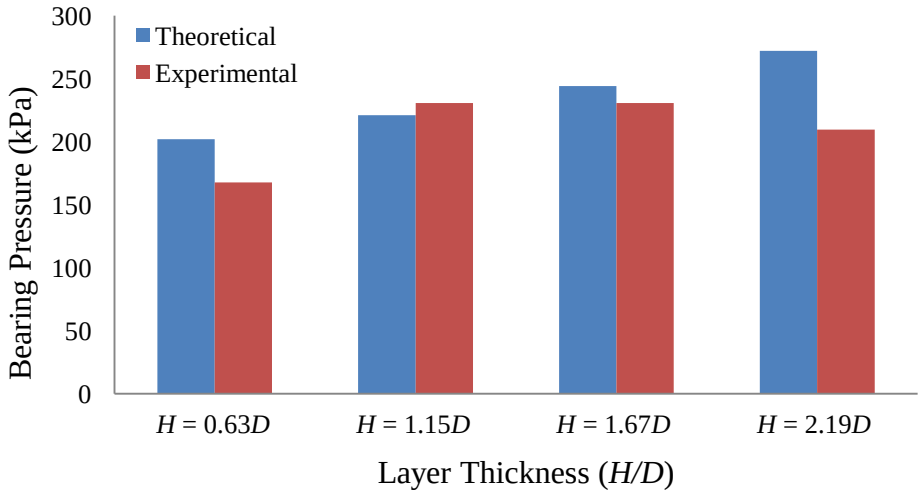

Fig. 6.25 Comparison of theoretical and experimental bearing pressure for different geocell-reinforced foundations for c_u = 30 kPa at s/D = 12%

6.4 POST EXPERIMENTAL OBSERVATIONS

Visual inspections for the physical behavior of the subgrades were performed after each test. A circular bowl shaped depression having a larger diameter than the footing was found just under the footing in case of unreinforced foundations (Fig. 4.20) for c_u = 7 kPa and H = 0.63D). It was the result of the penetrations of the truncated pyramidal sand column into the clay subgrade. The corresponding subgrade deformations for geogrid and geocell-reinforced are shown in Fig. 6.26. In geogrid reinforced case, bowled shaped depressions with traces of geogrid apertures were observed (Fig. 6.26a). However, in geocell-systems, the depression shapes were like the geocell-pockets as depicted in Fig. 6.26(b). Besides, the depths of depressions were reduced compared to the unreinforced and geogrid systems. It is signifying the reduction in load intensity transferred to the underlying subgrades which indicates better load carrying capacity of the geocell-reinforced foundations. In general, these depths of depressions were greater at the centre; while, it was reduced towards the edges of the test tank, increase in subgrade strength, and layer thickness.

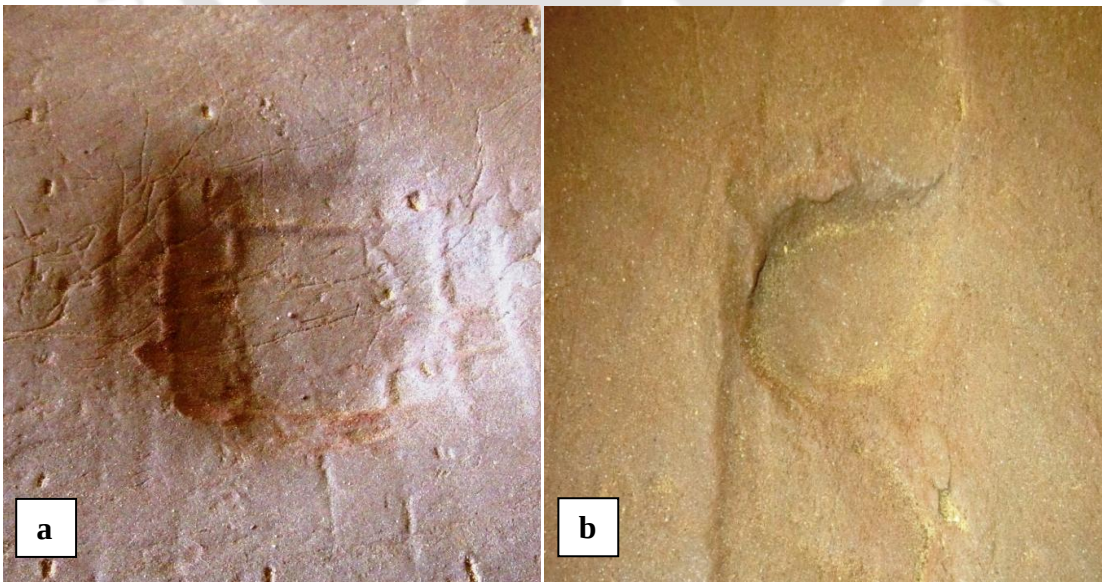

Fig. 6.26 Subgrade-deformation for (a) geogrid and (b) geocell-reinforced foundation systems (c_u = 7 kPa with H = 0.63D)

6.5 SUMMARY

In Chapter 6, responses of geocell-reinforced foundations are presented. In this series D, the heights of geocells (h) were so selected that in combination with the sand cushion (u = 0.1D), the thickness of the geocell-sand mattress should be the same as H (= h + u), as considered in series B and C. Thus, geocells-heights were varied as 0.53, 1.05, 1.57, and 2.09D overlying different clay subgrades having c_u = 7 to 60 kPa.

Substantial improvements in bearing pressure were observed with geocells as compared to unreinforced and/or geogrid-reinforced systems. The beneficial effect is attributed to the confinement of the in-filled sand and interception of potential failure planes of the sand to behave like a semi-rigid slab like structure. Besides, the interfacial resistance provides additional benefits in load bearing. The geocell-sand mattress redistributes the incoming load to a greater depth and wider area with lesser pressure intensity to the underlying subgrades to improve the bearing capacity of the foundation systems. The foundation performance was improved with increase in geocell-height and footing settlement. The increase in geocell-height increases the rigidity of the geocell-mattress due to increased number of joints and interfacial resistances derived through additional surface area. Higher bearing pressures were obtained in case of stiffer subgrades which is attributed to the greater subgrade support against the possible deformations. However, the improvement in bearing pressure, in terms of improvement factors, was decreased with subgrade strengths. Few adverse effects, such as buckling in geocell-walls, squeezing out of sand cushion etc were affected the foundation behavior, specially, for the stiffer subgrades and thicker geocells. Depending on the test results, the optimum geocell-height (h) can be considered as 1.05D. A maximum about 12-fold improvement (I_{fsgc}) in bearing pressure was observed for c_u = 7 kPa; while, that was only about 2.3 for c_u = 60 kPa.

Chapter 7. GEOCELL-GEOGRID REINFORCED FOUNDATIONS

7.1 INTRODUCTION

Conventionally, a layer of planar geogrid is laid over the soft ground before constructing the geocell-mattress. The geogrid layer serves in two ways; it facilitates the constructional movement over the soft ground and enhances the overall performance of the geocell-reinforcement by providing additional support (Bush et al., 1990; Cowland et al., 1993). In fact, researches have indicated the benefits of using base geogrid in addition to the geocell-reinforcement (Dash et al., 2001b; Sitharam et al., 2007).

Foundation configurations having a geogrid at the bottom of geocell-sand mattress overlying different clay subgrades were investigated under series E experiments. Schematic of a typical foundation configuration is shown in Fig. 7.1. Foundation configurations were almost similar to that followed in series D, except placing a geogrid of width '*b*' below the geocell mattress. The details of various tests performed under this test series are presented in Table 7.1. Test results and effect of various parameters on the foundation performance are presented in following sections.

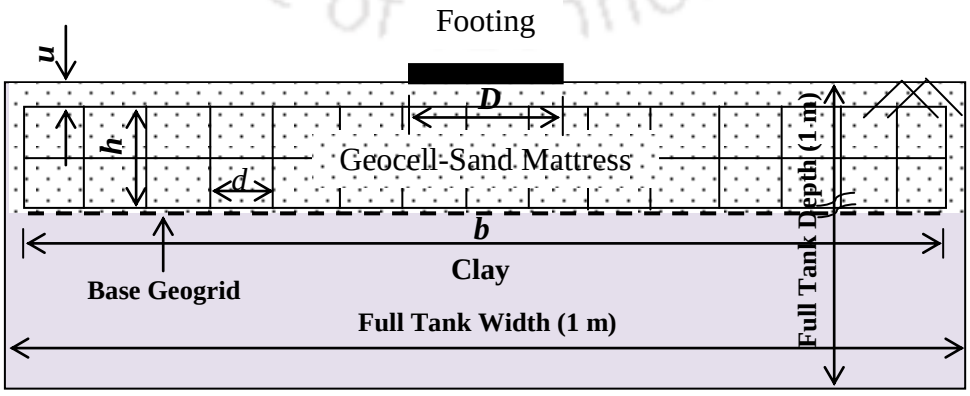

Fig. 7.1 Schematic configuration of geocell-geogrid reinforced foundations

Table 7.1 Details of test series E

Test Series	Foundation system	Test parameters		No. of Tests
		Variables	Constants	
E	Geocell-geogrid reinforced sand overlying clay subgrades	c_u = 7, 15, 30, 60 kPa h/D = 0.53, 1.05, 1.57, 2.09	D_r = 80% u = 0.1D, d/D = 0.8, b/D = 6	16

7.2 TEST RESULTS

The model tests were performed on geocell-geogrid foundation systems having different layered configurations (H = 0.63 to 2.19D) overlying different clay subgrades of varying undrained shear strengths (c_u = 7 to 60 kPa). The geocell-heights were kept similar to that followed in series D, i.e. h = 0.53 to 2.09D with u = 0.1D. A total of 16 tests were conducted in this series.

Pressure-settlement responses of geocell-geogrid reinforced foundations are presented in Fig. 7.2 to Fig. 7.5, for different clay subgrades having c_u = 7, 15, 30, and 60 kPa, respectively. Pressure-settlement responses of corresponding homogeneous clay beds (series A) are also shown in the figures. It is seen that the bearing pressures of the geocell-geogrid foundations were increased with footing settlement (s/D). For instance, for c_u = 7 kPa in Fig. 7.2, the variation in bearing pressures are about 119, 168, and 203 kPa corresponding to 6, 12, and 24% of s/D, respectively (at h = 0.53D). Similar variations were also found for the other foundation systems having different geocell-heights (h) and subgrade strengths (c_u). The results also indicate that the bearing pressures were influenced by the height of geocell beyond 6% settlement level. However, there is no consistent trended variation of bearing pressures with geocell heights. Higher bearing pressures were observed for thicker geocells, up to h = 1.05D. The variation in bearing pressures at s/D = 24%, for the change in geocell thickness from 0.53 to 1.05D, are 203 to 321 kPa, 265 to 349 kPa, 384 to 489 kPa,

and 622 to 720 kPa, for c_u = 7, 15, 30, and 60 kPa, respectively. In general, higher bearing pressures were observed for the geocell-reinforced foundations with base geogrid (series E), as compared to the geocell-alone systems (series D). Besides, higher bearing pressures were noticed for stiffer clay subgrades. In case of c_u = 7, 15, 30, and 60 kPa, the maximum bearing pressures were noted about 377, 405, 489, and 720 kPa, respectively (Fig. 7.2 to Fig. 7.5), as compared to 363, 377, 398, and 559 kPa for the corresponding geocell-alone systems (Fig. 6.2 to Fig. 6.5).

Typical variation of surface deformation profile with footing settlement is presented in Fig. 7.6, for geocell-geogrid reinforced foundation for clay subgrade of c_u = 7 kPa (at H = 0.63D). The deformation profile depicts higher heaving at a distance 2D from the centre of the footing. This trend is almost similar to the profiles obtained for the geocell-alone system which was presented in Fig. 6.6.

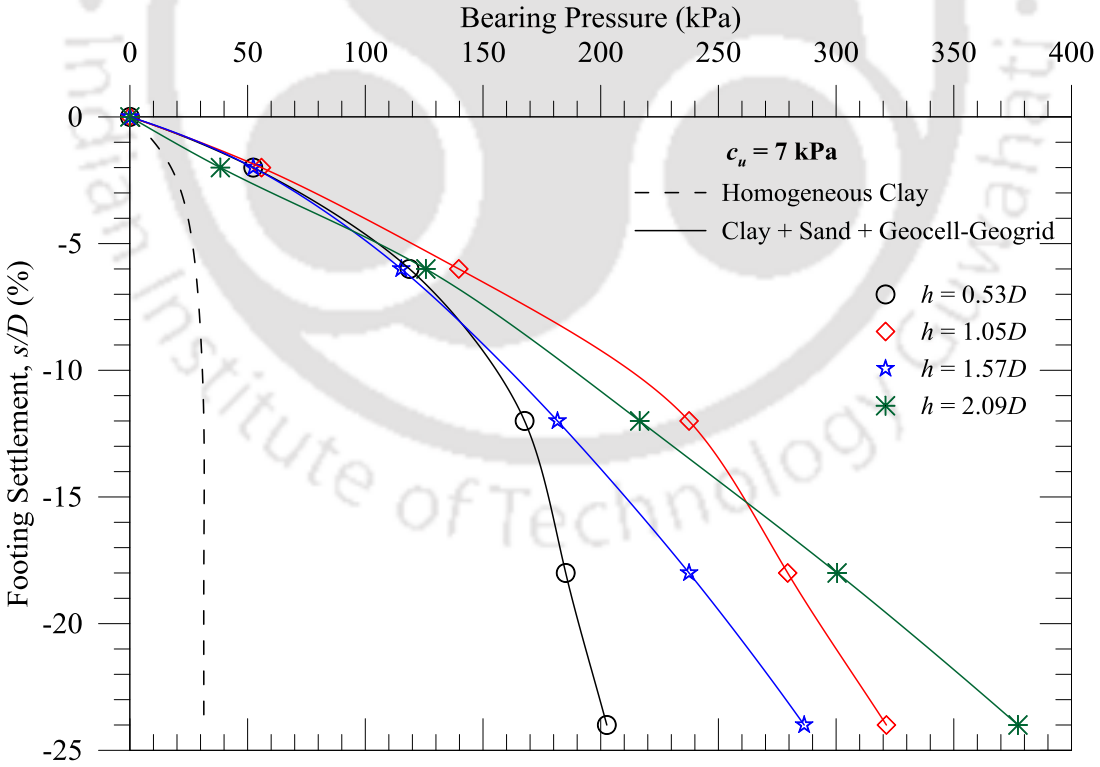

Fig. 7.2 Pressure-settlement responses of geocell-geogrid foundations: c_u = 7 kPa

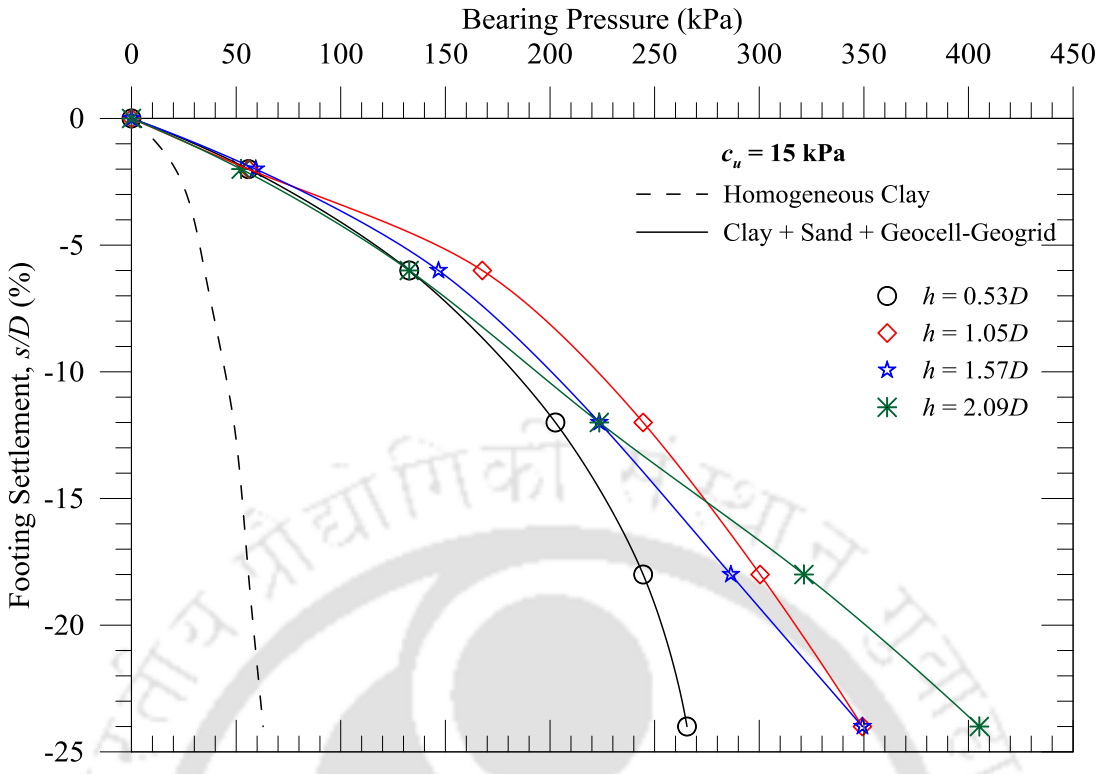

Fig. 7.3 Pressure-settlement responses of geocell-geogrid foundations: c_u = 15 kPa

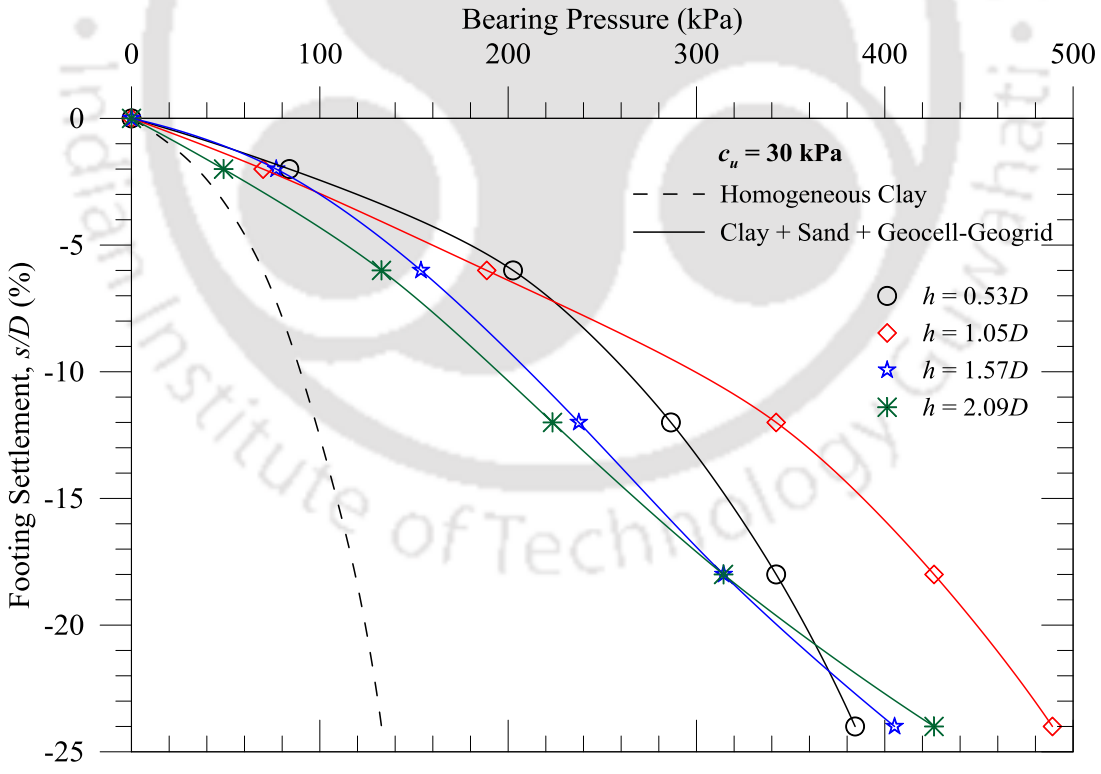

Fig. 7.4 Pressure-settlement responses of geocell-geogrid foundations: c_u = 30 kPa

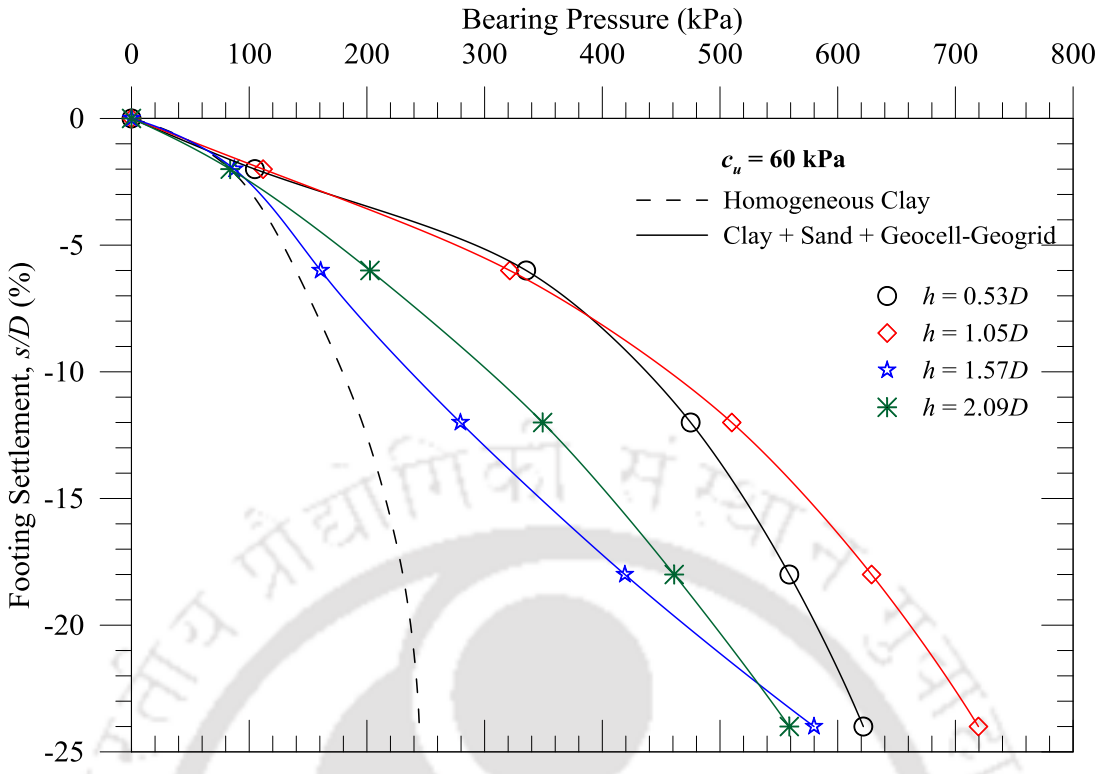

Fig. 7.5 Pressure-settlement responses of geocell-geogrid foundations: c_u = 60 kPa

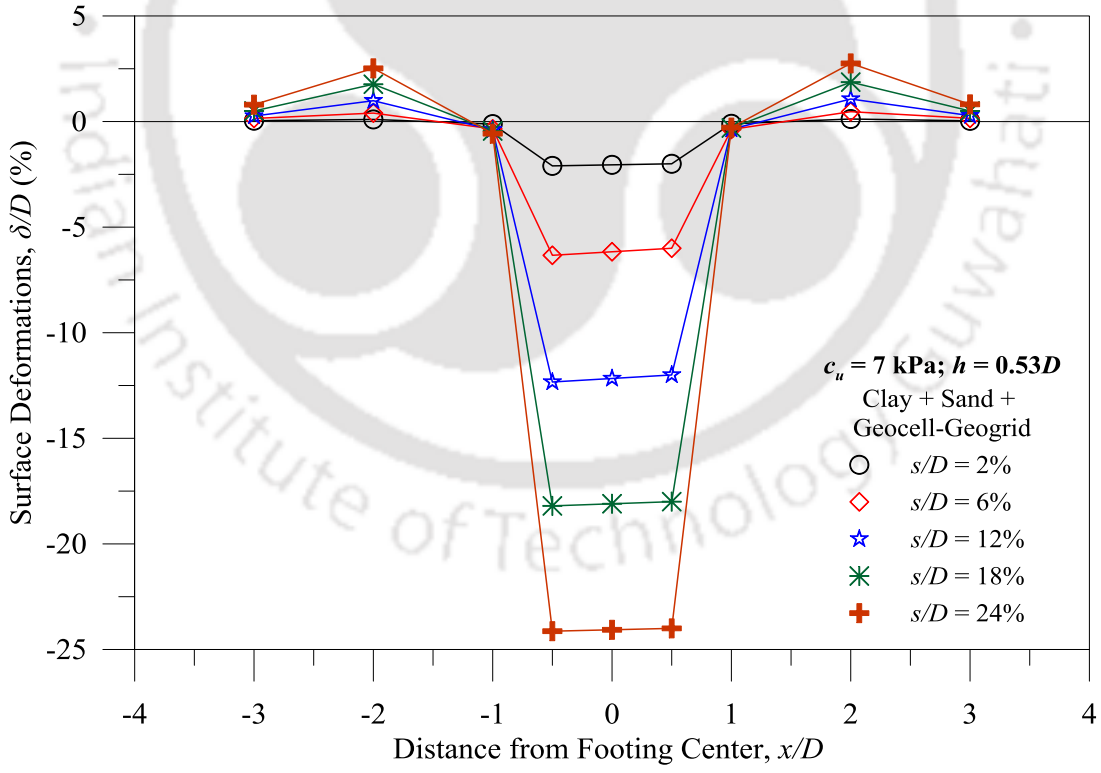

Fig. 7.6 Typical surface deformation profile for geocell-geogrid reinforced foundation (c_u = 7 kPa and H = 0.63D)

7.3 DISCUSSIONS ON TEST RESULTS

Performance of geocell-geogrid foundations are discussed in the following sections, bringing out the effect of various parameters: footing settlement (*s/D*), geocell-height (*h*), and subgrade strength (c_u). The obtained pressure-settlement responses from the model tests are further analyzed in terms of different bearing pressure improvement factors. Two new improvement factors are defined as the ratios of bearing pressures of two different foundation systems under consideration, at same footing settlement levels, as shown in Eqs. 7.1 and 7.2.

$$(I_{fsgcg}) = (\frac{q_{sgcg}}{q_c})_{\text{[at same } s/D \text{ level]}} \quad (7.1)$$

$$(I_{fbg}) = (\frac{q_{sgcg}}{q_{sgc}})_{\text{[at same } s/D \text{ level]}} \quad (7.2)$$

Where, q_{sgcg} is the bearing pressure of geocell-geogrid reinforced foundation system; while, the q_{sgc} and q_c are the bearing pressure of corresponding geocell-reinforced foundation and the homogeneous clay bed, respectively, at similar level of *s/D*. The evaluated improvement factors are summarized in Table 7.2.

7.3.1 Effect of Footing Settlement (s/D)

Pressure-settlement responses of geocell-geogrid reinforced foundations (Fig. 7.2 to Fig. 7.5) indicated significant influence of footing settlement on the foundation performances. Higher bearing pressures at greater footing settlement levels (*s/D*) were observed for all configurations. For instance, for c_u = 15 kPa and h = 1.05*D*, the variation in bearing pressures is 56 to 349 kPa for the variation in footing settlement as 2 to 24% of *s/D* (Fig. 7.3). Wherein, in similar foundation configuration (h = 1.05*D* and *s/D* = 2-24%), the variation of bearing pressures are 70 to 489 kPa (Fig. 7.4) and 112 to 720 kPa (Fig. 7.5), for c_u = 30 and 60 kPa, respectively.

Table 7.2 Summary of bearing pressure improvement factors

Footing Settlements (s/D)	Geocell Height (h/D)	Bearing Pressure Improvement Factor							
		c_u = 7 kPa		c_u = 15 kPa		c_u = 30 kPa		c_u = 60 kPa	
		I_{fsgcg}	I_{fbg}	I_{fsgcg}	I_{fbg}	I_{fsgcg}	I_{fbg}	I_{fsgcg}	I_{fbg}
2%	0.53	2.99	1.88	2.66	1.14	2.40	1.50	1.25	1.15
	1.05	3.19	1.33	2.66	1.14	2.00	1.00	1.33	1.14
	1.57	2.99	1.07	2.83	1.06	2.20	1.00	1.04	1.04
	2.09	2.20	1.10	2.50	1.07	1.40	1.00	1.00	1.00
6%	0.53	4.26	2.13	3.80	1.27	2.90	1.71	2.40	1.55
	1.05	5.01	1.48	4.80	1.14	2.70	1.13	2.30	1.18
	1.57	4.13	1.06	4.20	1.05	2.20	1.00	1.15	1.05
	2.09	4.51	1.06	3.80	1.06	1.90	1.00	1.45	1.00
12%	0.53	5.34	2.18	4.14	1.45	2.93	1.71	2.42	1.51
	1.05	7.56	1.89	5.00	1.25	3.50	1.48	2.60	1.28
	1.57	5.78	1.08	4.57	1.07	2.43	1.03	1.43	1.05
	2.09	6.90	1.07	4.57	1.07	2.29	1.07	1.78	1.00
18%	0.53	5.90	1.89	4.37	1.52	2.88	1.63	2.42	1.51
	1.05	8.90	1.86	5.37	1.30	3.59	1.53	2.73	1.34
	1.57	7.56	1.13	5.12	1.05	2.65	1.07	1.82	1.07
	2.09	9.57	1.05	5.75	1.05	2.65	1.07	2.00	1.00
24%	0.53	6.45	1.71	4.22	1.41	2.90	1.62	2.54	1.51
	1.05	10.23	1.84	5.55	1.32	3.69	1.56	2.94	1.41
	1.57	9.12	1.14	5.55	1.04	3.05	1.14	2.37	1.08
	2.09	12.01	1.04	6.44	1.07	3.21	1.07	2.29	1.00

Variation of improvements in bearing pressure for geocell-geogrid reinforced foundations, with respect to the corresponding homogeneous clay beds, are presented in terms of I_{fsgcg} (Eq. 7.1) in Fig. 7.7, for c_u = 7 kPa. Higher improvements in bearing pressures with footing settlement can be observed. The I_{fsgcg} is varied from 3 to 6.45 (for h = 0.53D) and 2.2 to 12 (for h = 2.09D) for s/D variation from 2 to 24%. The improvement factors, I_{fsgc}, obtained for geocell-alone reinforced foundations, are also presented in the figure for comparison. In similar foundation configurations (h = 0.53 and 2.09D, s/D = 2-24%), the variation in I_{fsgc} were 1.6-3.78 and 2-11.57, respectively. The additional improvements are attributed to the strain mobilized membrane resistance developed through the base geogrid.

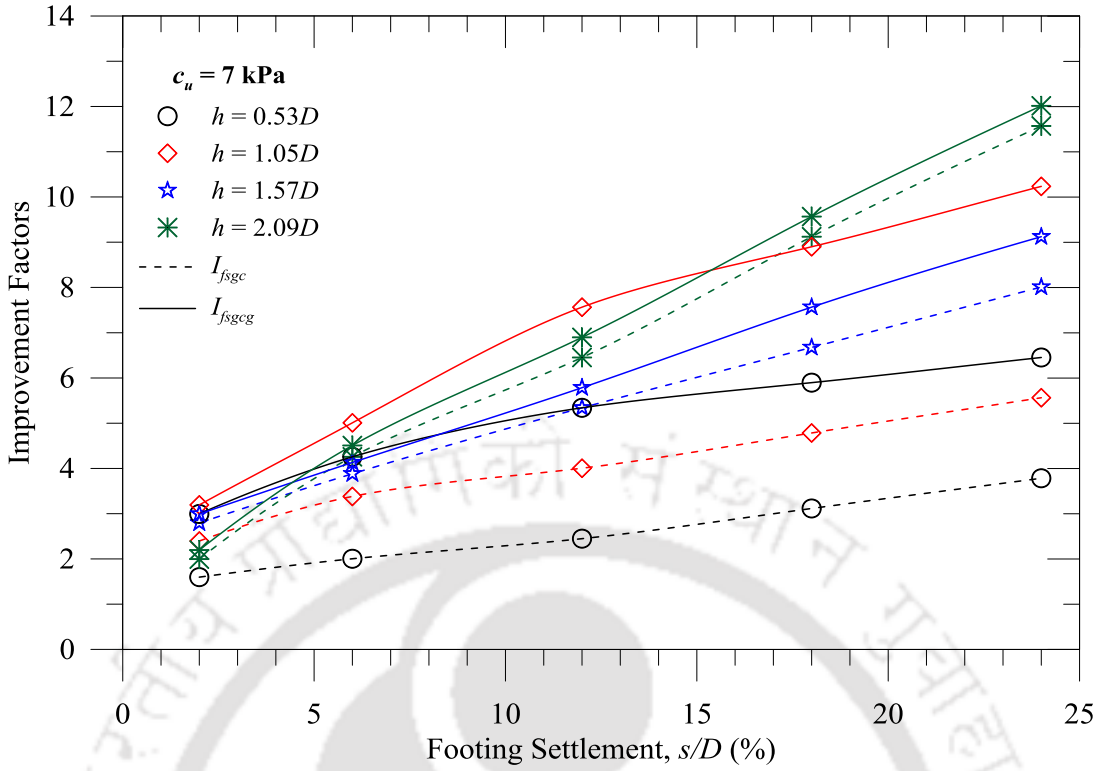

Fig. 7.7 Variation of I_{fsgcg} and I_{fsgc} for different h/D for c_u = 7 kPa

Typical variation in surface deformations for a geocell-geogrid reinforced foundation (c_u = 7 kPa; h = 0.63D), at x = D, 2D, and 3D from footing center, are presented in Fig. 7.8. The corresponding deformation variations of geocell-reinforced foundations are also presented in the figure. Reduced surface deformations can be noticed for the geocell-geogrid reinforced systems, as compared to geocell-reinforced foundations. It is attributed to the additional support provided by the base geogrid against the possible bending of the geocell-mattress. However, at x = 2D and 3D, marginally higher heaving can be observed at higher levels of footing settlements (s/D > 15%) for geocell-geogrid foundations, relative to the geocell systems. It is due to the interlocking of geocell-mattress at the base geogrid which effected as localized upward movements (rotational) of the geocell-mattress away from the footing center, causing higher heaving at the foundation surface.

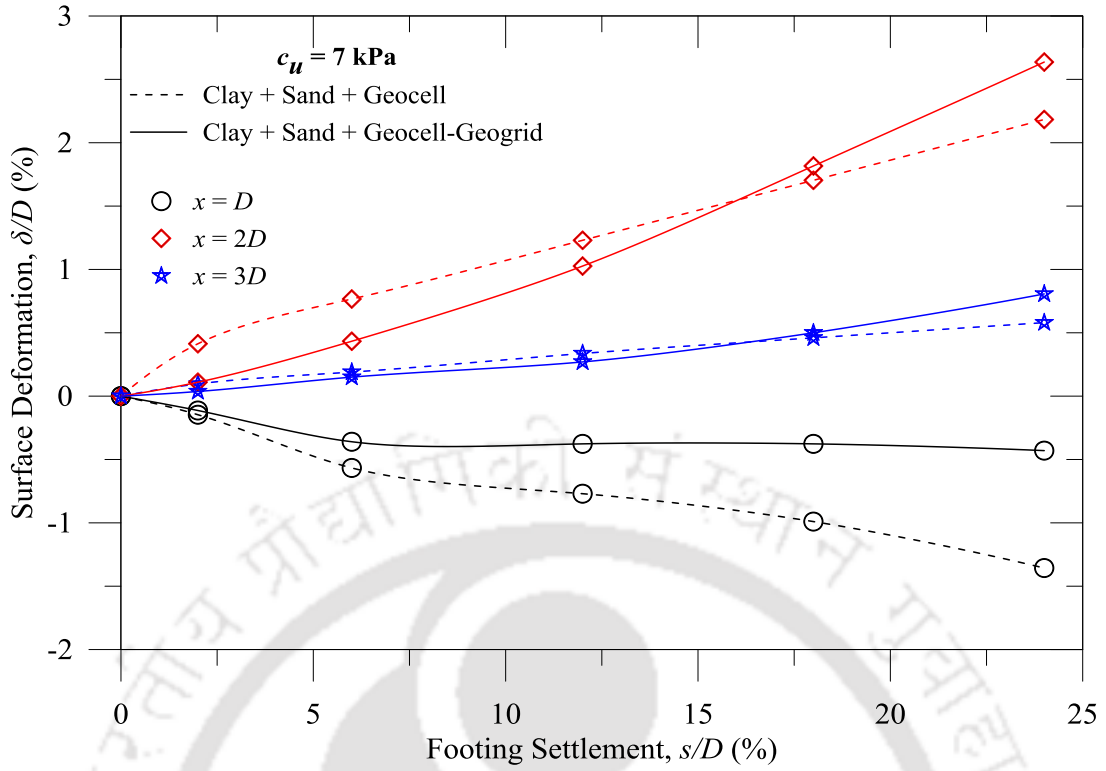

Fig. 7.8 Variation of δ/D with s/D at $x = D$, $2D$, and $3D$, for c_u = 7 kPa at $H = 0.63D$

7.3.2 Effect of Geocell-Height (h)

Influence of geocell-height (h) on the pressure-settlement responses of geocell-geogrid reinforced systems can be noticed in Fig. 7.2 to Fig. 7.5. In Fig. 7.2, variations in bearing pressures were about 168, 238, 182, and 217 kPa, for the variation in geocell height (h) as 0.53, 1.05, 1.57, and 2.09D, respectively (at s/D = 12% for c_u = 7 kPa), showing higher response at h = 1.05D. Similar higher bearing pressure responses can be seen for c_u = 30 and 60 kPa (Fig. 7.4 and Fig. 7.5, respectively). However, for c_u = 15 kPa, h = 2.09D showed highest response for $s/D \geq$ 18%. In Fig. 7.4 and Fig. 7.5, for h = 1.05D, considerable improvement in bearing pressure as compared to foundation with h = 0.53D can be noticed only at s/D > 6%. This behaviour depicts that the effect of geocell-height is sensitive to the footing settlement levels and subgrade strengths. This could be attributed to the buckling in geocell-walls which further affected by the mobilization of interfacial resistance due

to additional support of the base geogrid. These effects are very prominent for the geocell-geogrid configurations as compared to geocell-alone reinforced foundations.

Variation of improvement factors, I_{fsgcg} and I_{fsgc}, at s/D = 12%, with geocell heights (h) for different subgrade strengths (c_u) are presented in Fig. 7.9. It can be noticed that I_{fsgcg} variations do not follow a consistent trend with geocell heights. Maximum improvement of about 7.6-fold is seen for c_u = 7 kPa at h = 1.05D. Foundations with geocell heights (h) ≤ 1.57D showed higher improvement in the case of geocell-geogrid foundation than geocell alone systems (I_{fsgc}).

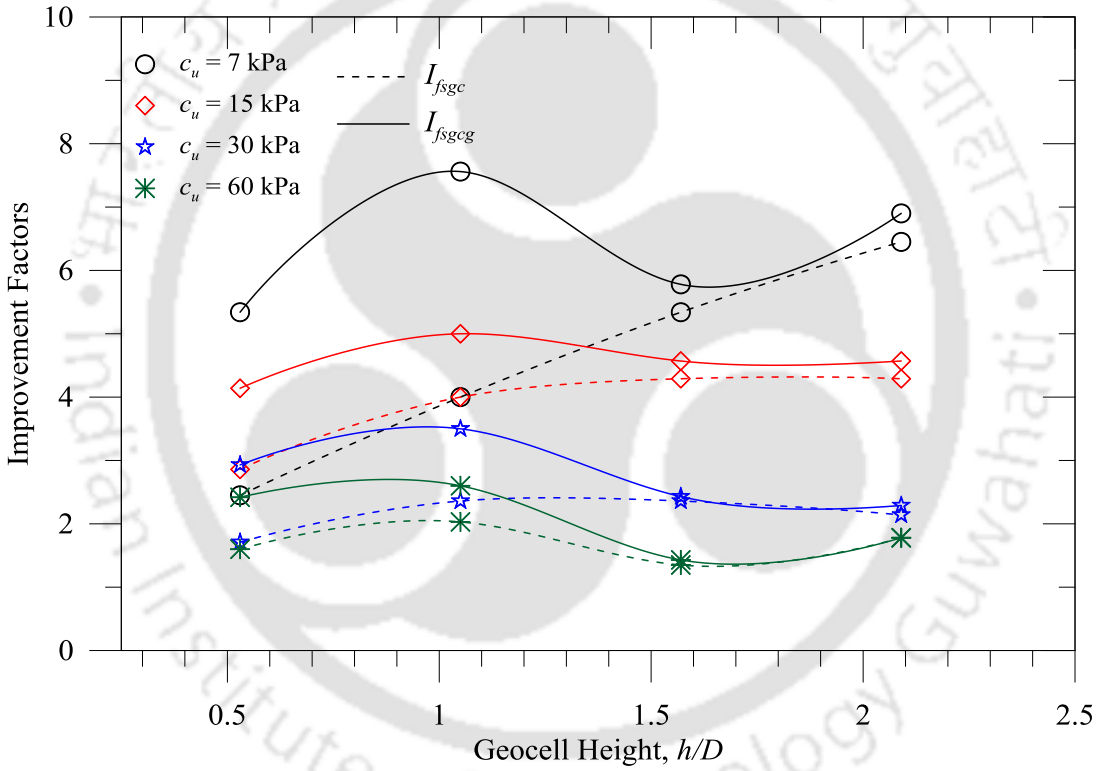

Fig. 7.9 Variation of I_{fsgcg} and I_{fsgc} for different h/D at s/D = 12%

The contribution of base geogrid, in terms of I_{fbg} (Eq. 7.2) at two different footing settlement levels (s/D = 12 and 24%) is presented in Fig. 7.10. It can be noticed that the beneficial effect of base geogrid is reduced for thicker geocells (h ≥ 1.57D), in which I_{fbg} values are about 1.0 (Fig. 7.10 and Table 7.2), indicating no additional contribution. This reduction is due to the insufficient strain generation at the base geogrid for membrane action. The shorter geocell-mattress (h < 1.57D),

owing to its low structural rigidity, deflects more upon loading which induces required strain in base geogrid for membrane resistance. Being stiffer, the thicker geocell-mattresses ($h \geq 1.57D$), offer more resistance against the possible bending that prevents from generating sufficient membrane resistances.

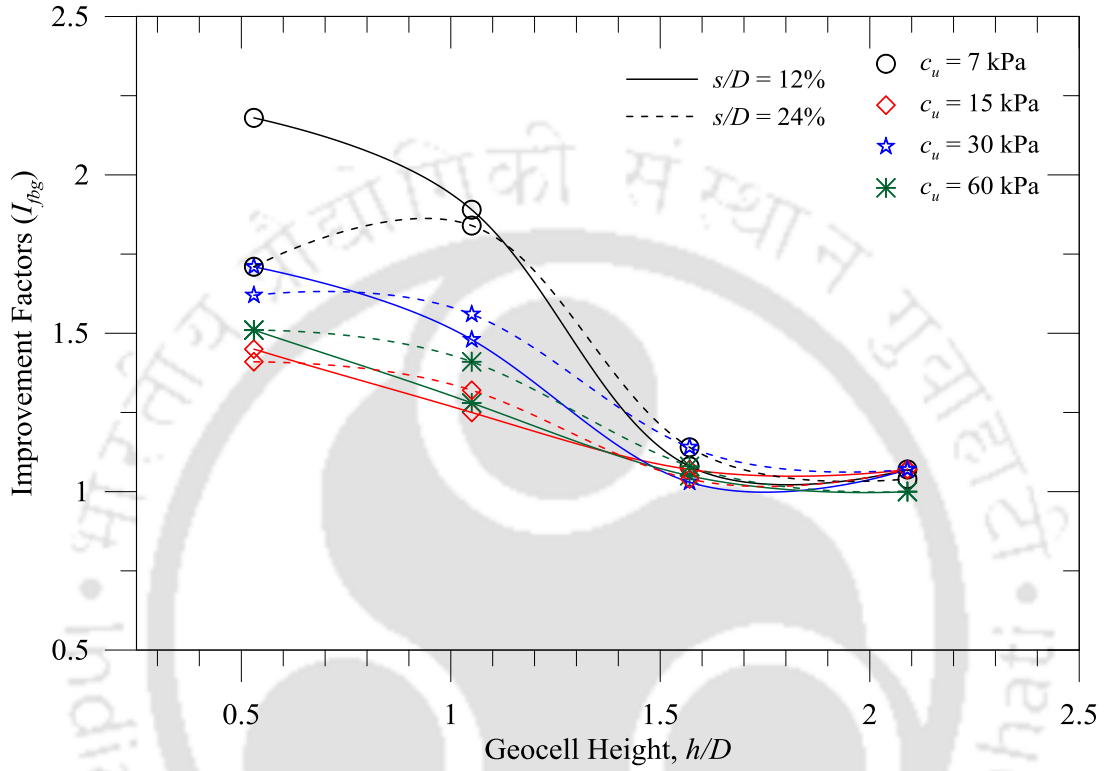

Fig. 7.10 Variation of I_{fbg} for different h/D at s/D = 12 and 24%

Variations of surface deformations, at $x = D$ and $2D$ from footing center, for geocell and geocell-geogrid reinforced foundations with c_u = 7 kPa are presented in Fig. 7.11 and Fig. 7.12, respectively. It is noticed that the deformation profiles, in both the foundation systems, are not consistent with respect to geocell heights. However, in geocell-geogrid foundations, at $x = D$, surface deformations were reduced compared to geocell-reinforced foundations. It is attributed to additional support provided by the base geogrid against the possible deformations in geocell-mattress. For thick geocell-mattress, such as $h = 2.09D$, the buckling effect in geocell-walls was more due to the restrain deformations. The higher buckling in geocell-walls resulted in greater surface settlement around $x = D$ (in Fig. 7.11). In Fig. 7.12, a

comparatively higher heaving can be noticed at x = 2D. It is due to the plate-like behavior of the base geogrid. Besides, the upward rotation of geocell-mattress, being interlocked at base, enhanced the heaving which increased with footing settlements.

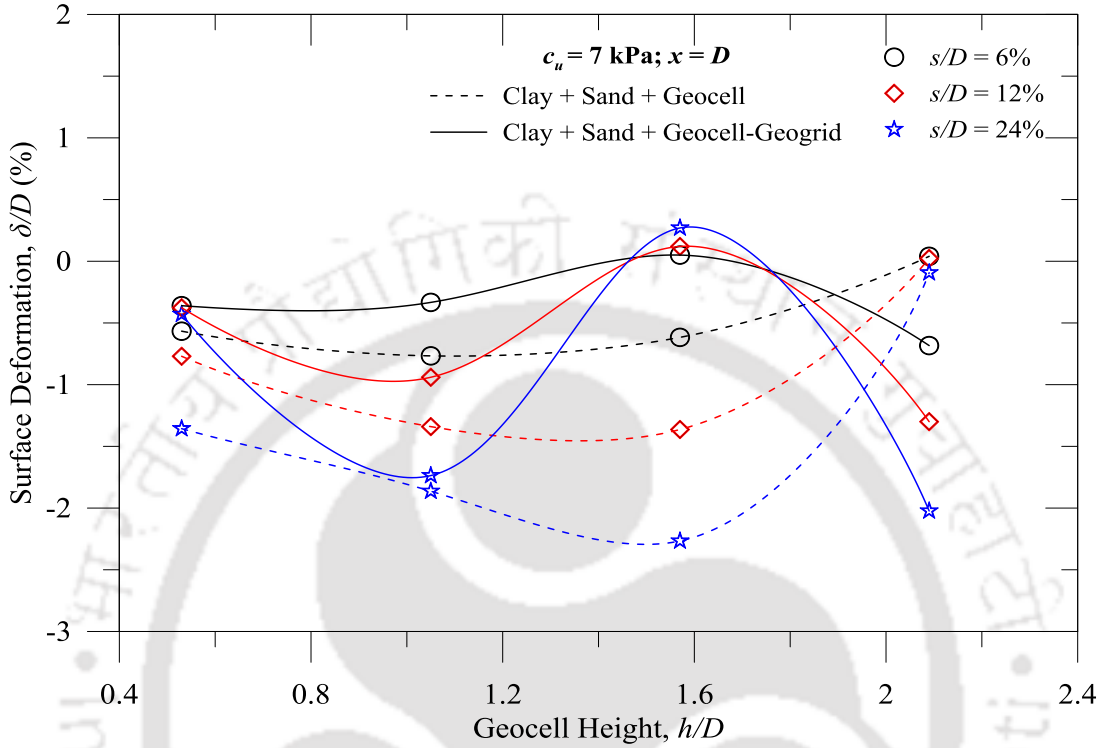

Fig. 7.11 Variation of δ/D at x = D of geocell and geocell-geogrid system: c_u = 7 kPa

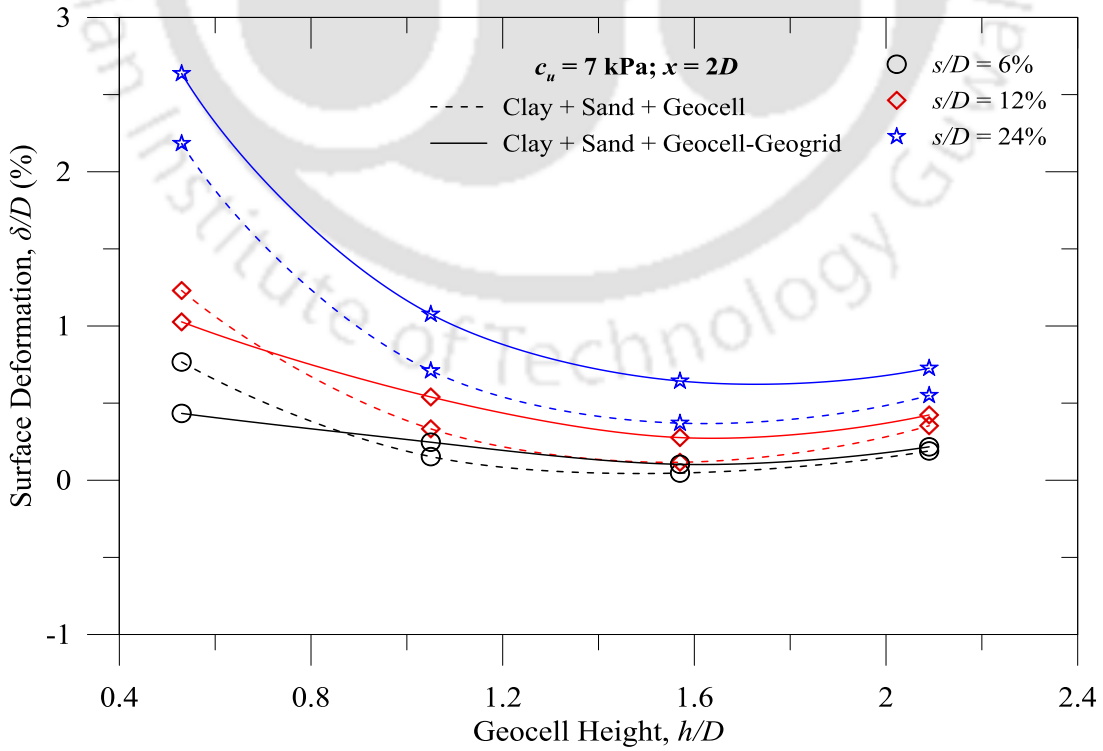

Fig. 7.12 Variation of δ/D at x = 2D of geocell and geocell-geogrid system: c_u = 7 kPa

7.3.3 Effect of Subgrade Strength (c_u)

Pressure-settlement responses of geocell-geogrid reinforced foundations with different subgrades (c_u), are presented in Fig. 7.13 (for h = 0.53D). Responses of the corresponding geocell foundations are also shown in Fig. 7.13. The figure depicts significant influence of subgrade strengths on the foundation behavior. Higher bearing pressures for stiffer subgrades (c_u) can be noticed for geocell-geogrid reinforced foundations. The maximum bearing pressures at s/D = 24% of about 203, 265, 384, and 621 kPa for c_u = 7, 15, 30, and 60 kPa, respectively, can be noted in Fig. 7.13. The corresponding bearing pressures for the geocell foundations were about 119, 189, 238, and 412 kPa, in the same order. This indicates significant improvements in bearing pressures for geocell-geogrid foundations as compared to that of geocell-reinforced systems. The increase in bearing pressure is about 40-70%. The improvement is attributed to membrane resistance of base geogrid as discussed earlier.

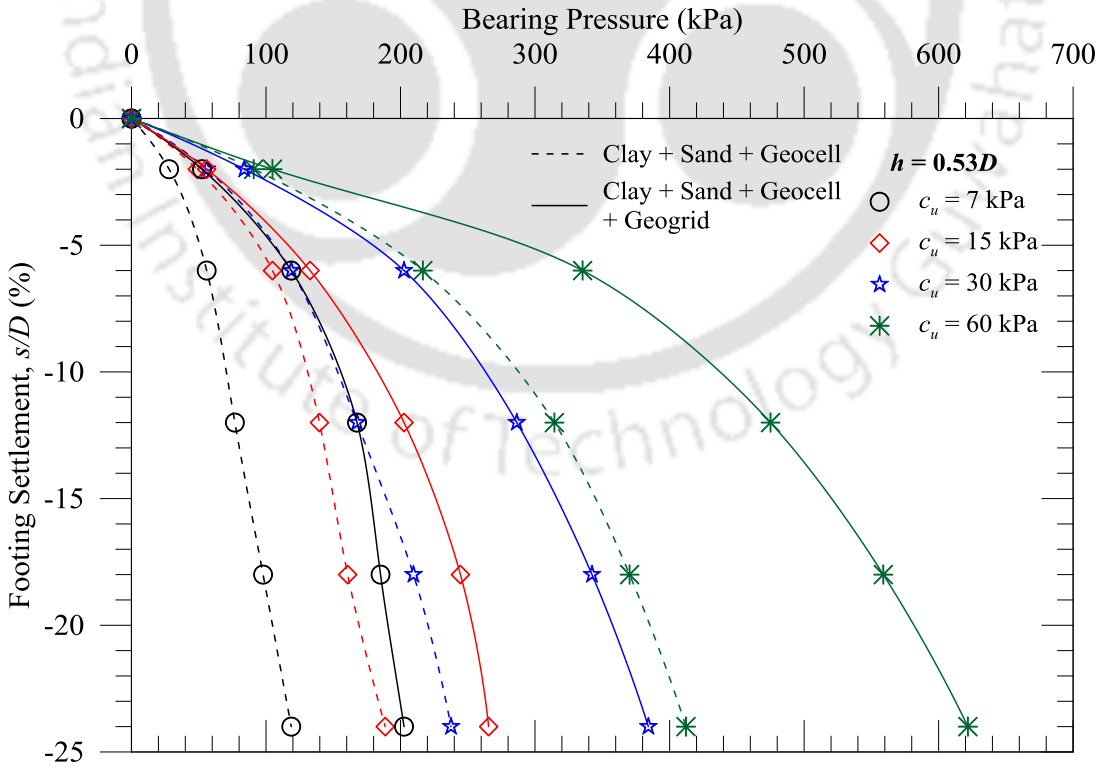

Fig. 7.13 Pressure-settlement responses of geocell (with and without base geogrid) reinforced foundations at h = 0.53D

The variations in improvement factors, I_{fsgcg} and I_{fsgc}, with subgrade strengths at different settlement levels are presented in Fig. 7.14, for geocell-geogrid and geocell reinforced systems, respectively, for a geocell height of 1.05*D*. Significant improvements for the geocell-reinforced foundations with the base geogrid can be noticed. In general, the improvement factors, I_{fsgcg} and I_{fsgc}, are reduced with increase in subgrade strength for all settlement levels. The variation in I_{fsgcg} is in the range of 10.23 to 2.94, for the change in subgrade strength (c_u) from 7 to 60 kPa (at *s/D* = 24%); while, for similar subgrade variations, the variation in I_{fsgc} is 5.56 to 2.09. The reductions in improvement factors are attributed to the stiffness of the clay subgrades which provides higher resistance against the possible deformations and thus, restricted the membrane resistances. Besides, it was also affected due to the geocell-buckling as discussed earlier. The base geogrid provides additional stiffness to the clay subgrades which enhanced the buckling in geocell-walls. The effect is even prominent for the very soft subgrade, in geocell-geogrid configuration.

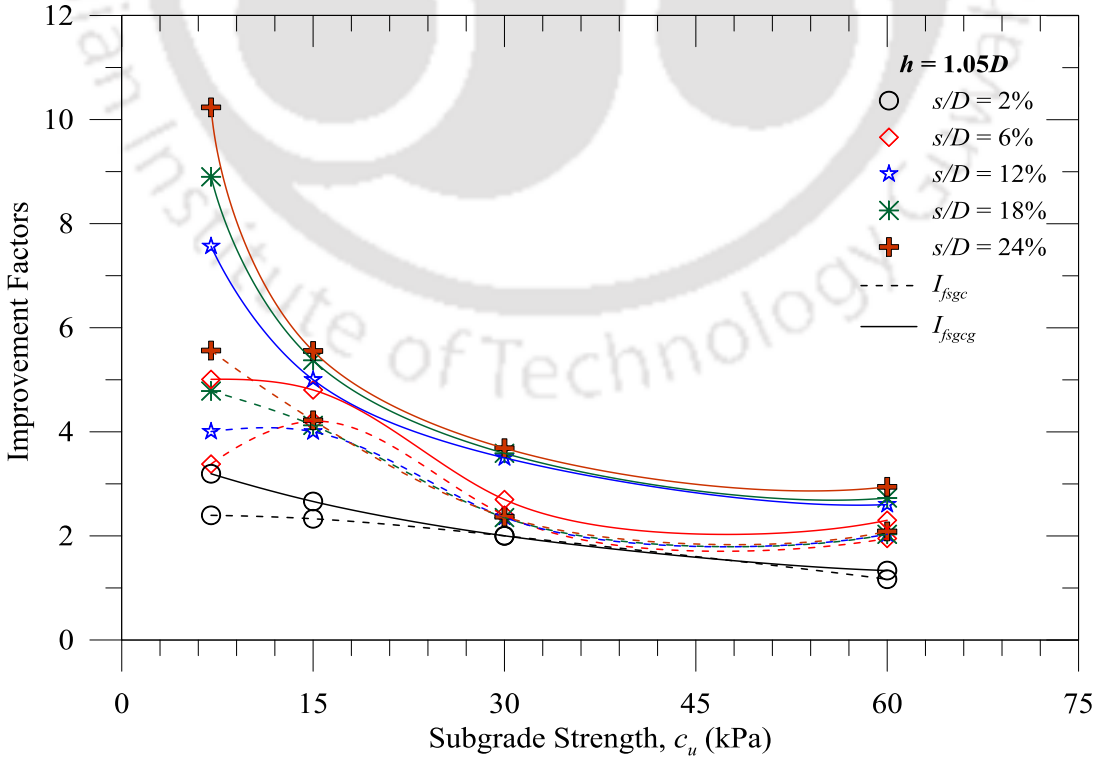

Fig. 7.14 Variation of I_{fsgcg} and I_{fsgc} for different *s/D* and varying c_u at *h* = 1.05*D*

Similar trends in variations of I_{fsgcg} and I_{fsgc} can also be noticed for h = 1.57 and 2.09D, as presented in Fig. 7.15. The ranges of variation of I_{fsgcg}, for h = 1.57 and 2.09D, are 1.15-9.12 and 1.45-12.01, respectively. The corresponding variations of I_{fsgcg} can be noted as about 1.10-8.01 and 1.15-9.12.

The contribution of base geogrid for different subgrades at h = 1.05D, in terms of I_{fbg}, is presented in Fig. 7.16, for different level of footing settlements. In Fig. 7.16, the I_{fbg} is in the range of 1.0-1.89. The variation of I_{fbg} for the case of 1.57D and 2.09D is presented in Fig. 7.17. Marginal contribution of base geogrid is noticed for the thicker geocells. In these cases, the ranges of I_{fbg} are about 1.0-1.14 and 1.0-1.07, for h = 1.57D and 2.09D, respectively. However, the variation of I_{fbg} is not consistent with respect to subgrade strengths and geocell heights, for all the settlement levels.

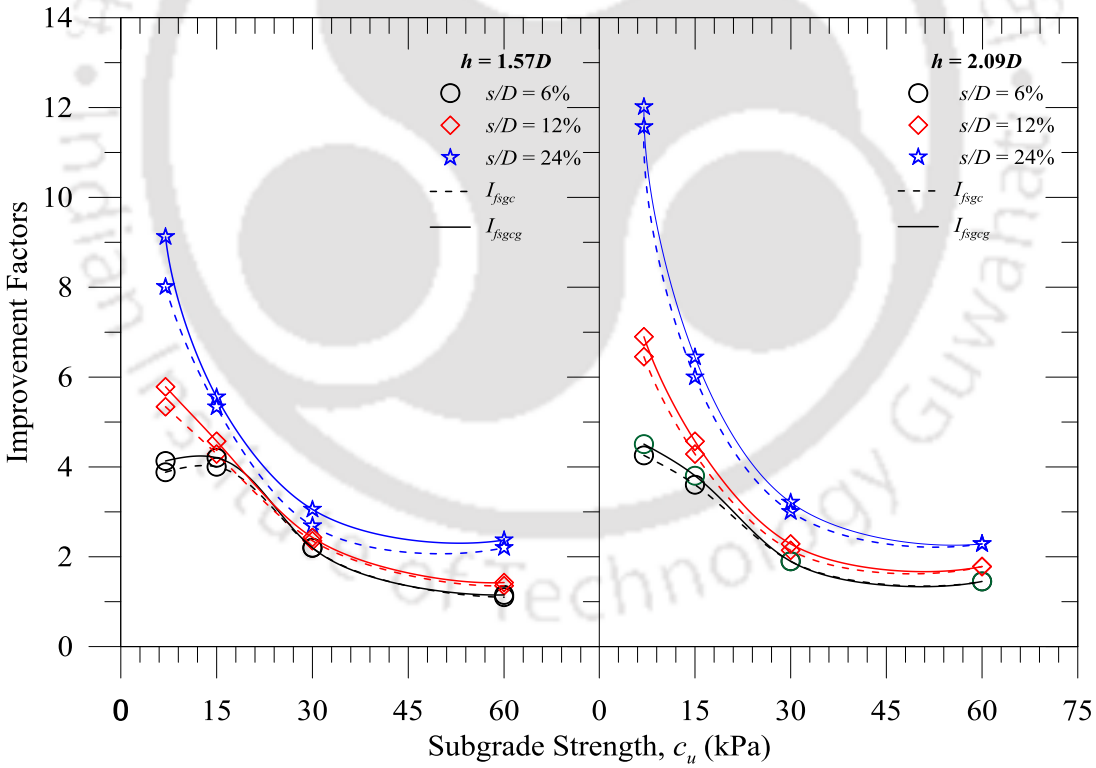

Fig. 7.15 Variation of I_{fsgcg} and I_{fsgc} with varying c_u for different s/D at h = 1.57 and 2.09D

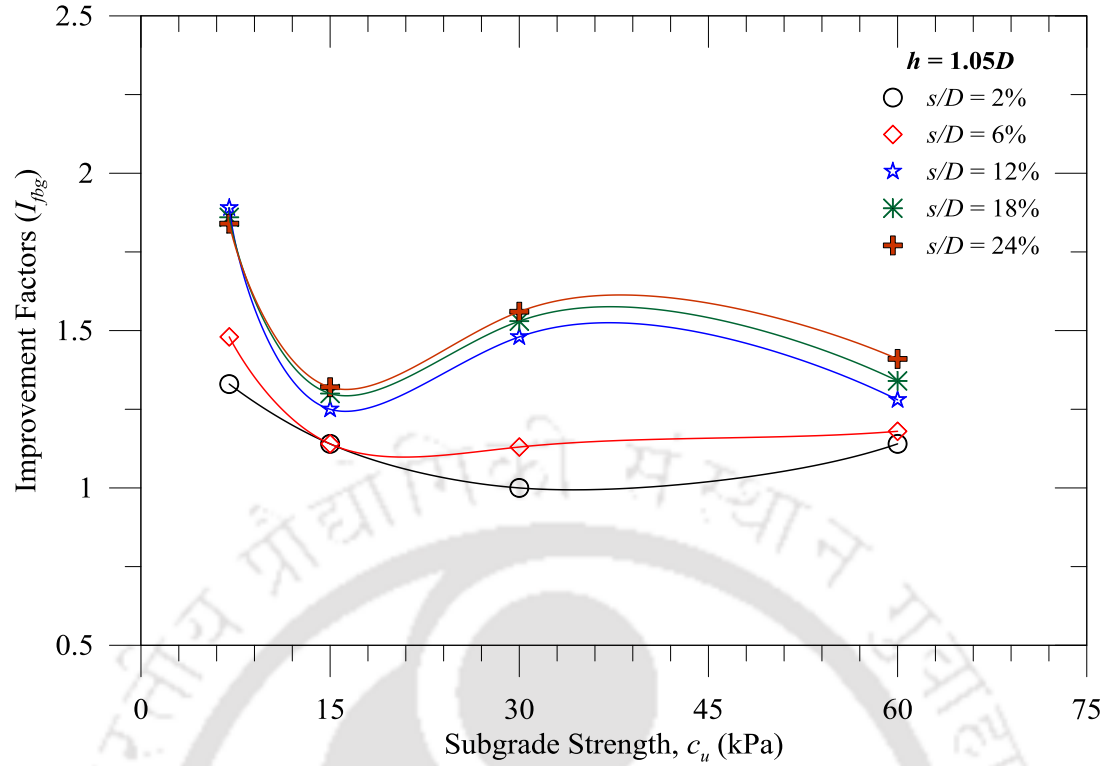

Fig. 7.16 Variation of I_{fbg} for varying c_u at h = 1.05D for different s/D

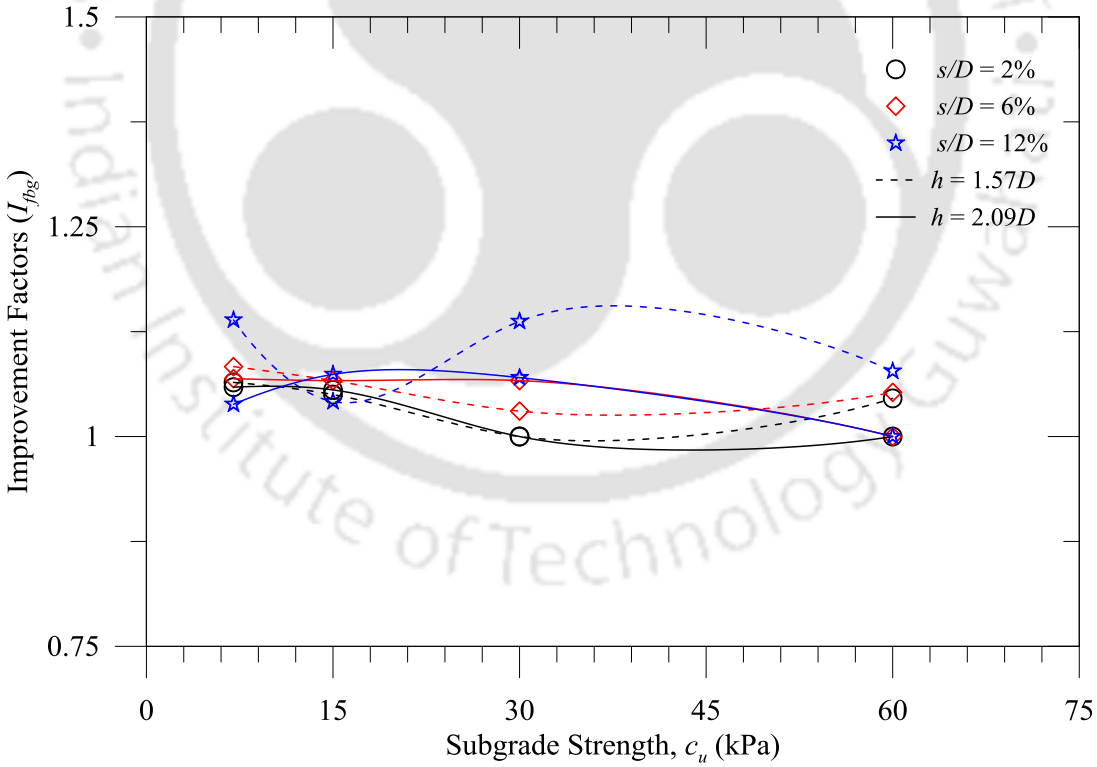

Fig. 7.17 Variation of I_{fbg} for varying c_u for different s/D at h = 1.57 and 2.09D

Typical surface deformation variations (at x = D and 2D) with subgrade strengths (c_u) for geocell-geogrid reinforced foundations (h = 0.53D) are presented in

Fig. 7.18 and Fig. 7.19, respectively, at footing settlements *s/D* = 6, 12, and 24%. Deformation behaviors of the corresponding geocell reinforced foundations are also presented in the figure for comparison. Almost similar deformation behaviors, with respect to subgrade strengths (c_u), can be noticed for both the foundation systems. However, comparatively reduced deformations at foundation surface were observed in the presence of base geogrid. A higher heaving at $x = 2D$, at greater level of footing settlement (*s/D* = 24%) can be noticed in Fig. 7.19. It is due to the localized upward bending of geocell-mattress, caused by the interlocking of geocell-mattress at the base, as discussed earlier.

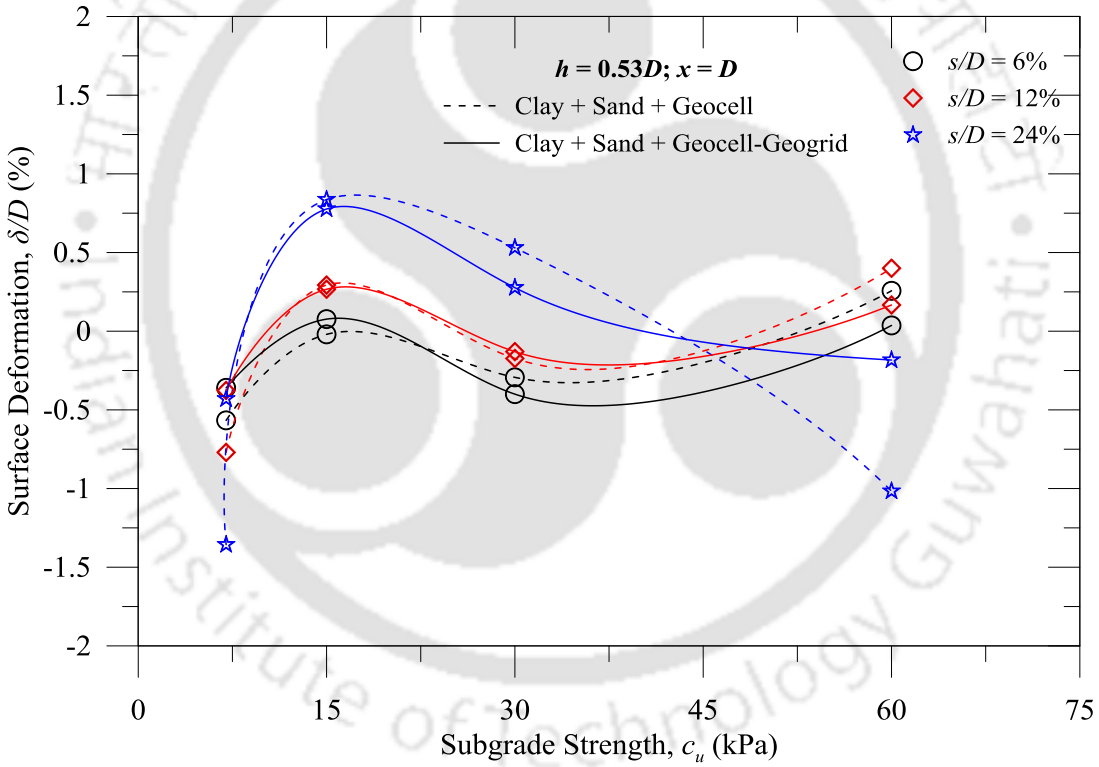

Fig. 7.18 Variation of δ/D at $x = D$ with c_u for different *s/D* levels ($h = 0.53D$)

7.4 POST EXPERIMENTAL OBSERVATIONS

Physical deformations of the clay subgrades were observed after each test. Photograph of a typical subgrade deformation for c_u = 7 kPa of geocell-geogrid reinforced foundation ($h = 0.53D$) is presented in Fig. 7.20a. Fig. 7.20b shows similar

figure for geocell reinforced foundation. Comparing both the figures, lesser depressions were observed for geocell-geogrid reinforced foundations than the geocell foundations. The depressions were more at the center and gradually reduced towards the tank boundary. For the geocell-geogrid foundations more uniform depression with impressions of geogrids was found instead of the clear shape of geocell-pockets. It was also observed from other tests that the depressions were reduced with increase in geocell-height and subgrade strengths. From the deformation profiles, it can be inferred that the load through the geocell-mattress is further redistributed and the footing settlement was restrained in the presence of base geogrid. The impressions of the geogrid aperture are signifying the interlocking between the subgrade and geogrid, indicating the generation of membrane resistance.

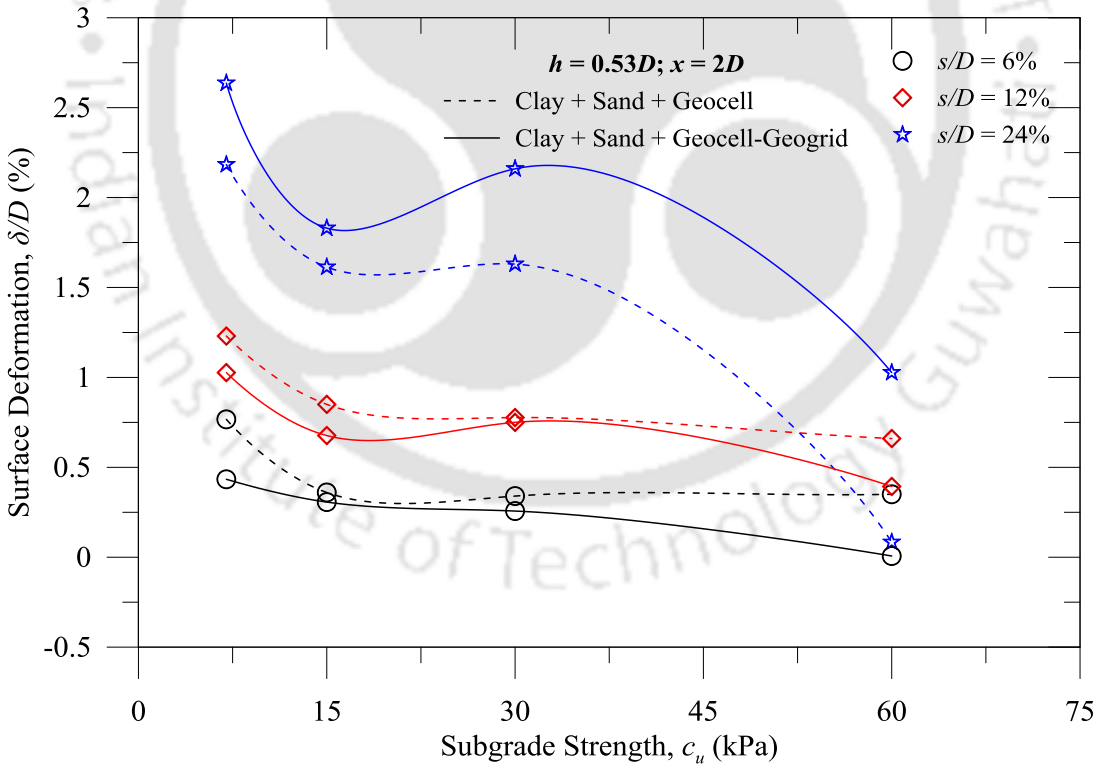

Fig. 7.19 Variation of δ/D at $x = 2D$ with c_u for different s/D levels ($h = 0.53D$)

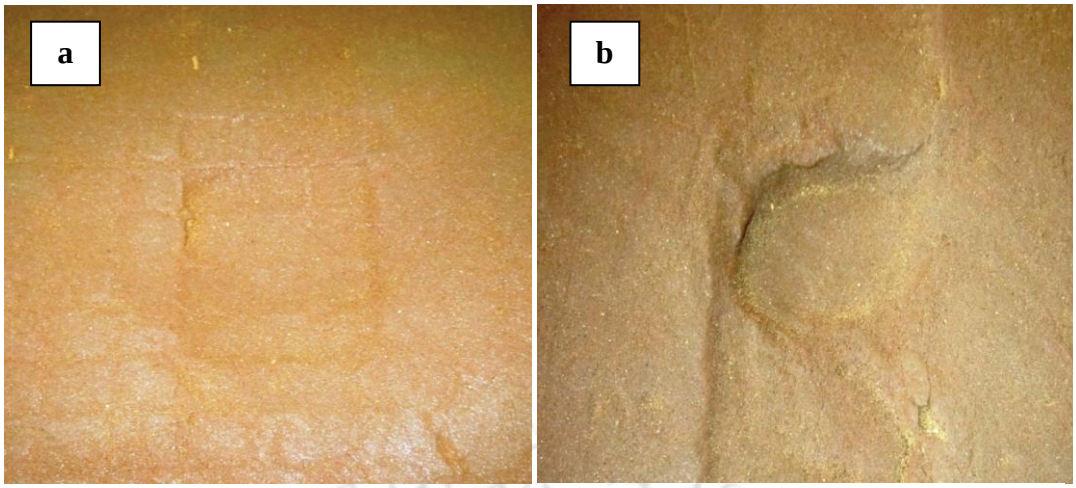

Fig. 7.20 Subgrade deformation for (a) geocell-geogrid and (b) geocell reinforced foundation (c_u = 7 kPa; h = 0.53D)

7.5 SUMMARY

Foundation behavior with a geogrid at the base of the geocell-sand mattress was presented in this chapter. In the test series E, for geocell-geogrid reinforced foundations, other than placing a geogrid of width 'b' at the bottom of geocell-sand mattress foundation configurations were kept same as followed in series D for geocell-alone reinforced systems.

The pressure-settlement responses have depicted further improvement in bearing pressure with the base-geogrid as compared to the geocell-reinforced foundation systems. The additional benefit is attributed to the membrane resistance of the base-geogrid. The improvements in bearing pressures were noticed with footing settlement. Higher bearing pressures were observed for thicker geocells and stiffer clay subgrades. However, it was also noticed that the base geogrid, in addition to the geocell-reinforcements, was mostly effective for softer subgrades having $c_u \leq 15$ kPa. Besides, for geocell-mattress of thickness $h > 1.05D$, reduction in bearing pressures were noticed. The reduction in bearing pressures is attributed to the intense buckling of the geocell-walls just at the bottom of the footing which was due to development of high stress concentration having restricted subgrade penetrations. In the experimental

program, maximum about 12-fold improvement in bearing pressure was achieved for c_u = 7 kPa; while, maximum bearing pressure was about 720 kPa, observed for c_u = 60 kPa. It can be concluded that the base geogrid is advantageous for the geocell-mattress having thickness of about the footing diameter (i.e. $h \sim 1.05D$) and will be effective for softer subgrades, such as $c_u \leq 15$ kPa, with the similar materials used as the present study.

Chapter 8. DESIGN IMPLICATIONS OF THE STUDY

8.1 INTRODUCTION

Present study has investigated the behavior of different foundation systems, with clay subgrade of varying strengths, through physical model tests. Model tests on different foundation configurations: homogeneous, unreinforced layered, and different reinforced systems (geogrid, geocell, and geocell-geogrid) have been conducted. Clay subgrade strengths (c_u) and thickness of layered configurations (H) were varied in the tests. Model tests were conducted under different series as presented in Table 3.3 and discussed in earlier chapters. This chapter presents the design implications of the study for practical purposes. A comparative discussion of the performances of different foundation systems, the critical observations and limitations of the study are also discussed. Regression analysis was performed for the test results to establish the inter-relationships among the variables used in the study. A design example is also presented to illustrate the implications of the present study.

8.2 COMPARATIVE DISCUSSION OF DIFFERENT FOUNDATIONS

The responses of homogeneous clay beds, obtained from series A, have indicated a non-linear increase of bearing pressure with the footing settlement. The homogeneous sand bed (at the relative density adopted, i.e. 80%) had indicated stiffer response (higher bearing pressures) as compared to the clay beds up to c_u = 30 kPa. The layered foundations of unreinforced sand of different thicknesses overlying clay subgrades of varying strengths (series B) have indicated that sand layer thickness (H) up to 1.67D would be beneficial for softer subgrades (i.e. $c_u \leq 30$ kPa). Beyond this

thickness, marginal benefits and/or reduced pressure-settlement responses were observed due to the failure of sand layer under shear. In case of the stiff clay subgrade of 60 kPa, all the layered configurations with unreinforced sand have resulted in reduced bearing pressure responses (Fig. 4.9) which is the typical foundation behavior of a softer layer overlying stiffer subgrade, as discussed by Meyerhof (1974).

Similar observations, in terms of optimum layer thickness, were found for geogrid reinforced foundations (series C). In this series, beyond the depth (H) of 1.67D, the influence of interface geogrid was negligible. It is attributed to the fact that a typical foundation behavior show a significant depth up to about 1 to 1.5 times diameter/width of the footing (Meyerhof, 1974; Terzaghi et al., 1996). However, for the stiff clay subgrade of 60 kPa, the interface geogrid was beneficial up to only H = 1.15D as seen in Fig. 5.5.

Significant improvements in bearing pressures were noticed for geocell-reinforced foundation systems for all the clay subgrades (series D). The improvements in bearing pressures were as high as 11.6 fold the corresponding homogeneous clay bed (c_u = 7 kPa). However, beyond the geocell-thickness (h) of 1.05D, the adverse effects, such as buckling in geocell-walls and squeezing out of sand cushion, lead to reduction in performances. Further improvements in bearing pressures were observed for geocell-reinforced foundations with a geogrid placed at the bottom of the geocell-sand mattress (series E). However, in geocell-geogrid reinforced systems, the negative effects (buckling in geocell-walls and squeezing out of sand cushion) were more pronounced as compared to the geocell-alone foundations. In geocell-geogrid systems, these effects were observed even for very soft clay bed (c_u = 7 kPa). As per the observations, the optimum geocell-height (h) is considered as 1.05D for geocell and geocell-geogrid reinforced foundation systems.

Referring to the above discussions, it can be stated that layer thickness of up to 1.67*D* for unreinforced and geogrid reinforced layered configurations and up to 1.15*D* for geocell and geocell-geogrid reinforced configurations can be considered for design purpose. Comparisons of the pressure-settlement responses obtained from different test series, for H = 1.15D cases, are presented in Fig. 8.1 to Fig. 8.4, for different clay subgrades, such as c_u = 7, 15, 30, and 60 kPa, respectively. This layered configuration (H = 1.15D) is chosen considering the foundation performances, in terms of the improvement trends and the negative effects such as geocell-buckling, sand squeezing etc. In general, instead of the limitations, it can be noticed that the load bearing capacity of the foundation beds were increased with increasing superiority of reinforcement types: i.e., unreinforced < geogrid < geocell < geocell-geogrid.

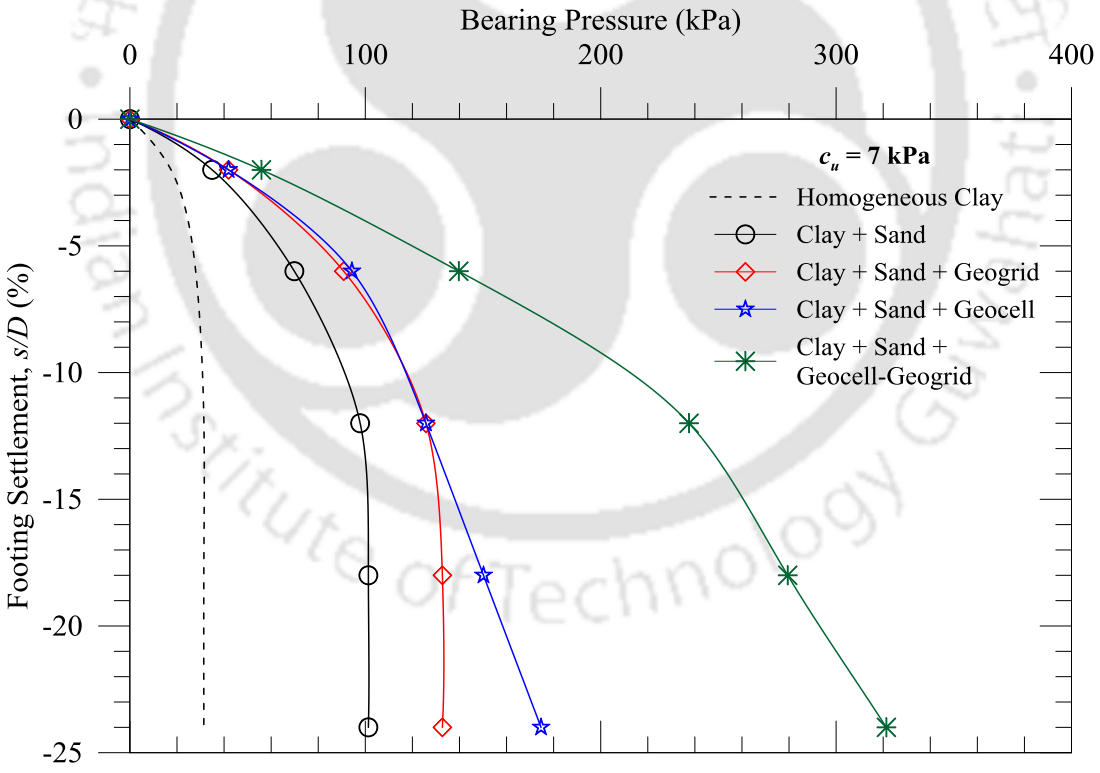

Fig. 8.1 Pressure-settlement responses of different foundations with c_u = 7 kPa (H = 1.15D)

In Fig. 8.1 to Fig. 8.4, significant improvements in bearing pressures for reinforced foundations, compared to the unreinforced systems, can be noticed.

However, for reinforced foundations, a comparatively higher level of footing settlements (s/D > 6%) is required for considerable improvement in bearing pressures, depending on subgrade clay strength and reinforcement superiority. For instance, in Fig. 8.1 for c_u = 7 kPa, improvement for geocell-reinforced configuration, compared to the geogrid reinforcement, was significant beyond 18% of s/D. It is attributed to the complex interaction in between foundation soil and the reinforcements. For very soft clay such as c_u = 7 kPa, the subgrade could easily be penetrated upon footing load. In this case, the interfacial resistance through reinforcement was considerable; however, due to less/no resistance against penetration, subgrade support was minimal. In case of comparatively stiffer subgrades ($c_u \geq$ 15 kPa), foundations were responded in other way; i.e. minimal interfacial resistance and maximum subgrade support.

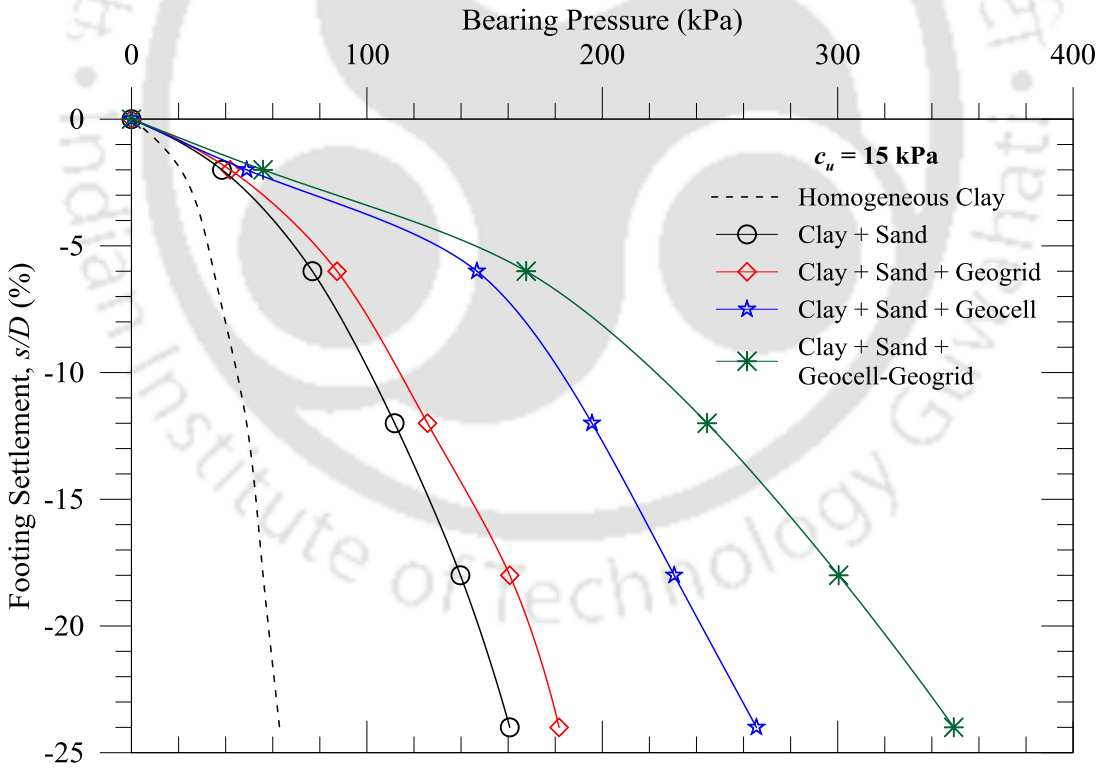

Fig. 8.2 Pressure-settlement responses of different foundations with c_u = 15 kPa (H = 1.15D)

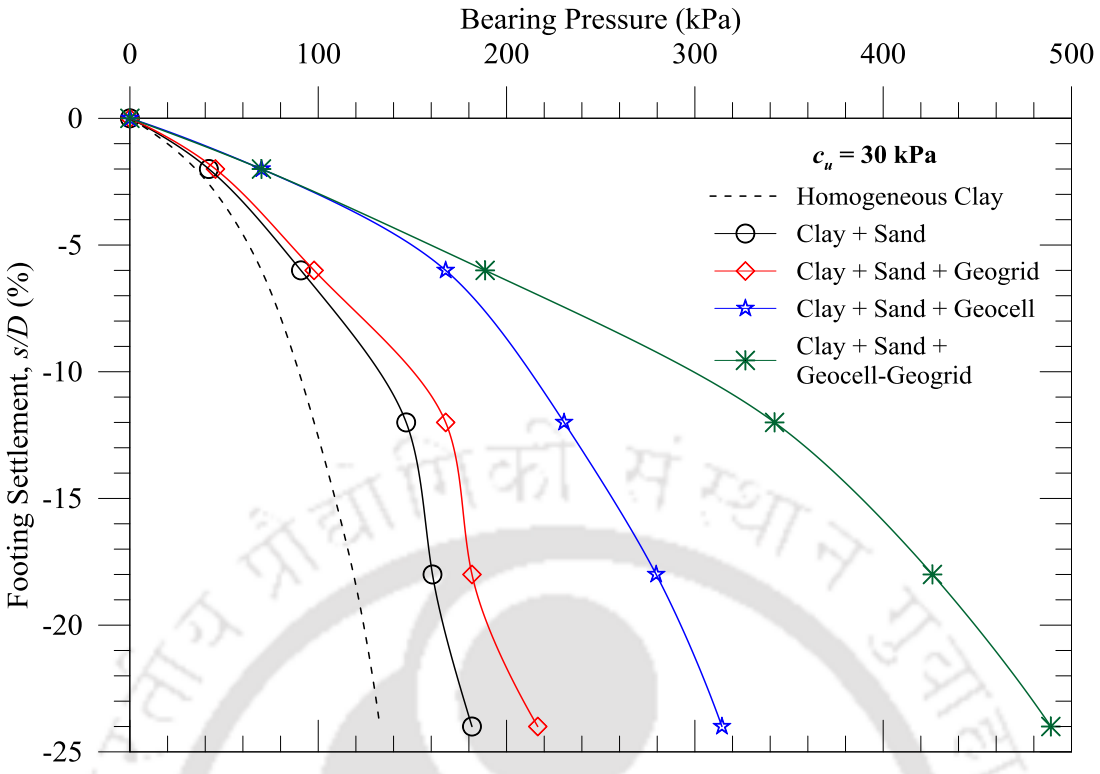

Fig. 8.3 Pressure-settlement responses of different foundations with c_u = 30 kPa (H = 1.15D)

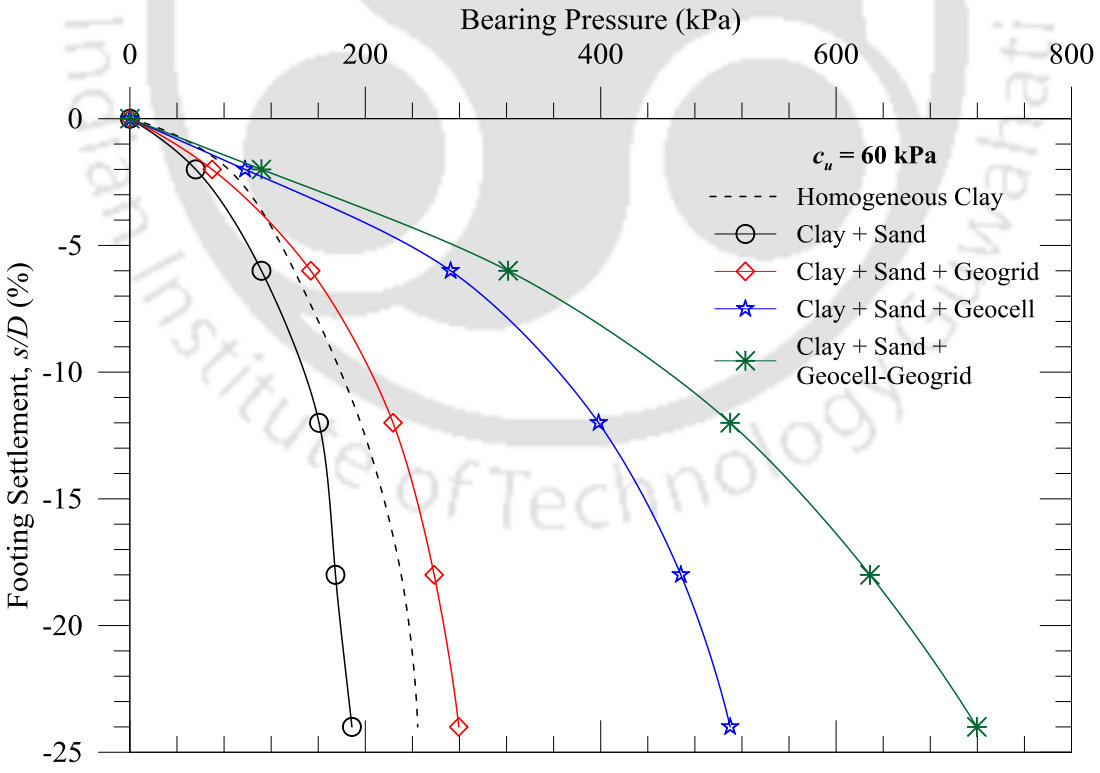

Fig. 8.4 Pressure-settlement responses of different foundations with c_u = 60 kPa (H = 1.15D)

The variations in different improvement factors (i.e. I_{fs}, I_{fsg}, I_{fsgc}, and I_{fsgcg}) for varying clay subgrades are presented in Fig. 8.5 to Fig. 8.8, corresponding to the pressure-settlement responses depicted in Fig. 8.1 to Fig. 8.4. It can be noticed that the improvements factors for bearing pressures, for a reinforcement of any type, are not same for all the subgrades. In general, the benefits of the geocell and geocell-geogrid reinforcements are mostly pronounced for comparatively stiffer subgrades in which c_u > 15 kPa. It is attributed to the higher support from the subgrades underlying, as discussed earlier. However, for thicker geocells ($h \geq 1.57D$), due to buckling in geocell-wall, the performances of geocell and geocell-geogrid reinforced foundations are decreased, as discussed in the respective chapters.

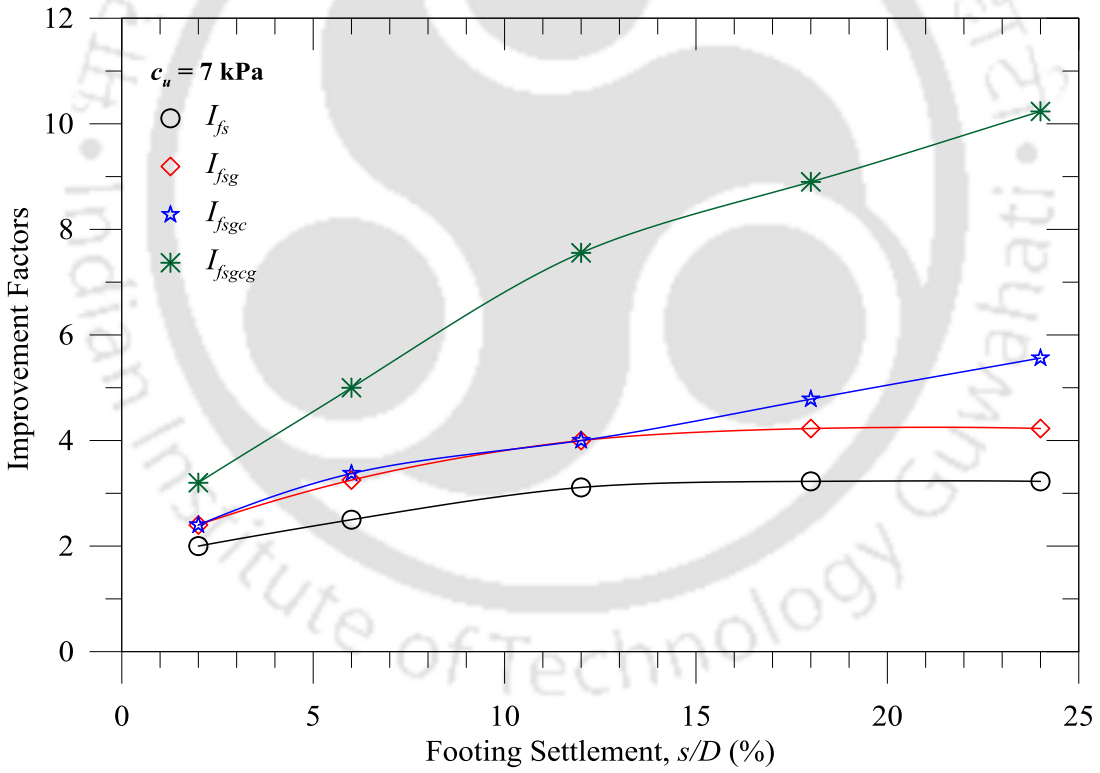

Fig. 8.5 Variation of improvement factors with *s/D* for c_u = 7 kPa (H = 1.15D)

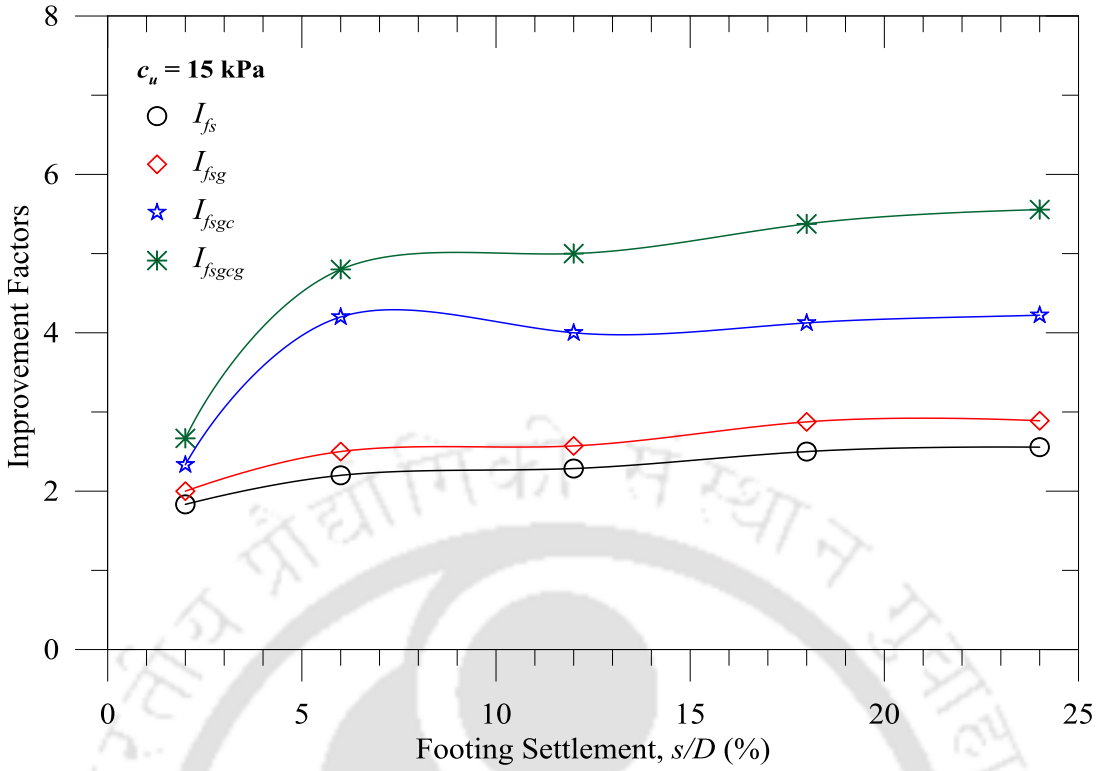

Fig. 8.6 Variation of different improvement factors with *s/D* for c_u = 15 kPa (*H* = 1.15*D*)

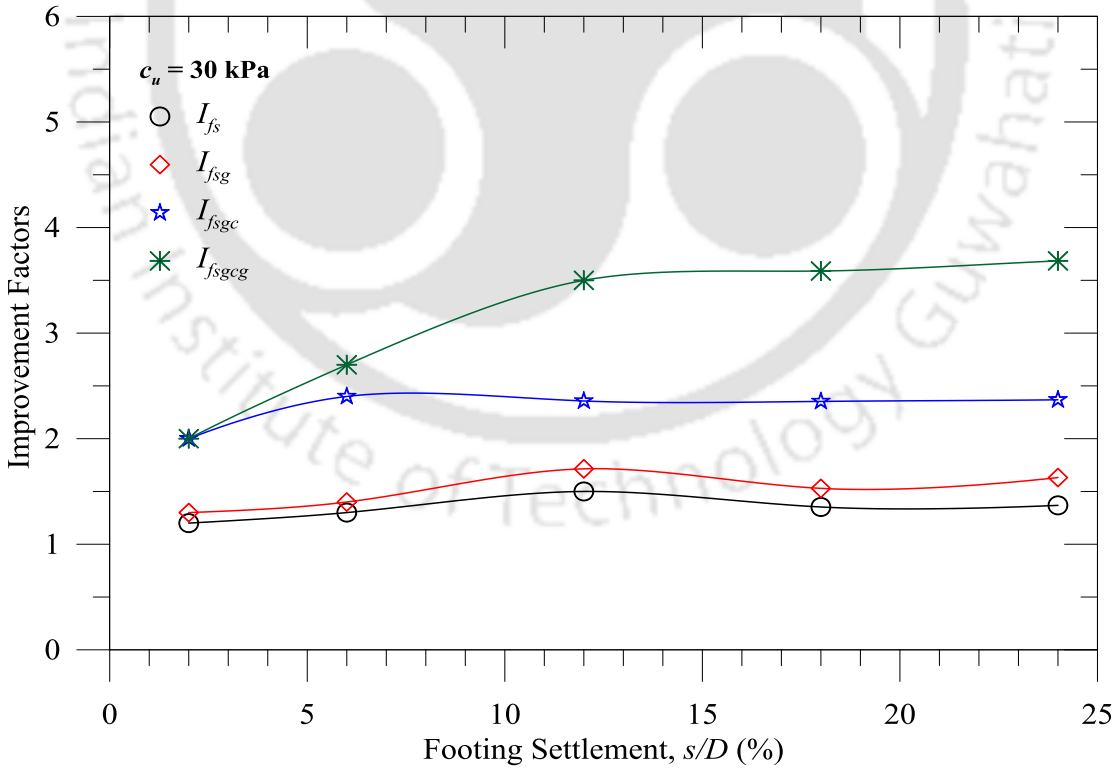

Fig. 8.7 Variation of different improvement factors with *s/D* for c_u = 30 kPa (*H* = 1.15*D*)

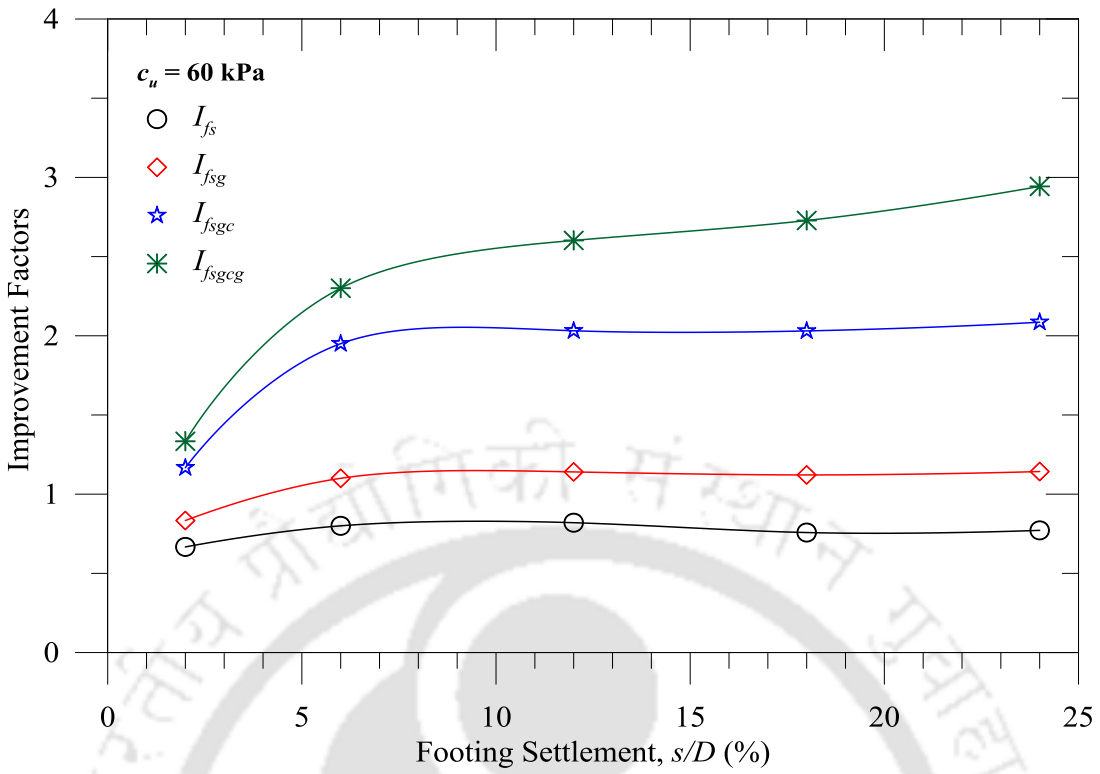

Fig. 8.8 Variation of different improvement factors with *s/D* at for c_u = 60 kPa (*H* = 1.15*D*)

In Fig. 8.9, contributions of geogrid and geocell reinforcements for different subgrades are presented in terms of I_{fg} and I_{fgc}, respectively, which were quantified at different levels of footing settlements. Higher contributions for the geocell-reinforcement can be noticed compared to the geogrid reinforcement, for all the subgrades and settlement levels. However, the variation in I_{fgc} is not consistent with the subgrade strengths and footing settlement levels. It could be attributed to the complex interaction between the reinforced-soil and the underlying subgrades. As discussed earlier, increase in subgrade stiffness improves the reinforcement-contribution, in the form of subgrade support; while, the interfacial resistances are being restricted due to reduced stain mobilization in the geocell-walls. Besides, with increase in subgrade strength and for $h \geq 1.57D$, the foundation performances were affected by geocell-buckling. Hence, as per the experimental observations, the geocell thickness of about footing diameter (~ 1.05*D*) is considered as optimum.

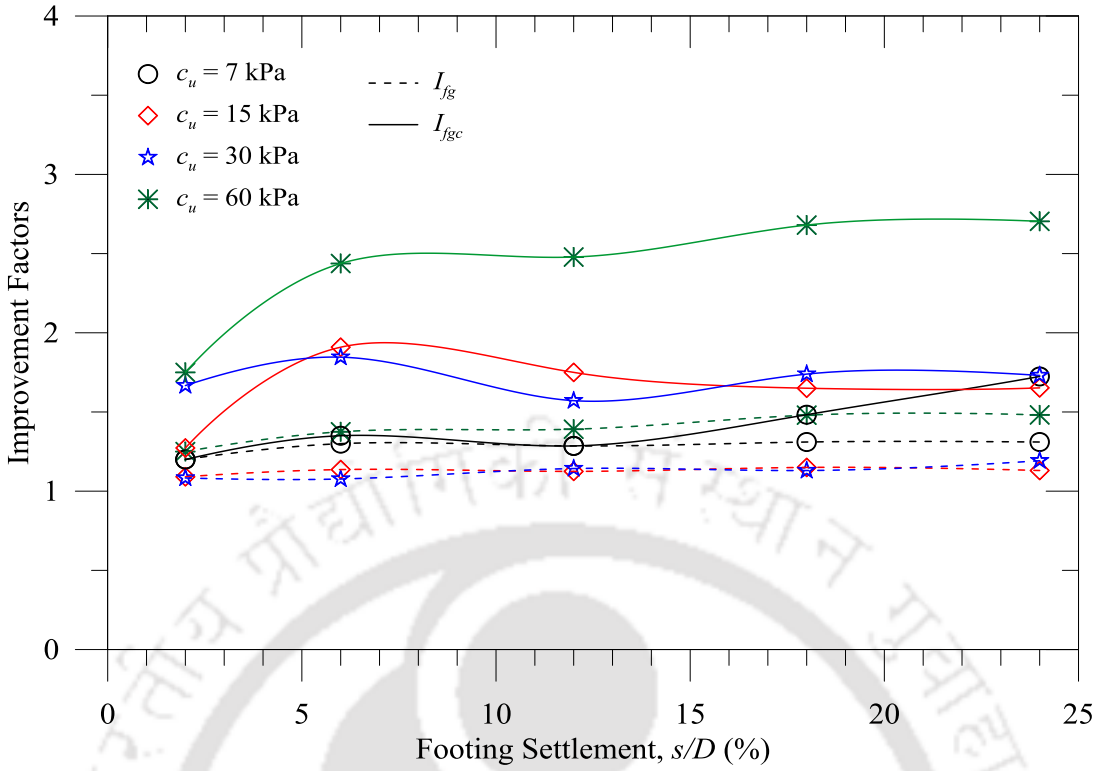

Fig. 8.9 Comparison of I_{fg} and I_{fgc} with s/D for different c_u at H = 1.15D

Contributions of geogrid as alone (series C) and together with geocell (series E) are presented in Fig. 8.10, in terms of I_{fg} and I_{fbg}, respectively, for different clay subgrades with H = 1.15D at different settlements. In this layer configuration, the range of variations of I_{fg} and I_{fbg} are 1.08-1.48 and 1.0-1.89, respectively. It can be noticed that the base geogrid (along with geocell) has performed in a better way as compared to the geogrid alone for the softer subgrades ($c_u \leq 30$ kPa). The behavior is attributed to the better strain mobilization at the base geogrid level in the case of geocell-sand mattress. At higher level of stress, the unreinforced sand was squeezed out from footing bottom inducing marginal strain to the interface geogrid leading to reduced membrane resistance. However, for the geocell-reinforced foundations, the sand was encapsulated within the geocell-pockets to behave as a semi rigid slab. Hence, it could carry higher stress and redistributed to the underlying base geogrid to derive the additional benefit and enhanced the overall foundation performance.

Reduced benefits of base geogrid, in case of the stiff clay subgrade of c_u = 60 kPa, can be attributed to the definition of quantifying the improvements. In case of geogrid-alone systems, the contribution was in terms of I_{fg}, comparing with the unreinforced sand in which case the bearing pressure was less than that of corresponding homogeneous clay bed (as discussed in context of Fig. 5.17). Hence, the I_{fg} is magnified as compared to the I_{fbg}, wherein, it (I_{fbg}) was compared to the geocell-reinforced system. Hence, from the observations, it can be noticed that significant contribution from the geogrid, in combination of unreinforced sand and the geocell-reinforced sand (series C and E), can be achieved for layer thickness H of 1.15D.

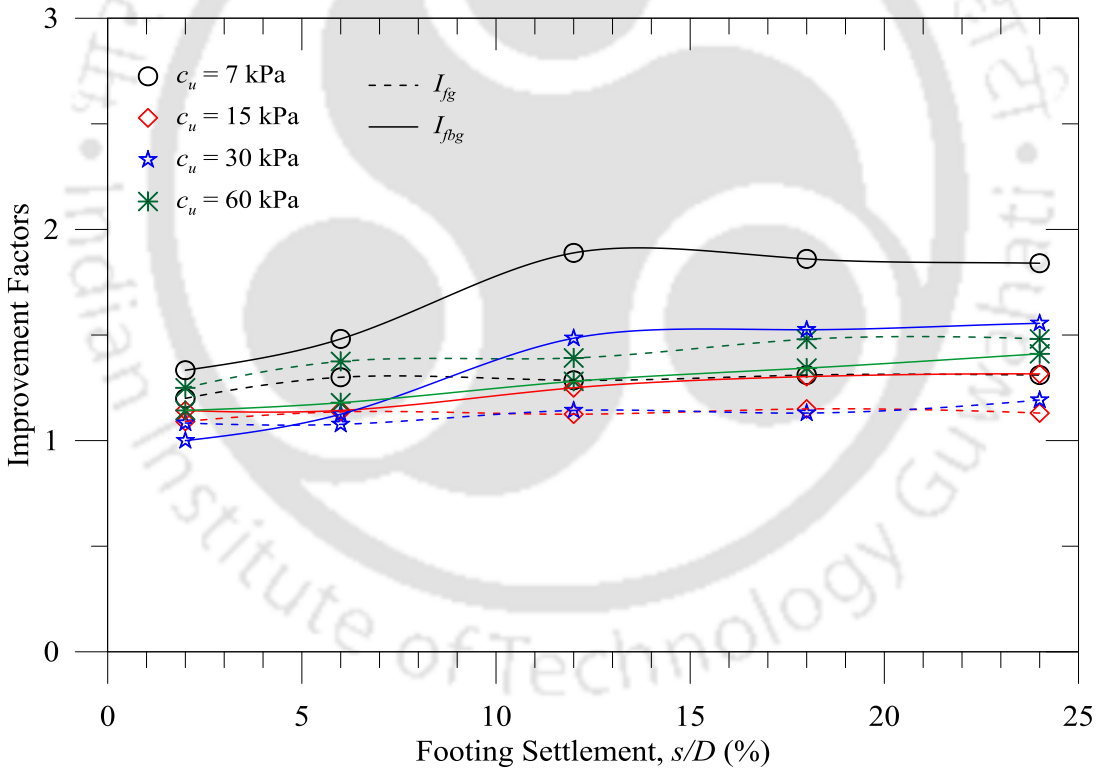

Fig. 8.10 Comparison of I_{fg} and I_{fbg} with s/D for different c_u at H = 1.15D

8.3 REGRESSION MODELS FOR BEARING PRESSURES

Model tests conducted on different unreinforced and reinforced foundation configurations indicated that the foundation behavior is significantly influenced by the subgrade clay strength (c_u), the unreinforced and/or reinforced sand layer thickness (H), and the footing settlements (s). Hence, quantification of the foundation behavior (in terms of bearing pressures) for different influencing parameters was attempted by regression analysis of the experimental data and presented in this section. Regression analysis methodology adopted by Ranjan et al. (1996), Bera et al. (2005), Rai (2010), Latha et al. (2013), and Bora and Dash (2014) has been followed for the purpose.

8.3.1 Regression Analysis

Regression analysis is a statistical tool used to establish relationship among a set of dependent and independent variables (Devore and Farnum, 1999; Dielman, 2001). In general, a non-linear regression model, as shown in Eq. 8.1 (Ranjan et al., 1996; Bera et al., 2005), is considered to explain the foundation behaviors.

$$Y_i = X_{i1}^{\beta i1} . X_{i2}^{\beta i2} . X_{i3}^{\beta i3} \ldots X_{ik}^{\beta ik} \quad (8.1)$$

Where, i = 1, 2, 3… n, are the number of data points (observations); the Y_i are the dependent variables and X_{ik} 's are the independent variables; k is the number of influencing parameters of Y_i and β_{ik} are the regression coefficients. The significance and accuracy of a regression model can be assessed through different indices and statistical parameters, such as standard errors (E_s), coefficient of determination (R^2) and adjusted coefficient of determination (R^2_{adj}), F-test, and t-test etc.

The 'standard error (E_s)' of a regression analysis is the measure of scatter of the variables; the smaller the E_s, the better is the fit. The 'E_s' is calculated as Eq. 8.2:

$$E_s = \sqrt{\frac{SSE}{n-k-1}} = \sqrt{MSE} \quad (8.2)$$

The *SSE* and *MSE* are the sum of squares and the mean square, respectively, due to 'error', defined as Eq. 8.3 and 8.4. The *SSR* and *MSR* are the sum of squares and the mean square due to 'regression', as defined in Eq. 8.5 and 8.6, respectively. The *SST* is defined and related with *SSE* and *SSR* as Eq. 8.7.

$$SSE = \sum_{i}^{i=n}(y_i - \hat{y}_i)^2 \tag{8.3}$$

$$MSE = \frac{SSE}{n-k-1} \tag{8.4}$$

$$SSR = \sum_{i}^{i=n}(\hat{y}_i - \bar{y})^2 \tag{8.5}$$

$$MSR = \frac{SSR}{k} \tag{8.6}$$

$$SST = \sum_{i}^{i=n}(y_i - \bar{y})^2 = SSR + SSE \tag{8.7}$$

Where, $\hat{y}_i$ is the predicted value and $\bar{y}$ is the mean of the dependent variables. The 'n' and 'k' represents the number of observations and the variables, respectively.

The correlation between the observed and the predicted values and effectiveness of the model can be assessed by R^2, which is defined as Eq. 8.8.

$$R^2 = 1 - \frac{SSE}{SST} \text{ ; Where, } 0 \leq R^2 \leq 1 \tag{8.8}$$

The closeness of R^2 to 1.0 signifies the betterment of the fit, and R^2 = 0 implies the absolute mismatch among the variables. In some models, having more number of variables will improve the R^2 spuriously. This deficiency can be overcome by checking the 'adjusted R^2' (R^2_{adj}; Bera et al. 2005) which can be evaluated as Eq. 8.9:

$$R^2_{Adj} = 1 - \frac{MSE}{MST} \tag{8.9}$$

The ***F***-test is performed to test the overall significance of the regression model. It can be calculated as Eq. 8.10. In the study, the significance level (α) is considered as 0.05 and the null hypothesis for the ***F***-test was, 'the independent variables are not related to the dependent variables'. The ***t***-test is to check the significance of individual

regression coefficients in the regression model. The decision rule for ***t***-test is as Eq. 8.11. The ***p***-value provides an additional estimation of the acceptance of the null hypothesis. The smaller the ***p***-value, the more convincing is the analysis.

$$F_{cal} = \frac{MSR}{MSE} \tag{8.10}$$

$$- t_{crit} > t_{cal} > +t_{crit} \tag{8.11}$$

8.3.2 Regression Models

The bearing pressures of different foundation systems, such as homogeneous and layered unreinforced and reinforced systems (i.e., q_c, q_s, q_{sg}, q_{sgc}, and q_{sgcg}) are considered as the dependent variables for the regression analysis. The influencing parameters, as per the foundation configurations, such as the undrained shear strength of clay (c_u), footing settlement levels (s/D), and the thickness of unreinforced and/or reinforced sand layers (H/D) overlying the clay subgrades are considered as the independent variables. The contribution of unreinforced sand is directly computed as the bearing pressures of the homogeneous sand bed as q_{os}. The effect of interfacial resistances in reinforced-systems is considered in terms of friction ratio, f (= δ_s/φ); where, δ_s is the interfacial frictional angle between sand and geogrid obtained in pull-out tests. Table 8.1 summarizes dependent and independent variables considered for different test series. The regression analysis was performed using built-in data analysis tool pack available in Microsoft Excel®.

Table 8.1 Variables for regression analyses

Test Series	Variables	
	Dependent	Independent
A	q_c	c_u, s/D
B	q_s	c_u, s/D, H/D, q_{os}
C	q_{sg}	c_u, s/D, H/D, q_{os}, δ_s/φ
D	q_{sgc}	c_u, s/D, H/D, q_{os}, δ_s/φ
E	q_{sgcg}	c_u, s/D, H/D, q_{os}, δ_s/φ

Bearing pressure data were obtained from the experimental investigations for the regression analysis. Referring to the experimental data analyses and inferences made, few set of experiments were excluded for the analysis. In the case of unreinforced and geogrid reinforced systems (series B and C), data from the experiments with layer thickness (H) up to 1.67D were considered for regression analysis. While, for geocell and geocell-geogrid reinforced systems (series D and E), test data up to H = 1.15D were used. For each foundation systems, a set of test data corresponding to s/D = 2, 6, 12, 18, and 24% are used to generate the regression coefficients and the remaining data (corresponding to s/D = 0.67, 4, 8, 10, 14, 16, 20, and 22%) were used for validation. For homogeneous clay beds, 20 such data points were used for analysis, while 40 data points were kept for validation.

Homogeneous Beds

In the series A, responses of homogeneous clay beds of different undrained shear strengths (c_u) were investigated. In regression analysis, the bearing pressure of the clay beds (q_c) are considered as a function of c_u and s/D, as presented in Eq. 8.12.

$$q_c = c_u^{x}.(s/D)^{y} \tag{8.12}$$

Where, x and y are the regression coefficients. The analysis results are presented in Table 8.2 to Table 8.4. Incorporating the coefficients, the final form of the expression (Eq. 8.12) is Eq. 8.13.

$$q_c = c_u^{0.99}.(s/D)^{0.49} \tag{8.13}$$

Table 8.2 Regression statistics (homogeneous clay beds)

Regression Statistics	
R^2	0.9978
R^2_{Adj}	0.9421
Standard Error	0.0902
Observations	20

Table 8.3 Analysis of variance (homogeneous clay beds)

	df	*SS*	*MS*	*F*
Regression	2	66.87	33.43	4102.53
Residual	18	0.14	0.008	
Total	20	67.02		

Table 8.4 Summary of ***t***-statistics (homogeneous clay beds)

	Coefficients	*Standard Error*	*t-Stat*	*p-value*
c	0.99	0.03	29.61	1.01E-16
s/D	0.49	0.04	11.24	1.43E-09

The overall significance of the regression model is assessed by *F*-test; whereas, significance of individual regression coefficients are evaluated through *t*-test. From the ***F***-distribution table, corresponding to the level of significance (α = 0.05), the value of $F_{crit,\,(2,\,18)}$ is found as 3.55, as compared to the F_{cal} = 4102 (Table 8.3). Hence, as $F_{cal} > F_{crit}$, the null hypothesis is rejected. In a similar way, the null hypothesis for the *t*-test is rejected for $t_{crit,\ (0.025,18)}$ = 2.101. A significantly good agreement is observed between the experimental and predicted bearing pressures, presented in Fig. 8.11.

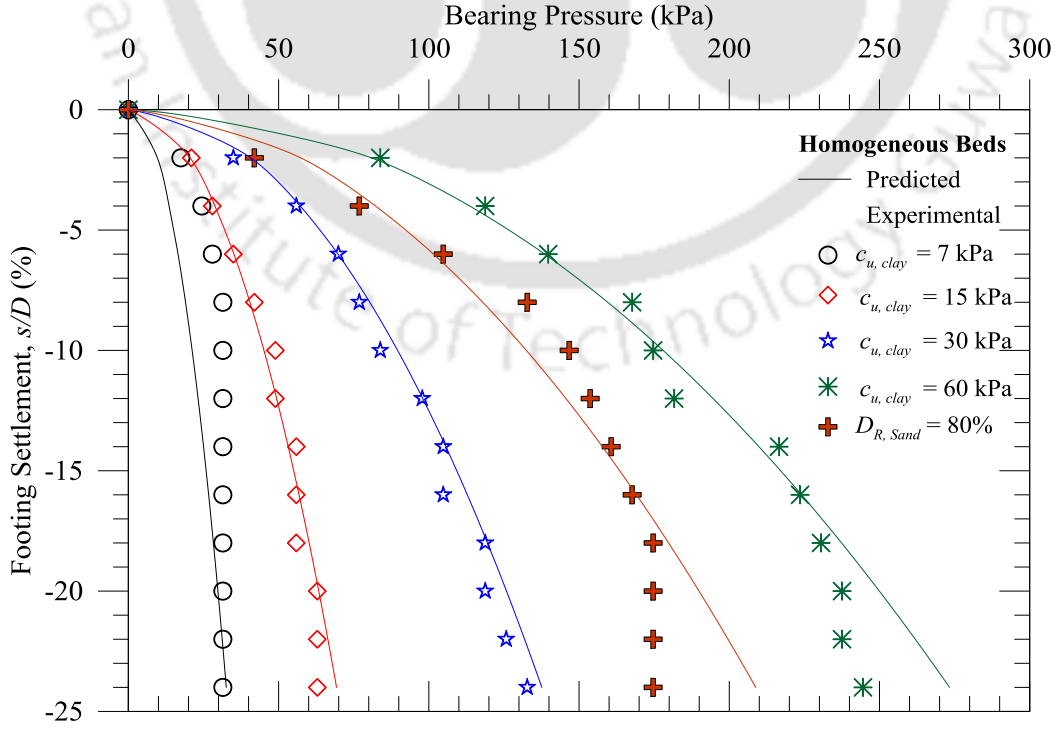

Fig. 8.11 Observed and predicted bearing pressures for homogeneous beds

In the test program, sand properties were not varied. However, an attempt is made similar to that of Eq. 8.13, where the bearing pressure of homogeneous sand bed (q_{os}) is considered as the function of the footing settlements levels (s/D). Through curve fitting, a relationship as shown in Eq. 8.14 was established.

$$q_{os} = 40\ (s/D)^{0.52} \tag{8.14}$$

Layered Foundations

Responses of unreinforced, geogrid, geocell, and geocell-geogrid reinforced foundations in different configurations were investigated in series B to E, respectively. Dependent bearing pressures and their independent influencing parameters are listed in Table 8.1. In layered systems, the bearing pressures are expressed as the function of subgrade strengths (c_u), homogeneous sand (q_{os}), footing settlement (s/D), layer thicknesses (H/D), and the friction factor, f ($= \delta_s/\varphi$). The regression model equation, in general, is shown in Eq. 8.15.

$$q_i = (c_u)^{ai1}(s/D)^{ai2}(H/D)^{ai3}(q_{os})^{ai4}(f)^{ai5} \tag{8.15}$$

Where, the q_i's are the bearing pressures of different foundation systems and a_i's are the regression coefficients. The results of the regression analysis are summarized in Table 8.5 to Table 8.7. Number of data points used (observations) for each class of dependent parameter is shown in Table 8.5. Regression coefficients for the regression model are shown in Table 8.7. Incorporating the coefficients, the final expressions are shown in Eqs. 8.16 to 8.19 for unreinforced, geogrid reinforced, geocell reinforced, and geocell-geogrid reinforced foundation systems, respectively.

$$q_s = (c_u)^{0.31}(s/D)^{012}(H/D)^{0.35}(q_{os})^{0.71} \tag{8.16}$$

$$q_{sg} = (c_u)^{0.32}(s/D)^{0.19}(H/D)^{0.13}(q_{os})^{0.64}(\delta_s/\varphi)^{-1.13} \tag{8.17}$$

$$q_{sgc} = (c_u)^{0.52}(s/D)^{0.28}(H/D)^{0.50}(q_{os})^{0.55}(\delta_s/\varphi)^{-1.05} \tag{8.18}$$

$$q_{sgcbg} = (c_u)^{0.42}(s/D)^{0.26}(H/D)^{0.26}(q_{os})^{0.72}(\delta_s/\varphi)^{-0.59} \quad (8.19)$$

Correlation of experimental and corresponding predicted bearing pressures are presented in Fig. 8.12. The fitted data points are corresponds to *s/D* = 2, 6, 12, 18, and 24%; whereas, the validated data points are corresponds to 0.67, 4, 8, 10, 14, 16, 20, and 22% of *s/D*. Depending on the overall performance and scattering of values, the proposed models can be judged good to estimate the foundation behavior.

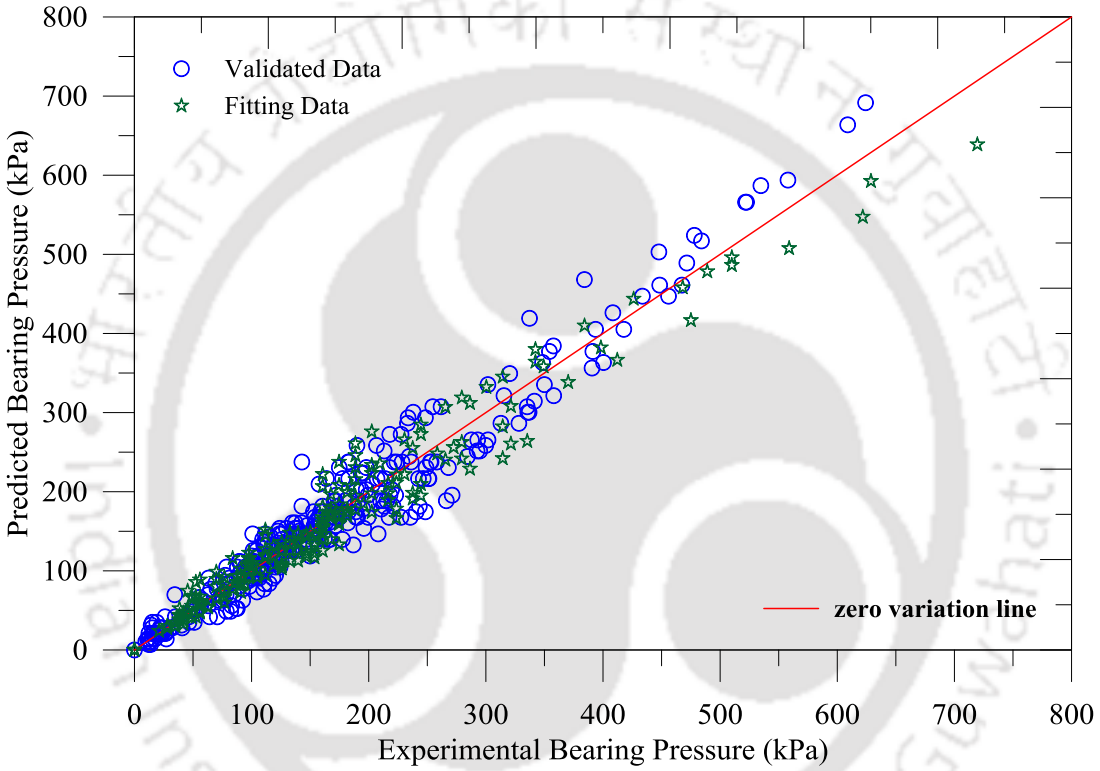

Fig. 8.12 Variation of observed and predicted bearing pressures

Table 8.5 Regression statistics (layered foundations)

	Foundation Condition			
	Unreinforced	**Geogrid**	**Geocell**	**Geocell-Geogrid**
R^2	0.998	0.998	0.999	0.999
R^2_{Adj}	0.980	0.981	0.971	0.971
Standard Error	0.085	0.076	0.047	0.057
Observations	60	60	40	40

Table 8.6 Analysis of variance (layered foundations)

	Foundation Condition															
	Unreinforced				**Geogrid Reinforced**				**Geocell Reinforced**				**Geocell-Geogrid Reinforced**			
	df	*SS*	*MS*	*F*	*df*	*SS*	*MS*	*F*	*df*	*SS*	*MS*	*F*	*df*	*SS*	*MS*	*F*
Regression	4	243.71	60.92	8473	5	261.39	52.27	9152	5	193.00	38.60	17182	5	222.99	44.59	13578
Residual	56	0.403	0.007		55	0.314	0.005		35	0.078	0.002		35	0.115	0.003	
Total	60	244.11			60	261.70			40	193.07			40	223.10		

Table 8.7 Summary of ***t***-statistics (layered foundations)

	Foundation Condition															
	Unreinforced				**Geogrid Reinforced**				**Geocell Reinforced**				**Geocell-Geogrid Reinforced**			
	Coefficients	Standard Error	t-stat	p-value	Coefficients	Standard Error	t-stat	p-value	Coefficients	Standard Error	t-stat	p-value	Coefficients	Standard Error	t-stat	p-value
c_u	0.31	0.031	10.03	4E-14	0.32	0.028	11.26	6E-16	0.52	0.022	24.19	2E-23	0.42	0.026	15.97	1.2E-17
q_{os}	0.71	0.034	21.10	2E-28	0.64	0.182	3.53	0.001	0.55	0.139	3.91	0.0004	0.72	0.168	4.27	0.0001
s/D	0.12	0.042	2.803	0.034	0.19	0.111	1.758	0.084	0.28	0.084	3.245	0.003	0.26	0.103	2.535	0.016
H/D	0.35	0.063	5.631	6E-07	0.13	0.056	2.398	0.019	0.50	0.50	8.77	2E-10	0.26	0.069	3.705	0.0007
δ_s/φ	-	-	-	-	-1.13	2.205	-0.511	0.611	-1.05	1.694	-0.623	0.54	-0.59	2.05	-0.286	0.776

8.4 LIMITATIONS OF THE STUDY

Limitations of the study are discussed in this section.

- Only one type of clay, sand, and reinforcement material were used.
- The footing size and shape were kept constant throughout the experimental investigation.
- Though the study considered different subgrade strengths but used only one clay material.
- The general dimensional analysis cannot be considered to the present study for applying the scaling laws, as it considered prototype materials.
- Proper measurements for deformation at geogrid and geocell-reinforcement were not taken.
- The regression models did not consider mechanics due to lack of proper observations. Hence, it is based only on the observed foundation data and applicable to predict the non-linear foundation behavior upto 15% footing settlements levels (*s/D*).

8.5 ILLUSTRATION OF DESIGN IMPLICATIONS OF THE STUDY

The following is the illustration for the design implications of the present study using the regression models. As an example, it is considered that a foundation configuration need to be identified for an isolated footing of diameter 1 m on a clay subgrade having c_u of 10 kPa. It is assumed that the capacity requirement (factored) for the said foundation is 100 kPa. For simplicity, the material properties of sand and reinforcements are considered as that of the materials adopted in the study. Further it is considered that the footing can sustain the maximum settlement about 5% the diameter.

As per the observations from the experimental study, different foundation systems will yield beneficial results with different layer thickness. A layer thickness up to 1.67*D* is implied to be beneficial for the unreinforced and geogrid reinforced foundations. While the same for geocell and geocell-geogrid reinforced foundations, it is considered as 1.15*D* (with u = 0.1*D*). A step wise procedure of determining the bearing pressures are as follows.

For the assumed settlement level, 5% of *s/D*, the bearing pressures of different foundation systems, having c_u = 10 kPa, have to be determined. The regression equations (Eqs. 8.16 to 8.19) are used for the purpose with the common layer thickness *H* of 1.15*D*.

i) For the homogeneous clay bed with c_u = 10 kPa, the bearing pressure at *s/D* = 5% is:

$q_c = c_u^{0.99}.(s/D)^{0.49} = (10)^{0.99}.(5)^{0.49}$ = 21.5 kPa

ii) For the unreinforced layered foundation with *H* = 1.15*D*, the bearing pressure at *s/D* = 5% is:

$q_s = (c_u)^{0.31}(s/D)^{0.12}(H/D)^{0.35}(q_{os})^{0.71}$

$= (10)^{0.31}(5)^{0.12}(1.15)^{0.35}(92.4)^{0.71}$ = 64.9 kPa

Where, q_{os} is determined as $\{40.(5)^{0.52}\}$ = 92.4 kPa

iii) For the geogrid-reinforced foundations with similar configurations, the bearing pressure can be estimated as the following.

$q_{sg} = (c_u)^{0.32}(s/D)^{0.19}(H/D)^{0.13}(q_{os})^{0.64}(\delta_s/\varphi)^{-1.13}$

$= (10)^{0.32}(5)^{0.19}(1.15)^{0.13}(92.4)^{0.64}(0.75)^{-1.13}$ = 72.9 kPa

iv) Similarly, for geocell and geocell-geogrid, the bearing pressures, q_{sgc} and q_{sgcg}, can be determined as below.

$q_{sgc} = (c_u)^{0.52}(s/D)^{0.28}(H/D)^{0.50}(q_{os})^{0.55}(\delta_s/\varphi)^{-1.05}$

$$= (10)^{0.52}(5)^{0.28}(1.15)^{0.50}(92.4)^{0.55}(0.75)^{-1.05} = 89.1 \text{ kPa}$$

$$q_{sgcg} = (c_u)^{0.42}(s/D)^{0.26}(H/D)^{0.26}(q_{os})^{0.72}(\delta_s/\varphi)^{-0.59}$$

$$= (10)^{0.42}(5)^{0.26}(1.15)^{0.26}(92.4)^{0.72}(0.75)^{-0.59} = 127 \text{ kPa}$$

Hence, it can be noticed the target capacity requirement can only be achieved with geocell-geogrid configuration. The regression equations can also be used to generate a general design chart for a given subsoil condition. Fig. 8.13 presents a complete range of estimated pressure-settlement responses for different foundation configurations. Based on the pressure-settlement responses, the appropriate foundation configuration as per design requirements can be selected. It can be noticed that the design pressure of 100 kPa (say) can be achieved as early as at a settlement of 3.5% (*s*/*D*) for geocell-geogrid foundation configuration with H = 1.15D. However, for geocell-foundation with similar layer configuration it can be reached at about 6% of *s*/*D*. Similarly, for geogrid and unreinforced foundations, the bearing pressures can be achieved no sooner than 8% and 9% of *s*/*D*, respectively, with H = 1.67D.

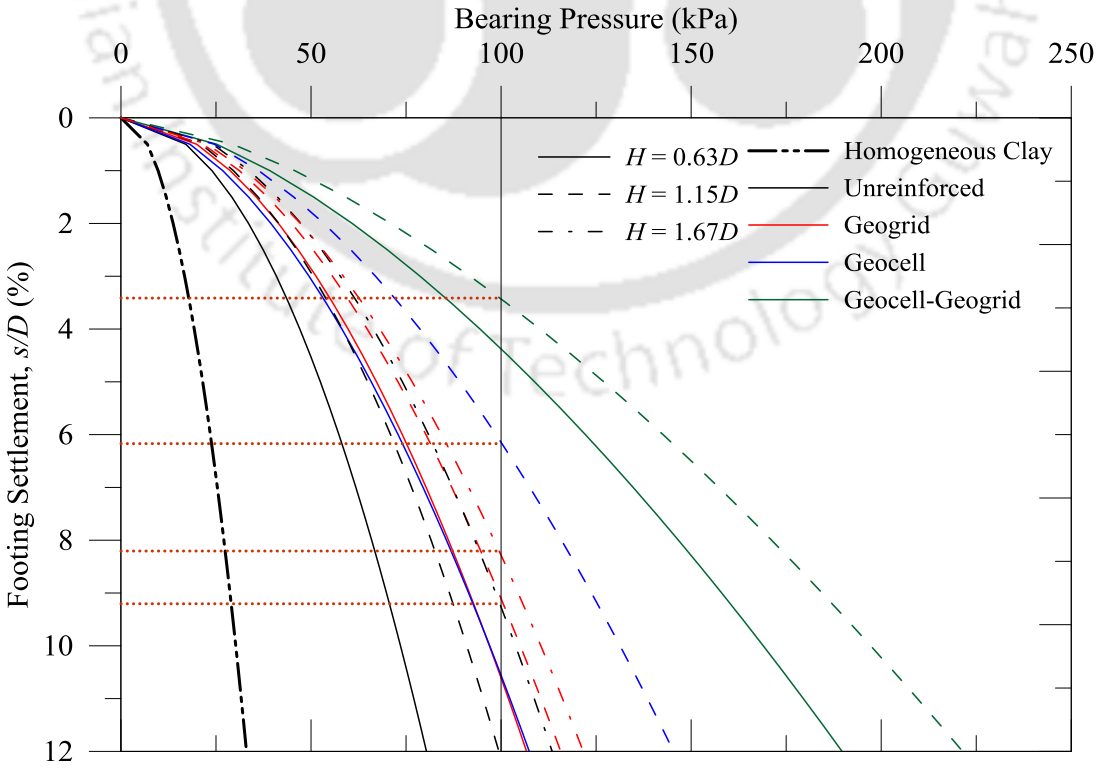

Fig. 8.13 Estimated pressure-settlement responses of different foundations

8.6 SUMMARY

This chapter presented a comparative study of the different foundation systems with their limitations. It is found that a layer thickness of 1.67*D* can be considered as optimum for unreinforced and geogrid reinforced foundations; while, for geocells, it was found as 1.15*D*. The regression analysis was performed on the experimental test results for inter-relationships between the bearing pressures (dependent variables) and the independent variables were the different influencing parameters, such as footing settlement, layer thickness, subgrade strengths and the interfacial properties. The experimental and predicted foundation behavior has shown good agreements. A detail step-wise design example is illustrated to show the use of the regression equations generated.

Chapter 9. CONCLUDING REMARKS

9.1 SUMMARY OF THE THESIS

The objective of the present study was to study the behavior of foundations on clay subgrades of varying strengths. The behaviors of different homogeneous and layered foundation systems (unreinforced and reinforced) of varying configurations, investigated through physical model tests, are presented in this thesis. Three types of reinforcements, such as planar geogrid, geocell, and a combination of geocell-geogrid, were considered with four different layer thicknesses and subgrade strengths.

The obtained test results from different foundation systems are discussed in four chapters, sequentially as unreinforced, geogrid reinforced, geocell reinforced, and geocell-geogrid reinforced foundation systems. The results are presented in terms of bearing pressure-settlement and surface deformation profiles. Besides, different bearing pressure ratios are introduced to compare the foundation behavior and reinforcement contributions. The subsequent chapter presented the practical design implications of the study along with the discussion on limitation of the study. Regression models were developed, based on the selected test data, to evaluate the bearing pressure at a given settlement level for a foundation system with any clay subgrade and reinforcement configuration. A detailed illustration for the applicability of the regression equations, defining the importance of subgrade strength in optimizing reinforced foundation design, was also presented.

9.2 CONCLUSIONS

The experimental study indicated that the performance of foundation systems, in unreinforced and reinforced configurations, is largely dependent on subgrade strength,

layer thicknesses, and footing settlement. In this section, conclusions drawn from this study are presented.

Homogeneous Foundations (Clay and Sand)

- The model tests performed on the homogeneous clay and sand beds (series A) depicted non-linear variations in pressure-settlement responses. Higher bearing pressures were noticed for stiffer clay beds at all settlement levels. The dense sand bed (D_r = 80%) showed stiffer response (higher bearing pressure) as compared to the clay beds up to c_u = 30 kPa, while it was softer w.r.t. 60 kPa (c_u) clay bed.
- Surface deformation profiles with footing settlement for homogeneous clay beds depicted pronounced heaving at foundation surface; while, initial settlement was seen for the dense sand bed followed by a surface heaving (at $x = D$). Such behavior was due to undrained behaviour of saturated clay and dilation of dense sand. The deformations were gradually reduced at $x = 2D$ and $3D$.

Unreinforced Layered Foundations (Sand over Clay)

- In case of layered foundations (series B) with unreinforced sand overlying the clay subgrades of different strength, the softer subgrades ($c_u \leq 30$ kPa) responded with improved bearing pressures at any level of footing settlements.
- For a stiff clay subgrade (c_u = 60 kPa), reduced bearing pressures were noticed as compared to corresponding homogeneous clay beds.
- Bearing pressures were improved with increase in H and s/D, for softer subgrades ($c_u \leq 30$ kPa). However, for $H > 1.67D$, the sand column was failed in shear and squeezed out from footing bottom leading to reduction in overall foundation performance.

- The improvement factor, I_{fs}, decreased with increase in subgrade strengths (c_u). Maximum improvement in bearing pressure of about 5.34-fold was seen for very soft subgrade (c_u = 7 kPa), whereas, it was about 2.3 for c_u = 30 kPa and about 0.90 for c_u = 60 kPa.
- Comparison of the experimentally obtained foundation responses with that of the theoretical approach are in considerably good aggrement.

Geogrid Reinforced Foundations

- Considerable improvement in bearing pressure was observed with planar geogrid reinforcement placed at the sand-clay interface (series C), compared to similar unreinforced foundation configurations (series B).
- Higher bearing pressures were noticed with increase in footing settlement (s/*D*), sand-layer thickness (*H*), and subgrade strength (c_u). The improvement is attributed to the membrane resistance developed at the interface-geogrid through soil-geosynthetic interaction.
- Optimum sand layer thickness (*H*) was 1.67*D* for softer subgrades ($c_u \leq$ 30 kPa), while the same was 1.15*D* in case of stiff clay subgrade of 60 kPa.
- The improvement factors, I_{fsg}, depicted a decreasing trend with increase in c_u. A maximum of 5.6-fold improvement (I_{fsg}) was observed for very soft clay subgrade while, the improvement factor is about 1.3 for stiff clay subgrade (c_u = 60 kPa). However, the contribution of planar geogrid (I_{fg}) was in the range of 1.0-1.75 depending on c_u value.
- Theoretical analysis depicted excellent aggrement of the foundation responses, in terms of bearing pressures, with that of the experimental results obtained in the present study.

Geocell Reinforced Foundations

- Beam like behavior and confinement action of geocell-sand mattress are inferred to be contributed for significant improvement in bearing pressure for all foundation systems with geocell reinforcement (series D). Higher bearing pressures were noticed with increase in footing settlement (s/D), geocell-height (h), and subgrade strength (c_u).
- The bearing pressure improvement factors (I_{fsgc}) were decreased with increase in subgrade strength (c_u) and geocell-height (h). For example: a maximum of about 11.6-fold improvement was observed for c_u = 7 kPa, while, it is 2.3 fold for 60 kPa subgrade.
- The geocells contribution (I_{fgc}), in improved bearing pressures, is higher for stiffer subgrades which is attributed to the semi-rigid slab like structure that offered greater subgrade support on stiffer subgrades.
- Optimum height of geocell-mattress for softer subgrades ($c_u \leq 15$ kPa) is 1.57D. In the case of stiffer subgrades ($c_u > 15$ kPa) the optimum height is 1.05D. Beyond these optimum heights buckling of geocell-walls and sand squeezing influenced the performance negatively.
- Surface heaving was significantly reduced around the footing (at $x = D$) and it increased at $x = 2D$ and $3D$ for geocell-reinforced foundations. It is due to the deep beam action of geocell-sand mattress which undergone sagging below the loading and hogging at away from footing.
- Bearing pressures calculated based on the theoretical approaches indicated a very good aggrement with that obtained through physical model tests.

Geocell-Geogrid Reinforced Foundations

- Geogrid placed at the base of geocells mattress enhanced the foundation performance, maximum up to 30%, compared to geocell-alone system which was inferred due to the membrane resistance of base geogrid.
- The optimum height of geocells with base geogrid is 1.05*D*, which can attain considerable beneficial effect could be obtained from the base geogrid. It is further inferred that the additional beneficial effect is reduced with increase in subgrade strength.

Design Implications of the Study

- The comparative performance analysis presented the superiority of reinforcement types in any layered configuration; i.e. higher bearing pressure can be obtained with higher reinforcement combinations (geocell-geogrid > geocell > geogrid > unreinforced).
- The comparative performance analysis and the regression models developed, optimized the use of reinforcements in foundation design. For example, a base geogrid with shorter geocell (h = 1.05D) would be more beneficial compared to thicker geocell ($h \geq 1.57D$) alone.

9.3 SCOPE FOR THE FUTURE RESEARCH

Following are some of the future scope options in the line of present research work.

- Detailed investigation by varying the soils and reinforcement types can be conducted to generalize the foundation behaviour. Besides, the parameters which were kept constant in the study can also be varied to investigate effects on overall foundation performance having different subgrades.

- Instrumentation facilities can be installed to measure the deformations in geogrid and geocell wall to estimate the membrane and interfacial resistances. Besides, it will be helpful in formulation of theoretical models.
- Numerical models can be developed and validated with the experimental observations. In future, these models can be used to analyse the behaviour of prototype foundations.
- In present study only incremental load was applied. A future investigation can be conducted with repeated (or cyclic) loading.

REFERENCES

1. Akinmusuru, J.O. and Akinbolade, J.A. (1981). Stability of loaded footings on reinforced soil. *Journal of the Geotechnical Engineering Division*, ASCE, 107(6), 819-827.

2. Alamshahi, S. and Hataf, N. (2009). Bearing capacity of strip footings on sand slopes reinforced with geogrid and grid-anchor. *Geotextiles and Geomembranes*, 27(3), 217-226.

3. Alawaji, H.A. (2001). Settlement and bearing capacity of geogrid reinforced sand over collapsible soil. *Geotextiles and Geomembranes*, 19(2), 75-88.

4. ASTM D0854 (2006). Standard test method for specific gravity of soil solids by water pycnometer. *ASTM International*, Vol. 04.09, West Conshohocken, PA.

5. ASTM D2487 (2011). Standard practice for classification of soils for engineering purposes (Unified Soil Classification System). *ASTM International*, Vol. 04.08, West Conshohocken, PA.

6. ASTM D2850 (2007). Standard test method for unconsolidated-undrained triaxial compression test on cohesive soils. *ASTM International*, Vol. 04.08, West Conshohocken, PA.

7. ASTM D4221 (2005). Standard test method for dispersive characteristics of clay soil by double hydrometer. *ASTM International*, Vol. 04.08, West Conshohocken, PA.

8. ASTM D4253 (2006). Standard test method for maximum index density and unit weight of soils and calculation of relative density. *ASTM International*, Vol. 04.08, West Conshohocken, PA.

9. ASTM D4254 (2006). Standard test method for minimum index density and unit weight of soils and calculation of relative density. *ASTM International*, Vol. 04.08, West Conshohocken, PA.

10. ASTM D4318 (2005). Standard test method for Liquid Limit, Plastic Limit, and Plasticity Index of soil. *ASTM International*, Vol. 04.08, West Conshohocken, PA.

11. ASTM D6528 (2007). Standard test method for consolidated undrained direct simple shear testing of cohesive soils. *ASTM International*, Vol. 04.09, West Conshohocken, PA.

12. ASTM D6637 (2009). Standard test method for determining tensile properties of geogrids by single or multi-rib tensile test methods. *ASTM International*, Vol. 04.13, West Conshohocken, PA.

13. ASTM D6913 (2004). Standard test method for particle size distribution (gradation) of soils using sieve analysis. *ASTM International*, Vol. 04.09, West Conshohocken, PA.

14. ASTM D698 (2012), Standard test methods for laboratory compaction characteristics of soil using standard effort (12 400 ft-lbf/ft^3 (600 kN-m/m^3)), *ASTM International*, Vol. 04.08, West Conshohocken, PA.

15. Basudhar, P.K., Saha, S. and Deb, K. (2007). Circular footings resting on geotextile reinforced sand bed. *Geotextiles and Geomembranes*, 25(6), 377-384.

16. Bathurst, R.J. and Jarrett, P.M. (1988). Large scale model tests of geocomposite mattresses over peat subgrades. *Transportation Research Record*, Transportation Research Board, Washington, D.C, 1188, 28-36.

17. Bathurst, R.J. and Karpurapu, R. (1993). Large-scale triaxial compression testing of geocell-reinforced granular soils. *Geotechnical Testing Journal*, 16(3), 296-303.

18. Bell, A.L. (1915). The lateral pressure and resistance of clay and supporting power of clay foundations. *In: A Century of Soil Mechanics*, ICE, London. 93-134.

19. Bera, A.K, Ghosh, A. and Ghosh, A. (2005). Regression model for bearing capacity of a square footing on reinforced pond ash. *Geotextiles and Geomembranes*, 23(3), 261-285.

20. Binquet, J. and Lee, K.L. (1975). Bearing capacity tests on reinforced earth slabs. *Journal of Geotechnical Engineering Division*, ASCE, 101(12), 1241-1255.

21. Bora, M.C. and Dash, S.K. (2014). Regression model for floating stone column improved soft clay. *Proc. of Indian Geotechnical Conference*, Kakinada, India, 1453-1459.

22. Brown, J.D. and Meyerhof, G.G. (1969). Experimental study of Bearing Capacity in Layered Clays. *Proc. of Seventh International Conference on Soil Mechanics and Foundation Engineering*, Vol. 2. 45-51.

23. Burd, H.J. and Frydman, S. (1997). Bearing capacity of plane-strain footings on layered soils. *Canadian Geotechnical Journal*, 34, 241-253.

24. Bush, D.I., Jenner, C.G. and Bassett, R.H. (1990). The design and construction of geocell foundation mattress supporting embankments over soft ground. *Geotextiles and Geomembranes*, 9(1), 83-98.

25. Button, S.J. (1953). The Bearing Capacity of Footings on a two-Layer Cohesive Sub-soil. *Proc. of Third International Conference on Soil Mechanics and Foundation Engineering*, Vol. 1, 332-335.

26. Carroll, R.G. and Curtis, V.C. (1990). Geogrid connections. *Geotextiles and Geomembranes*, 9(4-6), 515-530.

27. Cerato, A.B. and Lutenegger, A.J. (2006). Bearing capacity of square and circular footings on a finite layer of granular soil underlain by a rigid base. *Journal of Geotechnical and Geoenvironmental Engineering*, ASCE, 132(11), 1496-1501.

28. Choudhary, A.K., Jha, J.N. and Gill, K.S. (2010). Laboratory investigation of bearing capacity behaviour of strip footing on reinforced fly ash slope. *Geotextiles and Geomembranes*, 28(4), 393-402.

29. Chummar, A.V. (1972). Bearing capacity theory from experimental results. *Journal of the Soil Mechanics and Foundations Division*, ASCE, 98(12), 1311-1324.

30. Cooke, R.P. (1988). Contact stress distributions beneath a rigid circular plate resting on a cohesionless mass. *M.S. Thesis*, Clarkson University, Potsdam, New York.

31. Cowland, J.W. and Wong, S.C.K. (1993). Performance of a road embankment on soft clay supported on a geocell mattress foundation. *Geotextiles and Geomembranes*, 12(8), 687-705.

32. Das, B.M. and Khing, K.H. (1994). Foundation on layered soil with geogrid reinforcement-effect of a void. *Geotextiles and Geomembranes*, 13(8), 545-553.

33. Das, B.M. and Omar, M.T. (1994). The effects of foundation width on model tests for the bearing capacity of sand with geogrid reinforcement. *Geotechnical and Geological Engineering*, 12(3), 133-141.

34. Dash, S.K. (2010). Influence of relative density of soil on performance of geocell reinforced sand foundations. *Journal of Materials in Civil Engineering*, ASCE, 22(5), 533-538.

35. Dash, S.K. (2012). Effect of geocell type on load carrying mechanism of geocell reinforced sand foundations. *International Journal of Geomechanics*. ASCE, 12(5), 537-548.

36. Dash, S.K., Krishnaswamy, N.R. and Rajagopal, K. (2001a). Bearing capacity of strip footings supported on geocell-reinforced sand. *Geotextiles and Geomembranes*, 19(4), 235-256.

37. Dash, S.K., Rajagopal, K. and Krishnaswamy, N.R. (2001b). Strip footing on geocell reinforced sand beds with additional planar reinforcement. *Geotextiles and Geomembranes*, 19(8), 529-538.

38. Dash, S.K., Rajagopal, K. and Krishnaswamy, N.R. (2004). Performance of different geosynthetic reinforcement materials in sand foundations. *Geosynthetics International*, 11(1), 35-42.

39. Dash, S.K., Rajagopal, K. and Krishnaswamy, N.R. (2007). Behaviour of geocell-reinforced sand beds under strip loading. *Canadian Geotechnical Journal*, 44, 905-916.

40. Dash, S.K., Reddy, P.D. and Raghukanth, T.G. (2008). Subgrade modulus of geocell-reinforced sand foundation. *Ground Improvement*, 161(12), 79-87.

41. Dash, S.K., Sireesh, S. and Sitharam, T.G. (2003a). Model studies on circular footing supported on geocell reinforced sand underlain by soft clay. *Geotextiles and Geomembranes*, 21(4), 197-219.

42. Dash, S.K., Sireesh, S. and Sitharam, T.G. (2003b). Behaviour of geocell reinforced sand beds under circular footing. *Ground Improvement*, 7(3), 111-115.

43. Devore, J.L. and Farnum, N.R. (1999). Applied Statistics for Engineers and Scientists. *International Thomson Publishing Inc*., USA.

44. Dewar, S. (1962). The oldest roads in Britain. *The Countryman*, 59(3), 547-555.

45. Dielman, T.E. (2001). Applied regression analysis for business and economics. *Thomson Learning Inc*., USA.

46. Draper, N.R. and Smith, H. (1966). Applied regression analysis. *Wiley & Sons*, New York.

47. Duncan, J.M. and Seed, H.B. (1967). Corrections for strength test data. *Journal of the Soil Mechanics and Foundation Division*, ASCE, 93(5), 121-137.

48. Emersleben, A. and Meyer, N. (2008). The use of geocells in road construction over soft soil: Vertical stress and falling weight deflectometer measurements. *EuroGeo4*, Paper No. 132, 1-8.

49. Fragaszy, R.J. and Lawton, E. (1984). Bearing capacity of reinforced sand subgrades. *Journal of Geotechnical Engineering*, ASCE, 110(10), 1500-1507.

50. Gibson, R.E. (1953). Experimental determination of the true cohesion and true angle of internal friction in clays. *Proc. of the 3rd International Conference on Soil Mechanics and Foundation Engineering*, Zurich, 1, 126-130.

51. Giroud, J.P. and Noiray, L. (1981). Geotexti1e reinforced unpaved road design. *Journal of the Geotechnical Engineering Division*, ASCE, 107(9), 1233-1254.

52. Guido, V.A., Chang, D.K. and Sweeney, M.A. (1986). Comparison of geogrid and geotextile reinforced earth slabs. *Canadian Geotechical Journal*, 23, 435-440.

53. Hanna, A. M. (1981). Experimental study on footings in layered soil. *Journal of the Geotechnical Engineering Division*, ASCE, 107(8), 1113-1127.

54. Hanna, A. M. (1982). Bearing capacity of foundations on a weak sand layer overlying a strong deposit. *Canadian Geotechnical Journal*, 19, 392-396.

55. Hanna, A.M. and Meyerhof, G.G. (1980). Design charts for ultimate bearing capacity of foundations on sand overlying soft clay. *Canadian Geotechnical Journal*, 17, 300-303.

56. Hanna, A.M. and Meyerhof, G.G. (1981). Experimental evaluation of bearing capacity of footing subjected to inclined loads. *Canadian Geotechnical Journal*, 18, 599-603.

57. Hansen, J.B. (1970). A revised and extended formula for bearing capacity. *Danish Geotechnical Institute*, Bull no. 28, 21, Copenhagen.

58. Hendricker, A.T., Fredianelli, K.H., Kavazanjiam, E. Jr. and McKelvey III, J.A. (1998). Reinforcement requirements at a hazardous waste site. *Proc. of the Sixth International Conference on Geosynthetics*, Atlanta, Vol. 1, 465-468.

59. Henkel, D.J. and Gilbert, G.D. (1952). The effect of the rubber membrane on the measured triaxial compression strength of clay samples. *Geotechnique*, 3(1), 20-29.

60. Highter, W.H. and Anders, J.C. (1985). Dimensioning footings subjected to eccentric loads. *Journal of Geotechnical Engineering*, ASCE, 111(5), 659-665.

61. Huang, C.C. and Tatsuoka, F. (1990). Bearing capacity of reinforced horizontal sandy ground. *Geotextiles and Geomembranes*, 9(1), 51-82.

62. Indraratna, B., Biabani, M.M. and Nimbalkar, S. (2015). Behavior of geocell-reinforced sub-ballast subjected to cyclic loading in plane-strain condition. *Journal of Geotechnical and Geoenvironmental Engineering*, ASCE, DOI: 10.1061/(ASCE)GT.1943-5606.0001199

63. Johnson, J.E. (1982). Bridge over tidal waters. *Municipal Engineer*, 109(5), 104-107.

64. Jones, C.J.F.P. (1996). Earth reinforcement and soil structures. *Thomas Telford Publication*, London.

65. Jumikis, A.R. (1961). The shape of rupture surface in sand. *Proc.* of *Fifth International Conference on Soil Mechanics and Foundation Engineering*, Vol. 1, 693-698.

66. Kazi, M., Shukla, S.K. and Habibi, D. (2015). Effect of submergence on settlement and bearing capacity of surface strip footing on geotextile-reinforced sand bed. *International Journal of Geosynthetics and Ground Engineering*, 4 (1), DOI: 10.1007/s40891-014-0006-y.

67. Khing, K.H., Das, B.M., Puri, V.K., Cook, E.E. and Yen, S.C. (1993). The bearing capacity of a strip foundation on geogrid-reinforced sand. *Geotextiles and Geomembranes*, 12(4), 351-361.

68. Khing, K.H., Das, B.M., Puri, V.K., Yen, S.C. and Cook, E.E. (1994). Foundation on strong sand underlain by weak clay with geogrid at the interface. *Geotextiles and Geomembranes*, 13(3), 199-206.

69. Kim, S.I. and Cho, S.D. (1988). An experimental study on the contribution of geotextiles to bearing capacity of footings on weak clays. *Proc. of International Geotechnical Symposium on Theory and Practice of Earth Reinforcement*, Fukuoka, Japan, 215-220.

70. Koerner, R.M. (1997). Designing with geosynthetics. *Prentice Hall Inc*., New Jersey, USA.

71. Krishnaswamy, N.R., Rajagopal, K. and Latha, G.M. (2000). Model studies on geocell supported embankments constructed over soft clay foundation. *Geotechnical Testing Journal*, ASTM, 23(1), 45-54.

72. Latha G.M. and Somwanshi A. (2009). Bearing capacity of square footings on geosynthetic reinforced sand. *Geotextiles and Geomembranes*, 27(4), 281-294.

73. Latha, G.M, Rajagopal, K. and Krishnaswami, N.R. (2006). Experimental and theoretical investigation on geocell supported embankment. *International Journal of Geomechanics*, 6(1), 30-35.

74. Latha, G.M. and Murthy, V.S. (2007). Effects of reinforcement form on the behaviour of geosynthetic reinforced sand. *Geotextiles and Geomembranes*, 25(1), 23-32.

75. Latha, G.M., Dash S.K., and Rajagopa,l K. (2009). Numerical Simulation of the Behavior of Geocell Reinforced Sand in Foundations. *International Journal of Geomechanics*, 9(4), 143-152.

76. Latha, G.M., Dash, S.K. and Rajagopal, K. (2008). Equivalent continuum simulations of geocell reinforced sand beds supporting strip footings. *Geotechnical and Geological Engineering*, 26, 387-398.

77. Latha, G.M., Somwanshi, A. and Reddy, K.H. (2013). A multiple regression equation for prediction of bearing capacity of geosynthetic reinforced sand beds. *Indian Geotechnical Journal*, 43(4), 331-343.

78. Lau, A., Edil, T., Benson, C. and Tanyu, B. (2001). Use of geocells in flexible pavements over poor subgrades. *Geo Engineering Report No.01-05*. Department of Civil and Environmental Engineering, University of Wisconsin-Madison, USA.

79. Love, J.P., Burd, H.J., Milligan, G.W.E. and Houlsby, G.T. (1987). Analytical and model studies of reinforcement of a layer of granular fill on soft clay subgrade. *Canadian Geotechnical Journal*, 24(4), 611-622.

80. Mandal, J.N. and Gupta, P. (1994). Stability of geocell-reinforced soil. *Construction and Building Materials*, 8(1), 55-62.

81. Mandal, J.N. and Sah, H.S. (1992). Bearing capacity tests on geogrid-reinforced clay. *Geotextiles and Geomembranes*, 11(3), 327-333.

82. Mehrjardi, G.T., Tafreshi, S.N.M. and Dawson A. R. (2013). Pipe response in a geocell-reinforced trench and compaction considerations. *Geosynthetics International*, 20(2), 105-118.

83. Meyerhof, G.G. (1951). The ultimate bearing capacity of foundation. *Geotechnique*, 2(4), 301-332.

84. Meyerhof, G.G. (1953). The bearing capacity of foundations under eccentric and inclined loads. *Proc. of Third International Conference on Soil Mechanics and Foundation Engineering*, Zurich, Vol. 1, 440-445.

85. Meyerhof, G.G. (1957). The ultimate bearing capacity of foundations on slopes. *Proc. of Fourth International Conference on Soil Mechanics and Foundation Engineering*, London, Vol. 1, 384-387.

86. Meyerhof, G.G. (1963). Some recent research on bearing capacity of foundation. *Canadian Geotechnical Journal*, 1(1), 16-26.

87. Meyerhof, G.G. (1965). Shallow foundations. *Journal of Soil Mechanics and Foundations Division*, ASCE, Vol. 91, SM2. 21-31.

88. Meyerhof, G.G. (1974). Ultimate bearing capacity of footings on sand layer overlying clay. *Canadian Geotechnical Journal*, 11(2), 224-229.

89. Meyerhof, G.G. and Hanna, A.M. (1978). Ultimate bearing capacity of foundations on layered soil under inclined load. *Canadian Geotechnical Journal*, 15(4), 565-572.

90. Mhaiskar, S.Y. and Mandal, J.N. (1996). Soft clay subgrade stabilization using geocells. *Construction and Building Materials*, 10(4), 281-286.

91. Michael, A.T. and Collin J.G. (1997). Large model spread footing load tests on geosynthetic reinforced soil foundations. *Journal of Geotechnical and Geoenvironmental Engineering*, ASCE, 123(1), 66-72.

92. Mitchell, J.K., Kao, T.C. and Kavazanjiam, E. (1979). Analysis of grid cell reinforced pavement bases. *Technical Report GL-79–8*, US Army Engineers Waterways Experiment Station, Vicksburg, VA.

93. Omar, M.T., Das, B.M., Yen, S.C., Puri, V.K. and Cook, E.E. (1993). Ultimate bearing capacity of rectangular foundations on geogrid-reinforced sand. *Geotechnical Testing Journal*, ASTM, 16(2), 246-252.

94. Palmeira, E.M., Tatsuoka, F., Bathurst, R.J., Stevenson, P.E. and Zornberg (2008). Advances in Geosynthetics Materials and Applications for Soil Reinforcement and Environmental Protection Works. *Electronic Journal of Geotechnical Engineering*, Special Volume, Bouquet 08.

95. Pauker, H.E. (1889). An explanatory report on the project of a sea-battery. *Journal of the Ministry of Ways and Communications*, St. Petersburg, September.

96. Paul, J. (1988). Reinforced soil system in embankments-construction practices. *Proc. of International Geotechnical Symposium on practice of Earth Reinforcement*, Fukuoka, Japan, October, 461-466.

97. Pfeifle, T.W. and Das, B.M. (1979). Model tests for bearing capacity in sand. *Journal of Geotechnical Engineering Division*, ASCE, 105(9), 1112-1116.

98. Pokharel, S.K., Han, J., Leshchinsky, D., Parsons, R.L. and Halahmi, I. (2010). Investigation of factors influencing behavior of single geocell-reinforced bases under static loading. *Geotextiles and Geomembranes*, 28(6), 570-578.

99. Prandtl, L. (1921). Uber die eindringungsflstigkeit plastischer baustoffe und die festigkeit von schneiden. *Zeitschrift fur angewandte Mathematik und Mechanik*, 1(1), 15-20.

100. Rai, M. (2010). Geocell-sand mattress overlying soft clay subgrade: behaviour under circular loading. *Ph.D. Thesis*, IIT Guwahati, India.

101. Rajagopal, K., Krishnaswamy, N.R. and Latha G.M. (1999). Behaviour of sand confined with single and multiple geocells. *Geotextiles and Geomembranes*, 17(3), 171-184.

102. Rajyalakshmi, K., Madhav, M.R. and Ramu, K. (2012). Bearing capacity of reinforced strip foundation beds on compressible clays. *Indian Geotechnical Journal*, 42 (4), 294-308.

103. Ranjan, G., Vasan, R.M. and Charan, H.D. (1996). Probabilistic analysis of randomly distributed fiber-reinforced soil. *Journal of Geotechnical Engineering*, ASCE, 122(6), 419-426.

104. Rankine, W.J.M. (1857). On the stability of loose earth dams. *Philosophical Transactions of Royal Society*. London, Vol. 147, 9-27.

105. Raymond, G.P. (2001). Failure and reconstruction of a gantry crane ballasted track. *Canadian Geotechnical Journal*, 38(3), 507–529.

106. Rea, C. and Mitchell, J.K. (1978). Sand reinforcement using paper grid cells. *Reprint 3130, ASCE spring convention and exhibit*. Pittsburgh, PA, 24-28.

107. Robertson, J. and Gilchrist, A.J.T. (1987). Design and construction of a reinforced embankment across soft lakebed deposits. *Proc. of the International Conference on Foundations and Tunnels,* London, M. C. Forde. Engineering Technics Press, Edinburgh, 2, 84-92.

108. Rochelle et al. (1988). Observational approach to membrane and area correction in triaxial tests. *In: Advanced Triaxial Testing of Soil and Rock*, ASTM, STP 997, 715-731.

109. Samatani, N.C. and Sonpal, R.C. (1989). Laboratory tests of strip footing on reinforced cohesive soil. *Journal of Geotechnical Engineering*. ASCE, 115(9), 1326-1330.

110. Saran, S. (2005). Reinforced soil and its engineering applications. *I.K. International Pvt. Ltd*., India.

111. Sawwaf, M.E. and Nazer, A. (2005). Behaviour of circular footings resting on confined granular soil. *Journal of Geotechnical and Geoenvironmental Engineering*, ASCE, 131(3), 359-366.

112. Selig, E.T., and McKee, K.E. (1961). Static and dynamic behaviour of small footings. *Journal of Soil Mechanics and Foundations Division*, ASCE, 87, 29-47.

113. Shimizu, M. and Inui, T. (1990). Increase in the bearing capacity of ground with geotextile wall frame. *Proc of the Fourth International Conference on Geotextiles Geomembranes and Related Products*, Hague, Netherlands, 1, 254.

114. Shin, E.C., Das, B.M., Puri, V.K., Yen, S.C. and Cook, E.E. (1993). Bearing capacity of strip foundation on geogrid reinforced clay. *Geotechnical Testing Journal*, ASTM, 16(4), 534-541.

115. Simac M.R. (1990). Connections for geogrid systems. *Geotextiles and Geomembranes*, 9(4-6), 537-546.

116. Siraj-Eldine, K. and Bottero, A. (1987). Etude experimentale de la capacite portante d'une couche de sol pulverulent d'epaisseur limitee. *Canadian Geotechnical Journal*, 24, 242-251.

117. Sireesh, S., Gowrisetti, S., Sitharam, T.G. and Puppala, A.J. (2009). Numerical simulation of geocell reinforced sand and clay. *Ground Improvement*, 162(4), 185-198.

118. Sireesh, S., Sitharam, T.G. and Dash, S.K. (2009). Bearing capacity of circular footing on geocell–sand mattress overlying clay bed with void. *Geotextiles and Geomembranes*, 27(2), 89-98.

119. Sitharam, T.G. and Sireesh, S. (2004). Model studies of embedded circular footing on geogrid reinforced sand beds. *Ground Improvement*, 8(2), 69-75.

120. Sitharam, T.G., Sireesh, S. and Dash, S.K. (2005). Model studies of a circular footing supported on geocell-reinforced clay. *Canadian Geotechnical Journal*, 42, 693-703.

121. Sitharam, T.G., Sireesh, S. and Dash, S.K. (2007). Performance of surface footing on geocell-reinforced soft clay beds. *Geotechnical and Geological Engineering*. 25(5), 509-524.

122. Skempton, A.W. (1951). The bearing capacity of clays. *Proc. Building Research Congress*, London, Vol. 1, 180-189.

123. Tafreshi, S.N.M. and Dawson, A.R. (2010). Comparison of bearing capacity of a strip footing on sand with geocell and with planar forms of geotextile reinforcement. *Geotextiles and Geomembranes*, 28(1), 72-84.

124. Tafreshi, S.N.M., Khalaj, O. and Dawson, A.R. (2013). Pilot-scale load tests of a combined multilayered geocell and rubber-reinforced foundation. *Geosynthetics International*, 20(3), 143-161.

125. Tani, K. and Craig, W.H. (1995). Bearing capacity of circular foundations on soft clay of strength increasing with depth. *Soils and Foundations*, 35(4), 21-35.

126. Tanyu, B.F., Aydilek, A.H., Lau, A.W., Edil, T.B. and Benson, C.H. (2013). Laboratory evaluation of geocell-reinforced gravel subbase over poor subgrades. *Geosynthetics International*, 20(2), 47-61.

127. Teng, W.C. (1969). Foundation design. *Prentice Hall*, Englewood Cliffs, NJ.

128. Terzaghi, K. (1943). Theoretical soil mechanics. *Wiley & Sons*, New York.

129. Terzaghi, K., Peck, R.B. and Mesri, G. (1996). Soil mechanics in engineering practice. *John Wiley and Sons*. New York.

130. Tournier, J.P. and Milovic, D.M. (1977). Etude experimentale de la capacite portante d'une couche compressible d'epaisseur limitee. *Geotechnique*, 27(2), 111-123.

131. Vesic, A.S. (1973). Analysis of ultimate loads of shallow foundations. *Journal of Soil Mechanics and Foundations Division*, ASCE, Vol. 99, SM1, 45-73.

132. Vesic, A.S. (1975). Bearing capacity of shallow foundations. *Foundation Engineering Hand Book*, Van Nostrand Reinhold Book Co., N.Y.

133. Vidal, H. (1969). The principle of reinforced earth. *Highway Research Record*, 282, Washington, D.C.

134. Webster, S.L. (1979). Investigation of beach sand trafficability enhancement using sand-grid confinement and membrane reinforcement concepts. *Technical Report GL-79-20*. US Army Corps of Engineers, Vicksburg, MS.

135. Webster, S.L. and Alford, S.J. (1978). Investigation of construction concepts for pavements across soft ground. *Technical Report S-78-6*, United States Army Corps of Engineers, Waterways Experiment Station, Mississippi, USA.

136. Webster, S.L. and Watkins, J.E. (1977). Investigation of construction techniques for tactical bridge approach roads across soft ground. *Technical Report S-77-1*, United States Army Corps of Engineers, Waterways Experiment Station, Mississippi, USA.

137. Wesseloo, J., Visser, A.T. and Rust, E. (2009). The stress-strain behavior of multiple cell geocell packs. *Geotextiles and Geomembranes*, 27(1), 31-38.

138. Wu, C.S. and Hong, Y.S. (2009). Laboratory tests on geosynthetics-encapsulated sand column. *Geotextiles and Geomembranes*, 27(2), 107-120.

139. Yoon, Y.W., Heo, S.B. and Kim, K.S. (2008). Geotechnical performance of waste tires for soil reinforcement from chamber tests. *Geotextiles and Geomembranes*, 26(1), 100-107.

140. Zhang, L., Zhao, M., Shi, C. and Zhao, H. (2010). Bearing capacity of geocell reinforcement in embankment engineering. *Geotextiles and Geomembranes*, 28(5), 475-482.

141. Zhou, H. and Wen, X. (2008). Model studies on geogrid or geocell-reinforced sand cushion on soft soil. *Geotextiles and Geomembranes*, 26(3), 231-238.

PUBLICATIONS

Journals:

1. **Biswas, A.**, Krishna, A.M. and Dash, S.K. (2015). Behavior of geosynthetic reinforced soil foundation systems of different configurations over a stiff clay subgrade. *International Journal of Geomechanics*, ASCE, DOI:10.1061/(ASCE)GM. 1943-5622.0000559.
2. **Biswas, A**., Ansari, M.A., Dash, S.K. and Krishna, A.M. (2015). Behavior of geogrid reinforced foundation systems supported on clay subgrades of different strengths. *International Journal of Geosynthetics and Ground Engineering.* Springer, 1(3), 1-10.
3. **Biswas, A.**, Krishna, A.M. and Dash, S.K. (2013). Influence of subgrade strength on the performance of geocell-reinforced foundation systems. *Geosynthetics International*, 20(6), 376-388.

Conferences/Invited Lectures:

1. Krishna, A. M. and **Biswas, A.** (2015). Geocell Reinforced Foundations. *Invited lecture presented in Training Course on 'Introduction to Geosynthetics and Their Applications*, December 14, 2015, NIT Surat, Surat.
2. **Biswas, A.**, Krishna, A.M. and Dash, S.K. (2013). Behavior of circular footing on layered soil: sand overlying clay subgrades. *Proceedings of Fourth Indian Young Geotechnical Engineers Conference*, IIT Chennai, 157-160.
3. **Biswas, A.**, Krishna, A.M. and Dash, S.K. (2013). Applicability of planar geogrid reinforcement in geocell-reinforced foundation systems. *Proceedings of Indian Geotechnical Conference*, IIT Roorkee (CD-ROM).
4. **Biswas, A.**, Dash, S.K. and Krishna, A.M. (2012). Parameters influencing the performance of geocell-reinforced foundation system: a brief review. *Proceedings of Indian Geotechnical Conference*, IIT Delhi, Vol. 1, 365-368.